

# **THE MOLECULAR BASIS OF ANTAGONISM AT CARDIOVASCULAR P2X1 AND P2X4 RECEPTORS**

**Thesis Submitted for the Degree of**

**Doctor of Philosophy**

**at the University of Leicester**

**By Louise Farmer**

**Department of Cell Physiology and Pharmacology**

**University of Leicester**

**June 2014**

## ***Abstract***

### **The Molecular Basis of Antagonism at Cardiovascular P2X1 and P2X4 Receptors – Louise Farmer**

Structural information for the zebrafish P2X4 receptor in both an agonist bound and unbound resting state provided a major advance in understanding agonist action and has given insight into movement that occurs in the receptor upon ATP binding. Despite agonist action now being well characterised, the molecular basis of antagonism is poorly understood.

In this thesis the mechanism of antagonist action at the hP2X1 receptor has been investigated through determining properties of chimeras and mutant receptors based on differences between antagonist sensitive and insensitive P2X receptors. The antagonists suramin, NF449 and PPADS potently inhibit the human P2X1 receptor but have little or no action at the rat P2X4 receptor. The extracellular loop of the hP2X1 receptor was shown to determine antagonist sensitivity and was therefore split into four sections, residues of which were swapped with corresponding residues of the antagonist insensitive rP2X4 receptor and *vice versa*. Sub-chimeras and point mutations were then made to identify particular residues and regions which contribute to antagonist action. These experiments identified two regions important for NF449 binding at the receptor. These are a cluster of four positively charged residues at the base of the cysteine rich head region (136-140) and three residues located just below them (T216, H224 and Q231). An NF449 bound model of the hP2X1 receptor has been generated.

The introduction of the four positively charged residues at the base of the cysteine rich head region to the rP2X4 receptor introduced suramin and PPADS sensitivity to this previously insensitive receptor. This mutation is thought to cause a conformational change which allows the antagonist to bind at residues which are already present in the wildtype receptor. In summary this thesis has advanced the understanding of antagonist action at the hP2X1 receptor and the antagonist insensitivity of the rP2X4 receptor.

## **Publications**

### **Papers**

Allsopp RC, **Farmer LK**, Fryatt AG, Evans RJ (2013) P2X Receptor Chimeras Highlight Roles of the Amino Terminus to Partial Agonist Efficacy, the Carboxyl Terminus to Recovery from Desensitization, and Independent Regulation of Channel Transitions. *J Biol Chem.* 2013 Jul 19;288(29):21412-21.

### **Abstracts**

**Louise K Farmer**, Richard J Evans. The molecular basis of antagonist binding at the P2X1 receptor. *Poster presentation at UK Purines 2011, Cardiff, UK purines 2012, Norwich and Purines 2012 Fukuoka, Japan.*

**Louise K Farmer**, Richard J Evans. The molecular basis of antagonist binding at cardiovascular P2X receptors. *Poster presentation at IUPS 2013, Birmingham, BHF Fellows Meeting 2013, Cambridge and UK Purines 2013 Cambridge.*

### **Prizes**

East Midlands Science and Engineering Prize, June 2013.

## ***Acknowledgements***

Firstly I would like to thank my brilliant supervisor Prof. Richard Evans for his invaluable support, motivation, understanding and sense of humour. Without his vast knowledge, guidance and excellent teaching ability this thesis would not have been possible. He made my PhD a thoroughly enjoyable experience and I feel privileged to have been a part of his lab. I am also very grateful to the British Heart Foundation for funding my project and to all the academic staff who have given me feedback, particularly Dr Steve Ennion and Prof. Martyn Mahaut-Smith. I also owe a massive thank you to Dr Ralf Schmidt for carrying out the modelling and docking work and Dr Louise Fairall for her advice on HEK cell culture and protein purification.

I would also like to thank everyone in the lab for their advice and for teaching me practical skills. A particular thank you goes to Jon Roberts for his instruction in protein purification and to Becky Allsopp for her teaching of molecular biology and importantly for becoming a good friend. I am very grateful to Manijeh Maleki for her weekly oocyte preparation and general lab assistance and to Alistair Fryatt for providing entertainment! My friends in CPP, particularly Alex, Sophie, Kirk, and Harry have also been a huge support both in and out of work.

Another big thank you goes to two friends outside of CPP, Nic and Emily. Thank you for always being willing to celebrate the good times with me and cheer me up in the bad. I would have been lost without our weekly ‘girls-nights’! Also to Cengiz for always being there when needed, usually with a drink in hand!

I would like to say a huge thank you to Matt, without whom I am not sure I would have got through the write up! His encouragement, patience and laughter have been invaluable.

Finally I would like to dedicate this thesis to my parents. I am incredibly lucky to have been raised in such a loving and supportive home. Thank you for supporting every decision I’ve made and for always being at the end of the phone, willing to jump in the car to come and visit. I will be eternally grateful to you both.

## ***Abbreviations***

<b>2-MeSATP</b>	2-methylthio-adenosine-5'-triphosphate
<b>5-BDBD</b>	5-(3-Bromophenyl)-1,3-dihydro-2 <i>H</i> -benzofuro[3,2- <i>e</i> ]-1,4-diazepin-2-one
<b>ACh</b>	Acetylcholine
<b>ADP</b>	Adenosine diphosphate
<b>AIDS</b>	Acquired immunodeficiency syndrome
<b>ANAPP3</b>	Arylazido aminopropionyl ATP
<b>ATP</b>	Adenosine 5' Triphosphate
<b>ATP<sub>90</sub></b>	Concentration of ATP that gives 90% of the maximal response
<b>ATP<sub>low</sub></b>	Concentration of ATP that gives 10-20% of the maximal response
<b>ATP<sub>max</sub></b>	Concentration of ATP that gives a maximal response
<b>bp</b>	Base pairs
<b>Bz-ATP</b>	2'(3')-O-(4-Benzoylbenzoyl)adenosine-5'-triphosphate triethylammonium salt
<b>cAMP</b>	cyclic AMP
<b>cDNA</b>	complementary DNA
<b>CFTR</b>	Cystic fibrosis transmembrane conductance regulator
<b>CHF</b>	Congestive heart failure
<b>CNS</b>	Central nervous system
<b>DAG</b>	Diacylglycerol
<b>DDM</b>	n-dodecyl-β-D-maltopyranoside
<b>DNA</b>	Deoxyribonucleic acid
<b>E. Coli</b>	Escherichia coli

<b>EC<sub>50</sub></b>	Half maximal effective concentration of agonist
<b>EDTA</b>	Ethylenediaminetetraacetic acid
<b>EM</b>	Electron microscopy
<b>GFP</b>	Green fluorescent protein
<b>GPCR</b>	G-protein coupled receptor
<b>G-protein</b>	Guanosine nucleotide binding protein
<b>HEK</b>	Human embryonic kidney
<b>HIV</b>	Human immunodeficiency virus
<b>IC<sub>50</sub></b>	Half maximal effective concentration of antagonist
<b>IP<sub>3</sub></b>	Inositol triphosphate
<b>KO</b>	Knockout
<b>LTP</b>	Long term potentiation
<b>mRNA</b>	messenger RNA
<b>MS222</b>	Tricaine methanesulfonate
<b>MTS</b>	Methanethiosulfonate
<b>MTSES</b>	Sodium (2-sulfonatoethyl) methanethiosulfonate
<b>NA</b>	Noradrenaline
<b>NANC</b>	Non-adrenergic, non-cholinergic
<b>NF023</b>	8,8'-(Carbonylbis(imino-3,1-phenylene carbonylimino)bis(1,3,5-naphthalenetrisulfonic acid)
<b>NF279</b>	8,8'-(Carbonylbis(imino-4, 1-phenylenecarbonylimino-4,1-phenylenecarbonylimino)) bis(1,3,5-naphthalenetrisulfonic acid)
<b>NF449</b>	4,4',4'',4'''-(Carbonylbis(imino-5,1,3benzenetriylbis (carbonylimino)))
<b>NMDA</b>	N-methyl-D-aspartic acid

<b>NRK</b>	Normal rat kidney
<b>NT</b>	Neurotransmitter
<b>OG</b>	$\beta$ -octylglucoside
<b>P5P</b>	Pyridoxal 5'-phosphate
<b>PCR</b>	Polymerase chain reaction
<b>pEC<sub>50</sub></b>	Negative logarithm of the EC <sub>50</sub>
<b>pIC<sub>50</sub></b>	Negative logarithm of the IC <sub>50</sub>
<b>PKC</b>	Protein kinase C
<b>PLC</b>	Phospholipase C
<b>PNS</b>	Peripheral nervous system
<b>polyA</b>	Polyadenylated
<b>PPADS</b>	Pyridoxal-phosphate-6-azophenyl-2', 4'-disulfonate
<b>PSB-12054</b>	N-(benzyloxycarbonyl)phenoxazine
<b>PSB-12062</b>	N-(p-Methylphenyl)sulfonylphenoxazine
<b>RNA</b>	Ribonucleic acid
<b>Rpm</b>	Rotations per minute
<b>SEM</b>	Standard error of the mean
<b>SNP</b>	Single nucleotide polymorphism
<b>TM</b>	Transmembrane domain
<b>TNP-ATP</b>	[2'(3')-O-(2,4,6-Trinitrophenyl)adenosine 5'-triphosphate]
<b>UDP</b>	Uridine diphosphate
<b>UTP</b>	Uridine 5' triphosphate
<b>WT</b>	Wildtype
<b><math>\alpha,\beta</math>-meATP</b>	$\alpha,\beta$ -methylene ATP

## *Contents*

<b>Chapter 1: Introduction .....</b>	<b>1</b>
<b>1.1 ATP as a Signalling Molecule.....</b>	<b>2</b>
<b>1.2 P2Y Receptors .....</b>	<b>5</b>
<b>1.3 P2X Receptors .....</b>	<b>6</b>
<b>1.4 Properties of homomeric P2X Receptors.....</b>	<b>8</b>
<b>1.5 Heteromeric P2X Receptors .....</b>	<b>10</b>
<b>1.6 Physiological Roles of P2X Receptors .....</b>	<b>14</b>
1.6.1 The P2X1 Receptor .....	14
1.6.2 The P2X4 Receptor .....	19
1.6.3 Other P2X Receptor Subtypes.....	24
<b>1.7 Structure of P2X Receptors .....</b>	<b>31</b>
1.7.1 Pre-crystal Insights into Structure .....	31
1.7.2 Visualising the P2X Receptor Structure .....	33
1.7.3 The Crystal Structure of the P2X Receptor.....	34
1.7.4 The Location of the ATP Binding Site .....	37
1.7.5 Movement on Agonist Binding .....	40
<b>1.8 Antagonism at P2X Receptors .....</b>	<b>42</b>
<b>1.9 Antagonists at the P2X1 Receptor .....</b>	<b>42</b>
1.9.1 Suramin .....	43
1.9.2 Suramin Derivatives as Potent and Selective Antagonists.....	45
1.9.3 PPADS.....	47
<b>1.10 Inhibition of the P2X4 Receptor .....</b>	<b>49</b>
1.10.1 Ethanol Inhibits the P2X4 Receptor .....	50
1.10.2 Inhibition of the P2X4 Receptor by Antidepressants .....	51

1.10.3 5-BDBD.....	52
1.10.4 Phenoxazine and Acridone Derivatives as P2X4 Inhibitors.....	53
<b>1.11 Antagonists for Other P2X Receptor Subtypes .....</b>	<b>54</b>
1.11.1 Antagonists at the P2X2 Receptor.....	54
1.11.2 Antagonists at the P2X3 and P2X2/3 Receptors .....	54
1.11.3 Antagonists at the P2X7 Receptor .....	55
<b>1.12 Thesis Aims .....</b>	<b>58</b>
<b>Chapter 2: Materials and Methods .....</b>	<b>59</b>
<b>2.1 Molecular Biology.....</b>	<b>59</b>
2.1.1 WT P2X Receptor Constructs .....	59
2.1.2 Generation of chimeras.....	60
2.1.3 Point Mutations .....	62
2.1.4 Transformation and DNA Extraction .....	63
2.1.5 DNA Sequencing .....	64
2.1.6 mRNA Synthesis.....	64
<b>2.2 Expression in <i>Xenopus laevis</i> oocytes .....</b>	<b>65</b>
<b>2.3 Two Electrode Voltage Clamp Recordings .....</b>	<b>65</b>
2.3.1 Data Analysis.....	66
<b>2.4 Molecular Modelling .....</b>	<b>66</b>
<b>2.5 Protein Purification .....</b>	<b>67</b>
2.5.1 zfP2X4 constructs .....	67
2.5.2 HEK Cell Culture and Transfection .....	67
2.5.3 Membrane Isolation .....	68
2.5.4 Immunoprecipitation.....	69
<b>Chapter 3: Receptor Characterisation and the Contribution of the Extracellular Loop to Antagonism .....</b>	<b>71</b>

<b>3.1 Introduction .....</b>	<b>71</b>
3.1.1 The Use of Chimeras to Investigate P2X Receptor Properties .....	71
3.1.2 P2X Receptor Antagonism and the Extracellular Loop .....	72
3.1.3 Chapter Aims .....	73
<b>3.2 Results .....</b>	<b>73</b>
3.2.1 ATP Potency at WT Receptors .....	74
3.2.2 Time-course of the ATP Evoked Response .....	74
3.2.3 Antagonism at the WT Receptors .....	78
3.2.4 Suramin Action at WT Receptors.....	78
3.2.5 PPADS at WT Receptors.....	82
3.2.6 NF449 at WT Receptors .....	82
3.2.7 Chimeras and Antagonism.....	87
3.2.8 Chimeric Receptors and Suramin .....	88
3.2.9 Chimeric Receptors and PPADS .....	88
3.2.10 Chimeric Receptors and NF449.....	91
<b>3.3 Discussion .....</b>	<b>93</b>
3.3.1 Suramin is a Competitive Antagonist .....	93
3.3.2 NF449 is a Selective Competitive Antagonist .....	95
3.3.3 PPADS is a Non-Competitive Antagonist.....	95
3.3.4 Antagonist Sensitivity Tracks with the Extracellular Loop .....	97
3.3.5 The rP2X4 Receptor is Insensitive to Suramin, PPADS and NF449.....	97
<b>Chapter 4: ATP and Antagonist Action At Large Chimeras .....</b>	<b>99</b>
<b>4.1 Introduction .....</b>	<b>99</b>

4.1.1 Mutagenesis Studies into Suramin and NF449 Action at the P2X1 Receptor .....	100
4.1.2 Mutagenesis Studies into PPADS Action at the P2X1 Receptor.....	104
4.1.3 Chapter Aims .....	105
<b>4.2 Results .....</b>	<b>105</b>
4.2.1 Designing Chimeras.....	105
4.2.2 ATP Action at the hP2X1 Receptor Chimeras .....	109
4.2.3 NF449 Inhibition at the hP2X1 Receptor Chimeras .....	113
4.2.4 Suramin Inhibition at the hP2X1 Receptor Chimeras.....	113
4.2.5 PPADS Inhibition at the hP2X1 Receptor Chimeras.....	115
4.2.6 Generation of Inverse Chimeras X4-BX1 and X4-CX1 ...	119
4.2.7 ATP Action at Chimera X4-BX1 .....	119
4.2.8 NF449 Action at Chimera X4-BX1 .....	119
4.2.9 Suramin Inhibition at Chimera X4-BX1 .....	123
4.2.10 PPADS Inhibition at Chimera X4-BX1.....	123
<b>4.3 Discussion .....</b>	<b>127</b>
4.3.1 The Chimera Method Gives Insight into ATP Potency ....	127
4.3.2 Insight into the Time-course of the ATP Evoked Response .....	129
4.3.3 Insight into NF449 Binding .....	130
4.3.4 The Chimera Method Does Not Remove Suramin or PPADS Binding at the hP2X1 Receptor .....	133
4.3.5 Chimera X4-BX1 Introduced Suramin and PPADS Sensitivity to the rP2X4 Receptor .....	134
<b>Chapter 5: Sub-Chimeras and Point Mutations to Investigate NF449 Action .....</b>	<b>136</b>
<b>5.1 Introduction .....</b>	<b>136</b>

5.1.1 Previous Studies into NF449 Binding and <i>in silico</i> Models .....	136
5.1.2 Chapter Aims .....	138
<b>5.2 Results .....</b>	<b>138</b>
5.2.1 ATP Sensitivity of Chimeras X1-BX4(2+) and X1-BX4(4+) .....	138
5.2.2 Time-course of the ATP Evoked Response of Chimeras X1-BX4(2+) and X1-BX4(4+) .....	141
5.2.3 NF449 Action at X1-BX4 (2+) and X1-BX4(4+) Chimeras .....	142
5.2.4 X1-CX4 Sub-Chimeras .....	145
5.2.5 ATP at the Large X1-CX4 Sub-Chimeras .....	145
5.2.6 NF449 Action at the Large X1-CX4 Sub-Chimeras.....	148
5.2.7 Location of X1-CX4 Small Sub-Chimeras and ATP Sensitivity .....	148
5.2.8 NF449 Sensitivity at the Small Sub-Chimeras .....	150
5.2.9 ATP Action at X1-CX4 Point Mutations.....	153
5.2.10 NF449 Action at X1-CX4 Point Mutations .....	155
<b>5.3 Discussion .....</b>	<b>158</b>
5.3.1 Residues in Regions B and C that Contribute to the Time-course of the ATP Evoked Response of the hP2X1 Receptor.....	158
5.3.2 Residues in Regions B and C that contribute to ATP Sensitivity at the hP2X1 Receptor .....	161
5.3.3 The Positive Residues at Positions 136-140 are Essential for NF449 Antagonism .....	163
5.3.4 Contribution of region C to NF449 sensitivity .....	165

5.3.5 <i>In silico</i> Models of NF449 Binding at the hP2X1 Receptor.....	168
<b>Chapter 6: The Potential for Suramin and PPADS Bound P2X4 Crystal Structures.....</b>	<b>172</b>
<b>6.1 Introduction .....</b>	<b>172</b>
6.1.1 Introducing Antagonist Sensitivity to the P2X4 Receptor	172
6.1.2 The Cysteine Rich Head Region and Antagonist Sensitivity .....	174
6.1.3 Chapter Aims .....	174
<b>6.2 Results .....</b>	<b>175</b>
6.2.1 ATP Action at the rP2X4(2+) and rP2X4(4+) Mutants.....	175
6.2.2 Suramin Inhibition at the rP2X4(2+) and rP2X4(4+) Mutants.....	177
6.2.3 PPADS Inhibition at the rP2X4(2+) and rP2X4(4+) Mutants.....	179
6.2.4 NF449 Sensitivity at the rP2X4(4+) Receptor .....	179
6.2.5 ATP Action at the WT zfP2X4 Receptor .....	182
6.2.6 Suramin and PPADS at the zfP2X4 (FNDAR) receptor ..	184
6.2.7 ATP Action at zfP2X4 (KNKAR) and zfP2X4 (KNKRR) Receptors .....	184
6.2.8 Suramin Inhibition at the zfP2X4 Receptor Mutants.....	187
6.2.9 PPADS Inhibition at the zfP2X4 Receptor Mutants.....	189
6.2.10 Purification of the zfP2X4(KNKRR) Receptor .....	192
<b>6.3 Discussion .....</b>	<b>200</b>
6.3.1 Introduction of the Positive Charges to the Head Region of the P2X4 Receptor had no Impact on ATP Action .....	200
<b>6.3.2 Introduction of the Positive Charges Introduced both Suramin and PPADS Sensitivity .....</b>	<b>201</b>

6.3.3 The Presence of the Four Charges in Other P2X Receptors .....	202
6.3.4 Generation of an Antagonist Bound Crystal Structure ....	203
<b>Chapter 7: General Discussion.....</b>	<b>207</b>
<b>7.1 Regions of the hP2X1 Receptor Contributing to ATP Potency</b>	<b>207</b>
<b>7.2 Regions of the Receptor Contributing to the Time-course of the ATP Evoked Response .....</b>	<b>210</b>
<b>7.3 The Effects of Suramin and PPADS Track Together at Mutated Receptors .....</b>	<b>213</b>
<b>7.4. The Molecular Basis of Antagonism at the hP2X1 and rP2X4 Receptors .....</b>	<b>217</b>
<b>References .....</b>	<b>223</b>

## **Chapter 1: Introduction**

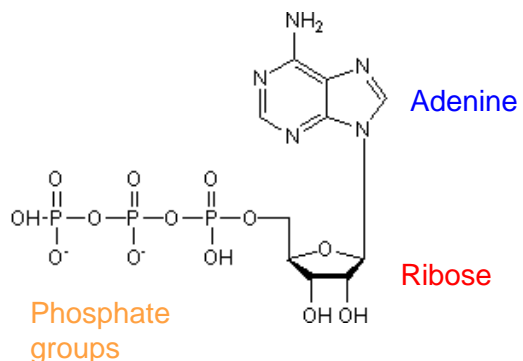
Receptors for extracellular adenosine 5' triphosphate (ATP) were formally proposed by Professor Geoffrey Burnstock in 1972 (Burnstock, 1972). The suggestion that ATP was a neurotransmitter (NT) was met with great scepticism but any uncertainty was answered in the 1990s when ligand gated P2X receptors and G protein coupled P2Y receptors were cloned. This cloning was proof that purinergic signalling existed and defined P2X receptors as a new class of ligand gated ion channel. It is now known that seven subunits of the mammalian P2X receptor exist, which come together to form both homomers and heteromers with widespread expression throughout the body and a variety of physiological and pathophysiological roles. The determination of crystal structures of a P2X receptor in the resting and agonist bound states has been a major advance in the field, providing information on the 3D structure and the location of the ATP binding site. Although agonist binding at the receptor is well defined, there is still a lack of understanding of antagonist action. The aim of this thesis was to further understand the molecular basis of how the antagonists suramin, NF449 and PPADS act at the P2X1 receptor, and to gain insight into how antagonists for the P2X4 receptor could be developed. These antagonists would have strong therapeutic potential in the treatment of a variety of conditions.

In this introduction I will give an overview of the history of the purinergic hypothesis and the properties, expression and physiological roles of the homomeric and heteromeric P2X receptors. An understanding of P2X receptor structure is necessary in order to relate this to function and antagonist action. Receptor structure is therefore described based on both the crystal structure and other mutagenesis and microscopy techniques. Existing antagonists may give insight into how to develop potent and selective novel P2X receptor antagonists and these are discussed at the end of the chapter.

## 1.1 ATP as a Signalling Molecule

The purine ATP was identified in 1929 by Lohmann and Fiske and its first known role was as an intracellular carrier of bioenergy for cell metabolism. The ATP molecule consists of an adenine base, ribose sugar and a tail made of three negatively charged phosphate groups. Energy is released to the cell from the molecule when one of these phosphates is cleaved from the molecule to hydrolyse ATP to adenosine 5' diphosphate (ADP). The structure of ATP is shown in figure 1.1.

(a)



(b)

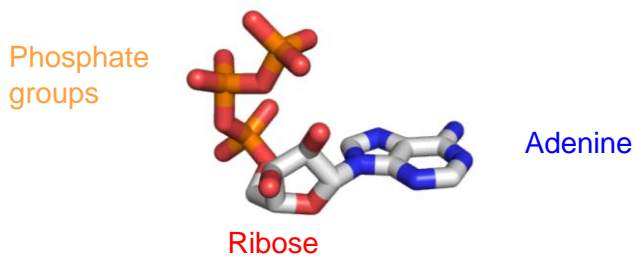


**Figure 1.1 Structure of ATP** (a) Cartoon of ATP structure. The molecule consists of an adenine ring, a ribose and three negatively charged phosphate groups. (b) The structure is also shown in the 3D conformation it takes when bound to the P2X receptor (Hattori & Gouaux, 2012).

The first suggestions that ATP could have an extracellular role as a NT were made by Professor Burnstock in the 1970s. It had been observed that various tissues had a component of the response to nerve stimulation that was not due to release of classical neurotransmitters. When adrenergic and cholinergic transmission was blocked and the nerves innervating the smooth muscle of guinea pig taenia coli were stimulated, hyperpolarisation and

relaxation of the muscle still occurred (Burnstock *et al.*, 1963). This signalling was named non-adrenergic non-cholinergic transmission (NANC) (Burnstock *et al.*, 1964). Excitation of the guinea pig colon also still occurred when cholinergic signalling was blocked (Bennett & Fleshler, 1969). In the guinea pig stomach, blocking adrenergic signalling did not prevent vagal inhibition (Beani *et al.*, 1971). As more and more responses that were neither cholinergic nor adrenergic began to be identified in an increasing number of tissues, a NT that could be responsible for this signalling was looked for.

For a substance to be a NT it must have several characteristics originally described by Jack Eccles (for a detailed review see (Burnstock, 2013)). It must be both synthesised and stored in the nerve terminals and released due to an influx of calcium ( $\text{Ca}^{2+}$ ). It must reproduce the effects of nerve stimulation when applied extracellularly to the tissue, and be inactivated or taken back into the nerve cell after its release. The response to extracellular application of NT and nerve stimulation must both be affected in a similar way by pharmacological agents e.g. antagonists and allosteric modulators. There were several historical studies which suggested ATP may fit these criteria and could be the NT responsible for the NANC signalling. In 1929 ATP and adenosine were injected into dogs and guinea pigs where they caused bradycardia and heart block (Drury & Szent-Gyorgyi, 1929). ATP was also shown to stimulate the superior cervical ganglion of the cat (Feldberg & Hebb, 1948) and injection of spinal root extracts thought to contain ATP and ADP to arteries caused vasodilation (HOLTON & HOLTON, 1954). ATP was subsequently shown to be present in sympathetic nerves in 1958 (SCHUMANN, 1958), and Pamela Holton was the first person to demonstrate the release of ATP from sensory nerves, as both mechanical and electrical stimulation of the great auricular nerves was shown to cause ATP release (HOLTON, 1959). Because of these and several other studies, ATP was investigated as the NT responsible for NANC transmission.

ATP was shown to mimic the actions of NANC transmission in the guinea pig taenia coli (Burnstock *et al.*, 1970). It also caused inhibition in gut preparations that were known to contain inhibitory nerves that were not adrenergic and was therefore suggested to be the NT responsible. With

evidence that ATP fit the criteria described by Eccles, the purinergic hypothesis, that ATP and related molecules could be NTs, was made in 1972 (Burnstock, 1972). The resistance the hypothesis received was mainly because ATP had such a vital intracellular role and it was not thought that a molecule that was so ubiquitous could be a NT. This controversy was fuelled when it was suggested that ATP was a co-transmitter, released alongside noradrenaline (NA) and acetylcholine (ACh) by various nerves, as it was widely considered that one nerve produced one NT (Burnstock, 1976; Westfall *et al.*, 1990)

Despite this, experiments demonstrated ATP co-transmission by sympathetic nerves innervating the guinea pig seminal vesicle, cat nictitating membrane and vas deferens (Nakanishi & Takeda, 1973; Langer & Pinto, 1976; Westfall *et al.*, 1978). Parasympathetic nerves were also shown to co-release ATP, with nerves innervating the urinary bladder releasing both ATP and ACh (Burnstock *et al.*, 1978). It is now known that ATP is a co-transmitter with all major NTs, including GABA, 5-HT, substance P, glutamate, nitric oxide and dopamine (Burnstock, 2009).

Once ATP had been identified as a NT, the receptors responsible for the purinergic response needed to be identified. The wide range of tissues that had shown responses to ATP led to a range of purinergic receptors being described, with initial characterisation based on the pharmacology of the receptors in native tissues. The purinergic receptors were originally divided into two classes, P1 receptors (now generally called adenosine receptors) which were activated by nucleosides and antagonised by methyloxanthines and P2 receptors which were activated by ADP or ATP (Burnstock, 2013). The P2 receptors were later split into two further subclasses based on the potency of agonists and antagonists. These were named P2X and P2Y receptors (Burnstock & Kennedy, 1985). P2X receptors were characterised by their sensitivity to  $\alpha,\beta$ -methylene ATP ( $\alpha,\beta\text{-meATP}$ ) and antagonism by arylazido aminopropionyl ATP (ANAPP3). P2Y receptors were most sensitive to 2-methylthio ATP and showed weak antagonism by ANAPP3. Further properties that allowed P2Y and P2X receptors to be distinguished were identified in

subsequent years, including the selective antagonists 2',3'-O-(2,4,6-trinitrophenyl) adenosine 5'-triphosphate (TNP-ATP) and PPADS for the P2X receptor and reactive blue 2 for the P2Y receptor. The cloning of the first P2Y and P2X receptors in the early 1990s led to a reclassification of the receptors based on their structure (Webb *et al.*, 1993; Lustig *et al.*, 1993; Valera *et al.*, 1994; Brake *et al.*, 1994). P2X receptors were defined as ligand gated ion channels, and P2Y receptors as seven transmembrane domain G-protein coupled receptors (GPCRs). Not only did expression cloning give insight into the structure of the receptors, it also allowed pharmacological characterisation without interference from other receptors present in native tissues.

## 1.2 P2Y Receptors

Before their cloning, P2Y receptors were distinguished from P2X receptors by the rank order of agonist potency, including high sensitivity to analogues of ADP and UTP. P2Y receptors were first expression cloned in 1993 from mouse neuroblastoma cells and a chick whole brain cDNA library (Webb *et al.*, 1993; Lustig *et al.*, 1993). Subsequent cloning identified a family of 8 different subtypes (Burnstock, 2004). They are G protein coupled receptors with seven transmembrane domains and, dependent on their subtype, can be activated by ATP, ADP, UTP, UDP or UDP-glucose. The P2Y<sub>1</sub>, P2Y<sub>2</sub>, P2Y<sub>4</sub> and P2Y<sub>6</sub> receptors are coupled to G<sub>q</sub> proteins, and P2Y<sub>12</sub>, P2Y<sub>13</sub> and P2Y<sub>14</sub> receptors are coupled to G<sub>i</sub>. The P2Y<sub>11</sub> subtype is coupled to both G<sub>i</sub> and G<sub>s</sub> proteins (Burnstock, 2004). The activation of the P2Y receptor subtypes that are coupled to G<sub>q</sub> proteins leads to the activation of phospholipase C (PLC) and generation of the second messengers inositol triphosphate (IP<sub>3</sub>) and 1,2-diacylglycerol (DAG). Activation of the G<sub>i</sub> coupled subtypes leads to a decrease in cyclic AMP (cAMP) by the inhibition of adenylate cyclase. As the P2Y<sub>11</sub> receptor is also coupled to G<sub>s</sub> its activation leads to an increase in cAMP. P2Y receptors have a range of physiological functions in the vascular system, immune system, brain, and bones. They could be targeted in the treatment of a variety of conditions including cystic fibrosis, diabetes and osteoporosis (Erlinge, 2011). P2Y receptors are of particular interest in the cardiovascular system as they are expressed by the endothelium, vascular smooth muscle,

heart, red blood cells and platelets. P2Y<sub>2</sub> receptor activation has been shown to reduce blood pressure making it a possible therapeutic target in hypertension (Rieg *et al.*, 2011). The P2Y<sub>6</sub> receptor has been linked to atherosclerosis (Guns *et al.*, 2010) and the P2Y<sub>1</sub> and P2Y<sub>12</sub> receptors are expressed on platelets and show contributions to blood clotting. The most commonly prescribed anti-coagulant clopidigrel is an antagonist for the platelet P2Y<sub>12</sub> receptor (Savi *et al.*, 2001).

### 1.3 P2X Receptors

The first direct evidence of P2X receptors was their expression cloning in 1994 from the rat vas deferens and rat pheochromocytoma cells (Valera *et al.*, 1994; Brake *et al.*, 1994). These receptors were named P2X1 and P2X2 receptors respectively, and subsequently cloned receptors were named in the order they were discovered. Three subunits come together to make a functional receptor and their trimeric structure means they are distinct from the cys-loop and glutamate classes of ion channel which have five and four subunits respectively. P2X receptors have been shown to form as both homomers and heteromers (North, 2002; Saul *et al.*, 2013). Receptor activation causes an influx of cations, with a particularly high Ca<sup>2+</sup> and sodium (Na<sup>+</sup>) conductance. Cloning has identified a family of seven P2X receptor subunits (P2X1-7) expressed in a wide range of tissues with 35-54% sequence homology between subtypes. There is sequence variation throughout the receptor sequence, however the extracellular loop region of the receptor has the most homology and the intracellular C termini (which show considerable variation in length) the least. The P2X6 subunit is the shortest, consisting of 379 amino acids and the P2X7 receptor is the longest at 595 residues long, these differences in length are largely due to the variation in length of their C-termini (North, 2002). Each subunit has not only a unique sequence, but also a different expression pattern in native tissues and a variant pharmacological profile, characterised by recombinant expression (North, 2002). Recombinant expression allows defined subunit combinations to be characterised that can then be compared to responses in native tissues. It is important that factors such as the recording solutions mimic the physiological environment as much as possible in order to

give physiologically relevant results. The predominant expression of different P2X receptor subunits is summarised in table 1.1, and the properties of different homomeric and heteromeric P2X receptors are discussed below.

<b>Subtype</b>	<b>Location</b>
P2X1	Smooth muscle, platelets, heart, sensory ganglia, cerebellum (Valera <i>et al.</i> , 1994; Scase <i>et al.</i> , 1998; Kidd <i>et al.</i> , 1995)
P2X2	Autonomic ganglia, sensory ganglia, brain, pituitary, retina, smooth muscle (Brake <i>et al.</i> , 1994; Chen <i>et al.</i> , 1995; Vulchanova <i>et al.</i> , 1996)
P2X3	Sensory ganglia, sympathetic neurons (Surprenant, 1996; Chen & Brosnan, 2006)
P2X4	Hippocampus, smooth muscle, microglia, colon, testes (Bo <i>et al.</i> , 1995; Buell <i>et al.</i> , 1996; Soto <i>et al.</i> , 1996a)
P2X5	Skeletal muscle, autonomic ganglia, bladder, gut, heart, spinal cord (Collo <i>et al.</i> , 1996)
P2X6	Autonomic ganglia, brain, skeletal muscle (Collo <i>et al.</i> , 1996; Soto <i>et al.</i> , 1996b)
P2X7	Apoptotic cells, lymphocytes, macrophages, CNS, skin (Surprenant <i>et al.</i> , 1996; Collo <i>et al.</i> , 1997)

**Table 1.1 Expression of the seven P2X receptor subunits in native tissues.**

## 1.4 Properties of homomeric P2X Receptors

Here I will give a summary of some of the properties of different recombinant homomeric P2X receptor subtypes characterised in *Xenopus* oocytes and HEK cells. These features include sensitivity to different agonists and antagonists and the time-course of the response to ATP. Heteromeric receptors are discussed in section 1.5.

In order for a receptor to be activated, the agonist must have affinity in order to bind to the receptor and efficacy to cause a response. The potency of a drug is the concentration needed in order to produce a given effect and is determined by both affinity and efficacy. The physiological agonist at P2X receptors is ATP and the potency of this agonist varies between the receptor subtypes. ATP potency is reported by measuring the concentration needed to cause 50% of the maximum response ( $EC_{50}$ ). The P2X1 and P2X3 receptors have the greatest ATP sensitivity, with  $EC_{50}$  concentrations of ~ 1  $\mu$ M (Chen *et al.*, 1995; Khakh *et al.*, 2001). The P2X2 receptor has been shown to have an  $EC_{50}$  value between 5 and 60  $\mu$ M depending on the expression system, and the P2X4, P2X5 and P2X6 receptors around 10-15  $\mu$ M (Buell *et al.*, 1996; Collo *et al.*, 1996). P2X7 receptors have greatly reduced ATP sensitivity compared to the other subtypes, with an  $EC_{50}$  of ~ 115  $\mu$ M (Surprenant, 1996). The most potent agonist at this receptor is 2'(3')-O-(4-Benzoylbenzoyl)adenosine-5'-triphosphate triethylammonium salt (BzATP). It has recently been suggested that the differences in ATP sensitivity between P2X receptor subtypes may be due to the different effects of divalent cations, particularly magnesium, at the receptors (Li *et al.*, 2013a). A variety of other ATP analogues can cause full or partial activation of different P2X receptors, including  $\alpha,\beta$ -meATP and 2-methylthio ATP (2-MeSATP). The order of potency of these agonists and partial agonists was originally used to define the receptor subtypes. For example  $\alpha\beta$ -meATP has a much higher potency at the P2X1 and P2X3 receptors compared to the other homomeric P2X receptors.

Another property that varies between subtypes is the time-course of the response to a sustained ATP application. During continued ATP application the current decays back toward baseline as the receptor desensitises and is

important in determining temporal signalling. This desensitisation varies between subtypes and has often been used to distinguish between them. As well as having the highest ATP potency, the P2X1 and P2X3 receptors also show the fastest desensitisation. The response to ATP of the P2X1 receptor decays by 50% within 300 ms (Valera *et al.*, 1994). The P2X2, P2X5 and P2X7 receptors are described as relatively non-desensitising, with the P2X2 receptor showing < 15% decay in two minutes (Evans *et al.*, 1996). The P2X4 receptor has a time-course intermediate between these fast desensitising and non-desensitising receptor subtypes (Garcia-Guzman *et al.*, 1997). The variation is due to differences in receptor gating. Gating is the movement in the receptor that is necessary in order for the channel to transition from one state to another. The inactivated receptor is in a resting, closed state, agonist binding causes the receptor to enter an agonist bound, open conformation. Further gating then causes the receptor to move into a desensitised state in the presence of ATP before returning to the resting, closed conformation in the absence of agonist.

Ions can act as allosteric modulators of P2X receptors and have been shown to affect different subtypes in different ways. A decrease in pH, leading to an increase in protons surrounding the extracellular loop of the P2X1 receptor, has been shown to decrease the current by ~ 50% (Stoop *et al.*, 1997). The P2X2 receptor has a greater sensitivity to pH than the P2X1 receptor, with acidification potentiating, and alkalinisation decreasing, the ATP evoked current (Stoop *et al.*, 1997). The P2X2 receptor is the only subtype which shows potentiation at an acidic pH, with all other subtypes being inhibited.

Trace metals can also affect P2X receptor signalling. The P2X1 receptor was inhibited by zinc, which had an IC<sub>50</sub> value of 1 µM. In contrast the P2X3 receptor was potentiated by zinc at low concentrations, with inhibition only being seen at a concentration > 10 µM (Wildman *et al.*, 1999). The presence of physiological concentrations of Mg<sup>2+</sup> has been suggested to alter the activity of the P2X1 – P2X4 receptors, and that in its absence these receptors all have similar potencies to ATP (Li *et al.*, 2013a). Mg<sup>2+</sup> can form a complex with free ATP to form MgATP<sup>2-</sup>. This form of ATP is less effective at activating the P2X2

and P2X4 receptors but shows increased efficacy at P2X1 and P2X3 receptors, accounting for the difference in ATP potency between them *in vivo* and in physiological recording solutions (Li *et al.*, 2013a).

A unique feature of the P2X4 receptor is its sensitivity to an antiparasitic drug called ivermectin (Khakh *et al.*, 1999). Ivermectin is thought to work by decreasing desensitisation and slowing deactivation of the receptor. This subtype is the only one shown to have ivermectin sensitivity and this property has therefore been used to identify this receptor subtype in native tissues. The effects of ions at the P2X receptors is summarised in table 1.2. It was known that other multimeric receptors formed heteromeric as well as homomeric channels and so it was likely that the same was true for the P2X receptor. The expression of heteromers was therefore looked for.

### 1.5 Heteromeric P2X Receptors

It was seen that co-expression of two different subunits led to the formation of a channel with properties distinct from either of the contributing subunits, demonstrating the likely formation of heteromeric P2X receptors (Lewis *et al.*, 1995). More than one P2X receptor subtype is often expressed in the same tissue *in vivo* and this heteromeric expression is an important factor that contributes to variation in P2X receptor properties. Identified heteromers are trimers consisting of a combination of two different subunits only and receptors containing three different subunits have not been identified to date (Saul *et al.*, 2013). Six of the P2X subunits have been shown to form heteromers (P2X1-6). Heteromer formation by the P2X7 subunit has been suggested in some circumstances but existence of P2X7 receptor heteromers *in vivo* is still a point of discussion (Nicke, 2008; Guo *et al.*, 2007; Antonio *et al.*, 2011). When different P2X receptor subunits come together, the heteromer generally has a mixture of properties of the two contributing receptor subtypes. It is usually seen that the receptor with the slowest time-course is dominant in the kinetics of the heteromer, and the heteromer adopts the agonist/antagonist sensitivity of the contributing subunit with the highest potency. For example, the P2X2/3 heteromer has the ATP and TNP-ATP potency of the P2X3 receptor but the time-course of the P2X2 receptor (Spelta *et al.*, 2002). An exception to

this rule is the P2X1/2 heteromer which adopts the fast desensitisation of the hP2X1 receptor (Brown *et al.*, 2002). The properties and physiological roles of known P2X heteromers are discussed below.

(i) P2X1/2

Biochemical studies have shown strong support for a heteromer between P2X1 and P2X2 subunits (Aschrafi *et al.*, 2004) and functional studies have demonstrated that the hP2X1/2 receptor has slightly different properties to the hP2X1 receptor, particularly in the effects of pH on receptor function (Brown *et al.*, 2002). In contrast to the biochemical evidence, there is little indication of the hP2X1/2 heteromer in native tissues despite the fact that subunits are often expressed alongside each other (Burnstock & Knight, 2004). The presence of the P2X1/2 heteromer has however been suggested in mouse sympathetic neurons (Calvert & Evans, 2004).

(ii) P2X1/4

Despite heteromer formation between P2X1 and P2X4 subunits originally thought to be unlikely (Torres *et al.*, 1999), this heterotrimer has been shown to be expressed by *Xenopus* oocytes (Nicke *et al.*, 2005). The receptor has intermediate levels of desensitisation, similar to the P2X4 receptor, but the agonist and antagonist sensitivity of the P2X1 receptor. There is little evidence that this receptor exists in native tissues to date (Saul *et al.*, 2013).

(iii) P2X1/5

There is a lot of evidence supporting the formation of P2X1/5 heteromeric receptors (Le *et al.*, 1999; Torres *et al.*, 1998c). The receptor shows the ATP, suramin, PPADS and NF449 sensitivity of the P2X1 receptor but the TNP-ATP sensitivity and slow desensitisation of the P2X5 receptor (Haines *et al.*, 1999). They have had suggested roles in

excitatory junction potentials in guinea pig arterioles (Surprenant *et al.*, 2000) and the excitability of cortical astrocytes (Lalo *et al.*, 2008).

(iv) P2X2/3

The P2X2/3 receptor is the most extensively characterised P2X heteromer. The receptor has an important role in sensory neurotransmission and is a target for the treatment of pain (Jarvis, 2010). The roles of this heteromer are discussed in section 1.6.3.

(v) P2X2/5

P2X2/5 trimers are expressed in the plasma membrane of human embryonic kidney (HEK) cells (Compan *et al.*, 2012). The properties of this receptor are surprisingly similar to the P2X7 receptor and its activation caused membrane blebbing and phosphatidylserine flip (Compan *et al.*, 2012). It has been suggested that these receptors could be expressed by a variety of tissues in the brain and br3ain stem including the dorsal root ganglion and spinal cord.

(vi) P2X2/6

The P2X6 subunit cannot form homotrimers, but it is co-expressed with the P2X2 receptor subunit and there is biochemical and functional evidence that these receptors can form functional trimers (Saul *et al.*, 2013). Their co-expression has been observed in the thalamus, hypothalamus, pineal gland, carcinoma cells and stem cells (Collo *et al.*, 1996; Resende *et al.*, 2008; Schwindt *et al.*, 2011). Despite this overlapping presence of the two receptor subunits there is no direct evidence that they form heteromers *in vivo*.

(vii) P2X4/6

P2X4 and P2X6 receptor expression overlaps widely in the central nervous system but the function of homomeric and possible heteromeric

receptors in the CNS is not yet known. The P2X4/6 receptor has properties quite similar to the homomeric P2X4 receptor, including potentiation by ivermectin (Le *et al.*, 1998). The receptors did have 3-5 fold increased sensitivity to partial agonists and increased inhibition by PPADS and suramin compared to the P2X4 receptor however (Le *et al.*, 1998).

(viii) P2X4/7

There is controversy over whether the P2X4 and P2X7 subunits can form heteromers or whether the homomeric P2X7 receptor associates with homomeric P2X4 receptors to form a complex (Nicke, 2008; Guo *et al.*, 2007; Boumechache *et al.*, 2009). Although the P2X4 receptor is predominantly intracellular in normal rat kidney (NRK) cells, when it is co-expressed with the P2X7 receptor its surface expression is increased ~ 2-fold, supporting an interaction between the two receptors. The surface expressed receptor also shows sensitivity to ivermectin and TNP-ATP, properties associated with the P2X4 receptor (Guo *et al.*, 2007). Cross-linking studies have shown the P2X7 receptor to interact with both P2X2 and P2X4 receptors but this interaction has been shown to be in the form of homomeric receptors forming a complex, i.e. dimers or trimers (Antonio *et al.*, 2011). Knockout of either the P2X4 or P2X7 receptor has also been shown to affect the expression of the other subunit, but this could be due to the P2X4 and P2X7 genes being located very close to each other and possibly sharing a promoter (Craigie *et al.*, 2013). The P2X4/P2X7 heteromers or complexes have been suggested to have roles in parotid acinar cells and rabbit airway epithelia (Casas-Pruneda *et al.*, 2009; Ma *et al.*, 2006)

The formation of heteromeric P2X receptors increases the variety of properties and roles of this receptor. The expression of these heteromers in native tissues remains to be fully identified, with convincing evidence only existing for the P2X1/5 and P2X2/3 receptors *in vivo*. Characterisation will allow further therapeutic exploitation of the P2X receptor.

## **1.6 Physiological Roles of P2X Receptors**

Many physiological roles of P2X receptors have been identified by their expression profiles and functional properties and these have often been verified by the generation of knockout (KO) mice. Where selective and potent antagonists are available, these have often confirmed these roles. Here I will summarise the known functions of P2X receptors *in vivo*, with particular focus on the P2X1 and P2X4 receptors. These receptors have been chosen as the focus of this thesis for two reasons. The first is their high expression, physiological roles and therapeutic potential in the cardiovascular system, and the second is the difference in properties between them. The P2X1 receptor shows fast desensitisation and is inhibited by the antagonists suramin, NF449 and PPADS. The P2X4 receptor shows much less desensitisation and is insensitive to these antagonists (table 1.2). These differences could be exploited to investigate the molecular basis of antagonist binding and develop novel drugs for the treatment of cardiovascular diseases and conditions.

### **1.6.1 The P2X1 Receptor**

The P2X1 receptor is highly expressed in smooth muscle and is found in a variety of preparations including the vas deferens (from which the receptor was first cloned), arteries and urinary bladder (Valera *et al.*, 1994; Mulryan *et al.*, 2000; Vial & Evans, 2000; Vial *et al.*, 2002). The receptor is expressed by blood cells where it has been found on both platelets and the megakaryocytes which produce them (Vial *et al.*, 1997) (Sun *et al.*, 1998). There have been reports of P2X1 receptors in human lung mast cells, neutrophils and mouse macrophages indicating a role in immune function (Sim *et al.*, 2007; Wareham *et al.*, 2009; Lecut *et al.*, 2009). In the CNS the receptor has been detected in the hippocampus (Cavaliere *et al.*, 2007) and as part of a heteromer with the P2X5 subunit in the cortical astrocytes (Lalo *et al.*, 2008). The widespread expression of the P2X1 receptor means that it contributes to a wide variety of physiological processes which are discussed in detail below.

(i) Fertility

The P2X1 receptor knockout mouse was generated in 2000 and KO males were ~ 90% less fertile than wildtype (WT) mice (Mulryan *et al.*, 2000). The P2X1 deficient mice copulated normally and the sperm was functional, but was absent from the ejaculate so conception could not occur. The P2X1 receptor was known to be present in the vas deferens (Valera *et al.*, 1994), and P2X1 receptor activation in response to sympathetic nerve stimulation was responsible for ~ 60% of the contraction (Mulryan *et al.*, 2000). This contraction propelled sperm into the ejaculate. The residual contraction of the vas deferens was mediated through  $\alpha_1$  adrenoceptors activated by noradrenaline which was co-released with ATP from sympathetic nerves (Mulryan *et al.*, 2000). These findings suggested the P2X1 receptor as a possible target as a male contraceptive. A contraceptive that was 90% effective would not be therapeutically viable, but it has recently been shown that knocking out both P2X1 receptors and  $\alpha_{1a}$  adrenoceptors caused 100% infertility in male mice (White *et al.*, 2013). A potent P2X1 receptor selective antagonist, given in combination with an  $\alpha_{1a}$  adrenoceptor antagonist, could therefore be developed as a non-hormonal contraceptive pill for men. The results also suggest that a potentiator of P2X1 receptor currents e.g. MRS 2219 could be useful to treat sub-threshold male fertility by increasing the amount of sperm in the ejaculate.

(ii) Thrombosis

Haemostasis is a vital process that prevents blood loss after injury. However pathological blood clots (thrombi) in vessels can cause pulmonary emboli, heart attacks and stroke when blood vessels become occluded. Anti-coagulants are used to treat and prevent pathological thrombi, but currently available anti-coagulants have the unwanted side-effect of bruising and bleeding, as physiological haemostasis is also inhibited (Hechler & Gachet, 2011). Therefore an antagonist that binds to a new target in thrombi formation, which did not cause the bleeding phenotype, would have huge therapeutic benefits.

Platelets are blood cells formed from megakaryocytes which are activated and aggregate in primary haemostasis. P2X1 receptors were identified on platelets using patch clamp and polymerase chain reaction (PCR) experiments (Vial *et al.*, 1997; MacKenzie *et al.*, 1996). The agonist  $\alpha,\beta$ -MeATP induced a rapid increase in platelet intracellular calcium that could be blocked by the P2X receptor antagonists PPADS and suramin. The role of the receptor in platelet function was supported by the generation of KO mice. The megakaryocytes from these mice (which are platelet progenitors) had a normal appearance but did not exhibit the rapid inward current in response to ATP (Vial *et al.*, 2002). Simultaneous activation of both P2X and P2Y receptors in the platelet amplified the calcium influx compared to individually stimulating the receptors, suggesting a synergy between these receptors in platelet function (Vial *et al.*, 2002).  $\text{Ca}^{2+}$  influx through the P2X1 receptor has a primary role in the subsequent activation of P2Y receptors.

P2X1 KO mice had normal bleeding times in response to tail snips, showing that the receptor does not play a critical role in physiological haemostasis. Interestingly, the receptors were seen to contribute to pathological clot formation. When thrombosis of mesenteric arterioles was induced by laser injury, less knockout mice died than wildtype (46.6% compared to 87.5%). In a second model where adrenaline and collagen induced thrombosis, P2X1 KO mice formed smaller clots that were easier to dislodge (Hechler *et al.*, 2003). Inhibition of clot formation was greater in smaller diameter vessels such as arterioles, which have high shear rates (Hechler *et al.*, 2003). In support of the role of the P2X1 receptor in thrombosis, overexpression of the P2X1 receptor was seen to cause a mild prothrombotic phenotype, as increased activation of P2X1 receptors caused an increase in clotting (Oury *et al.*, 2003). These findings demonstrated the activation of the P2X1 receptor as an important step in the formation of pathological thrombi but its removal did not prevent physiological clotting.

The generation of KO animals gave insight into physiological roles of the P2X1 receptor, however it is important that these effects can be mimicked pharmacologically in order to show them as a strong therapeutic target. This

was tested by applying the P2X1 receptor antagonist NF449 to WT mice *in vivo*. A concentration of 10 mg/kg NF449 selectively inhibited the P2X1 receptor (Hechler *et al.*, 2005). The mice treated with NF449 had reduced thrombosis and thromboembolism compared to untreated mice. As with the P2X1 receptor knockout mice, no effect was seen on bleeding time (Hechler *et al.*, 2005). This suggests the use of NF449 as a starting molecule in the development of a novel antithrombotic drug that, unlike current therapies, would have minimal bleeding risk. NF449 itself is not suitable for therapeutic use due to its large polyanionic structure (Kennedy, 2013).

(iii) Other Blood Cells

The presence of functional P2X1, P2X4 and P2X7 receptors has been identified in human lung mast cells (Wareham *et al.*, 2009). The role of the P2X1 receptor in mast cell function is thought to be transient with a greater contribution at lower ATP concentrations, and the P2X4 and P2X7 receptors contributing more when the ATP concentration is high (Bulanova & Bulfone-Paus, 2010). Mast cell activation is the first step in allergic reaction, so an understanding of how P2X receptors affect their function could help to treat conditions such as asthma. P2X1, P2X4 and P2X7 receptors have also been identified in mouse macrophages, and the activation of macrophage P2X1 receptors has been linked to cytokine release (Sim *et al.*, 2007; Coutinho-Silva & Persechini, 1997). The presence of P2X1 receptors on neutrophils has also been reported to have a role in chemotaxis (Lecut *et al.*, 2009). Their activation prevented endotaxis by reducing neutrophil function (Lecut *et al.*, 2012). There is a clear role of P2X receptors in immune cells, with a variety of subtypes being expressed. The understanding of how these P2X subtypes contribute to immune cell function could lead to new therapeutic targets.

(iv) Arteries

Sympathetic nerve stimulation of arteries has been shown to cause vasoconstriction *in vivo*, with both ATP and noradrenaline mediated components (Sneddon & Burnstock, 1984). Application of ATP and  $\alpha,\beta$ -MeATP

caused the vasoconstriction of mesenteric arteries in WT mice, but not in the P2X1 KO mouse, showing a role of the receptor in this process. The contraction of KO mouse arteries in response to nerve stimulation was also reduced by ~ 50% (Vial & Evans, 2002). P2X receptors mediated depolarisation and direct  $\text{Ca}^{2+}$  influx, but arteries also contain voltage operated L-type calcium channels which could be activated by depolarisation and be responsible for some of the  $\text{Ca}^{2+}$  influx. When extracellular calcium was removed, vasoconstriction was prevented, but a block of L-type calcium channels had no effect, demonstrating that calcium entry for contraction is occurring directly through the P2X1 receptor (Vial & Evans, 2002). Despite a clear effect on vasoconstriction, the P2X1 KO had no effect on blood pressure and P2X1,  $\alpha_1$ adrenoceptor double KO mice displayed a slight decrease in blood pressure, but no more than knock out of the  $\alpha_1$ adrenoceptor alone (White *et al.*, 2013). The control of blood pressure is a complex process with suggested compensation for a lack of P2X1 receptor function. Therefore the P2X1 receptor is unlikely to be a therapeutic target for hypertension. This also means that P2X1 receptor antagonists for the treatment of other conditions are unlikely to have hypotensive side effects.

(v) Heart Failure

The mRNA of the P2X1 receptor was upregulated in the myocardium of rats with induced congestive heart failure (CHF) compared to sham-operated rats (Hou *et al.*, 1999). In WT rats P2X1, P2Y1, P2Y2, P2Y4 and P2Y6 receptors are expressed in the myocardium, with P2Y6 being expressed at the highest levels. In CHF rats the mRNA levels of both P2X1 and P2Y2 receptors were increased 2.7 and 4.7 fold respectively (Hou *et al.*, 1999). A possible role of the P2X1 receptor in the pathophysiology of heart failure was therefore suggested. However the upregulation of the receptor may be part of a compensatory mechanism that occurs in this disease state and be protective, helping to slow the progression of the disease. The contribution of the P2X1 receptor to heart failure therefore needs to be investigated further to see whether it is contributing to the condition or slowing its progression. This information could be used in the treatment of CHF.

(vi) The Urinary Bladder

The human P2X1 receptor was first isolated from the urinary bladder (Valera *et al.*, 1995). KO mice identified that this receptor subtype had a 30% contribution to parasympathetic nerve evoked contraction (Vial & Evans, 2000), with the remaining 70% mediated by muscarinic acetylcholine (mACh) receptors. The P2X1 receptor is responsible for the initial increase in contractile force, while the mACh receptor determines the length of the contraction (Heppner *et al.*, 2009). It was suggested that the P2X1 receptor may actually be limiting the extent to which the bladder contracts, as in KO mice there was an increase in the force transient (Heppner *et al.*, 2009). Differences in P2X1 receptor expression between rodent and human bladders have been seen. In the healthy human bladder P2X1 expression is low, but in pathophysiological states such as bladder instability and cystitis P2X1 receptor expression is upregulated (Tempest *et al.*, 2004). This suggests that there could be an important role of the P2X1 receptor in human bladder disorders and this could be a therapeutic target in the treatment of such conditions.

(vii) Fast Neuronal – Glial Signalling

ATP plays an important role in signalling between neurons and glia in the CNS, and glial cells express a variety of P2 receptors (Verkhratsky & Steinhauser, 2000). The presence of P2X1/5 heteromers was identified on cortical astrocytes by Lalo *et al* (Lalo *et al.*, 2008). The rapid opening of the P2X1 receptor leads to a  $\text{Ca}^{2+}$  increase in the cell and enables fast signalling between neurons and glia (Palygin *et al.*, 2010). The P2X5 subunit is non-functional in > 95% of the human population and therefore any therapeutic potential of these heteromers is likely to be minimal.

### **1.6.2 The P2X4 Receptor**

The P2X4 receptor was first isolated and cloned in 1995 by Bo *et al* from the hippocampus (Bo *et al.*, 1995). The receptor was also cloned from whole brain and cervical ganglion cDNA libraries shortly after (Soto *et al.*, 1996a; Buell *et al.*, 1996). It is known to be expressed in the central nervous system

(CNS), peripheral nervous system (PNS), epithelial and endothelial cells, reproductive organs and skeletal and smooth muscle cells and often overlaps with the expression of the P2X6 receptor, with which it can form heterotrimers (Collo *et al.*, 1996; Kaczmarek-Hajek *et al.*, 2012). This extensive expression suggests a large number of possible physiological roles of the P2X4 receptor. A lack of antagonists for the receptor has made its characterisation *in vivo* more difficult than for the P2X1 receptor. However P2X4 currents are potentiated by zinc and the antiparasitic drug ivermectin which has been used to distinguish them from other P2X receptors in native tissues (Khakh *et al.*, 1999; Xiong *et al.*, 1999). Known and hypothesised roles and any therapeutic potential of the P2X4 receptor are discussed below.

(i) Pain

Chronic pain is pain which has no physiological or protective benefit and is often extremely debilitating to the person affected. There are two types, inflammatory pain which occurs due to tissue damage and the subsequent inflammatory responses, and neuropathic pain which is felt after injury to a nerve (Trang & Salter, 2012). There are various treatment options for inflammatory pain, however currently available analgesics are often ineffective at treating neuropathic pain (Tsuda *et al.*, 2013). Neuropathic pain occurs after peripheral nerves are damaged due to conditions such as diabetes mellitus, autoimmune disorders, cancer, infections or a traumatic injury (Tsuda *et al.*, 2013). The injury can cause molecular changes that affect the neuronal plasticity and the organisation of pain sensing pathways which leads to an enhancement of pain sensation (Woolf, 2004). Treatments for these pain conditions have often been targeted to neurons, but have been largely ineffective and therefore a new target was looked for (Beggs & Salter, 2010).

Microglial cells are known to migrate to the site of an injury. P2X4 receptors are expressed on microglia and their expression has been shown to be upregulated in the ipsilateral spinal cord and the microglia after injury. A direct role of the receptor was shown when overexpression of P2X4 receptors in rat microglia led to increased pain sensation (Tsuda *et al.*, 2003). Supporting

this, pharmacological block of the P2X4 receptor by TNP-ATP in mice with peripheral nerve injuries caused a reduction in pain behaviours (Tsuda *et al.*, 2003). P2X4 knock-down and knockout animals also did not show increased pain sensation after a peripheral nerve injury (Tsuda *et al.*, 2009). KO mice have reduced brain derived neurotrophic factor (BDNF) and lack prostaglandin E2 (PGE2) in tissue exudates, showing a role of the receptor in the production of both these inflammatory mediators (Ulmann *et al.*, 2008; Ulmann *et al.*, 2010). It has recently been shown that the analgesic effects of morphine act via the P2X4 receptor in a BDNF, K<sup>+</sup>-Cl<sup>-</sup> co-transporter (KCC2) disinhibition cascade between microglia and the spinal dorsal horn neurons, which led to a disruption of Cl<sup>-</sup> homeostasis (Ferrini *et al.*, 2013). The upregulation of the P2X4 receptor on the microglia and subsequent production of inflammatory mediators is therefore a key process in the development of neuropathic pain.

(ii) Regulation of Blood Pressure

The P2X4 receptor is present on endothelial cells and its activation in response to shear stress leads to calcium release from the endoplasmic reticulum (Yamamoto *et al.*, 2000a; Yamamoto *et al.*, 2000b). In WT mice an increase in shear stress causes a dilation of the blood vessel in response to Ca<sup>2+</sup> increase and NO production. When blood flow (and hence shear stress) was increased through a vessel in P2X4 KO mice, no increase in vessel diameter was seen as neither the Ca<sup>2+</sup> increase nor NO production occurred (Yamamoto *et al.*, 2006). Dilation of vessels could still occur in response to acetylcholine (ACh) in these mice. It is therefore thought that the P2X4 receptor transduces changes in shear stress to the interior of the blood vessels via calcium influx, leading to vasodilation. In human patients it has been seen that the inheritance of a Tyr215Cys polymorphism in the P2X4 receptor leads to decreased receptor function, associated with an increased pulse pressure, demonstrating the physiological importance of the P2X4 receptor in control of vasodilation and blood pressure (Stokes *et al.*, 2011). It is known that in disease states which lead to reduced blood flow through vessels, vascular remodelling occurs to permanently decrease vessel diameter (Kamiya & Togawa, 1980). When blood flow was reduced through vessels in a disease

model in P2X4 KO mice this decrease in lumen size was not seen (Yamamoto *et al.*, 2006). This shows a role of the P2X4 receptor in the structural remodelling of blood vessels in disease states. A potent and selective P2X4 antagonist could be used to prevent remodelling of blood vessels in disease states, maintaining a normal diameter of these vessels. This is currently an unmet clinical need.

(iii) Cystic Fibrosis

As well as being expressed by endothelial cells of blood vessels, P2X4 receptors are also present in airway epithelial cells (Ma *et al.*, 2006). In cystic fibrosis the epithelia fail to transport chloride ( $\text{Cl}^-$ ) and water due to the dysfunction of the cystic fibrosis transmembrane conductance regulator (CFTR)  $\text{Cl}^-$  channel, leading to progressive lung disease (Ehre *et al.*, 2014). Activation of epithelial P2X4 receptors increases intracellular calcium which could be useful in the treatment of cystic fibrosis by activating calcium dependent chloride channels and increasing  $\text{Cl}^-$  secretion (Zsembery *et al.*, 2003). Application of ATP and the P2X4 potentiator zinc was seen to restore the  $\text{Cl}^-$  secretion across airway epithelia from human cystic fibrosis patients (Zsembery *et al.*, 2004). This gives a possible treatment option which does not involve the CFTR channels. The full therapeutic potential of P2X4 receptor activation in cystic fibrosis is yet to be explored.

(iv) Heart Failure

P2X4 receptors are expressed in cardiomyocytes where their high calcium permeability contributes to contraction of the heart (Mei & Liang, 2001). Overexpression of the P2X4 receptor in these cells caused an increase in cardiomyocyte contractility in response to 2-meSATP and thereby enhanced the contractile state *in vivo* (Hu *et al.*, 2001). Despite this contribution of the P2X4 receptor to contractility, no cardiac phenotype of the P2X4 receptor KO mice has been reported, however a strong contribution of the receptor in heart failure has been described. The effect of increasing P2X4 receptor expression in models of heart failure was studied. Mice overexpressing the receptor

showed an increased survival in these models (Sonin *et al.*, 2008; Shen *et al.*, 2009). It is not fully understood how the P2X4 receptor exhibits these protective effects but it has been speculated that in states of ischemia or heart failure the receptor could increase the release of vesicular contents, which may include cardioprotective factors such as vascular endothelial growth factor (Yang & Liang, 2012). The cardioprotective effect of P2X4 receptor overexpression makes it a potential target in heart failure research.

(v) Learning and Memory

P2X4 receptors are expressed in the CA1 area of the hippocampus, on the postsynaptic membrane of synapses with Schaffer collaterals (Rubio & Soto, 2001). Calcium influx can lead to a long lasting increase in synaptic strength called long term potentiation (LTP), which is a critical process in learning and memory. The high calcium permeability and location of P2X4 receptors led to their role in LTP being investigated. P2X4 KO mice showed reduced LTP compared to WT mice (Sim *et al.*, 2006) and ivermectin and low concentrations of zinc which potentiate P2X4 receptor currents, were able to cause an increase in LTP in WT mice (Sim *et al.*, 2006; Lorca *et al.*, 2011). The activation and upregulation of P2X4 receptors has also been linked to LTP in the spinal dorsal horn (Gong *et al.*, 2009). It is known that NMDA receptors provide the majority of the calcium influx that leads to LTP, but it is possible that the additional calcium permeability of the P2X4 receptor may fine tune the LTP induced by these NMDA receptors.

(vi) Lysosomes

A unique feature of the P2X4 receptor is its expression within the cell on lysosomal membranes. Proteins are normally degraded by these lysosomes, but the P2X4 receptor is able to be stably expressed in their membrane (Qureshi *et al.*, 2007). The predominant expression of the P2X4 receptor in microglia, vascular endothelial cells and peritoneal macrophages has been shown to be in the lysosomes (Qureshi *et al.*, 2007). The expression of P2X4 receptors is upregulated at the cell surface during lysosome exocytosis,

suggesting that the receptor can traffic out of the lysosome to regulate P2X4 receptor expression. The receptors can also traffic to phagosomes, and are seen to be upregulated after phagocytosis. This upregulation increases currents through the membrane receptors and can contribute to the function of P2X4 receptors in these cell types.

The P2X4 receptor has a wide range of physiological roles and there is therefore a strong therapeutic potential of targeting these receptors. The development of potent and selective antagonists at the receptor would be an important step in gaining further understanding of the therapeutic potential of these receptors.

### **1.6.3 Other P2X Receptor Subtypes**

The P2X receptor family has a diverse expression and range of functions. Although the focus of this thesis is on the P2X1 and P2X4 receptors, a summary of the roles of other P2X receptor subtypes is given below.

#### (i) P2X2 Receptors

The P2X2 receptor was isolated from pheochromocytoma PC12 cells in 1994 and was seen to be very widely expressed throughout the body (Brake *et al.*, 1994). There is particularly high expression of the receptor in the brain, including the basal ganglia, cerebellum, cerebral cortex, diencephalon, mesencephalon, medulla oblongata and the dorsal horn of the spinal cord (Kaczmarek-Hajek *et al.*, 2012). This widespread expression suggests a variety of roles of P2X2 receptors in the CNS which remain to be fully understood, but a contribution of the receptor to fast synaptic transmission in learning, memory, motor function and sensory integration has been identified (Gever *et al.*, 2006). P2X2 receptors have a role in sensory functions including detection of odorants (Spehr *et al.*, 2004). P2X2 deficient mice had no signalling in the gustatory nerves responsible for taste sensation (Finger *et al.*, 2005) and the receptor acts in conjunction with P2X3 receptors to detect taste (Huang *et al.*, 2011). P2X2 receptors have been located in the inner ear of developing and adult mice (Housley *et al.*, 1998). This expression has been seen to be upregulated

in response to sustained loud noise (Wang *et al.*, 2003) however another study reported that this upregulation was only in young mice (Telang *et al.*, 2010). A loss of function of the P2X2 receptor with age has been described, and an SNP in the P2X2 receptor has been linked to age induced hearing loss (Yan *et al.*, 2013).

P2X2 receptor KO animals have given further insight into roles of the receptor. Despite widespread expression of the receptor, P2X2 KO mice had no obvious differences from WT mice in appearance or blood and urine analysis (Cockayne *et al.*, 2005). KO mice did show a decreased peristalsis in the small intestine but not the colon, suggesting that P2X2 action in the mesenteric plexus contributes to peristalsis (Ren *et al.*, 2003; Devries *et al.*, 2010). The KO mice also showed reduced responses of the carotid sinus nerve to hypoxia which in turn affected the ability to mediate ventilatory responses to low oxygen concentrations (Rong *et al.*, 2003). There is currently a lack of potent and subtype selective antagonists for the P2X2 receptor, with generic P2X receptor antagonists such as PPADS and suramin being used in most studies.

(ii) P2X3 and P2X2/3 Receptors

P2X3 receptors and the P2X2/P2X3 heteromers are both sensitive to the agonist  $\alpha\beta$ -meATP but show a difference in the time-course of their responses to ATP. The P2X3 receptor was first isolated from DRG neurons (Chen *et al.*, 1995), and its co-expression with the P2X2 subunit was identified shortly after (Lewis *et al.*, 1995). They are mainly located on the peripheral and central terminals of C-fibers and A $\delta$  sensory afferent fibres, and account for nearly all the response of the dorsal root ganglion to ATP (Burgard *et al.*, 1999). They have an important role in nociception in sensory afferents (Cook *et al.*, 1997). A role of the receptor in pain sensation was illustrated by P2X3 KO mice which displayed highly reduced responses to formalin pain tests and the injection of ATP (Cockayne *et al.*, 2000; Souslova *et al.*, 2000). Increased P2X3 expression has also been shown to contribute to bone cancer pain in rats (Liu *et al.*, 2013). Antagonism of the P2X3 receptor reduced pain behaviour in mice (Jarvis *et al.*,

2004), as did reducing the expression of the P2X3 receptor (Li *et al.*, 2013b). The P2X3 receptor is often expressed alongside the P2X2 subunit *in vivo* and these receptors readily form heteromers. These findings show a strong link between P2X2/3 and P2X3 receptor expression and nociception and suggest that potent and selective antagonists have therapeutic potential in the treatment of pain.

As well as the contribution to nociception, P2X3 deficient mice also had a phenotype of reduced bladder function, with decreased voiding frequency and increased bladder capacity (Cockayne *et al.*, 2000). This is because the absence of the P2X3 receptor of the afferent nerves in the pelvis means the ATP released by the stretching of the bladder is not detected (Cockayne *et al.*, 2000; Vlaskovska *et al.*, 2001). As well as detecting the stretching of the bladder, P2X3 receptors are thought to detect the distension of the ileum, oesophagus and gut (Bian *et al.*, 2003; McIlwraith *et al.*, 2009). This suggests a possible role of the receptor in the perception of fullness or nausea and demonstrates further therapeutic potential of the receptor.

(iii) The P2X5 Receptor

The P2X5 receptor was isolated in 1996 from the rat cervical ganglion and rat heart (Collo *et al.*, 1996; Garcia-Guzman *et al.*, 1996). The receptor is also present in the adrenal gland, kidney, cardiac and skeletal muscle, testis and the central and enteric nervous system (Kaczmarek-Hajek *et al.*, 2012). In humans the receptor shows highest expression in the CNS and immune system (Le *et al.*, 1997). There is currently no P2X5 knockout animal, but > 95% of humans express a non-functional isoform of the receptor, suggesting that it does not have a vital role in human physiology (Kotnis *et al.*, 2010). In rats the P2X5 receptor has been shown to have a role in cell differentiation. It is expressed on satellite cells and promotes differentiation of these cells into muscle fibres (Ryten *et al.*, 2002). It has also been shown to be involved in the differentiation of osteoblasts and epithelial cells, however the fact that the non-functional receptor is predominantly expressed in humans suggests that there is little role of the human receptor in these processes (Hoebertz *et al.*, 2000;

Gayle & Burnstock, 2005). Consistent with a receptor involved in differentiation, P2X5 receptor expression has been identified in various tumour cells. These include prostate cancer and basal cell carcinomas (Calvert *et al.*, 2004; Greig *et al.*, 2003). The expression of the receptor in some cancer cells may make it a therapeutic target.

(iv) The P2X6 Receptor

The P2X6 receptor is the only P2X receptor subtype which does not readily form homotrimers, and it is often expressed alongside P2X2 and P2X4 receptor subunits with which it forms heterotrimers (Kaczmarek-Hajek *et al.*, 2012). It was first isolated from the rat superior ganglion and a rat brain cDNA library (Collo *et al.*, 1996; Soto *et al.*, 1996b). Four splice variants of the human P2X6 receptor have been identified to date (Urano *et al.*, 1997; Nawa *et al.*, 1999) and the highest expression levels of the P2X6 receptor are in skeletal muscle and the brain (Urano *et al.*, 1997). Co-localisation of the P2X6 receptor with P2X2 and P2X4 receptors is seen in the central and peripheral nervous systems (Rubio & Soto, 2001), and the expression of P2X4 and P2X6 receptors has been reported in epithelial cells and the female reproductive system (Collo *et al.*, 1996; Glass *et al.*, 2002). The receptor has been seen to be expressed when muscles are regenerating in a mouse model of muscular dystrophy, suggesting a possible role in this process (Ryten *et al.*, 2004). Its upregulation has also been described in patients with chronic heart failure, although it is not known if this increased expression is causative or protective (Banfi *et al.*, 2005). As with the P2X5 receptor, there is no P2X6 knockout animal, meaning that the full range of functions of the P2X6 receptor remains to be explored and further work remains to be done to identify P2X6 receptor function, particularly in heterotrimers with the P2X2 and P2X4 subtypes.

(v) The P2X7 Receptor

A pore forming receptor that responded to ATP was identified on T-lymphocytes and macrophages and shown to have a role in cytolysis (Di Virgilio *et al.*, 1990; Blanchard *et al.*, 1995). It was originally named as the P2Z

receptor, however a receptor with similar properties was isolated from a rat brain cDNA library and it was shown that the P2Z receptor was a subtype of P2X receptor, named P2X7 (Surprenant *et al.*, 1996). The P2X7 receptor has several unique phenotypes compared to most P2X receptor subtypes. The most potent agonist at this receptor is BzATP, with ATP having a much lower potency than at other subtypes (Surprenant *et al.*, 1996). The pore of the receptor has also been seen to dilate during continued agonist application, allowing larger molecules to move into the cell and is linked with membrane blebbing and cell death (Rassendren *et al.*, 1997b). This pore formation has also been reported in P2X2 and P2X4 receptors (Virginio *et al.*, 1999). The intracellular C-terminal of the receptor is much longer than those of other subtypes and contains a cysteine rich insertion (Surprenant *et al.*, 1996). This region may be responsible for the functional differences of the P2X7 receptor. The receptor is most abundantly expressed on dendritic cells, lymphocytes, macrophages, mast cells and monocytes, all of which are hematopoietic (Collo *et al.*, 1997). It is also present on glial cells in the central and peripheral nervous system and epithelial and endothelial cells (Kaczmarek-Hajek *et al.*, 2012). There have been studies both supporting and disputing the expression of P2X7 receptors on neurons with the presence of P2X7 mRNA and the detection of the P2X7 protein by antibodies having been reported (Deuchars *et al.*, 2001; Ishii *et al.*, 2003). The reason for some groups disputing this is due to the lack of selectivity of the P2X7 antibody, with some antibody binding being reported in P2X7 KO animals (Anderson & Nedergaard, 2006). It is now generally accepted that the antibody was binding to P2X7 splice variants (discussed below) and that neurons do express the P2X7 receptor.

There have been 9 splice variants of the human P2X7 receptor identified to date, which have different properties to the full length P2X7 receptor and contribute to their diverse functions (Cheewatrakoolpong *et al.*, 2005; Feng *et al.*, 2006). The P2X7B variant is prevalent in humans. This receptor has a large deletion in its C-terminus but retains function. A non-functional splice variant has been seen to be expressed in cervical cancer cells and contribute to the dysregulation of cell proliferation (Feng *et al.*, 2006). The various splice variants have caused issues with P2X7 KO mice, with variant

forms of the receptor still functional in the Pfizer and Glaxo mice. The P2X7K splice variant is still present and active in the Glaxo KO mouse (Nicke *et al.*, 2009). Two splice variants have been shown to be present in the spleen and superior ganglion of the Pfizer mouse (Masin *et al.*, 2012). The presence of splice variants in these mice may explain some of the contrasting physiological roles of the P2X7 receptor that have been identified by these mice, discussed later. There are also reports of over 650 single nucleotide polymorphisms (SNPs) in the receptor (Bradley *et al.*, 2011). Some of the SNPs have been linked to diabetes, leukaemia, tuberculosis and mood disorders although they are not always seen in all subjects with these mutations (Ben-Selma *et al.*, 2011; Dao-Ung *et al.*, 2004; Elliott & Higgins, 2004; Lucae *et al.*, 2006).

P2X7 knockout mice have given insight into a variety of roles of the P2X7 receptor. The bones of the KO mice developed abnormally, with a reduction in total bone content, reduced periosteal bone formation and increased trabecular bone resorption in tibias (Ke *et al.*, 2003). Due to these defects the mice had reduced sensitivity to mechanical loading (Li *et al.*, 2005). P2X7 receptors have been located on the osteoclast cells and were identified as a possible target in the treatment of osteoporosis.

P2X7 deficient mice have decreased IL-1 beta cytokine production and little/no inflammatory response after LPS or ATP injection (Solle *et al.*, 2001). When arthritis was induced in these animals the incidence and severity of the disease was reduced in KO mice compared to WT (Labasi *et al.*, 2002). The P2X7 receptor is therefore involved in the activation of leukocytes and the production of IL-1 beta in the inflammatory response. Mice lacking the P2X7 receptor maintain normal responses to nociceptive stimuli, but do not develop the hypersensitivity to mechanical and thermal stimuli seen in inflammatory and neuropathic pain (Chessell *et al.*, 2005). The nerves of human patients who suffer from chronic neuropathic pain have also been seen to have an increased P2X7 receptor expression, consistent with the involvement of the receptor in this process (Chessell *et al.*, 2005). P2X7 receptor selective antagonists decreased neuropathic pain sensation in WT, but not P2X7 KO, rodents and

research is ongoing into a P2X7 receptor antagonist as a treatment for neuropathic pain (Honore *et al.*, 2009; McGaraughty *et al.*, 2007).

There has been particular interest in the P2X7 receptor as a possible target in the treatment of neurodegenerative disease including Alzheimer's, Parkinson's and multiple sclerosis (MS) (Sanz *et al.*, 2009) (Hracsiko *et al.*, 2011). This is due to the upregulation of the receptor in both animal models of, and human patients with, these diseases. In Huntingdon's disease this upregulation has been shown to contribute to the death of neurons in cellular and mouse models of the disease, and this effect was inhibited by a P2X7 receptor antagonist (Diaz-Hernandez *et al.*, 2009). P2X7 receptor antagonists also have therapeutic potential in spinal injury as recovery was improved after increasing their expression (Peng *et al.*, 2009). The contribution of the P2X7 receptor to the pathology of MS is unclear. This is partly due to different strategies for the generation of P2X7 KO mice. In the Glaxo P2X7 KO mouse, the P2X7K splice variant is still functional. Studies on the brain of the Pfizer mouse have detected the presence of a P2X7 receptor splice variant. The Glaxo KO mouse strain had a reduction in the occurrence of multiple sclerosis in a model of the disease compared to WT mice, and antagonism of the receptor reduced MS symptoms (Sharp *et al.*, 2008) (Matute *et al.*, 2007). However the Pfizer P2X7 KO mouse had an enhancement of MS symptoms compared to WT, questioning the role of the receptor in the disease state (Chen & Brosnan, 2006). Similarly the activation of the P2X7 receptor has been seen to both prevent and enhance Parkinson's disease in rodent models. Studies have shown therapeutic benefits of application of a P2X7 receptor antagonist which prevented the loss of dopamine nerve cells (Hracsiko *et al.*, 2011; Marcellino *et al.*, 2010) and reduced neurotoxicity (Carmo *et al.*, 2014). However it has also been shown that the P2X7 receptor is neuroprotective and its depletion advances the progression of the disease (Hracsiko *et al.*, 2011). The differing proposed roles of the P2X7 receptor in these diseases may be due to the splice variants present in the KO mice. The full role of the P2X7 receptor in neurodegenerative disease therefore remains to be understood.

The P2X7 receptor has been shown to have a possible role in cancer with links to tumour metastasis (Jelassi *et al.*, 2011) and breast cancer (Jelassi *et al.*, 2011; Huang *et al.*, 2013). Research into the P2X7 receptor as a drug target has recently been advanced by the development of potent and selective antagonists for the receptor, which will be discussed later. However there are large differences in P2X7 receptor expression and pharmacology between species, meaning that information gained in rodent models may not be relevant in humans.

It has been demonstrated that the homomeric and heteromeric P2X receptors have a vast expression, with almost every tissue in the body expressing at least one P2X receptor subtype. This broad expression leads to a huge variety of proven and potential roles of the P2X receptor *in vivo* which in turn demonstrates a strong therapeutic potential of P2X receptor targeted drugs. In order to deduce the molecular basis of the differences in properties between the receptor subtypes it is first necessary to understand P2X receptor structure and how this relates to function.

## 1.7 Structure of P2X Receptors

### 1.7.1 Pre-crystal Insights into Structure

The P2X receptor subtypes do not share sequence homology with any other known ion channels or proteins. Following initial cloning, experiments were performed to establish the topology of the receptor. Two regions of hydrophobicity were identified in each subunit, and it was proposed that the subunits consisted of two transmembrane domains (Valera *et al.*, 1994; Brake *et al.*, 1994). The N terminal did not contain a leader signal peptide, suggesting that it was intracellular (Brake *et al.*, 1994). It was also shown that antibodies that recognised N and C terminal sequences of the P2X receptor could only bind if the cells had been permeabilised (Torres *et al.*, 1998b; Torres *et al.*, 1998a). Glycosylation is a post-translational modification that adds sugars to asparagine residues in the extracellular portion of P2X receptors. N-linked glycosylation sequences are present in the loop of the receptor and their glycosylation assists with protein folding and trafficking (Torres *et al.*, 1998a).

The P2X receptor was therefore predicted to have intracellular N and C termini with two transmembrane domains and a large extracellular loop (figure 1.2a). This identified it as being structurally distinct from receptors in the existing cys-loop and glutamate ligand gated ion channel families which have four and three transmembrane domains respectively. The receptor does share a topology with the acid sensing ion channels (ASICs) and the inward rectifying potassium channel but the lack of sequence homology with these channels means the P2X receptor forms its own class of ligand gated ion channel (Nichols & Lopatin, 1997; Saugstad *et al.*, 2004).

It is unlikely that a receptor pore would form from two transmembrane domains (i.e. a single subunit) and so multimeric assembly of the P2X receptor was looked for. The concentration response curve of the P2X receptor of rat and bullfrog sensory neurons had a Hill coefficient of ~3, suggesting that 3 molecules of ATP were required for its opening (Bean *et al.*, 1990). This led to speculation that the receptor formed as a trimer, with each subunit containing an ATP binding site. Co-expression of two separate P2X subunits also led to the generation of a novel phenotype, suggesting that at least two subunits were coming together to form a multimer (Lewis *et al.*, 1995). Cross linking and blue native page gels were used to show that the receptor formed a trimer (Nicke *et al.*, 1998).

Mutagenesis studies contributed to the understanding of P2X receptor tertiary structure. There are 10 conserved cysteine residues located in the extracellular loop of all mammalian P2X receptors (Ennion *et al.*, 2000; Clyne *et al.*, 2002). These were predicted to form 5 disulphide bonds which are involved in the trafficking of the receptor to the cell surface and contribute to the protein structure (Clyne *et al.*, 2002; Ennion & Evans, 2002a). The loop region also contains several conserved residues important for ATP potency that were predicted to form part of an extracellular ATP binding pocket. The location of this pocket and the residues which contribute it are discussed in more detail below.

The intracellular portions of the P2X receptor have been shown to have various roles in the control of receptor time-course and trafficking. The N terminus contains a consensus sequence for protein kinase C (PKC), mutation of which has been shown to be involved in the time-course kinetics of the P2X1 and P2X2 receptors (Ennion & Evans, 2002b; Boue-Grabot *et al.*, 2000). The carboxy terminus contains a YXXXXK motif that is conserved in all subunits. The sequence is located next to the second transmembrane domain in all subunits apart from in the P2X7 receptor where there are 18 amino acids in between TM2 and this sequence. It is responsible for stabilising the surface expression of the P2X receptor (Chaumont *et al.*, 2004).

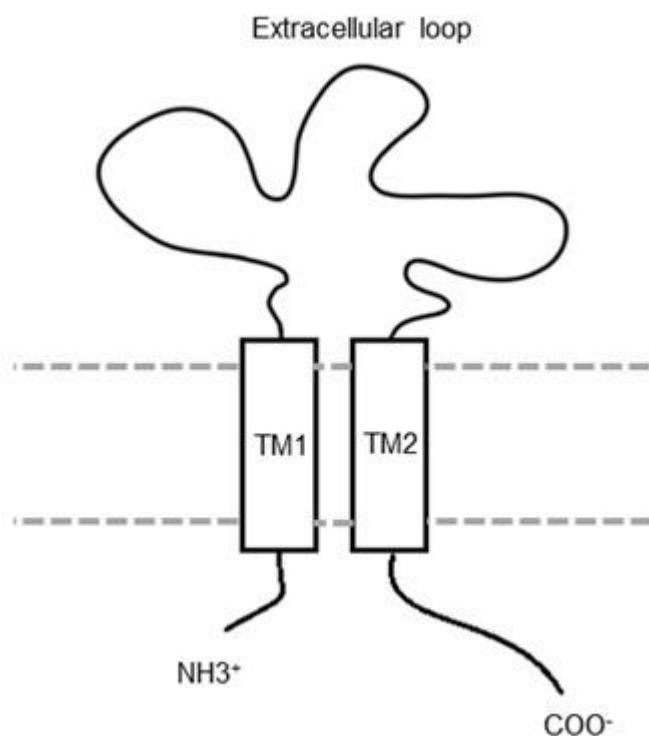


**Figure 1.2 Structure of the P2X Receptor Subunit.** Basic cartoon representation of an individual subunit showing the intracellular N and C termini, transmembrane domains and large extracellular loop.

### 1.7.2 Visualising the P2X Receptor Structure

The first 3D information on the structure of P2X receptors came from atomic force microscopy (AFM) and electron microscopy (EM) experiments. AFM allows visualisation of the topology of an isolated protein and showed that

the P2X receptor formed as a trimer (Barrera *et al.*, 2005). EM of the P2X2 receptor showed that the structure of this receptor resembled a pyramid with a crown cap (Mio *et al.*, 2005). Another EM study likened the P2X4 receptor to a torpedo, with the ectodomain taking a similar shape to a propeller (Young *et al.*, 2008). These experiments were performed on full length WT receptors and therefore provide information on the structure of P2X receptor intracellular termini that was not obtained from later crystallisation of the receptor. FRET experiments have predicted that the C-terminal tails of the P2X4 receptor were 5.6nm apart, and labelling of these termini with gold particles predicted that the distance between them was 6.1 nm, suggesting that these predictions are reasonably accurate (Young *et al.*, 2008).

In 2009 the first P2X receptor crystal structure was produced, and this was followed by two further structures in 2012 (Hattori & Gouaux, 2012; Kawate *et al.*, 2009). These studies have given valuable insight into the 3D structure of the receptor, allowing it to be visualised at high resolution for the first time. Below I will give an overview of the structure of P2X receptors, with emphasis on the crystal structure but also drawing on previous mutagenesis studies.

### 1.7.3 The Crystal Structure of the P2X Receptor

The crystallised receptor was a truncated form of the zebrafish P2X4.1 (zfP2X4.1) receptor in its closed, resting state (Kawate *et al.*, 2009). In 2012 this structure was refined, increasing the resolution and an additional structure was produced in an agonist bound state (resolutions of 2.9 and 2.8 Å respectively) (Hattori & Gouaux, 2012). The structures were consistent with predictions made in many mutagenesis and biochemical experiments which had been performed before the crystal was available (Young, 2010).

The zfP2X4 receptor was chosen after extensive screening of many different P2X receptor subtypes as it was seen that the zfP2X4 receptor formed stable trimers in crystallisation conditions (Kawate *et al.*, 2009). A variety of different mutants of this receptor were screened to identify which allowed crystal formation. The mutant that was crystallised was zfP2X4-C which had N and C termini truncations. 26 residues were removed from the N terminus, and

6 from the C terminus. There were also three point mutations made C51F, N78K and N187R, the latter two were to remove glycosylation sites (Kawate *et al.*, 2009). These mutations were predicted to have minimal effects on receptor structure compared to the WT receptor.

Crystallisation allowed visualisation of the 3D structure of the receptor and showed the interlocking nature of the three subunits. Each individual subunit was described as having a dolphin-like shape, with the extracellular domain forming the upper body, and the transmembrane domains forming the fluke (Kawate *et al.*, 2009) (figure 1.3a). The upper body could be further split into the head, body, right flipper, left flipper and dorsal fin sections. The truncation of the intracellular termini meant that information on their structure could not be obtained. Three of these subunits were present in the functional receptor.

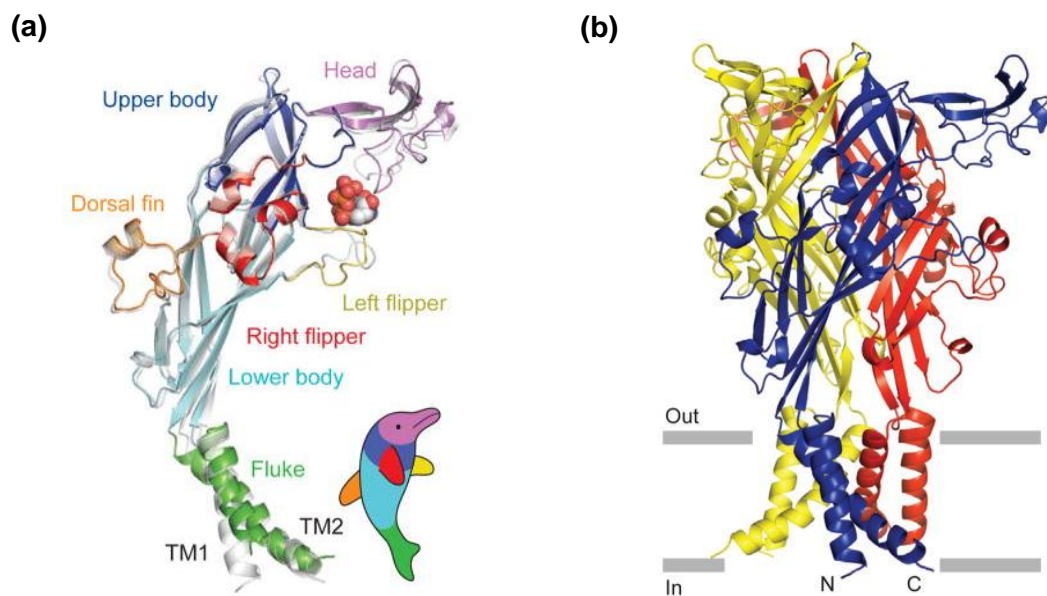


**Figure 1.3** (a) Structure of an individual zfP2X4 subunit. The structure has been compared to a dolphin, with head, body, left flipper, right flipper, dorsal fin and fluke regions. (b) Structure of a trimeric P2X receptor. Each subunit wraps around the one to its right. Taken from (Hattori & Gouaux, 2012).

The trimeric P2X receptor forms a chalice shape containing four vestibules, the intracellular, extracellular, central and upper vestibules (Hattori

& Gouaux, 2012). The extracellular domain extends ~ 70 Å above the membrane and the loop of each subunit twists around the neighbouring subunit to the right (figure 1.3b). The interfaces between subunits form mainly in the extracellular domain, with minimal contact occurring at the transmembranes. The three main points of contact for the subunits are between the bodies, the head and the body and the left flipper and dorsal fin of two subunits. Of these regions, only the body has a high level of conservation between different P2X receptor subunits and therefore amino acid differences at other subunit interfaces may allow for some of the variations in properties between the receptor subtypes. Within the extracellular region were five disulphide bonds which formed between ten cysteine residues and had been predicted in previous mutagenesis studies (Clyne *et al.*, 2002; Ennion & Evans, 2002a). Three of these bonds formed between six cysteine residues in the head region of the receptor. A further disulphide bond was located at the bottom of the body, and one was located at the dorsal fin (Kawate *et al.*, 2009; Young, 2010).

The transmembrane domains are approximately 28 Å long and twisted to the left within the membrane in the unbound state with the second transmembrane domains crossing over one another, allowing a mechanism of closing the pore of the channel (figure 1.3b). TM2 lined the pore of the receptor, as had been predicted (Li *et al.*, 2008; Rassendren *et al.*, 1997a). Ion access through the pore region was blocked by a run of hydrophobic residues in this closed state, with the narrowest part of the pore at alanine 344. Using the original crystal structure, two possible pathways for ion access to the pore were put forward by Kawate *et al.* The first was that ions entered through three lateral fenestrations which were located immediately above the transmembrane domains and were up to 8 Å in diameter, wide enough to allow ion access. The second possible pathway was from the apex of the extracellular domain, along the axis of symmetry through the upper and central vestibule. In the closed state the pathway was too narrow for ions to pass through, but it was postulated that the diameter could increase with conformational changes upon ATP binding, allowing ion flow. The open structure allowed the ion access pathway to be deduced (Hattori & Gouaux, 2012). It was seen that only the lateral fenestration pathway, located above the pore, was wide enough to allow

ions to enter in the ATP bound state. Ion entry through these lateral fenestrations was supported by cysteine mutagenesis studies (Kawate *et al.*, 2011; Samways *et al.*, 2011).

The crystal structures were supported by previous mutagenesis studies and function in response to ATP was retained at the mutated zfP2X4 receptor, demonstrating that ATP could still bind. This suggests that the changes to structure due to the mutations introduced are not likely to be extreme and it can therefore be assumed that the crystallised receptors are a good representation of the WT (Young, 2010; Silberberg & Swartz, 2009). Despite this it is important to remember that the mutations made will have introduced some differences compared to WT, the most important of these being the truncation of the intracellular termini, as no structural information could be obtained for these. There have also been questions raised about the accuracy of the structure of the transmembrane domains. Experimental data has shown that upon ATP binding there must be a large amount of movement in the inner part of the TM2 helices, which was not seen in the crystal structure (Jiang *et al.*, 2013). Previous studies had also suggested that residues D349 and V343 must be accessible to ions flowing through the pore, but this was again not seen in the ATP bound structure (Kracun *et al.*, 2010; Li *et al.*, 2010). These discrepancies could be due to the truncation of the intracellular regions of the crystallised receptor, or these residues may be accessible in another activation state that is yet to be crystallised.

#### 1.7.4 The Location of the ATP Binding Site

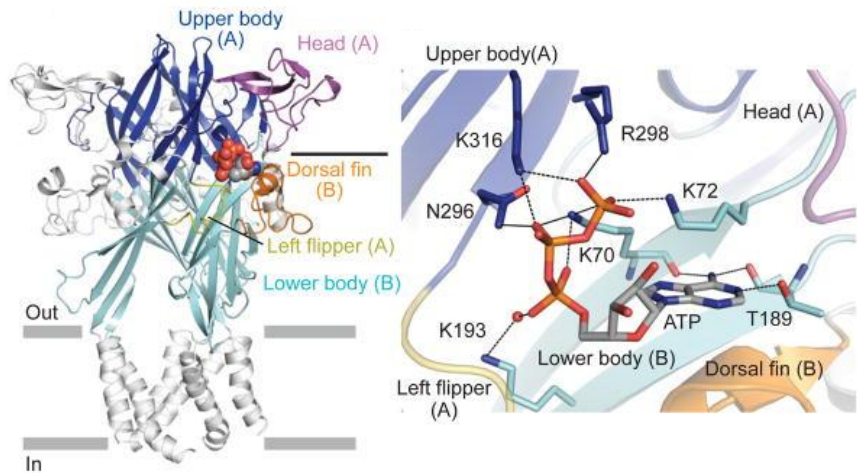
Although ATP is the physiological agonist at P2X receptors, when the receptors were cloned it was seen that they did not contain a classical motif for ATP binding such as the Walker motif (Walker *et al.*, 1982). Therefore it was likely that the P2X receptor contained a novel ATP binding pocket, distinct from other ATP binding proteins. As all P2X receptor subtypes are activated by ATP it was probable that the binding site consisted of residues conserved between all subunits. Mutagenesis of the conserved residues was performed to identify where ATP was binding at the P2X receptor. The residues identified as being involved in binding the negative charge of ATP (P2X1 numbering) were Lys 68,

Lys70, Arg292 and Lys309 (Ennion & Evans, 2002a; Jiang *et al.*, 2000)(Ennion *et al.*, 2000). The aromatic residues Phe185 and Phe291 were also thought to be involved in agonist action (Roberts & Evans, 2004), along with the polar amino acids Thr186 and Asn290 (Jiang *et al.*, 2000; Roberts & Evans, 2006). Nicke *et al* predicted that the binding site formed by these residues was formed at the interface between two subunits of the receptor (Marquez-Klaka *et al.*, 2007; Marquez-Klaka *et al.*, 2009).

When the receptor was first crystallised in the absence of ATP, it was seen that all these predicted residues lined a pocket that formed between two adjacent subunits (Kawate *et al.*, 2009). Residues Lys70, Lys72, Phe188 and Thr189 were located on one subunit (zfP2X4 numbering) while residues Asn296 Phe297, Arg298 and Lys316 were on the second subunit. There are three of these sites in the trimeric structure, and using the dolphin analogy, they are made up of the head and body domains, left flipper and dorsal fin. (Kawate *et al.*, 2009). The residues were positioned too far apart for the ATP molecule to interact with all of them in this resting state, however it was thought that on agonist binding conformational changes in the receptor would bring the residues closer together to enable strong interaction/binding. The first crystal structure therefore supported the findings of many mutagenesis studies and identified the probable location of ATP binding.

Definitive proof of the location of the ATP binding site was obtained when the zfP2X4 receptor was crystallised in the agonist bound state. The orientation of the bound ATP molecule could also be seen (figure 1.4a) (Hattori & Gouaux, 2012). The structure confirmed that the ATP pocket predicted in 2009 was the location of ATP binding and was located ~ 40 Å from the boundary between the extracellular loop and transmembrane domains. A surprising finding was that the ATP molecule was in an unusual conformation, making a 'U' shape (Hattori & Gouaux, 2012). Lys70 (Lys68 P2X1 numbering) was seen to make various important interactions with the ATP molecule, the centre of the ATP molecule was positioned above this residue, allowing for interactions with the oxygen atoms of α, β, and γ phosphate groups of the ATP

**(a)**



**(b)**

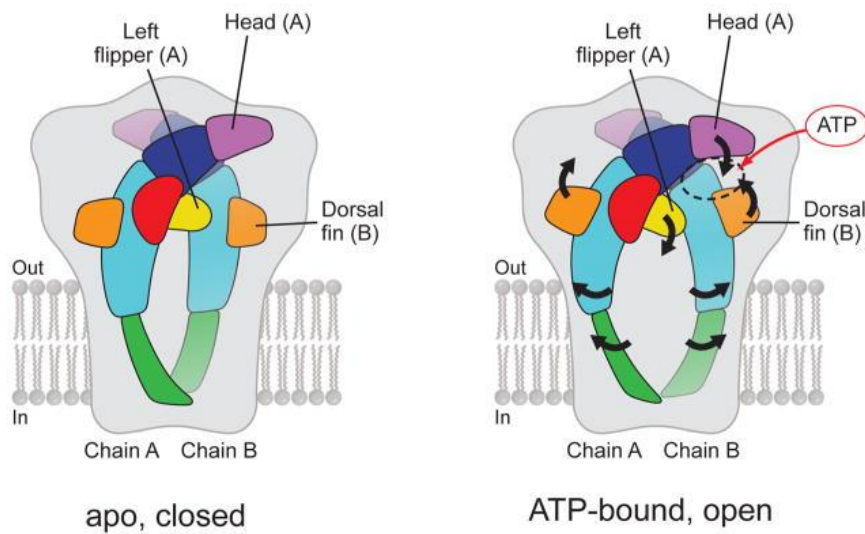


**Figure 1.4 Location of the ATP Binding Site and Movement Upon ATP Binding**

**(a)** Location of the ATP binding site of the zfP2X4 receptor. Residues which interact with the ATP molecule are labelled **(b)** Movement of the P2X receptor upon ATP binding. Arrows represent the direction of movement. Taken from (Hattori & Gouaux, 2012).

molecule (figure 1.4a). The  $\beta$  phosphate formed additional interactions with Asn296 and Lys316 (Asn290 and Lys309 P2X1 numbering) and the  $\gamma$  phosphate also interacted with Lys72, Arg298 and Lys316 (Lys70, Arg292 and Lys309 P2X1 numbering). The adenine ring of the ATP molecule was buried further into the pocket, where it formed interactions with the side chain and oxygen atoms of Thr189, and with the oxygen atoms of Lys70 (Thr186 and Lys68 P2X1 numbering) (Hattori & Gouaux, 2012). No interactions were identified with the phenylalanine residues corresponding to Phe185 and Phe291 in the P2X1 receptor, suggesting that they may be involved in transducing ATP binding through the receptor, rather than recognising the ATP molecule itself. Hydrophobic interactions were seen with residues Leu191 and Ile232. These residues show a conservation of hydrophobicity between P2X receptor subtypes and are the equivalent to residues Leu191, Leu186 of the rat P2X2 receptor had previously been identified as contributing to ATP binding (Jiang *et al.*, 2011). The crystallisation therefore verified numerous mutagenesis studies that had been performed previously, demonstrating the success of structure function mutagenesis as a technique in understanding molecule binding when a crystal structure is not available.

### 1.7.5 Movement on Agonist Binding

A comparison of the agonist bound and unbound crystal structures demonstrated substantial movement of the receptor on ATP binding (figure 1.4b) (Hattori & Gouaux, 2012). At the ATP binding site the left flipper moved out to allow agonist binding. The dorsal fin moved upward, and the head region downward, to close the protein around the ATP molecule. This was similar to the movement predicted by Kawate *et al* and brought the residues involved in ATP binding close enough together to allow all the residues to interact with the ATP molecule (Hattori & Gouaux, 2012). This tightening of the P2X receptor around ATP has also been described by Jiang *et al* (Jiang *et al.*, 2012). Binding leads to movement in the rest of the receptor. Using the dolphin analogy, most movement was seen in the lower body, which flexed outwards, increasing the size of the extracellular vestibule by  $\sim 10 \text{ \AA}$ . This in turn caused the transmembrane domains to also move outwards, opening the pore of the

receptor and allowing the flow of ions into the cell. This movement in the transmembranes was described as iris-like. Of the two transmembranes, TM2 displayed the most movement, rotating by ~ 55° anticlockwise and forming a kink at position Gly350. This residue had previously been predicted to form a hinge in TM2 (Fujiwara *et al.*, 2009). TM1 showed less movement, with a rotation of 10° in the same direction. It was the movement of both TM domains combined that caused an expansion of the pore. This was now seen to be uninterrupted, with the narrowest part ~7 Å, wide enough to allow ion flow. The importance of the movement of the transmembrane domains has recently been demonstrated by the activation of P2X receptors by photoswitchable ligands, in the absence of an agonist (Lemoine *et al.*, 2013). It was shown that P2X2 and P2X3 receptors could be activated by conformational changes in the light activated ligand 4,4'-bis(maleimido)azobenzene which had been attached to the end of the second transmembrane domain. These currents imitated those produced by ATP binding (Browne *et al.*, 2014). Photoactivation of propyl-methanethiosulfate (MTS) that had been covalently attached to the end of the second transmembrane domain in the absence of agonist has been shown to have similar effects as conformational changes in the activated ligand force the TMs apart (Rothwell *et al.*, 2014). This again caused the activation of the channel as effectively as ATP binding and the properties of the MTS induced current were similar to ATP induced current, showing that movement in the transmembranes can lead to channel gating.

The generation of the crystal structures was an important advance in the understanding of P2X receptor structure, proving the location of agonist binding and showing two conformations that the receptor adopts. These crystal structures however are only single molecular snapshots of the receptor and it is likely that additional conformational states exist. The conformation of the intracellular termini, and any effect the presence of these structures may have on the extracellular portion of the receptor, also remains to be seen. An important question that the crystallised receptor has not answered is how antagonists are binding at the P2X receptor. The only receptor subtype which has been successfully crystallised so far, the zfP2X4 receptor, is insensitive to commonly used antagonists. In order to obtain an antagonist bound structure,

mutations need to be introduced to the zfP2X4 receptor which induce antagonist sensitivity, or another antagonist sensitive P2X receptor subtype needs to be crystallised. Our current understanding of how antagonists are acting at the P2X receptor therefore comes from mutagenesis studies.

### **1.8 Antagonism at P2X Receptors**

Antagonists are drugs which have affinity to bind to a receptor but no efficacy in order to activate it. Antagonists are an important research tool in the understanding of receptor function and the P2X receptor field has historically been disadvantaged by the lack of potent and subtype selective antagonists for different subtypes. Most prescribed medications are antagonists and there is a lot of evidence that the inhibition of P2X receptors could have strong therapeutic potential. This highlights the importance of the development of potent and selective P2X receptor antagonists. An understanding of how existing P2X receptor antagonists work at the receptor can assist in this development. Recently, antagonists with good potency and selectivity at some receptor subtypes, particularly P2X3 and P2X7 receptors, have begun to become available, and some of these drugs have been entered into clinical trials. However a lot of work remains to be done in the development of potent and selective P2X receptor antagonists.

Here the focus will again be at the P2X1 and P2X4 receptors which have been demonstrated to have therapeutic potential in the treatment of several cardiovascular conditions, and also have a marked difference in antagonist sensitivity. There are several P2X1 receptor antagonists, but the P2X4 receptor is often insensitive to these drugs, even at high concentrations. The contrast in antagonism between these two receptors can be exploited in further studies to gain valuable insight into how these existing antagonists are binding at the receptor.

### **1.9 Antagonists at the P2X1 Receptor**

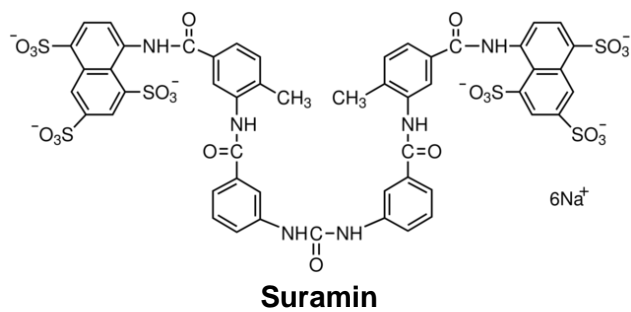
There are a variety of antagonists at the P2X1 receptor, but the ones most commonly used are suramin, PPADS and NF449. Suramin and PPADS are fairly non-selective between P2X receptor subtypes, but NF449 is potent

and selective for the P2X1 receptor. These three antagonists, along with two other suramin derivatives, are described below.

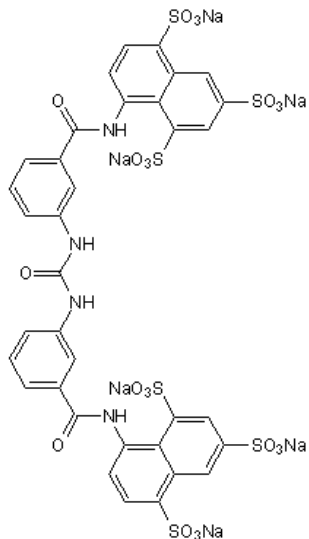
### 1.9.1 Suramin

Suramin (8-[4-methyl-3-{[3-({[3-(2-methyl-5-[(4,6,8-trisulfo-1-naphthyl) carbamoyl] phenylcarbonyl) phenyl] carbamoyl} amino)-benzoyl] amino}-benzoyl amino] naphthalene-1,3,5-trisulfonic acid) is a polysulphonated derivative of urea that was developed in the early 20<sup>th</sup> century as an anti-protozoal drug for the prevention of conditions such as sleeping sickness (Fourneau, 1924). After its discovery, it was widely used in Africa to treat the early stages of human trypanosomiasis (Voogd *et al.*, 1993). The effects of suramin at other proteins, viruses and enzymes were subsequently investigated and it was shown to be an inhibitor at various targets. These include enzymes involved in carbohydrate breakdown (TOWN *et al.*, 1950), lysozymes (LOMINSKI & GRAY, 1961), Na-K-ATPase (Fortes *et al.*, 1973), Mg<sup>2+</sup>-ATPase (Smolen & Weissmann, 1978), and melanoma heparanase (Nakajima *et al.*, 1991). The interest in suramin as a possible therapeutic drug peaked after it was shown to block the reverse transcriptase of RNA tumour viruses (De Clercq, 1979). Suramin was entered into clinical trials as a treatment for Acquired Immunodeficiency Syndrome (AIDS) after it was discovered that it could block the human immunodeficiency virus (HIV) in vitro (Mitsuya *et al.*, 1984; Cheson *et al.*, 1987). However these trials were unsuccessful and a variety of toxicities were reported (Kaplan *et al.*, 1987). A similar scenario was seen for the use of suramin in cancer treatment where various clinical trials were performed but these were unsuccessful, with toxicity being high and benefits minimal (Kaur *et al.*, 2002).

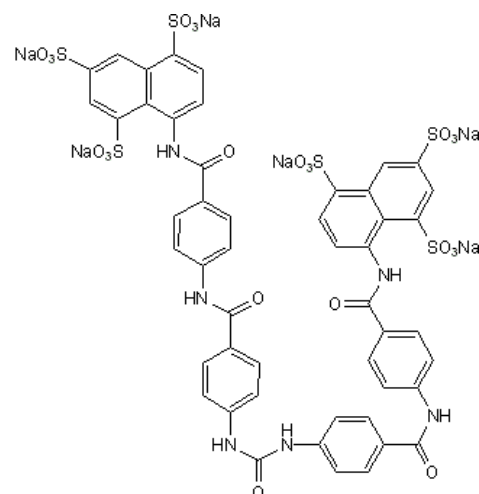
Suramin inhibited both the Mg<sup>2+</sup>-ATPase and the Na-K-ATPase and it was thought that this inhibition may be occurring through an interaction with the ATP binding site. As P2X receptors are activated by ATP, the action of suramin at these receptors was also investigated. Suramin was first identified as a P2X receptor antagonist at the University of Leicester in 1988, before the receptor had been isolated, when it was seen that suramin acted at a P2 purinoceptor to reversibly inhibit contractions in the vas deferens (Dunn & Blakeley, 1988).



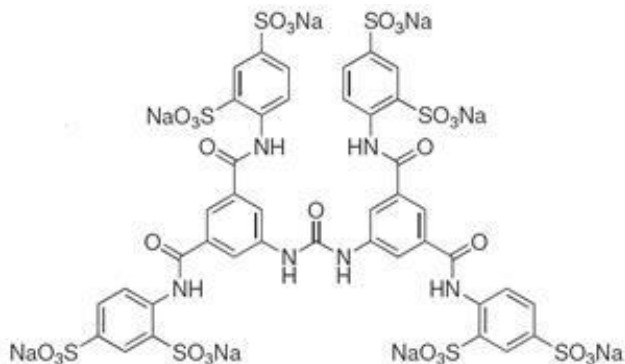
**Suramin**



**NF023**



**NF279**



**NF449**

**Figure 1.5 Structure of Suramin and its Derivatives.** Suramin consists of a central urea, 2 negatively charged naphthyl rings and four amide groups. NF023, NF279 and N449 are all derivatives of the suramin molecule with slight variations in structure.

Sneddon *et al* subsequently saw an effect of suramin in the vas deferens, where it inhibited excitatory junction potentials (Sneddon, 1992). This led to the drug being tested in a variety of native tissues thought to express purinergic receptors, and it was identified as a competitive antagonist at P2X receptors expressed in tissues including the cat colon (Venkova *et al.*, 1994) rat vas deferens (Khakh *et al.*, 1994; Mallard *et al.*, 1992) and rat vagus nerve (Trezise *et al.*, 1994).

Suramin was profiled at recombinant P2X receptors and acted as an antagonist at most of the receptor subtypes. It was most effective at the P2X1 receptor ( $IC_{50} \sim 1\mu M$ ) and had little action at the P2X4 receptor (Buell *et al.*, 1996; Evans *et al.*, 1995). The P2X2 receptor is 10-fold less sensitive to suramin than the P2X1 receptor (North & Surprenant, 2000). Sensitivity to the antagonist was also seen to differ between the same P2X receptor but from different species, for example the mouse P2X1 receptor is insensitive to 10  $\mu M$  suramin while the human variant is nearly completely inhibited by this concentration (Sim *et al.*, 2008). Suramin could not be used as a therapeutic treatment for any P2X receptor related pathologies as toxicity was high and selectivity low, with many P2X receptors and other proteins being suramin sensitive. However, the drug has been useful for identifying and characterising P2X receptors, and its structure has been used as the starting point for a series of suramin derivatives with P2X1 antagonist properties. The structure of suramin is shown in figure 1.5. It is a symmetrical molecule with the urea at the centre. Two arms extend from this urea, each containing 4 benzene rings, of which two are fused together to form a naphthyl ring on each arm. Each of the naphthyl rings contains 3 polysulphonates which are negatively charged causing the molecule to have a negative charge over all.

### 1.9.2 Suramin Derivatives as Potent and Selective Antagonists

As suramin was an effective, but non-selective, P2X receptor antagonist, it could not be used to differentiate between P2X receptor subtypes *in vivo* and had limited use therapeutically. Various suramin derivatives were therefore synthesised by Lambrecht *et al* and their potency and selectivity at different P2X receptor subtypes tested to see if a molecule of increased potency and

selectivity could be generated (Lambrecht *et al.*, 2002). This led to the identification of three suramin derivatives with high potency and/or selectivity at P2X receptor subtypes, NF023, NF279 and NF449 (Bultmann *et al.*, 1996). NF023 (8,8'-(carbonylbis(imino-3,1-phenylene carbonylimino) bis(1,3,5-naphthalenetri-sulfonic acid)) was a truncated form of suramin and the first potent and selective suramin derived antagonist to come from these studies (Bultmann *et al.*, 1996). Like suramin, NF023 was a reversible competitive antagonist. It was most potent at the human and rat P2X1 receptors with IC<sub>50</sub> values of ~ 0.2 µM, ~ 5-fold more potent than suramin (Soto *et al.*, 1999). It had good selectivity for the P2X1 over the P2X2 and P2X3 receptors, with the P2X2 receptor and P2X3 receptor being > 300-fold and ~ 35-fold less sensitive respectively. The structure of NF023 is shown in figure 1.5. This highlighted the generation of suramin derivatives as a strong possibility for the development of a potent hP2X1 receptor antagonist that could be used therapeutically.

Another suramin derived, potent P2X1 antagonist was NF279 (8,8'-carbonylbis(imino-4,1-phenylene carbonylimino-4,1-phenylene carbonylimino) bis(1,3,5-naphthalenetrisulfonic acid)) (Damer *et al.*, 1998). This molecule was very similar to suramin in its structure, but with two methyl groups removed (figure 1.5). NF279 was shown to be ~ 11-fold more potent at P2X receptors in the rat vas deferens than either suramin or NF023 (Damer *et al.*, 1998). The effects of NF279 were also studied at recombinant rat P2X1, P2X2 and P2X3 receptors and human P2X4 receptors expressed in *Xenopus laevis* oocytes (Rettinger *et al.*, 2000). The human variant of the P2X4 receptor was used as this showed a higher sensitivity to suramin. NF279 was even more potent at the rat P2X1 receptor than NF023, and had an IC<sub>50</sub> value of 19 nM (Rettinger *et al.*, 2000). It was reasonably selective for P2X1 over the P2X2 receptor, with the latter having an IC<sub>50</sub> value of ~ 800 nM. The P2X3 receptor had an IC<sub>50</sub> of ~ 1 µM. The antagonist also showed some effect at the P2X4 receptor where 300 µM was seen to cause ~ 40% inhibition (Rettinger *et al.*, 2000).

The most potent and selective of the suramin derived antagonists was NF449 (4,4',4'',4'''-(carbonylbis(imino-5,1,3-benzenetriylbis(carbonylimino))) tetrakis-benzene-1,3-disulfonic acid) (Braun *et al.*, 2001). Like suramin, the

structure of NF449 is based around a urea group, with two benzenes extending from this central molecule. In the NF449 molecule each of these benzene rings has two branches, each containing a further benzene ring with 2 negatively charged polysulfonates (figure 1.5) (Braun *et al.*, 2001). Therefore NF449 has eight negative charges, two more than suramin, which are spread around the molecule. This could account for the increased potency compared to the parent molecule. NF449 has nanomolar potency at the P2X1 receptor, with an IC<sub>50</sub> concentration of ~1nM (Braun *et al.*, 2001), although there has been some suggestion that it is more potent, with an IC<sub>50</sub> of 0.05 nM (Hulsmann *et al.*, 2003). NF449 is highly selective for the P2X1 receptor subtype, with IC<sub>50</sub> values of 47, 1.8 and > 300 μM at the P2X2, P2X3 and P2X4 receptors respectively (Hulsmann *et al.*, 2003; Rettinger *et al.*, 2005). The antagonist has not been used in clinical trials as the polyanionic structure of the molecule is not favoured for drug development (Kennedy, 2013). Various toxicities were also seen for its parent molecule suramin when used therapeutically (described above). Several P2X1 antagonists with distinct structures have been developed, e.g. the benzimidazole-2-carboxamide derivative RO-1, but these have not shown the same potency at the receptor as NF449 (Jaime-Figueroa *et al.*, 2005).

### 1.9.3 PPADS

Pyridoxalphosphate-6-azophenyl-2',4'-disulphonic acid (PPADS) was first characterised as a P2X receptor inhibitor in the rabbit vas deferens in 1992 (Lambrecht *et al.*, 1992). PPADS was seen to inhibit contraction at concentrations < 10 μM showing it to be a more potent P2X receptor antagonist than suramin. PPADS also inhibited the P2X receptor in the rabbit urinary bladder at concentrations of 1 – 30 μM, where it was shown to be selective at the receptor (Ziganshin *et al.*, 1993). This inhibition was thought to be mostly irreversible, with only a 15-20% recovery of αβ-meATP induced contraction after > 2 hours of washing. Several more studies suggested PPADS to be acting as a

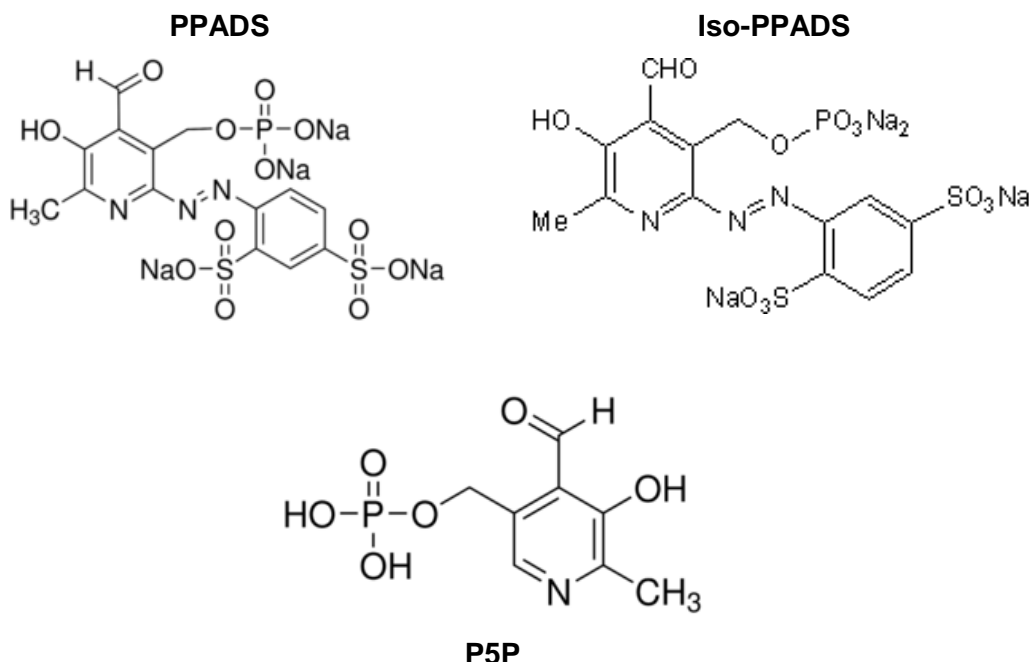


**Figure 1.6 Structure of PPADS and related molecules.** PPADS consists of a phosphate moiety and two polysulfonates. Iso-PPADS is an isomer of PPADS with the disulfonic acid at the 5' position. P5P is a precursor of the PPADS molecule.

selective P2X receptor inhibitor in native tissues such as the rabbit ear artery (Ziganshin *et al.*, 1994), guinea pig taenia coli and rat duodenum (Windscheif *et al.*, 1995). However PPADS was later shown to be a non-selective, but non-universal purinergic receptor antagonist as it can inhibit recombinant P2X1, P2X2, P2X3 and P2X5 receptors with pIC<sub>50</sub> values of 1 - 2.6 µM (Collo *et al.*, 1996; Ralevic & Burnstock, 1998). It was seen that the rat P2X4 receptor was insensitive to micromolar levels of PPADS (Buell *et al.*, 1996), but that the human receptor had an IC<sub>50</sub> < 30 µM (Garcia-Guzman *et al.*, 1997). PPADS has also been seen to have an effect at various P2Y receptors. The P2Y1 receptor was shown to be inhibited by PPADS at a concentration of 30 µM (Schachter *et al.*, 1996). There is also evidence of PPADS inhibition of P2Y4 and P2Y6 receptors (von Kugelgen & Wetter, 2000).

The PPADS molecule consists of a phosphate moiety and two polysulfonates. Each of these three components contains a negative charge.

As ATP also contains phosphates it is possible that PPADS may bind in the ATP active site. The structure of PPADS is shown in figure 1.6.

Some analogues and isoforms of PPADS have been shown to also have antagonist action at P2X receptors and have given insight into structural elements of the PPADS molecule that are important for inhibition. Iso-PPADS is an isomer of PPADS with the disulphonic acid at the 5' instead of the 4' position in the molecule (figure 1.5). It was seen to have a similar level of inhibition as PPADS and therefore the position of the disulphonic acid does not seem to be important to antagonism (Connolly, 1995). Pyridoxal 5'-phosphate (P5P) is a PPADS precursor that lacks the 6-azophenyl disulphonic acid (figure 1.6). This molecule was seen to antagonise P2X receptors but with a much lower potency than PPADS or Iso-PPADS. This suggests that the 5-phosphate aspect of the PPADS molecule has some antagonistic effect at the P2X receptor, but that the disulphonic acid greatly increases potency (Connolly, 1995).

Despite various antagonists acting at the P2X1 receptor, very little is known about the molecular basis of their action. Understanding the molecular basis of how existing antagonists bind at the hP2X1 receptor, would assist in the development of novel, potent and selective antagonists for this receptor. The aim of this thesis was therefore to gain further insight into the action of the existing antagonists suramin PPADS and NF449. The rP2X4 receptor is insensitive to these antagonists at micromolar concentrations.

### **1.10 Inhibition of the P2X4 Receptor**

When the rat P2X4 receptor was first cloned in 1996 it was observed that the subtype was insensitive to the commonly used antagonists suramin and PPADS (Buell *et al.*, 1996). Very high concentrations of the antagonists did show some inhibition, but this was only ~ 60% at 1000 µM PPADS, ~ 30% at 1000 µM P5P and ~ 20% at 300 µM suramin. It has since been shown that the potent P2X1 receptor antagonist NF449 is also ineffective at this subtype, with 300 µM NF449 producing just ~ 20% inhibition (Rettinger *et al.*, 2005). The human P2X4 receptor has been reported to have greater sensitivity to these antagonists, however the levels of inhibition are still much reduced compared to

at the P2X1 receptor (Garcia-Guzman *et al.*, 1997). A lack of potent and selective P2X4 antagonists makes identifying the physiological functions of this subtype of P2X receptor more difficult. There are some inhibitors and antagonists available which are discussed below, but none with the potency and selectivity of those available for other subtypes.

### **1.10.1 Ethanol Inhibits the P2X4 Receptor**

Ethanol was first reported to inhibit a neuronal ATP gated ion channel in 1993, (Li *et al.*, 1993). The ATP activated currents seen in the central and peripheral nervous system were seen to be reduced by 3-500 mM ethanol, with an IC<sub>50</sub> value of 68 mM (Li *et al.*, 1993). This effect was subsequently shown to be through the P2X4 receptor, with the recombinant receptor shown to have an IC<sub>50</sub> concentration of 58 mM (Xiong *et al.*, 2000). Further investigation suggested that this inhibition was via an allosteric mechanism and could be due to an increase in the dissociation constant of ATP (Li *et al.*, 1998; Weight *et al.*, 1999). This finding has been disputed by Ostrovskaya *et al* in 2011, who found that there was no change in the dissociation constant when performing single cell analysis (Ostrovskaya *et al.*, 2011). It was seen that application of ethanol had to be extracellular to cause inhibition, suggesting that the binding site for ethanol at the receptor is in the extracellular loop region. Inhibition was also only seen when the molecular volume of the ethanol was < 46.1 ml/mol (Weight *et al.*, 1999). The amount of inhibition by ethanol can be decreased by increasing the proton concentration (pH) of the extracellular solution and can be increased by the presence of Zn<sup>2+</sup> (Weight *et al.*, 1999).

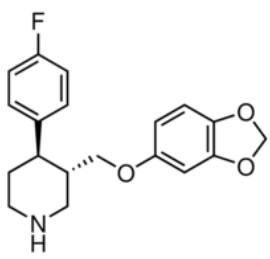
Various mutagenesis studies have given insight into where the binding site for ethanol at the P2X4 receptor may be located. Mutation of the histidine at position 241 to alanine (H241A) in the rat P2X4 receptor altered the mechanism by which ethanol acted at the receptor (Xiong *et al.*, 2005). At this mutant ethanol did not alter the IC<sub>50</sub> concentration, as was seen at the WT receptor, but instead decreased the maximal response to ATP. Mutation of the residues asparagine 331 and methionine 336 to alanine have been shown to reduce ethanol inhibition. These residues are located in the second transmembrane domain, close to the extracellular loop suggesting that they

may be part of the ethanol binding site (Popova *et al.*, 2010). Using mutagenesis studies and the crystal structure the location of the ethanol binding site has been identified. It is centred around Trp46 and Trp50 in TM1 and Asp331 and Met336 in TM2 (Popova *et al.*, 2010; Asatryan *et al.*, 2010).

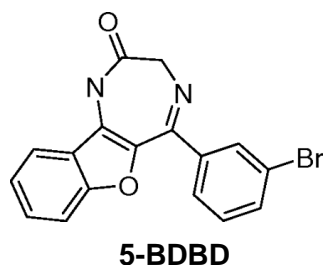
It can be seen that while the P2X4 receptor is not sensitive to the commonly used P2X receptor antagonists such as suramin and PPADS, it can be inhibited by ethanol, and that the P2X4 receptor is more sensitive to ethanol than any other subtype.

### **1.10.2 Inhibition of the P2X4 Receptor by Antidepressants**

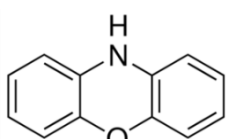
Patients taking antidepressants, who also suffered from neuropathic pain often reported alleviation of their pain due to the antidepressants, and these are now a prescribed treatment for the condition (Sindrup *et al.*, 2005). As P2X4 receptors were known to be upregulated in pain sensation it was investigated to see whether the antidepressant drugs were inhibiting the P2X4 receptor and thus reducing pain (Nagata *et al.*, 2009). In 1321N1 cells expressing P2X4 receptors there was a strong inhibition of the ATP induced  $\text{Ca}^{2+}$  responses by cyclic antidepressants. Both human and rat responses were inhibited by paroxetine ( $\text{IC}_{50}$  values of 2.45 and 1.8  $\mu\text{M}$  respectively). It was thought that this inhibition was non-competitive (Nagata *et al.*, 2009). These findings were questioned by Khakh's group in 2010, who found little evidence to suggest that antidepressants acted as P2X4 receptor antagonists in C8-B4 cells, but instead suggested that the reduction in response may be due to down regulation of the receptor (Toulme *et al.*, 2010). The structure of paroxetine is shown in figure 1.7. Any inhibition by antidepressant drugs, in particular the selective serotonin inhibitor paroxetine, remains to be fully investigated at the P2X4 receptor. If they do act as P2X4 receptor antagonists, the characterisation of how these drugs are working could lead to insights into the development of new potent and selective P2X4 receptor antagonists.



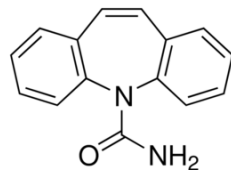
**Paroxetine**



**5-BDBD**



**Phenoxazine**



**Carbamazepine**

**Figure 1.7 Structures of P2X4 receptor antagonists.** Four molecules that have been shown to have an inhibitory effect at the P2X4 receptor are shown.

### 1.10.3 5-BDBD

A benzodiazepine derivative, 5-(3-bromophenyl)-1,3-dihydro-2H-benzofuro[3,2-e]-1,4-diazepin-2-one (5-BDBD) has recently been named as a selective P2X4 receptor antagonist with an  $IC_{50}$  of  $\sim 0.5 \mu\text{M}$  (Kaczmarek-Hajek *et al.*, 2012), although reports into its effectiveness have been contradictory. No papers are available simply showing the characterisation of the drug in different tissues or at recombinant receptors. Instead there are reports of its use as a tool in several different papers. At recombinant human P2X4 receptors 5-BDBD showed weak potency and the same was seen at native guinea pig P2X4 receptors in vascular endothelial cells, with both studies showing 5-BDBD to have an  $IC_{50}$  concentration of  $\sim 30 \mu\text{M}$  (Norenberg *et al.*, 2012; Wu *et al.*, 2011). In contrast a recent study demonstrated a complete block of human P2X4 receptors in a prechondrogenic cell line by  $10 \mu\text{M}$  5-BDBD (Kwon, 2012). Balazs *et al* also reported an  $IC_{50}$  value of  $\sim 1 \mu\text{M}$  for 5-BDBD at recombinant human P2X4 receptors (Balazs *et al.*, 2013). The effectiveness of 5-BDBD at P2X4 receptors from other species is yet to be reported.

#### **1.10.4 Phenoxazine and Acridone Derivatives as P2X4 Inhibitors**

N-substituted phenoxazine derivatives have been shown to have a variety of inhibitory effects in the CNS, a region in which the P2X4 receptor is highly expressed (Thimmaiah *et al.*, 1992). It was thought that these molecules may be having their effects via P2X4 receptors and therefore a series of N-substituted phenoxazine derivatives were synthesized and their antagonist effects on the P2X4 receptor examined (Hernandez-Olmos *et al.*, 2012). The inhibition by the different compounds was tested at human P2X4 receptors expressed in 1321N1 astrocytoma cells, and the most effective were also tested at mouse and rat receptors. From these studies two compounds were seen to strongly inhibit the P2X4 receptors and be reasonably selective over the human P2X1, P2X2, P2X3 and P2X7 receptors. The most potent was N-(benzyloxycarbonyl)phenoxazine, called PSB-12054, which had an IC<sub>50</sub> of 0.189 µM at the human P2X4 receptor, and < 2.5 µM at the rat and mouse homologues. The receptor function could not be completely blocked, with maximal inhibition of 77% being seen (Hernandez-Olmos *et al.*, 2012). The IC<sub>50</sub> of this compound at the human P2X1 and P2X3 receptors was 6.52 and ~ 10 µM respectively, and > 10 µM at the P2X2 and P2X7 receptors. This shows selectivity for the P2X4 receptor.

The second compound with good potency for the P2X4 receptor was N-(p-Methylphenyl)sulfonylphenoxazine, called PSB-12062. This compound was ~ equipotent at the human, mouse and rat P2X4 receptors with IC<sub>50</sub> concentrations of 1.38, 1.76 and 0.928 µM respectively (Hernandez-Olmos *et al.*, 2012). PSB-12062 was also reasonably selective for the P2X4 receptor, with the IC<sub>50</sub> value at other P2X receptors tested being > 10 µM. The structure of phenoxazine is shown in figure 1.7. The two phenoxazine compounds show potential for the development of potent and selective P2X4 receptor antagonists for therapeutic use.

Due to the effects of phenoxazine, Tian *et al* decided to look at the possible P2X4 receptor antagonist properties of carbamazepine and its derivatives as it is structurally similar to the phenoxazine derivatives and is used as an anti-epileptic treatment (Tian *et al.*, 2014). Of the carbamazepine

derivatives, *N,N*-diisopropyl-5*H*-dibenz[*b,f*]azepine-5-carboxamide was the most potent with an IC<sub>50</sub> of 3.44 μM. However it was not selective for the P2X4 receptor, with the P2X1 receptor having an IC<sub>50</sub> value of 5.32 μM (Tian *et al.*, 2014). Both carbamazepine and phenoxazines have tricyclic heterocycles and as both can inhibit the P2X4 receptor this structure may be one on which to base a future potent P2X4 receptor antagonist, however more studies will be needed to increase the selectivity of the compounds for the P2X4 receptor.

## **1.11 Antagonists for Other P2X Receptor Subtypes**

### **1.11.1 Antagonists at the P2X2 Receptor**

There is a lack of potent and selective antagonists for the P2X2 receptor. The non-selective antagonists PPADS and suramin both show antagonism at the P2X2 receptor, PPADS is most potent with an IC<sub>50</sub> of ~ 1 μM while suramin has an IC<sub>50</sub> of ~ 10 μM (Jarvis & Khakh, 2009). There has only been one report of a potent P2X2 antagonist and this was NF770, a suramin derivative (Wolf *et al.*, 2011). NF770 was identified in a similar way to NF449, with derivatives of suramin being examined for their antagonistic effects at P2X receptors. NF770 was seen to have an IC<sub>50</sub> value of 19 nM at the P2X2 receptor, but only had ~ 4-fold selectivity over the P2X3 receptor which had an IC<sub>50</sub> value of 74 nM (Wolf *et al.*, 2011). This shows that although a potent antagonist for the P2X2 receptor has been developed, the selectivity is low, as is often seen for P2X receptor antagonists.

### **1.11.2 Antagonists at the P2X3 and P2X2/3 Receptors**

There has been much more success at developing potent and selective antagonists for the P2X3 and P2X2/3 receptors. The first to be developed was A-317491 which was a competitive antagonist and had an IC<sub>50</sub> value of 97 nM (Jarvis *et al.*, 2002). It was shown to have > 100-fold selectivity for the P2X3 and P2X2/3 receptors over other P2X receptor subtypes. In the same study the compound was shown to be effective at reducing neuropathic pain sensation of mice *in vivo*, however it was later seen that the drug had poor distribution in the CNS, and therefore was not pursued as a therapeutic agent (Gever *et al.*, 2006). More success has been seen with diaminopyrimidine derivatives RO-4

(renamed AF-353) and RO-51 (Gever *et al.*, 2006; Gever *et al.*, 2010; Jahangir *et al.*, 2009). RO-4 had a pIC<sub>50</sub> of 8.0 at the P2X3 receptor and 7.1 at the P2X2/3 receptor. This drug was shown to be bio-available and to prevent the pain as a result of bone cancer in rats (Gever *et al.*, 2010; Kaan *et al.*, 2010). In the same set of experiments compound RO-51 was also found to be potent and selective at the P2X3 and P2X2/3 receptors, with pIC<sub>50</sub> values of 8.7 and 8.3 respectively. Both compounds showed no or very little antagonism at the other P2X receptor subtypes.

Based on these findings several more P2X3 antagonists have been developed which have strong potency and selectivity. These include RO-85 by Roche (Brotherton-Pleiss *et al.*, 2010), compounds A, B and C by GlaxoSmithKline (Ballini *et al.*, 2011) and AF-219 by Afferent Pharmaceuticals (Kaczmarek-Hajek *et al.*, 2012). AF-219 is an aryloxy-pyrimidinediamine with an IC<sub>50</sub> of ~ 30 nM at hP2X3 receptors and ~ 100 – 250 nM at the hP2X2/3 receptor, with no inhibition at receptors that did not contain a P2X3 subunit. This molecule has been through four separate phase 1 clinical trials, completed one phase 2 clinical trial and is involved in three further phase 2 trials. The clinical trials still under way are for treatment of osteoarthritic joint pain, asthma and interstitial cystitis (Ford & Undem, 2013). The completed trial was for chronic cough and was successful, with patients seeing a reduction in cough rate and frequency and any symptoms related to their cough (Ford & Undem, 2013). This is an example of the potential of potent and selective P2X receptor antagonists in the treatment of disease.

### **1.11.3 Antagonists at the P2X7 Receptor**

The development of potent and selective antagonists for the P2X7 receptor has peaked in recent years due to the involvement of the receptor in pain, inflammation and neurodegenerative disease. There are now a variety of P2X7 receptor antagonists available. In vitro inhibition of P2X7 has been shown for a range of compounds. A-804598 was developed by Abbot and has an IC<sub>50</sub> of 11 nM at the human P2X7 receptor (Donnelly-Roberts *et al.*, 2009). AZ11645373 has an IC<sub>50</sub> value of 90 nM at the human P2X7 receptor, but is > 500-fold less sensitive at the rat P2X7 receptor (Stokes *et al.*, 2006). A range of

antagonists have been produced by GlaxoSmithKline, including 2-oxo-N-(phenylmethyl)-4-imidazolidinecarboxamides, (1H-pyrazol-4-yl)acetamides and tetrasubstituted-imidazoles (Abberley *et al.*, 2010; Chambers *et al.*, 2010; Gleave *et al.*, 2010). Pfizer have also produced a P2X7 antagonist 2-chloro-N-((4,4-difluoro-1-hydroxycyclohexyl) methyl)-5-(5-fluoropyrimidin-2-yl)benzamide that has been studied in vitro (Chen *et al.*, 2010). Johnson&Johnson have also recently produced a P2X7 receptor antagonist, JNJ-47965567 (Bhattacharya *et al.*, 2013). The fact that many different pharmaceutical companies are generating P2X7 receptor antagonists shows the strong therapeutic potential of these drugs. Several P2X7 receptor antagonists have shown analgesic effects when administered to rodent models of inflammatory pain. These include pyroglutamic acid amides (Abdi *et al.*, 2010), GSK314181A (Broom *et al.*, 2008), A-839977 (Honore *et al.*, 2009) and A-740003 (Honore *et al.*, 2006). These molecules are yet to be put into clinical trials.

A variety of P2X7 receptor antagonists have been, or are currently, in clinical trials but with so far little / no success. AZD9056 was put into a clinical trial for the treatment of rheumatoid arthritis but did not show any beneficial effect in patients (Keystone *et al.*, 2012). Although there was no effect on rheumatoid arthritis patients AZD9056 has since been entered into clinical trials for inflammatory bowel disease, osteoarthritis and chronic obstructive pulmonary disease. The drug CE-224535 was also tested in a clinical trial for the treatment of rheumatoid arthritis where it was seen to have no effect (Duplantier *et al.*, 2011). The effects of this drug on Alzheimer's and pain are now being tested. The compound GSK1482160 was also entered into phase I clinical trials, but the results led to its development being discontinued as it was not possible to get to the necessary >90% inhibition of IL-1 $\beta$  release that was required (Ali *et al.*, 2013). These results show that while the *in vitro* and *in vivo* rodent experiments suggest that P2X7 antagonists have strong therapeutic potential, a compound that can be released to the drugs market is yet to be found. This may be due to the differences in the pharmacological properties of rodent and human P2X7 receptors.

Receptor	Agonists	Desensitisation	ATP EC <sub>50</sub> (μM)	Antagonists
P2X1	2-mesATP>ATP>Ap6A>α,β-meATP >βγ-L-meATP	Fast	1	PPADS, suramin, TNP-ATP, NF279, NF023, NF449
P2X2	ATP>2-meSATP >ATPγS	Slow	5-60	PPADS, suramin, reactive blue 2
P2X3	2-meSATP>ATP >α,β-meATP >ATPγS>AP3A	Fast	1	PPADS, suramin, A-317491, RO-85, AF-219
P2X4	ATP>ATPγS>2-meSATP	Slow	10	Phenoxazine, carbamazepine, Paroxetine, 5-BDBD
P2X5	ATP=2- meSATP > ATPγS>2CIATP	Minimal	15	PPADS, suramin
P2X7	BzATP>ATP>2meSATP	Minimal	115	AZD9056,CE-224535, GSK1482160

**Table 1.2 Pharmacological profile of agonists and antagonists at the homomeric P2X receptors.** Order of agonist potency, ATP EC<sub>50</sub>, and antagonists that inhibit homomeric P2X receptors.

In this introduction I have given an overview of the physiological roles of P2X receptors, the structure of the receptor and the therapeutic potential of a range of P2X receptor antagonists. Although a range of P2X1 receptor antagonists have been described and their effects at the recombinant receptor characterised, the basis of how these antagonists are binding remains to be deduced.

### **1.12 Thesis Aims**

In this thesis I aim to demonstrate the molecular basis of antagonist binding at the hP2X1 receptor. The contribution of residues in the extracellular loop to the antagonist sensitivity of the hP2X1 receptor will be investigated. This will be done through the generation of chimeras and point mutations between this receptor and the antagonist insensitive rP2X4 receptor. The residues identified by these techniques will be used to generate an antagonist bound homology model of the hP2X1 receptor. The chimeras can also be used to gain insight into the low potency of the antagonists at the P2X4 receptor. It is important that the molecular basis of antagonism is understood in order to design now potent and selective hP2X1 receptor antagonists with therapeutic potential.

## Chapter 2: Materials and Methods

### 2.1 Molecular Biology

#### 2.1.1 WT P2X Receptor Constructs

The WT hP2X1, hP2X2 and rP2X4 receptor complementary DNAs (cDNAs) had previously been used in the laboratory. The hP2X1 receptor cDNA was originally cloned from the bladder (Ennion *et al.*, 2000) and the hP2X2 receptor from the pituitary gland (Lynch *et al.*, 1999). The rP2X4 receptor DNA was a gift of Dr. Francois Rassendren, (CNRS, Montpellier, France). A mutation (Y378A) had been introduced to the rP2X4 receptor template by Dr Helen Digby, a previous lab member, and allowed for more stable and reproducible currents (Royle *et al.*, 2002). The zfP2X4.1 construct was kindly given to the lab by Mark Voigt (St Louis University, USA). All constructs were contained within the pcDNA3.1 vector plasmid which had an ampicillin resistance gene to allow for selection of the correct plasmid (figure 1.1). A *Mlu*I restriction enzyme site linearised the plasmid in order to generate messenger RNA (mRNA) for injection into *Xenopus laevis* oocytes. For effective expression of P2X receptors in oocytes, the vector contained T7 promoter sites to allow expression of protein, and a polyadenylated (polyA) tail which is positioned at the 3' end of the P2X1 receptor. This polyA tail has been shown to increase expression and currents in *Xenopus* oocytes by protecting the mRNA from exonucleases (Ennion & Evans, 2002a).

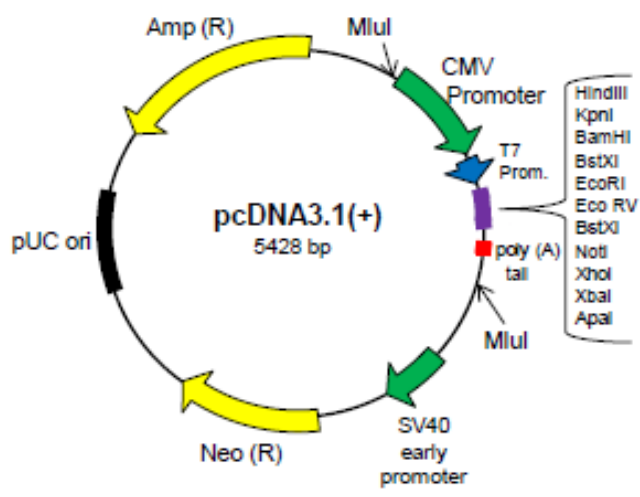


**Figure 2.1 pcDNA3.1 Plasmid.**  
Plasmid map of the pcDNA3.1 vector. Taken from (El-Ajouz, 2011)

### 2.1.2 Generation of chimeras

Chimeras were generated using domain swapping, a two-stage polymerase chain reaction (PCR) (figure 2.2). The first PCR generated a megaprimer of the insert from the first receptor, and the second incorporated the megaprimer into the template receptor. To make the megaprimer, primers were designed by hand to amplify the region of the receptor (e.g. rP2X4) that was to be swapped with the template receptor (e.g. hP2X1). The primers also contained a section ~ 15 bp in length at either end, complementary to the hP2X1 receptor sequence. This increased insertion efficiency. The primers used to make the megaprimer for chimera X1-AX4 are shown below, the sequence corresponding to the hP2X1 receptor is shown in black, and to the rP2X4 receptor is shown in red.

Forward primer to make X1-AX4 megaprimer (5' to 3')

CTCATCAGCAGT**GTCTCTACCAAAGCCAAAGGTGTG**

Reverse primer to make X1-AX4 megaprimer (5' to 3')

**GGCCTTCCCAGGGGTACA**GTCGGCGTCTGAATTACA

Primers were custom ordered from Sigma and diluted to 10 pmol/μl in nuclease free water. A PCR of these primers with the rP2X4 receptor template was performed to generate the megaprimer. Reactions were conducted with the following components:

- 5 μl 10 x Pfu reaction buffer
- 0.4 μl dNTPs
- 2.5 μl forward primer (250 ng)
- 2.5 μl reverse primer (250 ng)
- 1-2 μl template DNA (50 ng)
- 0.5-1 μl Pfu turbo enzyme
- Nuclease free water to 50 μl

The reaction was performed in a Techne Genius thermocycler with the following settings:

Denaturation	95°C	3 minutes	
Denaturation	95°C	30 seconds	
Annealing	55-75°C	60 seconds	
Extension	68°C	60 seconds	30 cycles

To check if the reaction had worked the PCR product was run out on a 1% agarose gel stained with ethidium bromide (EtBr) to see if there was a band present at the size of the megaprimer. If the PCR had not worked it was repeated at variant temperatures. If successful, the PCR product was treated with DpnI for 1 hour at 37°C to remove the template DNA. The DpnI enzyme was then inactivated by heating to 85°C for 10 minutes and the DNA purified using a PCR clean-up kit (Qiagen, Sussex, UK). The product was the purified megaprimer of rP2X4 with hP2X1 receptor overhangs.

This megaprimer was then used in a second PCR (figure 2.2) with the hP2X1 receptor template, with similar components to those above. Instead of using separate forward and reverse primers, 2.5 µl of the megaprimer was used and the water volume adjusted to keep the reaction at a volume of 50 µl. The PCR was run with the following settings:

Denaturation	95°C	3 minutes	
Denaturation	95°C	30 seconds	
Annealing	55-75°C	60 seconds	
Extension	72°C	16 minutes	16 cycles
Final extension	72 °C	10 minutes	

This PCR inserted the rP2X4 receptor residues into the hP2X1 receptor, producing the chimera contained within the pcDNA3.1 vector. The product was again run on an EtBr stained, 1% agarose gel and if correct was DpnI treated. The final chimera could then be transformed and DNA extraction performed.

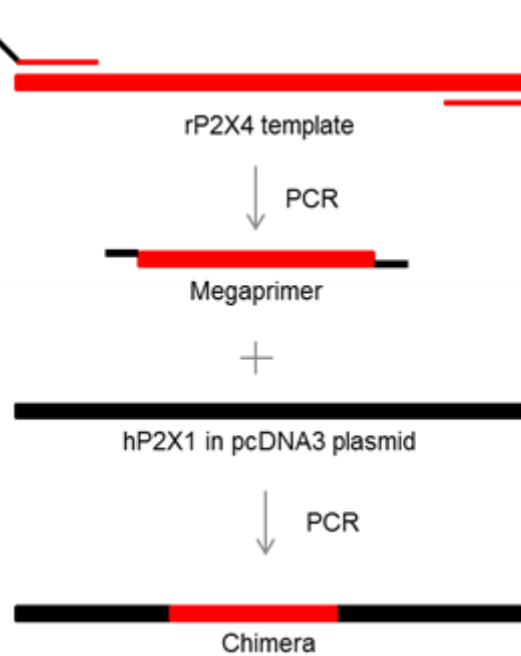


**Figure 2.2 Chimera Generation.** Primers were designed to amplify the section of the rP2X4 receptor that was to be swapped into the hP2X1 receptor, and also add hP2X1 receptor overhangs corresponding to the point where the rP2X4 sequence was to be inserted. PCR generated a megaprimer of the rP2X4 receptor sequence with the hP2X1 receptor overhanging ends. The megaprimer was then used in a second PCR with the hP2X1 receptor template. This produced the desired chimera (a section of the rP2X4 receptor swapped into the hP2X1 receptor).

### 2.1.3 Point Mutations

Primers were designed using the PrimerX website ([www.bioinformatics.org/primerx](http://www.bioinformatics.org/primerx)) and diluted to a concentration of 10 pmol/μl in nuclease free water. PrimerX was chosen as it allowed optimisation of the GC base content, melting temperature and primer length. PCRs were performed:

5 μl 10 x Pfu reaction buffer  
 0.4 μl dNTPs  
 2.5 μl forward primer (250 ng)  
 2.5 μl reverse primer (250 ng)  
 1-2 μl template DNA (50 ng)  
 0.5-1 μl Pfu turbo enzyme  
 Nuclease free water to 50 μl

The reaction was carried out at the following parameters:

Denaturation	95°C	3 minutes
Denaturation	95°C	30 seconds
Annealing	55-75°C	60 seconds
Extension	68°C	16 minutes
Final extension	68°C	10 minutes

16 Cycles

The PCR products were ran on an EtBr stained, 1% agarose gel and Dpn1 treated as above. Once complete the DNA was transformed as described below.

#### 2.1.4 Transformation and DNA Extraction

The chimeric or point mutated DNA was transformed into *Escherichia Coli* (*E. Coli*) and selected for using the ampicillin resistance gene present in the pcDNA3.1 vector. To do this, plasmid DNA was transformed into supercompetent XL-1 blue cells (Stratagen, Aligent technologies). 50 µl of the cells were placed in a 15ml Corning centrifuge tube on ice. 1 µl of DNA was added and gently flicked to mix before being left on ice for 30 minutes. The cells were then heat shocked in a 42°C water bath for 45 seconds and incubated on ice for 2 minutes. 0.5 ml of S.O.C medium (Invitrogen) which has a refined salt balance and contains ions optimal for transformation, was then added to the tube to allow for maximal transformation efficiency. Tubes were incubated at 37°C in a shaking incubator at 250 rotations per minute (rpm) for 1 hour. After incubation, 50-100 µl of the cells and SOC medium were added to the agar plates containing 50 µg/ml ampicillin which had been made previously. They were incubated overnight in a 37°C incubator. Only cells containing the pcDNA3.1 vector with the ampicillin resistance gene could grow in the presence of the antibiotic.

The next day three individual colonies were picked from the plate with a sterile pipette tip. These were each placed in an individual 30 ml universal tube (Sterilin, UK) containing 6 ml of LB broth and 50 µg/ml of ampicillin. These were incubated overnight in a shaking incubator at 37°C, 250 rpm. DNA was

extracted from the cultures the following day using a Wizard plus SV miniprep kit (Promega). The final product was 50-200 ng of DNA (quantified by a nanodrop spectrophotometer) contained in 100 µl of nuclease free water.

### **2.1.5 DNA Sequencing**

The extracted DNA was sent for sequencing to check that the desired regions had been swapped and that no unwanted mutations had been introduced during the process. Sequencing was performed by the Protein and Nucleic Acid Chemistry Laboratory (PNACL), University of Leicester. The sequence was analysed using Seqman II software (DNASTAR).

### **2.1.6 mRNA Synthesis**

Once the DNA had been correctly sequenced, it could be used to generate mRNA for expression of the protein in oocytes. DNA was linearised in a digest containing 41 µl DNA (50-200 ng), 5 µl buffer H and 4 µl *Mlu*I enzyme (Roche) at 37°C for 4 hours. The linearised product contained the T7 promoter site before the P2X receptor sequences and the polyA tail after it. The product was treated with 1 µl proteinase K and 5 µl 10% SDS and left at 50°C for 1 hour. DNA was extracted with Phenol/Chloroform/Isoamyl (25:24:1) and precipitated overnight at -20°C in 2x volume of 100% ethanol. The following day tubes were centrifuged at 13000 rpm at 4°C for one hour. The DNA pellet was washed with 70% ethanol (0.5 ml). Ethanol was removed from the pellet and heated to 50°C for 1-2 minutes to completely evaporate ethanol from the tube. 6 µl nuclease free water was added and the DNA resuspended by vortexing.

mRNA synthesis was performed using the mMessage mMachine T7 kit (Ambion). To the 6 µl of DNA, was added 2 µl of reaction buffer, 10 µl of NTP/CAP ribonucleotides and 2 µl of T7 enzyme mix and incubated at 37°C for 2 hours. 1 µl TURBO DNase was added to remove template DNA and incubated at 37°C for 15 minutes. 30 µl lithium chloride precipitation solution (7.5 M LiCl, 50 mM EDTA) was then added and stored at -20°C overnight. This precipitated the RNA, purifying the product and removing any excess nucleotides or other proteins. Samples were centrifuged for an hour at 13000 rpm, 4°C, to form a pellet of RNA. The pellet was washed with 1 ml 70%

ethanol, which was again removed by pipette and drying at 50°C. The pellet was resuspended in 3-6 µl of nuclease free water and quantified using a nanodrop spectrophotometer (Labtech international). RNA was diluted to a final concentration of 1 µg/µl and run on an RNA gel in order to make sure it was not degraded.

## **2.2 Expression in *Xenopus laevis* oocytes**

The RNA was expressed in *Xenopus laevis* oocytes. These were chosen as an expression system as their large size makes them easy to take electrophysiological recordings from. They allow rapid and efficient translation of RNA and this means that many ion channels can be expressed and large currents recorded (Buckingham *et al.*, 2006). *Xenopus laevis* frogs were anaesthetised using tricaine methane sulfonate (MS222) solution and decapitated. Oocytes were extracted at stage V; this stage can be easily identified as the oocytes are clearly split into a dark brown animal half and a yellow vegetal half. Lobes of oocytes were cut into small clumps and digested with collagenase (1 mg/ml) for ~ 20 minutes until manual defolliculation was easy. Oocytes were kept at 16°C in ND96 solution (96 mM NaCl, 2 mM KCL, 1.8 mM CaCl<sub>2</sub>, 1 mM MgCl, 5 mM sodium pyruvate, 5 mM HEPES, pH 7.6). 50 µg/ml gentamycin was added to the solution to maintain the oocytes. An Inject+Matic microinjector (J. Alejandro Gaby, Geneva, Switzerland) was used to inject 50 ng of RNA into the oocyte. Recordings were made 3-10 days later with the ND96 solution being changed daily.

## **2.3 Two Electrode Voltage Clamp Recordings**

The two-electrode voltage clamp technique was used to record currents in oocytes. Oocytes were held in a 2 ml recording chamber which was perfused at ~ 3 ml/min with a recording solution of ND96 (1.8 mM BaCl<sub>2</sub> replaced the 1.8 mM CaCl<sub>2</sub> from the storage solution to prevent any calcium sensitive chloride channels present in the oocyte from being activated). Electrodes made from capillary glass (TW150F-4 World Precision Instruments Inc) were pulled using a two stage puller (Narishige, Japan) until the tip diameter was 1-2 µm. They were filled with a 3M KCl solution to allow effective

conductance of current. The resistance of the electrodes was between 0.2 and 0.4 MΩ and they were inserted into oocytes that were then voltage clamped at -60 mV using the Geneclamp 500B amplifier (Axon Instruments, Union City, CA, USA). A Digidata 1322A analog to digital converter was used to digitise the data and this was collected on a computer using pClamp 8.2 acquisition software (Molecular devices, Menlo Park, CA, USA). A U-tube perfusion system was used to deliver agonists and antagonists for 3 second periods with 5-10 minutes of recovery time between each application dependent on the construct. Antagonists were pre-perfused around the oocyte for 5 minutes before co-application with ATP.

### 2.3.1 Data Analysis

Data are reported as the mean ± standard error of the mean (SEM). The analysis software used was GraphPad Prism 6 (GraphPad Software Inc., San Diego, USA). All experiments were repeated ≥ 3 times. Significant differences for data sets comparing more than two receptors were calculated by one-way ANOVA followed by either Dunnett's test to compare the means vs a control column, or Tukey's multiple comparison test to compare the means of all columns. Concentration response curves were fitted with the Hill equation:  $Y = [(X)^H \times M] / [(X)^H + (EC_{50})^H]$ , Y is the response, X is the agonist concentration, H is the Hill coefficient, M is the maximum response and EC<sub>50</sub> is the concentration of ATP that evokes 50% of the maximum response. Inhibition curves were fitted with the same formula, with IC<sub>50</sub> values instead of EC<sub>50</sub> values. The curves were fitted to mean, normalised data.

## 2.4 Molecular Modelling

The homology models of the ATP bound and closed hP2X1 receptors used in this thesis was constructed by Ralf Schmid (Department of Biochemistry, University of Leicester) and assembled using Modeller v9.7 software. The structure of the ATP bound and closed zfP2X4 receptors (PDBid = 4DW1 and 4DW0) were used as a basis for this modelling. Various models were generated and those likely to be most accurate identified using Modeller's scoring function and external validation via Whatcheck and PROSA.

The homology model of the closed resting hP2X1 receptor was used to generate NF449 docked models (Ralf Schmid, University of Leicester). The NF449 molecule was built using Hyperchem 8.0 and steepest descent energy minimisation was performed. The molecule was docked to the structure using the GOLD package (Verdonk *et al.*, 2003). The location of NF449 binding was defined as within a 20 Å radius of residues K136, K136, R139, K140 or T216, H224, Q231 which were identified in later chapters as being important in NF449 action. The docked poses of NF449 were then ranked by their ChemScores and those that fit best with the data were chosen by hand. All images of the homology model were assembled in PyMOL (Molecular Graphics System, Version 1.2r3, Schrodinger, LLC.).

## 2.5 Protein Purification

### 2.5.1 zfP2X4 constructs

The zfP2X4C(FNDAR) receptor cDNA was a gift from Professor Eric Gouaux (Vollum Institute, Portland, OR, USA). Two plasmids were supplied, one in the pcDNA3.1 vector and one in the pFastBac vector. For expression in HEK cells the zfP2X4C(FNDAR) DNA was sub-cloned into the pLEICS12 vector, an adapted version of the pcDNA3.1 vector (figure 6.10). This vector had Histidine and FLAG tags as well as a T7 promoter, TEV site and ampicillin resistance gene. Sub-cloning was performed by the Protein Expression Laboratory (PROTEX), University of Leicester, and the 3 point mutations F139K, D141K and A142R introduced at the same time to produce the zfP2X4C(KNKRR) receptor. The DNA was transformed into *E. Coli* and maxipreps were performed using a maxiprep kit (Qiagen) to obtain the high concentrations of DNA required for transfection.

### 2.5.2 HEK Cell Culture and Transfection

HEK293F cells (Invitrogen) were grown in Gibco® FreeStyle™ 293 Expression Medium. 30 ml cultures in 250 ml Corning Erlenmeyer Polycarbonate flasks were grown at 37°C in a shaking incubator and gassed with 5% CO<sub>2</sub> mix. Cells were split to a density of 0.5 x 10<sup>6</sup>/ml every 2 days as a stock concentration. Transfection of cells with zfP2X4C(FNDAR) and

zfP2X4C(KNKRR) was performed at a density of  $1 \times 10^6$ /ml. For the transfection 3 ml PBS was mixed with 30 µg DNA and vortexed briefly. 120 µl polyethylenimine at 0.5mg/ml (Sigma) was added and the mixture vortexed and incubated for 20 minutes at room temperature. This was added to 27 ml of the cell culture and mixed by swirling. Cells were stored in the shaking CO<sub>2</sub> incubator at 37°C for 48 hours before harvesting. To harvest cell cultures (30-120 ml) were spun for 5 minutes at 5000 x g to collect cells in a pellet. The pellet was resuspended in either lysis buffer A or lysis buffer B, vortexed and sonicated for 10 s on a medium setting. Lysis buffer A consisted of 150 mM NaCl, 40 mM Tris HCl (pH7.5), 8 mM Tris base and protease inhibitor mixture (Sigma). Lysis buffer B was 50 mM Tris, pH to 7.4, 0.5 M NaCl, 10% glycerol. The sample was then either mixed directly with magnetic beads for immunoprecipitation or membrane isolation was performed before adding to the beads.

### **2.5.3 Membrane Isolation**

To increase the purity of the protein sample obtained, membrane proteins were isolated from the rest of the cell protein. The protocol was performed on ice or at 4°C.

- (a) The pellet of cells was resuspended in 5 ml buffer B (50 mM Tris, pH to 7.4, 0.5 M NaCl, 10% glycerol) and vortexed.
- (b) The suspension was sonicated for 10 s on a medium setting.
- (c) Cell debris was removed by centrifugation at 5000 x g for 5 min at 4°C and the supernatant containing the membrane proteins retained.
- (d) Cell membranes were pelleted by ultracentrifugation for 1 hour at 125,000 x g at 4°C
- (e) Pellet was resuspended and lysed in 0.5 ml buffer B + 1% DDM and homogenised gently using a Dounce homogeniser.
- (f) Sample was left on a shaking platform for 2 hours at 4°C

(g) Membrane proteins were collected by ultracentrifugation at 125,000 x g for 1 hour at 4°C and the supernatant containing the P2X receptor retained.

#### **2.5.4 Immunoprecipitation**

Samples of 200 µl of either total cell proteins or membrane proteins were added to 70 µl antibody-coupled beads and the mixture rolled overnight at 4°C to allow any tagged proteins to bind to the beads. Two types of antibody coupled beads were used, either anti-FLAG or nickel (anti-His). For flag beads buffer A/B + 1% DDM was used for washes and protein was eluted using 0.5 mg/ml flag peptide contained in this buffer. For nickel beads washes were performed in buffer A (1% DDM) + 25 mM imidazole. Elutions were performed using buffer A + 250 mM imidazole.

- (a) Beads were spun at 13000 rpm, 4°C for 5 minutes and the flow through collected and retained.
- (b) Beads were washed with the appropriate buffer, vortexed and spun for 5 minutes at 13000 rpm, 4°C and supernatant removed. This was repeated four times to remove any protein that did not include the appropriate tag.
- (c) Tagged proteins were eluted by addition of 70 µl of either 0.5mg/ml flag peptide or 250 mM imidazole. In order to increase the amount of protein eluted, beads were left to roll with the eluting buffer for 10 minutes before spinning for 5 minutes at 13000 rpm, 4°C. Supernatant containing the protein was retained. 3 elutions were performed.
- (d) A final elution in SDS + 10% 2-Mercaptoethanol was performed to remove all protein from the beads.

- (e) Samples were mixed with LDS running buffer (1:1) and 5% 2-mercaptoethanol and 30  $\mu$ l was loaded onto precast NuPAGE 4-12% Bis-Tris gels (Novex). Gels were run at 150 V for 100 minutes.
- (f) The gel was placed in InstantBlue (Expedian) a coomassie based protein stain for one hour to identify any protein in the gel.
- (g) Bands of the correct size (~65 kDa) were cut out of the gel and sent for mass spectrometry by PNACL so that the protein could be identified.

## **Chapter 3: Receptor Characterisation and the Contribution of the Extracellular Loop to Antagonism**

### **3.1 Introduction**

The properties of recombinant P2X receptors vary dependent on the subunit composition (see section 1.4) and are due to differences in the amino acid sequences between the subunits. Chimeras have often been generated between subunits with contrasting properties to identify which variant amino acids are contributing to the different characteristics. This chimera technique allows the contribution of sections of the receptor incorporating several variant residues to be determined at the same time. Important variant regions, and those which are not contributing to the differences in properties, can then be identified.

#### **3.1.1 The Use of Chimeras to Investigate P2X Receptor Properties**

The first use of chimeras to investigate properties of P2X receptors looked at regions involved in the control of the time-course of the ATP evoked response. The WT P2X1 receptor displayed rapid desensitisation during a 10 s, ATP (100 µM) application whilst the P2X2 receptor showed little decay in current during this period (90% and 14% respectively) (Werner *et al.*, 1996). There is 37% sequence homology between these receptors and chimeras were generated in order to determine the contribution of regions of the receptor to desensitisation. Three initial chimeras were made to swap the N terminus and TM1, the extracellular loop, and TM2 and the C-terminus of the receptors. When either the N terminus and TM1 or C terminus and TM2 of the P2X1 receptor was replaced with that of the P2X2 receptor, desensitisation was greatly reduced, with only 2% and 13% desensitisation being seen for these chimeras respectively (Werner *et al.*, 1996). Generation of smaller sub-chimeras identified that it was the swap of residues 14-47 of the N-terminus and TM1 within the first chimera and 332-365 of TM2 and the C terminus in the second that was vital for the decrease in desensitisation. Swapping the extracellular loop had no effect on desensitisation. Interestingly both termini and parts of the transmembrane domains of the P2X1 receptor had to be introduced to the P2X2 receptor in order to confer P2X1-like desensitisation

(Werner *et al.*, 1996). This suggests that an interaction between the two TMs and the intracellular sections is required for the receptor to exhibit rapid desensitisation, but which particular residues within these sections are important was not investigated.

Further chimeric studies have been performed on the P2X1 and P2X2 receptors looking at the interdependence of the transmembrane domains and intracellular regions in the control of time-course (Allsopp & Evans, 2011). This study aimed to identify smaller regions and specific residues within the sections identified by Werner *et al* that were contributing to this property. There was no contribution of variant amino acids within the extracellular loop to the difference in desensitisation between the WT receptors. Swapping the extracellular loops or both transmembrane domains of the P2X2 receptor into the P2X1 receptor showed no effect on the response, but there was an effect of chimeras which swapped one TM at a time and intracellular region chimeras. The chimeras which swapped the extracellular loops in this study were called P2X1-2EXT and P2X2-1EXT and are further characterised for antagonists later in this chapter. The N-terminus was highlighted as having a considerable role in desensitisation, as swapping this region of the P2X1 receptor with corresponding residues of the P2X2 receptor decreased desensitisation ~ 3.5 fold (Allsopp & Evans, 2011). The reciprocal chimera which swapped the N-terminus of the P2X1 receptor into the P2X2 receptor introduced P2X1 like desensitisation. Using sub-chimeras and point mutations, the variant residues responsible for this response were identified as 17 and 20-23 (Allsopp & Evans, 2011). These studies are an example of how chimeras can be used to identify regions contributing to a particular property that can be further divided into subchimeras to highlight specific residues that are contributing.

### 3.1.2 P2X Receptor Antagonism and the Extracellular Loop

Allsopp *et al* developed a range of chimeras which allowed the identification of residues contributing to time-course and partial agonism. However antagonism at these chimeras was not tested. There is a difference in suramin, NF449 and PPADS antagonism between the WT hP2X1 and hP2X2 receptors as described in chapter 1.9. The P2X2 receptor shows an ~ 10-fold

decrease in suramin and PPADS potency compared to the P2X1 receptor and an ~ 1000-fold decrease in NF449 sensitivity. The chimeras swapping regions between the hP2X1 and hP2X2 receptors could therefore be used to investigate residues involved in antagonist action at the receptors. As suramin, NF449 and PPADS are all unable to cross the cell membrane and are applied extracellularly, it was hypothesised that they bind to the extracellular loop of the receptor. The P2X1-2EXT and P2X2-1EXT chimeras were therefore used to test if residues in the extracellular loop of the receptor determined antagonist sensitivity. The rP2X4 receptor was also characterised in this chapter. This receptor is insensitive to the P2X1 receptor antagonists suramin, NF449 and PPADS and it was hoped that this antagonist insensitivity could be exploited in later chapters to give insight into antagonist binding.

### **3.1.3 Chapter Aims**

In order to exploit the differences between the hP2X1, hP2X2 and rP2X4 receptors through chimera generation, it was first necessary to characterise the responses of the WT receptors to ATP and antagonists. This allows any differences between the WT and chimeric receptors to be determined. The second aim was to identify if the extracellular loop region of the receptor was responsible for antagonist sensitivity. To do this suramin, NF449 and PPADS antagonism was determined at chimeras P2X1-2EXT and P2X2-1EXT between the P2X1 and P2X2 receptors, that had previously been made by Dr Allsopp (Allsopp & Evans, 2011).

## **3.2 Results**

Two-electrode voltage clamp experiments were performed in order to characterise the properties of ATP gated P2X receptors expressed in *Xenopus laevis* oocytes. The responses of wild-type hP2X1, hP2X2 and rP2X4 receptors to ATP were studied. The membrane potential of the oocyte was held at -60 mV and ATP was applied for 3 seconds via a U-tube perfusion system. The channel activity of the expressed P2X receptors was recorded by measuring the amount of current required to maintain the membrane potential at -60 mV. In order to get a stable, reproducible response a period of time in the absence

of agonist was needed between each application to allow complete solution exchange and for the receptors to recover from any desensitisation. This was 5 minutes for the hP2X1 receptor, 2 minutes for the hP2X2 receptor and 7-10 minutes for the rP2X4 receptor.

### **3.2.1 ATP Potency at WT Receptors**

Responses to ATP at the three WT receptors were concentration dependent (figure 3.1a). The concentration of ATP at which a maximal response was reached ( $ATP_{max}$ ) varied among receptors (100  $\mu$ M ATP at the hP2X1 and rP2X4 receptors, 300  $\mu$ M at the hP2X2 receptor). The mean peak amplitudes to  $ATP_{max}$  at the hP2X1, hP2X2 and rP2X4 receptors were  $7598 \pm 793$ ,  $4279 \pm 327$  and  $5320 \pm 586$  nA respectively. Once reproducible responses to  $ATP_{max}$  had been obtained, lower concentrations of ATP could be applied and a full sigmoidal concentration response curve generated (figure 3.1b). The  $pEC_{50}$  value was used as a measure of potency. This is the negative logarithm of the concentration of ATP required to evoke 50% of the maximal response. ATP was most potent at the hP2X1 receptor, where the  $pEC_{50}$  value was  $6.31 \pm 0.04$ . The hP2X2 and rP2X4 receptor curves were rightward shifted  $\sim 18$  and  $\sim 8$  fold respectively compared to the hP2X1 receptor, signifying a decreased ATP potency ( $pEC_{50} = 5.04 \pm 0.07$ ,  $p < 0.0001$  and  $5.37 \pm 0.05$ ,  $p < 0.001$  respectively). These values are consistent with previous studies at these receptors (North, 2002).

### **3.2.2 Time-course of the ATP Evoked Response**

Application of ATP to the oocytes expressing hP2X1, hP2X2 or rP2X4 receptors caused a rapid influx of ions through the channel, recorded as a downward deflection in current from the baseline (figure 3.2b). At the hP2X1 and rP2X4 receptors this inward current decayed back toward baseline during the continued  $ATP_{max}$  application; this is called desensitisation (figure 3.2c). An obvious difference in the amount of desensitisation could be seen between the WT receptors (figure 3.2a). At the end of the application, ATP was washed out

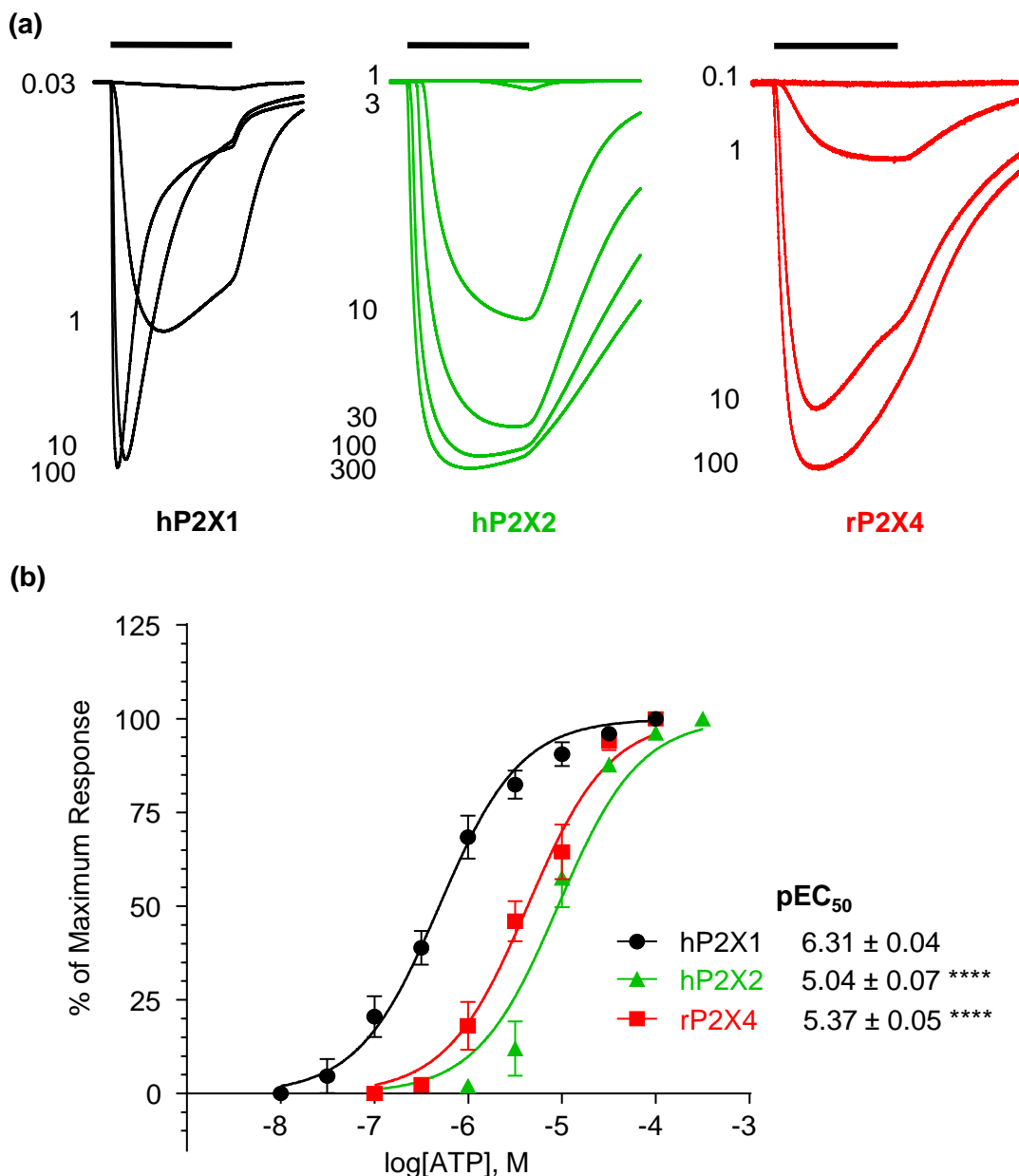


**Figure 3.1 ATP Evoked Concentration Dependent Currents at the WT hP2X1, hP2X2 and rP2X4 Receptors.** (a) Representative traces of different ATP concentrations ( $\mu\text{M}$ ) applied to *Xenopus* oocytes expressing the WT hP2X1, hP2X2 and rP2X4 receptors, with 5 -10 min intervals between each application dependent on subtype. Traces were normalised for peak currents to allow comparison. The bar indicates a 3 s ATP application. (b) Concentration response curves for the WT receptors,  $pEC_{50}$  values are given ( $n \geq 5$ ). Stars indicate a significant difference from the hP2X1 receptor \*\*\*\*  $p < 0.0001$ .

and any remaining current decayed back to basal levels. The time-course of the response of each of the WT receptors to ATP was both concentration and subtype dependent. To observe the effects on time-course, two concentrations were chosen at which the differences were most evident. These were ATP<sub>max</sub> and a concentration which gave 10-20% of the maximal response (ATP<sub>low</sub>). The low ATP concentration was 0.1 µM for the hP2X1 receptor, 3µM at the hP2X2 receptor and 1µM at the rP2X4 receptor.

The rise time and percentage decay of each receptor were calculated in order to give a comparison of the time-course of the responses. The rise time was defined as the time it takes the current to increase from 10% to 90% of the maximum response (figure 3.2b). At ATP<sub>max</sub> the rise time was fastest at the hP2X1 receptor ( $95.7 \pm 5.1$  ms) and ~ 4-fold slower at the hP2X2 and hP2X4 receptors,  $p < 0.0001$  ( $402.8 \pm 23.9$  and  $393.3 \pm 88.6$  ms respectively). The rise times were significantly slower at each receptor when ATP<sub>low</sub> was applied compared to ATP<sub>max</sub>; hP2X1 =  $667 \pm 264$  ms,  $p < 0.01$ , hP2X2 =  $1141 \pm 169$  ms,  $p < 0.05$ , and rP2X4 =  $1795 \pm 310$  ms,  $p < 0.0001$  (figure 3.2b).

Dependent on receptor subtype, the current did not always decay to 50% of maximum within the 3 second ATP application, the most commonly used measurement of desensitisation in the literature, and so the time at which the current has decreased by 50% from the peak, could not be used. I therefore measured the % desensitisation that had occurred from the peak current at the end of the 3 second ATP application (figure 3.2c). At ATP<sub>(max)</sub> the hP2X1 receptor current showed near complete desensitisation during the ATP application ( $80.3 \pm 4.3\%$ ). The rP2X4 and hP2X2 receptors desensitised significantly less within the three seconds ( $31.9 \pm 3.5\%$ ,  $p < 0.0001$  and  $3.6 \pm 0.2\%$ ,  $p < 0.0001$  respectively), see figure 3.2c. There was very little desensitisation at the hP2X2 receptor which allows sustained current flow at ATP<sub>max</sub>. A comparison was also made of % desensitisation at maximal and low concentrations of ATP at each receptor (figure 3.2c). Although all 3 receptors showed a decrease in the % desensitisation at ATP<sub>low</sub> compared to ATP<sub>max</sub>, this was only significant for the hP2X1 receptor ( $37.1 \pm 11.6\%$ ,  $p < 0.0001$ ).

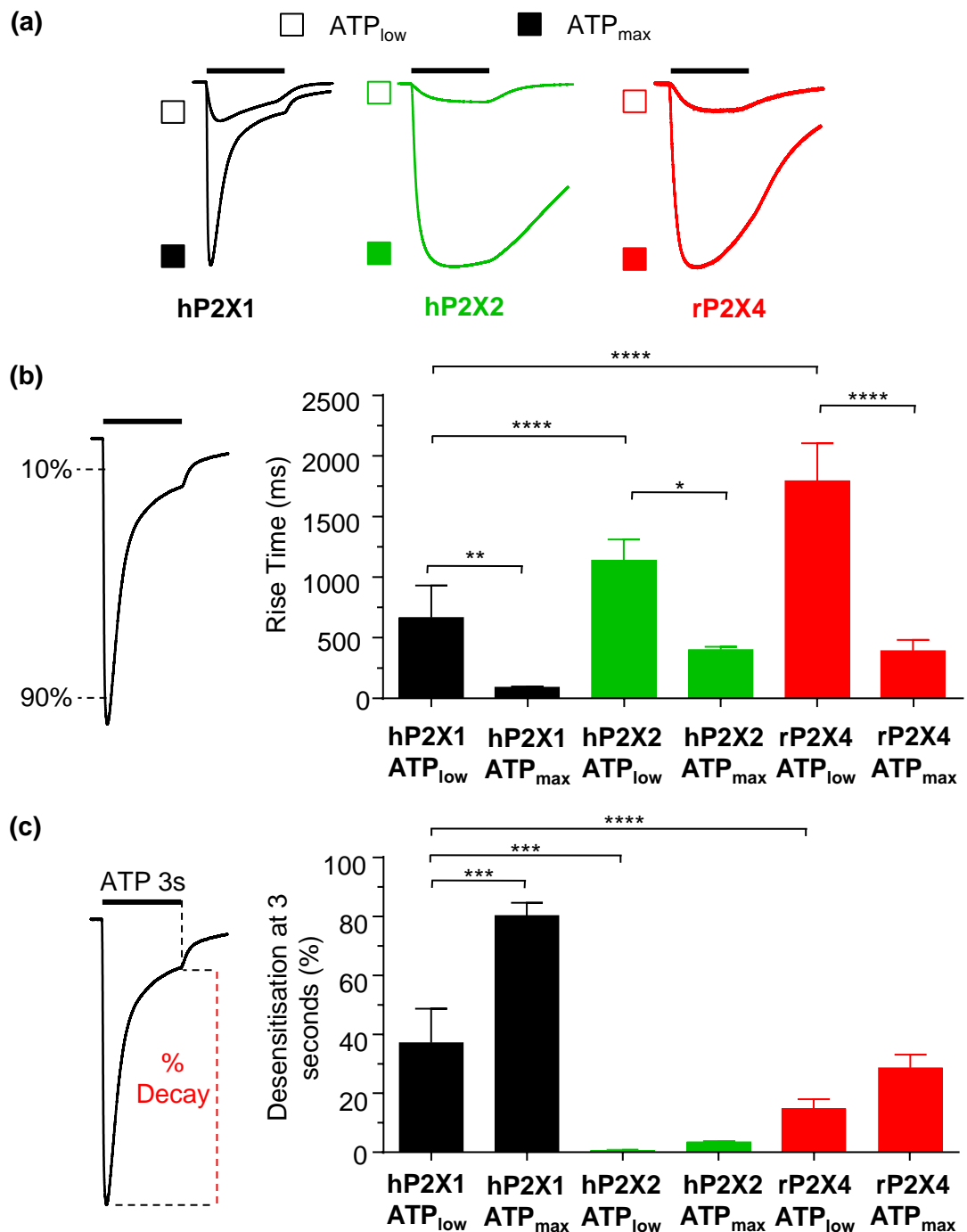


**Figure 3.2 Time-course of the WT Receptors in Response to ATP** (a) Representative traces of application of ATP<sub>max</sub> and ATP<sub>low</sub> to Xenopus oocytes expressing WT hP2X1, hP2X2 and rP2X4 receptors. Traces were normalised for peak currents to allow comparison. Bars represent a 3 s ATP application. (b) Rise time was the time taken for current to increase from 10 to 90% of the peak amplitude. A comparison is shown of the rise times at each receptor for ATP<sub>low</sub> and ATP<sub>max</sub>. (c) % desensitisation was measured as the % of peak current remaining at the end of the 3 s ATP application. % desensitisation at ATP<sub>max</sub> and ATP<sub>low</sub> were compared for each receptor. Stars indicate significance \* p<0.05, \*\* p<0.01, \*\*\* p<0.001. \*\*\*\* p<0.0001

### **3.2.3 Antagonism at the WT Receptors**

There are a variety of P2X receptor antagonists available; the three most commonly used for the hP2X1 receptor subtype are suramin, NF449 and PPADS. The molecular basis of how they bind to the hP2X1 receptor is largely unknown. The effects of these antagonists on the three WT receptors were therefore examined.

To account for the varied ATP potency between the receptors a standardised ATP concentration needed to be used when the antagonist was applied. Therefore the individual EC<sub>90</sub> concentration of ATP was deduced from the concentration response curves and used at each receptor in all antagonism experiments. Each antagonist was bath perfused around the oocyte for 5 minutes prior to a 3 s U-tube co-application of the antagonist and EC<sub>90</sub> ATP. This bath perfusion was to allow equilibration and was utilised before each application of antagonist throughout the thesis. A high concentration of each antagonist was also applied at the three receptors in the absence of agonist to see if it had any agonist effects. These concentrations were 100 µM for suramin and PPADS and 1 µM NF449. None of the antagonists had an effect at any of the receptors when applied alone as was seen for all WT, chimeric and point mutated receptors in this thesis. Each antagonist concentration was also initially applied at least twice to make sure the response had stabilised before further applications were made. This protocol was used for all antagonist experiments throughout this thesis.

### **3.2.4 Suramin Action at WT Receptors**

The effect of suramin application on both time-course and peak currents of the response to ATP at the three WT receptors was examined. There was an ~ 100-fold difference in suramin sensitivity between the hP2X1 and hP2X2 receptors with ~ 50% inhibition evoked by 1 µM suramin at the hP2X1 receptor and by 100 µM suramin at the hP2X2 receptor. There was no inhibition at the rP2X4 receptor up to a concentration of 100 µM (figure 3.3a). Inhibition by suramin was concentration dependent at the hP2X1 and hP2X2 receptors, with % inhibition increasing with suramin concentration until no current was

produced by ATP at the highest suramin concentrations tested (figure 3.3b). The  $\text{pIC}_{50}$  was used as a measure of antagonist potency in this thesis. The  $\text{pIC}_{50}$  is the negative logarithm of the concentration of antagonist required to cause 50% inhibition. Suramin was most potent at the hP2X1 receptor, causing a total block of the receptor at 100  $\mu\text{M}$  suramin and a  $\text{pIC}_{50}$  of  $5.98 \pm 0.04$ . The hP2X2 receptor was  $\sim$  40-fold less sensitive to suramin than the hP2X1 receptor compared to the hP2X1 receptor,  $\text{pIC}_{50} = 4.36 \pm 0.05$ ,  $p<0.0001$ . The rP2X4 was insensitive to suramin at the concentrations tested (figure 3.3b). These results are consistent with the literature (North, 2002).

The presence of suramin also affected the time-course of responses to ATP of the hP2X1 and hP2X2 receptors. The rise time for the hP2X1 and hP2X2 receptors was  $\sim$  7-fold and  $\sim$  3-fold slower when a high concentration of suramin was co-applied (fig 3.4 a,b). This was a concentration that gave  $> 80\%$  inhibition at the hP2X1 and hP2X2 receptors (10 and 300  $\mu\text{M}$  respectively), and was the maximum concentration tested at the rP2X4 receptor (100  $\mu\text{M}$ ). There was no effect of 100  $\mu\text{M}$  suramin on the rise time of the rP2X4 receptor. The hP2X1 receptor had an  $\sim$  7-fold decrease in % desensitisation in the presence of suramin ( $73.2 \pm 4.8\%$  in  $\text{EC}_{90}$  ATP alone and  $11.7 \pm 2.1\%$  in  $\text{EC}_{90}$  ATP and suramin,  $p<0.0001$ ). The hP2X2 receptor showed very little desensitisation in either condition (figure 3.4c) and the rP2X4 receptor showed  $\sim$  20% desensitisation in both the presence and absence of suramin, again showing that the antagonist has no effect on this receptor (figure 3.4c). These results show that suramin both decreases the amount of current recorded at the hP2X1 and hP2X2 receptors, and has an effect on the time-course of their response to ATP, consistent with a competitive mode of action of the antagonist. In contrast the rP2X4 receptor was unaffected by suramin in either current amplitude or time-course.

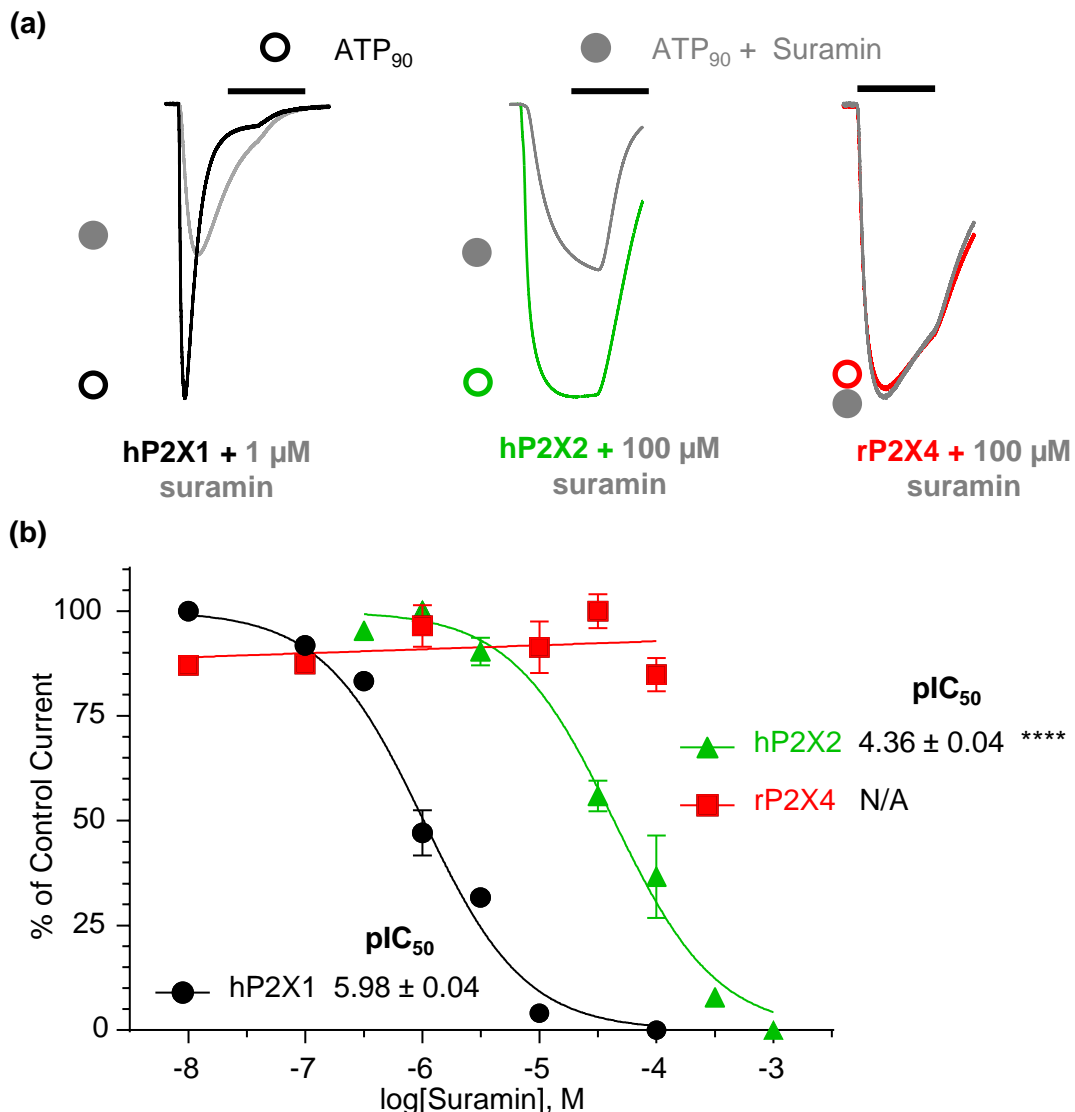


**Figure 3.3 Inhibition of ATP Currents by Suramin.** (a) Representative traces for EC<sub>90</sub> ATP (ATP<sub>90</sub>, open circles) and ATP<sub>90</sub> + suramin (closed circles) application to *Xenopus* oocytes expressing the WT hP2X1, hP2X2 and rP2X4 receptors. Bars represent a 3 s application. Traces are normalised to peak currents to allow comparison. Suramin was perfused around the oocyte for 5 minutes before application of ATP and there was a 5-10 min recovery period between each application dependent on subtype. (b) Inhibition curves for suramin at the WT receptors. pIC<sub>50</sub> values are shown. Stars indicate a significant difference from the hP2X1 receptor. \*\*\*\* p<0.0001.

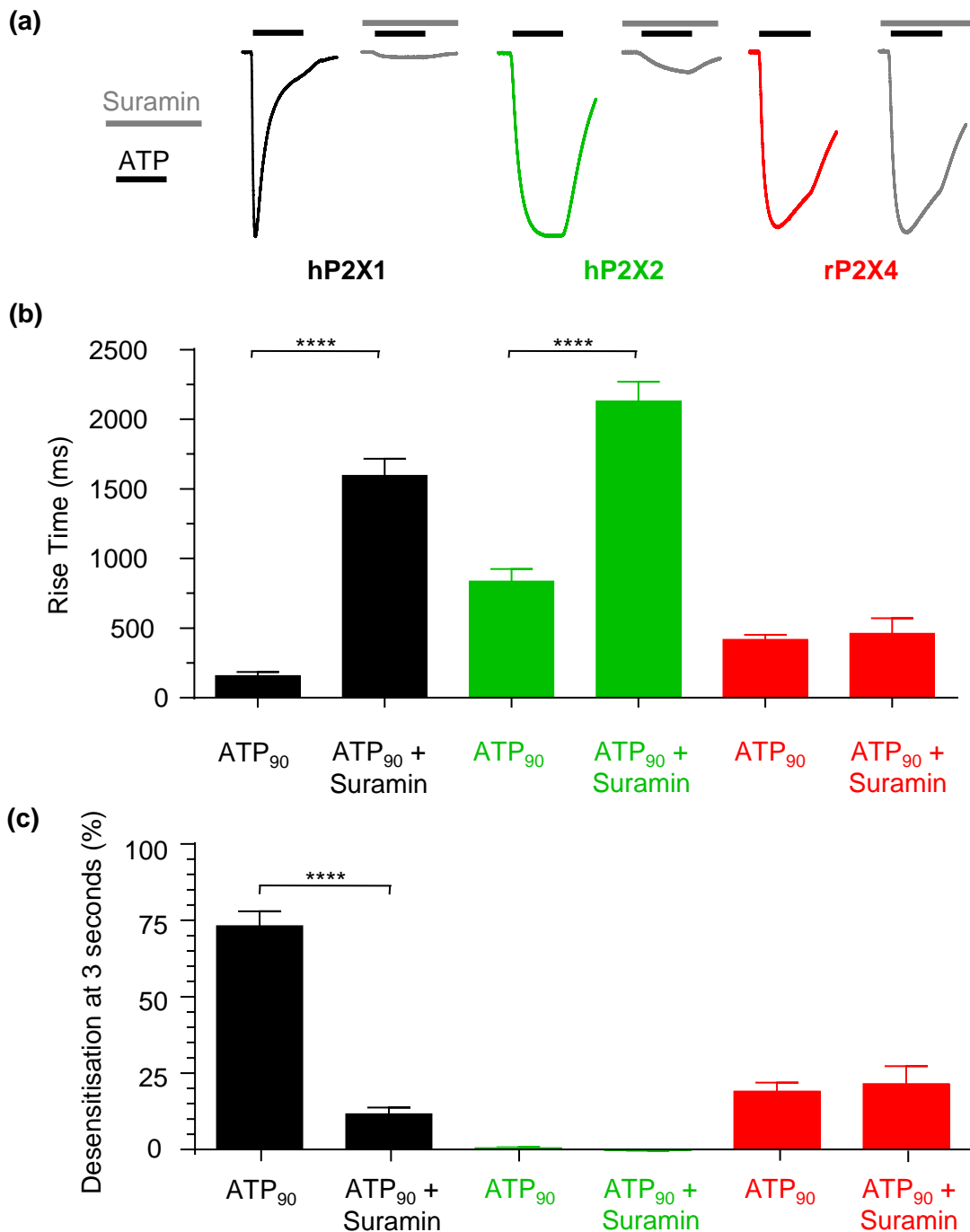


**Figure 3.4 Rise Times and % Desensitisation of WT Receptors in the Presence of Suramin.** (a) Representative traces for each of the conditions tested. Black bars represent a 3 s ATP application, dark grey bars show suramin application. Traces have been normalised to peak currents for comparison (b) A comparison of the rise time of each receptor in ATP<sub>90</sub> only and ATP<sub>90</sub> plus suramin. At hP2X1 and hP2X2 receptors this concentration gave > 80% inhibition. At the rP2X4 receptor 100  $\mu$ M suramin was applied. (c) Comparison of the % desensitisation at the end of the ATP application in ATP<sub>90</sub> and ATP<sub>90</sub> plus suramin. Stars indicate a significant difference. \*\*\* p<0.0001.

### **3.2.5 PPADS at WT Receptors**

PPADS inhibition was also determined at the WT receptors (figure 3.5). Co-application of PPADS (0.03 – 100  $\mu$ M) with EC<sub>90</sub> ATP inhibited the ATP evoked current at the hP2X1 and hP2X2 receptors. This inhibition was concentration dependent and a maximal concentration of PPADS (PPADS<sub>max</sub>) caused a total block of the receptors. Only ~ 25% inhibition was seen at the rP2X4 receptor at a concentration of 100  $\mu$ M PPADS, making the receptor relatively insensitive to PPADS (figure 3.5b). Inhibition curves showed that the pIC<sub>50</sub> of the hP2X1 receptor was 5.80 ± 0.03. PPADS was more potent at the hP2X2 receptor where 1  $\mu$ M caused an ~ 70% inhibition, pIC<sub>50</sub> 6.40 ± 0.05, p<0.01 (figure 3.5b).

PPADS had less of an effect on receptor time-course than was seen with suramin. A concentration of PPADS that caused > 80% inhibition was used at the hP2X1 and hP2X2 receptors (10  $\mu$ M and 3  $\mu$ M respectively) and the maximum concentration tested (100  $\mu$ M) was used at the rP2X4 receptor. There was an ~ 1.8-fold slowing in the rise time of the hP2X2 receptor in the presence of PPADS (1.60 ± 0.18 with PPADS and 0.91 ± 0.10 without, p<0.0001, figure 3.6 a,b). However, the rise times of the hP2X1 and rP2X4 receptors were unaffected. There was no effect of PPADS on the % desensitisation of any of the WT receptors (figure 3.6b).

### **3.2.6 NF449 at WT Receptors**

NF449 potently inhibited the hP2X1 receptor, 1 nM NF449 inhibited currents by ~50% (figure 3.7a). A concentration of 1  $\mu$ M was required to cause a similar amount of inhibition at the hP2X2 receptor. Inhibition curves showed that at the hP2X1 receptor, NF449 had a pIC<sub>50</sub> of 8.94 ± 0.05 (figure 3.8b). The hP2X2 receptor was ~ 1400-fold less sensitive to the antagonist than the hP2X1 receptor, pIC<sub>50</sub> = 5.78 ± 0.05, p<0.0001. At the rP2X4 receptor 1  $\mu$ M NF449 had no effect on ATP responses indicating that the receptor is insensitive to this antagonist.

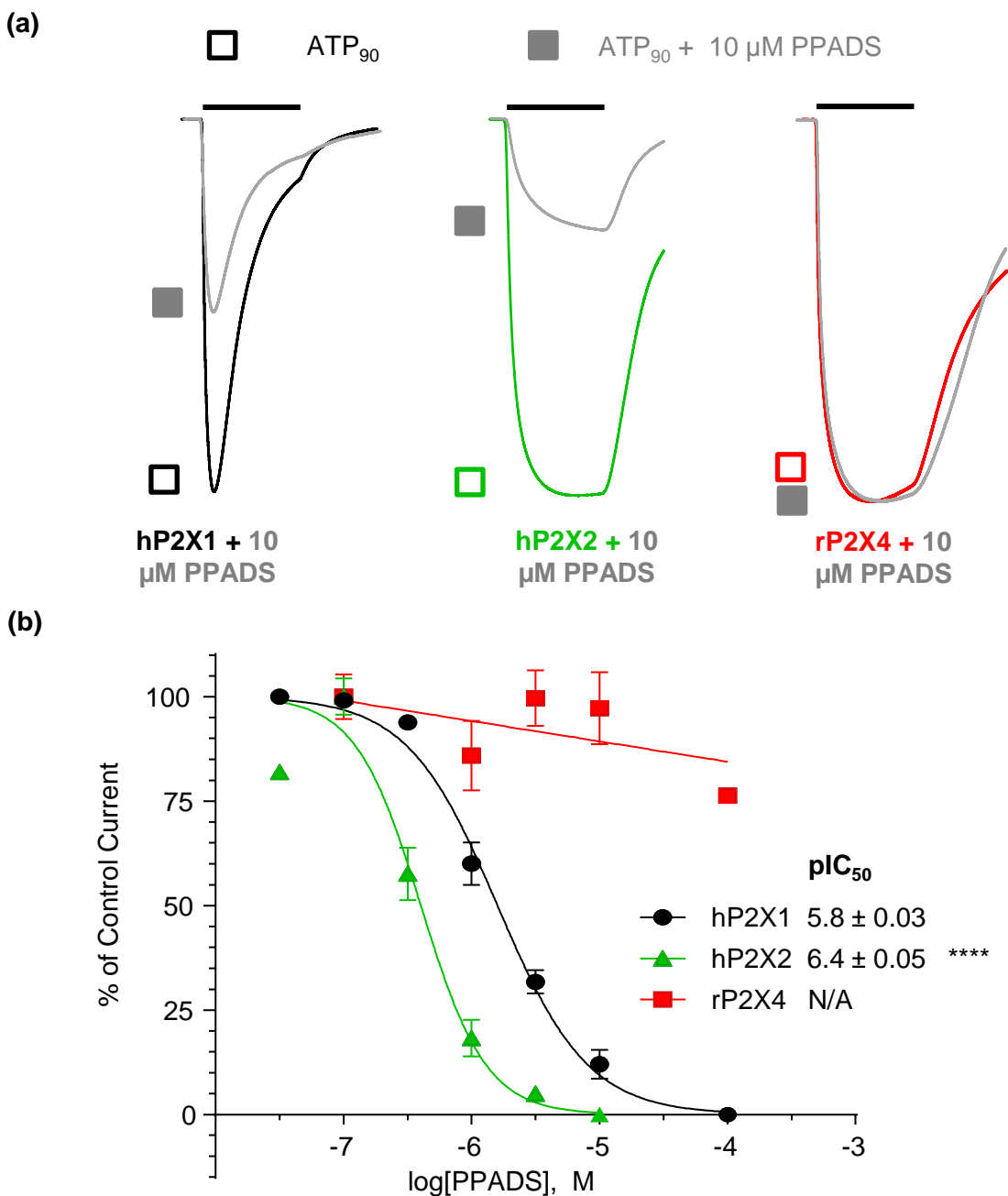


**Figure 3.5 Inhibition of ATP Induced Currents by PPADS.** (a) Representative traces of 10  $\mu$ M PPADS action at *Xenopus* oocytes expressing the WT hP2X1, hP2X2 and rP2X4 receptors. There was a 5-10 minute recovery period between each application to allow for recovery from desensitisation. Bars indicate a 3 s ATP<sub>90</sub> or ATP<sub>90</sub> + PPADS application. PPADS was perfused around the oocyte for 5 minutes before co-application of ATP. Traces are normalised to peak currents for comparison. (b) Inhibition curves for PPADS at WT receptors. The pIC<sub>50</sub> values are shown. Stars indicate a significant difference from the hP2X1 receptor. \*\*\*p<0.0001.

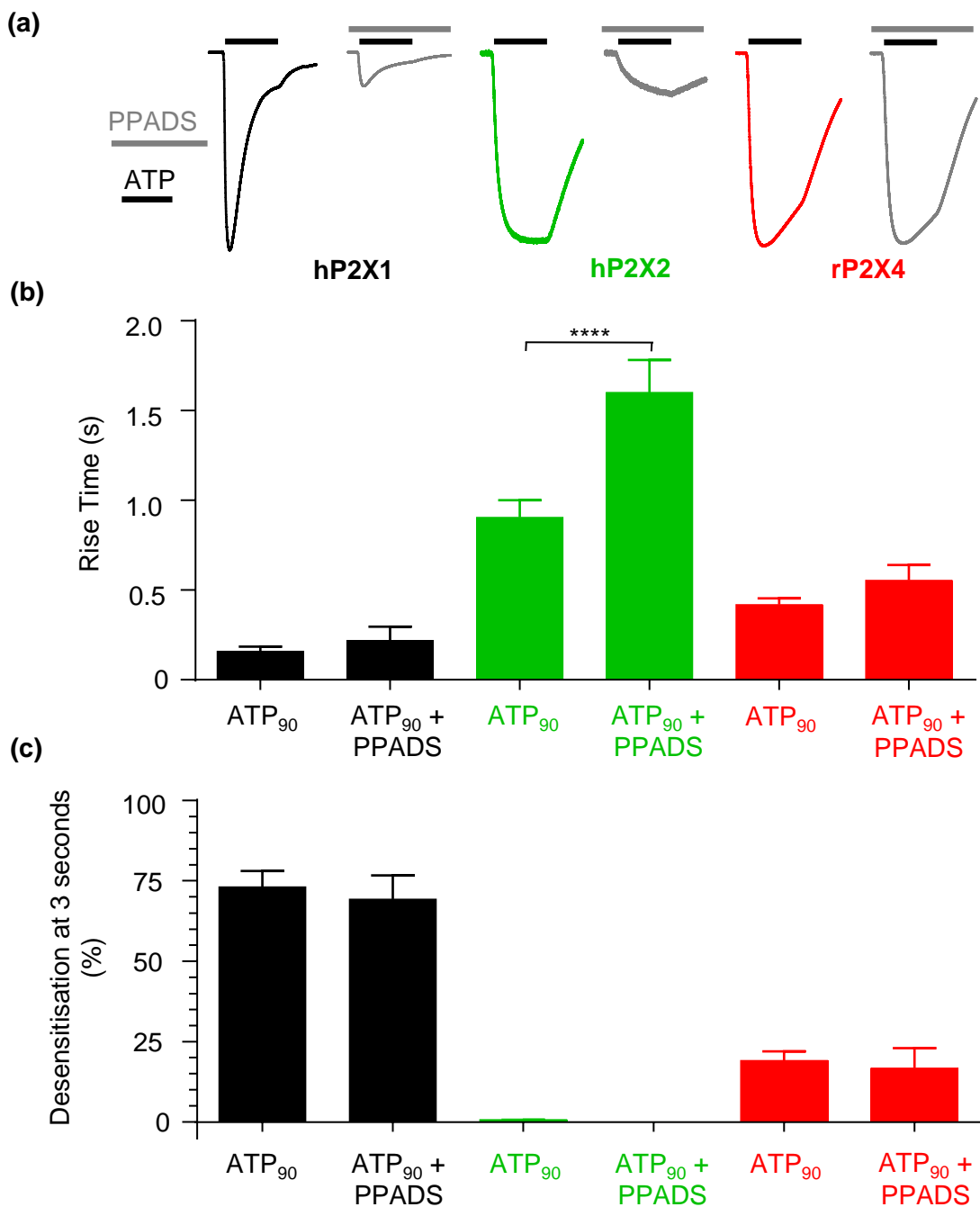


**Figure 3.6 Effects of PPADS on the Time-course of the WT Receptors.** (a) Representative traces of each of the conditions at the WT receptors. Black bars represent a 3 s ATP application. Dark grey bars show PPADS application. At hP2X1 and hP2X2 receptors a PPADS concentration was used that gave > 80% inhibition. At the rP2X4 receptor 100  $\mu$ M PPADS was applied. Traces have been normalised to the peak currents to allow for comparison. (b) A comparison of the rise time of each receptor in ATP<sub>90</sub> only and ATP<sub>90</sub> plus PPADS. (c) Effects of PPADS on the % desensitisation at the end of the ATP application. Stars indicate a significant difference. \*\*\* p<0.0001

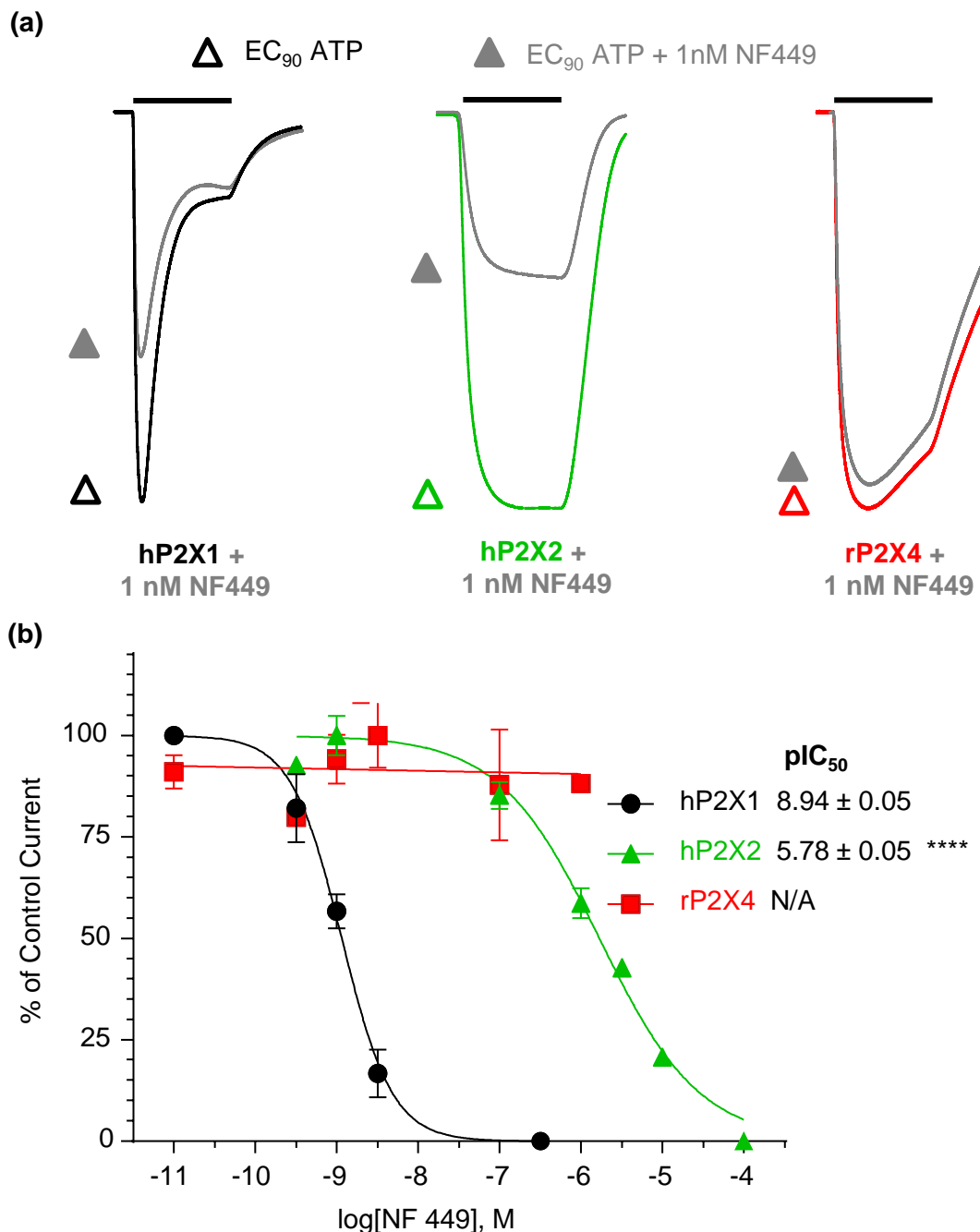


**Figure 3.7 NF449 inhibition at the WT receptors.** (a) Representative traces to show inhibition by NF449 at the WT hP2X1, hP2X2 and rP2X4 receptors. Bars indicate a 3s application. Traces were normalised to peak currents to allow comparison. A 5-10 minute period was given between each application to allow for recovery from desensitisation. (b) Inhibition curves for the WT receptors. pIC<sub>50</sub> values are shown. Stars indicate a significant difference from the hP2X1 receptor. \*\*\*\* p < 0.0001.

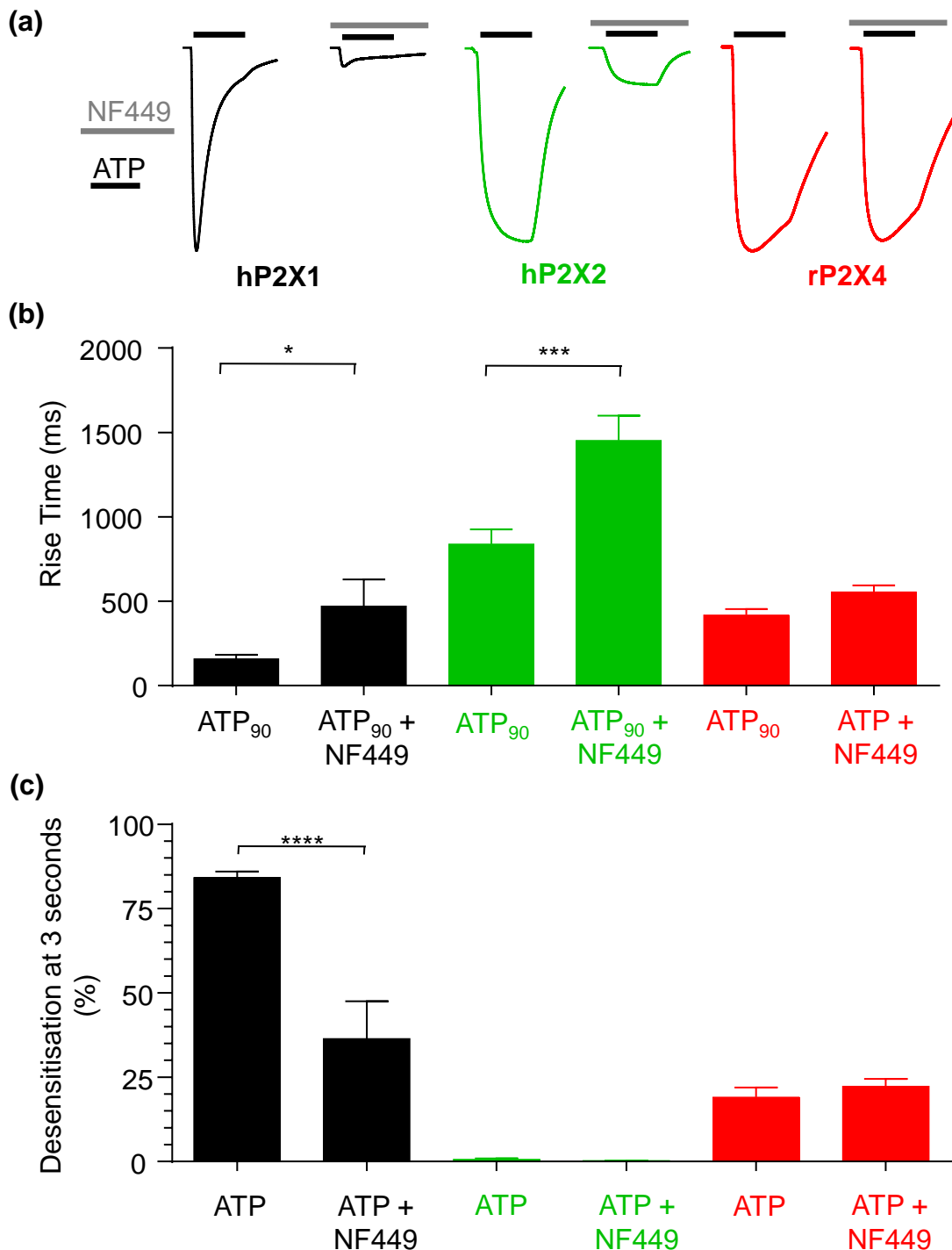


**Figure 3.8 The Influence of NF449 on the Time-course of the hP2X1 and hP2X2 and rP2X4 receptors** (a) Representative traces of each of the conditions tested. Bars represent a 3 s application. (b) Comparison of the rise time of each receptor in ATP<sub>90</sub> only and ATP<sub>90</sub> plus NF449. At hP2X1 and hP2X2 receptors a NF449 concentration which gave > 80% inhibition was used. At the rP2X4 receptor 1  $\mu$ M NF449 was applied. (c) Effects of NF449 on the % desensitisation at the end of the ATP application. Stars indicate a significant difference. \* p<0.05, \*\*\* p<0.001, \*\*\*\* p<0.0001.

Inhibition by NF449 of ATP evoked currents resulted in a slowing in their time-course. An NF449 concentration that caused > 75% inhibition was used at the hP2X1 and hP2X2 receptors (10 nM and 10 µM respectively) and the maximum concentration tested (1 µM) was used at the rP2X4 receptor. At the hP2X2 receptor the rise time was ~ 1.5-fold slower in the presence of NF449 than ATP alone ( $1.3 \pm 0.3$  and  $0.85 \pm 0.09$  ms respectively,  $p<0.05$ ), figure 3.8a. The rise times of the hP2X1 and rP2X4 receptors did not differ in the presence of NF449. Only the hP2X1 receptor differed in desensitisation in the presence of NF449, where the amount of desensitisation was 2.3-fold reduced compared to ATP only conditions ( $36.5 \pm 11.1$  and  $84.3 \pm 11.1\%$  respectively,  $p<0.0001$ ), figure 3.8c. Again there was very little desensitisation seen at the hP2X2 receptor in either condition which may be why no effect of NF449 application on desensitisation can be seen.

### 3.2.7 Chimeras and Antagonism

The aim of this thesis was to identify how antagonists were acting at the hP2X1 receptor. As the application of antagonists is extracellular and the antagonist molecules cannot cross the cell membrane, it was hypothesised that the binding sites of the antagonists must be in the extracellular portion of the receptor, the large loop region. In order to test this, two chimeras were used which swapped the loop regions of the hP2X1 and hP2X2 receptors with each other. The WT hP2X1 and hP2X2 receptors were both sensitive to all three antagonists, however there was a clear difference in antagonist sensitivity between them, making chimeras between them appropriate to study antagonism. The chimeras had previously been generated by Dr Allsopp and used in the lab, but not characterised to antagonists (Allsopp *et al.*, 2013). The first was P2X1-2EXT which consisted of the hP2X1 receptor intracellular and transmembrane domains and the extracellular loop of the hP2X2 receptor (figure 3.9a). The second was P2X2-1EXT which was the reciprocal chimera, consisting of the hP2X1 receptor loop and the rest of the protein was the hP2X2 receptor (figure 3.9a). Antagonists were applied to these chimeras to see if antagonism was similar to either the hP2X1 receptor or the hP2X2

receptor. As the receptors had previously been characterised to agonists in the lab these experiments were not repeated in this thesis.

### **3.2.8 Chimeric Receptors and Suramin**

First, suramin inhibition at the chimeras was studied to test the contribution of the loop region to suramin sensitivity. 1  $\mu$ M suramin inhibited the ATP induced current by ~ 50% at the hP2X1 and P2X2-1EXT receptors (figure 3.9a). The same concentration of suramin had no effect on the P2X1-2EXT or hP2X2 receptors. A 100-fold higher concentration of 100  $\mu$ M was required for these receptors to be inhibited by ~ 40% (figure 3.9a). There was no significant difference between suramin action at the hP2X1 and P2X2-1EXT receptors which showed  $53.0 \pm 5.4\%$  and  $49.1 \pm 21.5\%$  of maximum response respectively. The effect of suramin was also similar at the hP2X2 and P2X1-2EXT receptors at both suramin concentrations (figure 3.9a). The receptors which showed similar levels of inhibition were the ones which contained the same extracellular loop regions. Receptors with contrasting loop regions showed significant differences in the amount they were inhibited by suramin. For example the hP2X1 and P2X1-2EXT receptors had  $53.0 \pm 5.5$  and  $93.6 \pm 2.1\%$  of current remaining in 1  $\mu$ M suramin respectively,  $p < 0.05$ . This suggests that it is the extracellular loop region which determines suramin sensitivity at the P2X receptors.

### **3.2.9 Chimeric Receptors and PPADS**

The suramin sensitivity of the hP2X1 and hP2X2 receptors tracked with the extracellular loop region of the receptors and so it was tested to see if the loop also contributed to PPADS antagonism. When 1  $\mu$ M PPADS was co-applied with an EC<sub>90</sub> concentration of ATP there was no significant difference between the amount of inhibition caused at P2X1-2EXT and hP2X2 receptors ( $35.5 \pm 3.8$  and  $22.4 \pm 5.3\%$  of maximum response respectively, figure 3.10). The hP2X1 and P2X2-1EXT receptors also showed no significant difference in PPADS potency, with 1  $\mu$ M PPADS causing  $61.3 \pm 4.1$  and  $69.7 \pm 6.6\%$  of maximum response respectively. The amount of inhibition seen at these receptors, which contain the entire extracellular loop of the hP2X1 receptor,

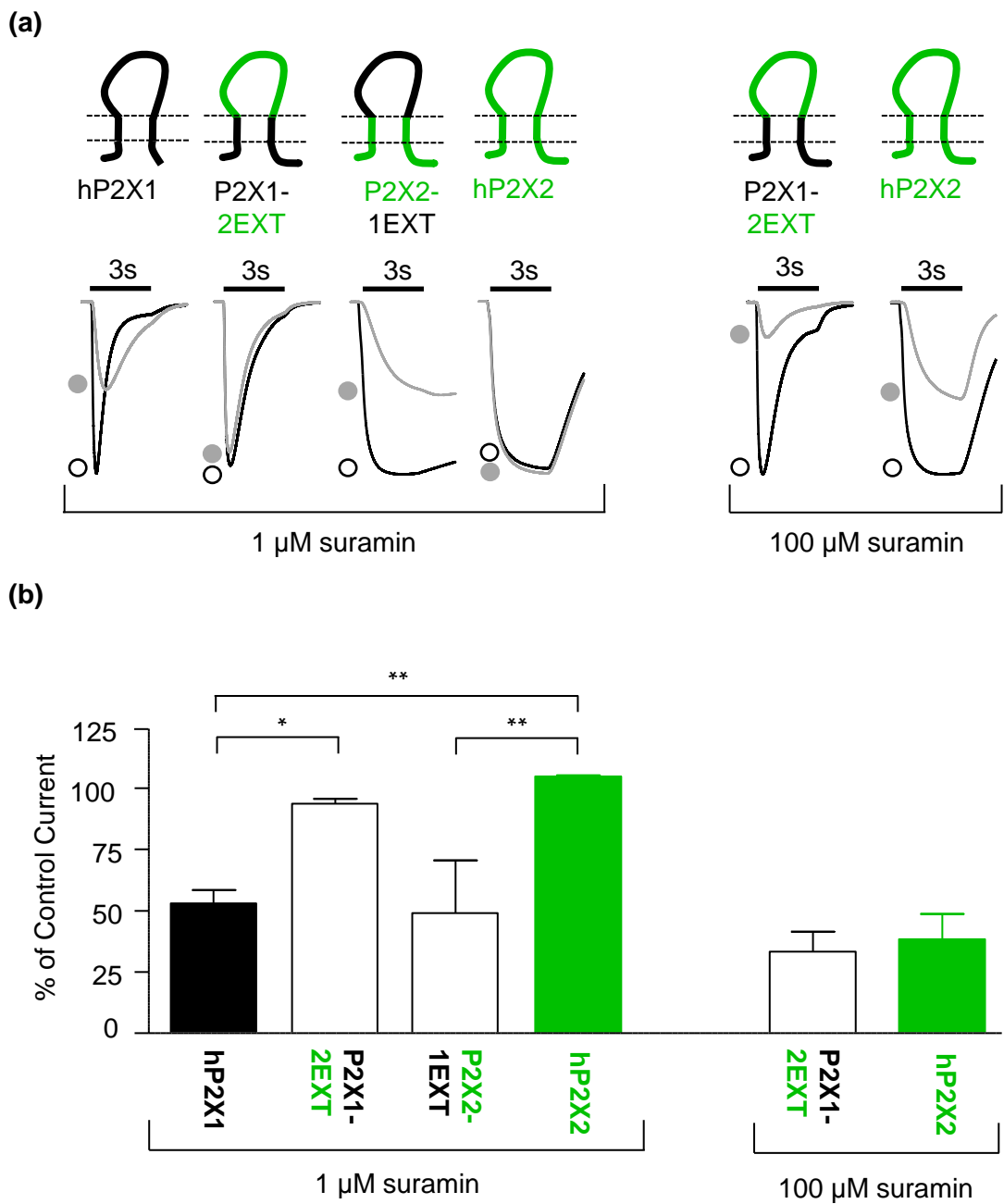


**Figure 3.9 Suramin Sensitivity Tracked with the Extracellular Loop. (a)** Schematic shows the hP2X1 (black) and hP2X2 (green) receptors and chimeras P2X2-1EXT and P2X1-2EXT. Representative current traces in response to an EC<sub>90</sub> concentration of ATP (open circle) and ATP plus suramin (filled circle). Traces have been normalised to peak currents to allow comparison. **(b)** Histogram to show percentage of control current when suramin was co-applied with ATP. Stars indicate significance. \* p < 0.05, \*\* p < 0.01.

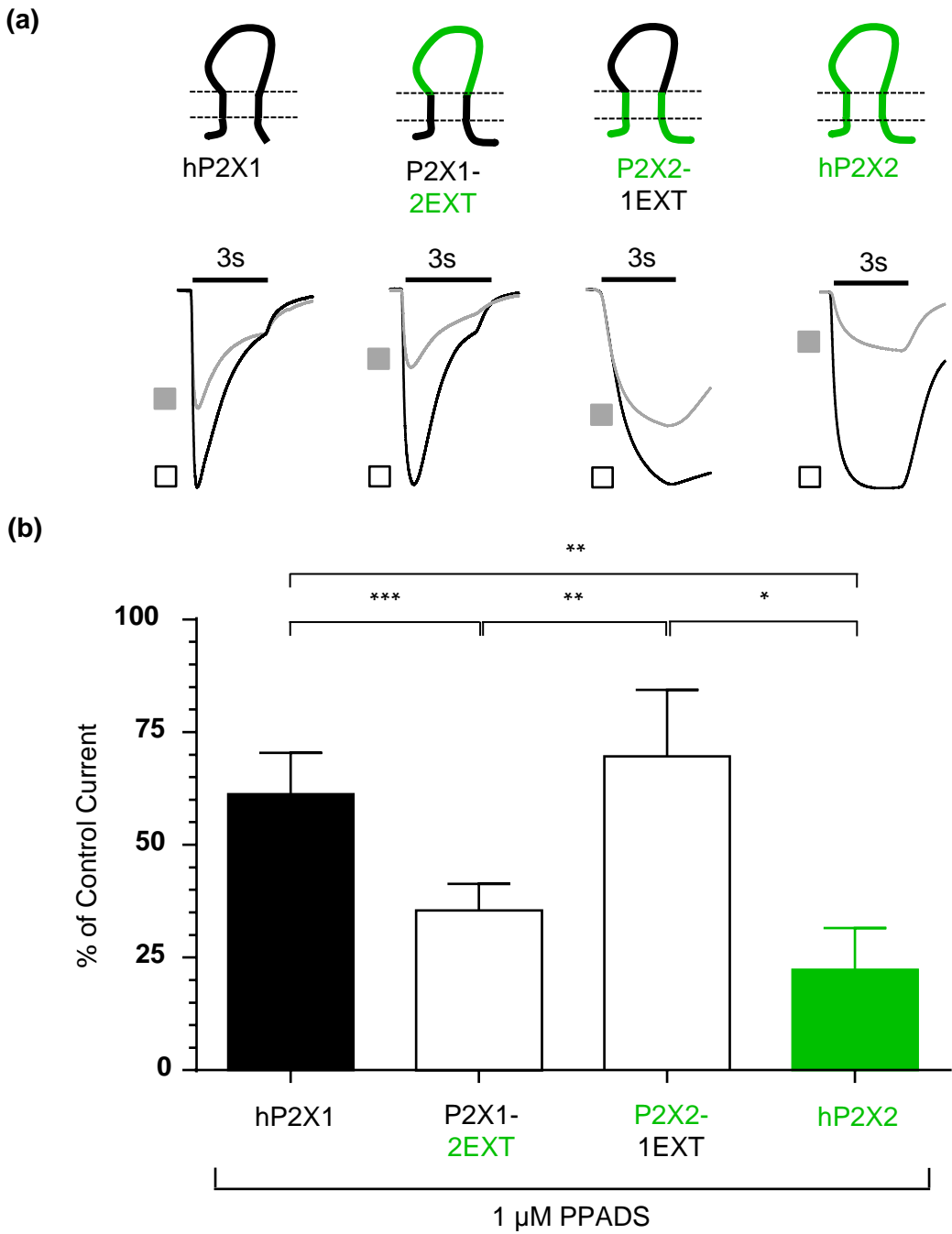


**Figure 3.10 PPADS Sensitivity Tracked with the Extracellular Loop.** (a) Schematic shows the hP2X1 (black) and hP2X2 (green) receptors and chimeras P2X1-2EXT and P2X2-1EXT. Representative current traces mediated by a 3 s application (indicated by bar) of an EC<sub>90</sub> concentration of ATP (open square) and ATP plus PPADS (filled square). Traces have been normalised to peak currents to allow comparison. (b) Histogram to show percentage current change when PPADS was co-applied with ATP. Stars indicate significance. \* p<0.05, \*\* p<0.01, \*\*\* p<0.001.

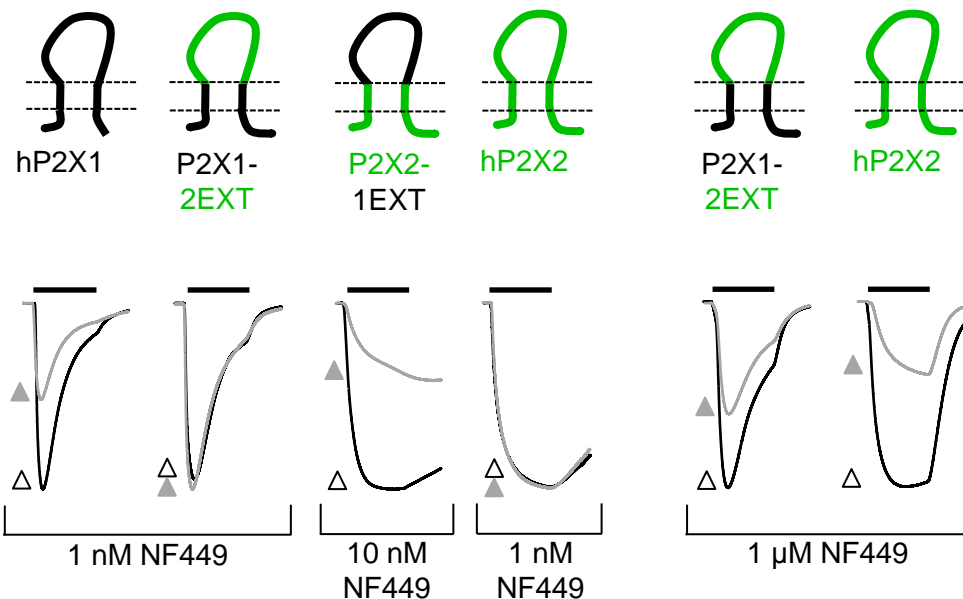
was however significantly different from that seen at the hP2X2 and P2X1-2EXT receptors (which contain the loop of the hP2X2 receptor, figure 3.10b). The results show that PPADS potency tracks with the extracellular loop.

### 3.2.10 Chimeric Receptors and NF449

The contribution of the extracellular loop region to NF449 action was also determined. 1 nM NF449 had no effect at either the hP2X2 or the P2X1-2EXT receptors when co-applied with EC<sub>90</sub> ATP (figure 3.11a). In contrast, nanomolar concentrations of NF449 were able to inhibit the hP2X1 and P2X2-1EXT receptors, pIC<sub>50</sub> = 8.94 ± 0.04 and 8.15 ± 0.08 respectively (figure 3.11b). The P2X2-1EXT receptor was ~ 6-fold less sensitive to NF449 than the hP2X1 receptor, p <0.0001. However, the hP2X2 receptor was > 300-fold less sensitive to NF449 than the P2X2-1EXT chimera p<0.0001 (figure 3.11b). The P2X2-1EXT chimera, which contains the extracellular loop of the hP2X1 receptor, is therefore much closer in antagonist sensitivity to the hP2X1 receptor than to the hP2X2 receptor. The P2X1-2EXT chimera had a similar NF449 sensitivity to the hP2X2 receptor (pIC<sub>50</sub> = 5.8 ± 0.10 and 5.67 ± 0.05 respectively). This again showed a strong link between the loop region that is present in a receptor and the receptor's antagonist sensitivity.

From these results it can be seen that the sensitivity of the hP2X1 and hP2X2 receptors to suramin, PPADS and NF449 tracks with the extracellular loop of the receptor, suggesting that this is the part of the receptor that determines antagonist action.

(a)



(b)

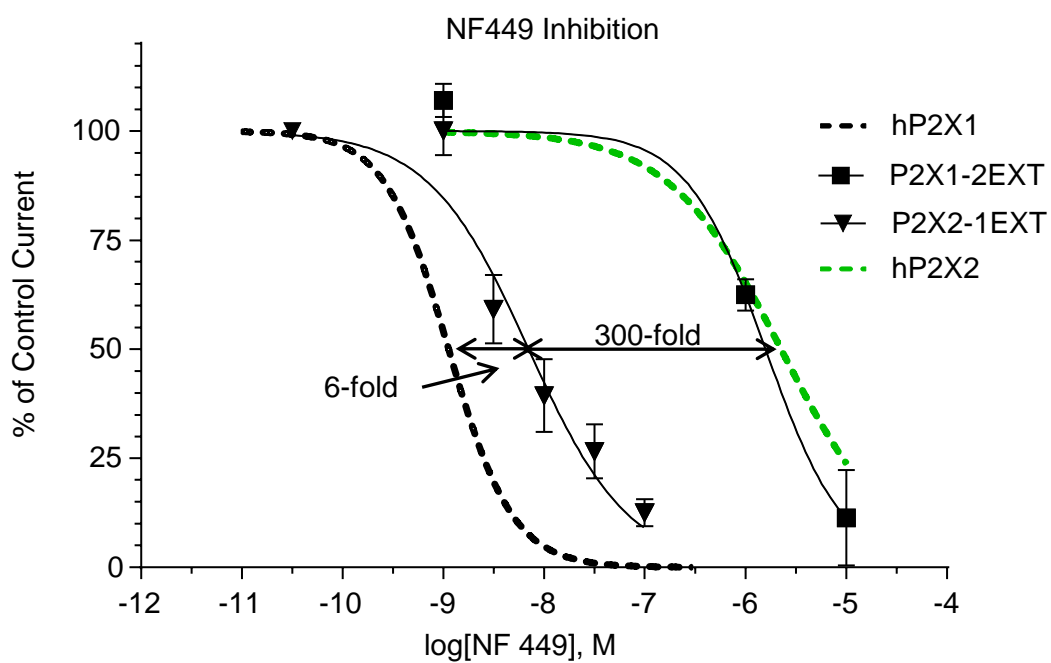


**Figure 3.11 NF449 sensitivity tracked with the extracellular loop.** (a) Representative current traces in response to an EC<sub>90</sub> concentration of ATP (open triangle) and ATP plus NF449 (filled triangle). Traces have been normalised to peak currents to allow comparison. Bars represent a 3 s ATP application (b) Inhibition curves showing the effects of NF449 on WT and chimeric receptors. Arrows show the fold difference between receptors.

### **3.3 Discussion**

The properties of the WT hP2X1, hP2X2 and rP2X4 receptors were consistent with previous studies. The experiments showed that the hP2X1 receptor could be distinguished from the hP2X2 and rP2X4 receptors due to its rapid time-course and high ATP potency. The rP2X4 receptor could be distinguished from the other WT receptors by its insensitivity to the antagonists suramin, NF449 and PPADS. These antagonists had inhibitory effects on the ATP evoked responses at the WT hP2X1 and hP2X2 receptors. Suramin and NF449 were competitive antagonists, and PPADS was non-competitive at these receptors. The difference in ATP and antagonist action at the WT receptors may arise from differences in amino acids, not just in the extracellular loop but also in the transmembrane domains and intracellular regions.

#### **3.3.1 Suramin is a Competitive Antagonist**

When co-applied with ATP, suramin caused a concentration dependent inhibition of current. This inhibition was reversible within 5 minutes. Suramin was also shown to decrease the rise time at the hP2X1 and hP2X2 receptors and the desensitisation seen at the hP2X1 receptor. These results are consistent with previous studies which have shown that suramin is a reversible competitive antagonist at the hP2X1 and hP2X2 receptors (North, 2002; Leff *et al.*, 1990; Zhong *et al.*, 1998). 1 µM suramin has been shown to shift the ATP concentration response 10-fold (Evans *et al.*, 1995). The competitive nature has been demonstrated on both native tissues and at recombinant receptors where increasing agonist concentration has overcome the effects of suramin (Leff *et al.*, 1990; King *et al.*, 1998). Radioligand binding has also shown that suramin inhibition is surmountable at P2X receptors in native rat vas deferens, as inhibition was decreased when the concentration of ATPγS was increased. Binding sites have been labelled by [<sup>3</sup>H]α,β-MeATP and suramin has been shown to compete for these sites, again showing its competitive nature (Khakh *et al.*, 1994).

Although suramin is generally accepted to be a competitive antagonist, there have been some suggestions that the action of suramin may

be non-competitive at some P2X receptors. When suramin was applied to a P2X receptor expressed in hippocampal granule cells, single channel recordings demonstrated an ~20% increase in current and an ~ 40% decrease in open probability in the presence of 40 µM suramin (Wong *et al.*, 2000). The subtype of P2X receptor characterised in these experiments was unclear, but it was thought to be a heteromeric channel. The non-competitive nature of suramin could therefore be unique to this subtype of P2X receptor (which was not identified). Suramin action has also been suggested to be non-competitive at P2X receptors expressed on the murine myenteric plexus (Guerrero-Alba *et al.*, 2010). When 30 µM suramin was applied to the receptors, ATP potency decreased but so did the maximum response. Suramin inhibition was not surmountable when ATP concentration was increased. These are properties of a non-competitive antagonist. It has also been shown that suramin application at the P2X2 receptor does not affect the binding of [ $\alpha$ -<sup>32</sup>P]ATP. This suggests that the two molecules have separate binding sites (Trujillo *et al.*, 2006). Despite these few studies suggesting suramin may act as a non-competitive antagonist, the vast majority of studies on suramin inhibition, including this one, suggest it to be a competitive antagonist at P2X receptors.

Another finding supporting the competitive nature of suramin is that suramin has been shown to be a partial agonist at a constitutively active P2X2 receptor mutant (T339S) (Cao *et al.*, 2007). The partial agonist effects of suramin suggest that it could bind in the ATP binding pocket. This is supported by Hausmann *et al* who produced models of the P2X2 receptor with suramin docked in the ATP binding pocket, where it was suggested to interact with residues Gly72, Glu167 and Arg290 (Wolf *et al.*, 2011). However mutants at residues involved in ATP action at the P2X1 receptor have been shown to have little effect on suramin action (Ennion *et al.*, 2000). This suggests that the individual key residues in the ATP binding pocket are not involved in suramin inhibition. ATP has three negative charges, but suramin has six, therefore mutation of more than one of these residues at a time may be required to have an effect on suramin action. The residues that ATP binds to are also conserved between P2X receptors, but not all receptors are suramin sensitive, suggesting that these residues are unlikely to determine suramin inhibition at the receptor,

as if the antagonist bound at the conserved ATP binding site you might expect similar inhibition to be seen at all P2X receptors. Residues located outside the ATP binding pocket have also been shown to contribute to suramin action (chapter 4.1.1). The location of suramin binding will be investigated in chapters 4 and 6 of this thesis.

As suramin was not selective between P2X receptor subtypes, and also had effects on P2Y receptors and other proteins, suramin derivatives were generated with the hope that potent and selective P2X receptor antagonists could be generated. The most successful of these was the P2X1 receptor selective antagonist NF449 which has also been studied in this thesis.

### **3.3.2 NF449 is a Selective Competitive Antagonist**

NF449 inhibited currents at the hP2X1 and hP2X2 receptors but with different potencies. NF449 had nanomolar potency at the hP2X1 receptor and was ~ 1400-fold more sensitive at this subtype than at the hP2X2 receptor. This is consistent with previous studies of NF449 action at P2X receptors (Braun *et al.*, 2001; Rettinger *et al.*, 2005). As with suramin, NF449 also affected the time-course of the ATP evoked response at the hP2X1 and hP2X2 receptors. The rise time of the hP2X2 receptor was decreased and less desensitisation was seen at the hP2X1 receptor in the presence of NF449 compared to ATP only conditions. Inhibition by NF449 was reversible with a 5 minute wash out of ATP. This is also consistent with previous studies into NF449 action (Hulsmann *et al.*, 2003). NF449 is a competitive antagonist, as an increase in the concentration of ATP shifted the NF449 inhibition curve to the right (Hulsmann *et al.*, 2003). The fact that the mechanism of action of suramin and NF449 is similar was expected as NF449 is a suramin derivative.

### **3.3.3 PPADS is a Non-Competitive Antagonist**

PPADS inhibited ATP evoked currents at the hP2X1 and hP2X2 receptors in a concentration dependent manner. The hP2X2 receptor was most sensitive to PPADS inhibition, but the hP2X1 receptor was also potently inhibited. There was little to no effect of PPADS on the time-course of the ATP evoked response at these receptors. There was no effect on the time-course of

the hP2X1 receptor, and the desensitisation of the hP2X2 receptor was also unaffected but there was a small (< 2-fold) increase in the rise time of this receptor. This is consistent with previous reports of PPADS antagonism (Lambrecht *et al.*, 1992; McLaren *et al.*, 1994). The lack of effect on time-course supports a non-competitive mode of action by PPADS as it suggests there is no apparent change in ATP sensitivity. Instead the concentration response curve has shown a collapse in the maximum current with no change in the EC<sub>50</sub> value (El-Ajouz *et al.*, 2012). PPADS inhibition at both the hP2X1 and hP2X2 receptors was reversible in this thesis, with current returning to maximum after a 5 minute wash off period. Both reversible and irreversible inhibition by PPADS has been reported in the literature. In native bullfrog DRG neurons the recovery from inhibition was reported to take 8 minutes (Li, 2000). It has also been reported that ATP induced currents at the native P2X1 receptor in the rat vas deferens had not fully recovered after 40 minutes of washing (Khakh *et al.*, 1994). The variation in recovery time from PPADS inhibition may be due to expression in different tissues or different receptor subtypes may show a difference in reversibility. The suggestion that PPADS forms a Schiff base with lysine 249 of the P2X1 receptor in order to antagonise the P2X1 receptor (described in chapter 4.1.2) is also supportive of irreversible antagonism (Buell *et al.*, 1996). The Schiff base theory of PPADS action has been questioned however as the P2X3 receptor is also inhibited by PPADS but does not have a lysine in an equivalent position to the P2X1 receptor.

The fact that suramin is a competitive antagonist and PPADS is non-competitive suggests that the two molecules do not share a binding site at the P2X receptor. Several point mutations have been identified in P2X receptors which affect either suramin or PPADS binding and may therefore form part of their respective binding sites and will be discussed in later chapters (Buell *et al.*, 1996; Garcia-Guzman *et al.*, 1997; Sim *et al.*, 2008; El-Ajouz *et al.*, 2012). The mutations which impacted on suramin action did not necessarily affect PPADS inhibition and vice versa, suggesting the antagonists have different binding sites. However a study by Xiong et al has demonstrated that a single point mutation (H241A) in the rP2X4 receptor affects both suramin and PPADS inhibition. Mutations which affect suramin action often also affect NF449

inhibition, suggesting a common or similar binding site for these two antagonists.

As with suramin, PPADS can also antagonise P2Y receptors (Windscheif *et al.*, 1994), and other proteins including ecto-ATPases (Chen *et al.*, 1996) and therefore does not have potential to be used therapeutically. However, insight into the molecular basis of how this drug is acting could help in the design of potent and subtype selective P2X1 receptor antagonists which would have huge therapeutic potential.

### **3.3.4 Antagonist Sensitivity Tracks with the Extracellular Loop**

The differences in antagonist sensitivity between the hP2X1 and hP2X2 receptors were investigated using chimeras originally generated by Dr Allsopp (Allsopp & Evans, 2011). The chimeras swapped the loops of the receptors and it was seen that the sensitivity of the receptor to all three antagonists tracked with the loop region of the receptor. The results of antagonist action at the chimeras described in this thesis was published in 2013 (Allsopp *et al.*, 2013). This suggests that the antagonist binds to the loop and this region determines how effective the inhibition is. This is consistent with previous studies, as all residues which have been implicated in antagonist action are located within the extracellular loop of the P2X receptor (Buell *et al.*, 1996; Sim *et al.*, 2008; El-Ajouz *et al.*, 2012). These residues will be discussed in chapter 4.

### **3.3.5 The rP2X4 Receptor is Insensitive to Suramin, PPADS and NF449**

The rP2X4 receptor displayed no inhibition or alteration of time-course of the ATP evoked currents by suramin, NF449 or PPADS, even at high concentrations of these drugs. This is consistent with the literature (Buell *et al.*, 1996). The reason for this antagonist insensitivity is unclear, however a few mutations have been identified which can induce sensitivity at this receptor subtype (Buell *et al.*, 1996; Garcia-Guzman *et al.*, 1997; Xiong *et al.*, 2004b). These mutations will be discussed in chapter 4.

The rP2X4 receptor may be insensitive to the antagonists as it lacks the residues necessary for the antagonist molecules to bind to the receptor. If

variant residues of the rP2X4 receptor are contributing to its antagonist insensitivity then mutation of residues in the hP2X1 receptor to the equivalent residue of the antagonist insensitive rP2X4 receptor would decrease or remove antagonism at the receptor. As well as identifying residues responsible for the antagonist insensitivity of the rP2X4 receptor the reciprocal mutations could give insight into residues which are responsible for antagonist binding at the hP2X1 receptor. This demonstrates that the antagonist insensitivity of the rP2X4 receptor could be exploited to gain insight into antagonist binding at the hP2X1 receptor. This method has been used in chapters 4, 5 and 6. Sequence comparison and mutation of variant residues between receptors with different properties has regularly been used in the literature to identify possible residues responsible for these differences. The contribution of some of these studies to the understanding of antagonism and time-course are discussed in chapters 4 and 5.

In summary, this initial chapter has characterised the WT hP2X1, hP2X2 and rP2X4 receptors to ATP and the three antagonists suramin, PPADS and NF449. The results were consistent with previous findings suggesting that suramin and NF449 act as competitive antagonists and PPADS is non-competitive at the hP2X1 and hP2X2 receptors, and have no effect on the rP2X4 receptor at the concentrations tested. It has also shown that the extracellular loop of the receptor strongly contributes to antagonist sensitivity of the hP2X1 and hP2X2 receptors. Despite the nature of the antagonism being well understood, the molecular basis of how antagonists bind to the hP2X1 and hP2X2 receptors remains to be identified. This understanding could help in the development of potent subtype selective antagonists for the hP2X1 receptor. In chapters 4,5 and 6 chimera generation and point mutations between the hP2X1 and rP2X4 receptors have been used to gain further understanding of this antagonism.

## **Chapter 4: ATP and Antagonist Action At Large Chimeras**

### **4.1 Introduction**

Antagonists cause varying amounts of inhibition at different P2X receptor subtypes. Variation in the sequence between subunits give rise to these differences. For an antagonist to bind to a receptor it must interact with specific residues at the surface which form a binding site. This binding site is likely to consist of numerous residues, some which form the core binding site and are vital to antagonism and others which have a smaller contribution. A potent and selective antagonist will have specific and high affinity interactions with one receptor but will be unable to dock at another. If the molecule acts at more than one receptor subtype then it is likely that the residues that form the binding site will be conserved between subunits. The binding site for ATP at the P2X receptors is a good example of this (Ennion *et al.*, 2000; Jiang *et al.*, 2000). Variation in antagonist sensitivity between subunits can therefore be due to a lack of conservation of these residues. If the residues that form the binding site are not present, the molecule will have reduced or no affinity.

The results from the P2X1/2 chimeras in chapter 3 show that the extracellular loop determines how effective an antagonist is at P2X receptors. It was thought that the generation of smaller chimeras and point mutations may be useful to determine which variant residues within the loop were important. In order to optimise the chimeric study of the contribution of these residues, chimeras were generated between receptors with large differences between them. The hP2X1 and rP2X4 receptors had a much greater difference in inhibition by suramin, NF449 and PPADS than the hP2X1 and hP2X2 receptors. These antagonists potently inhibited the hP2X1 receptor, but had little or no effect at the rP2X4 receptor at the concentrations tested. The receptors also show differences in other properties, including time-course, ATP potency and sensitivity to allosteric modulators (North, 2002). Chimeras were therefore generated between these two receptors to exploit the difference in antagonist sensitivity between them and gain insight into the molecular basis of how these antagonists bind to the hP2X1 receptor. If the difference in antagonism is due to the rP2X4 receptor not containing the antagonist binding

sites then replacing residues of the hP2X1 receptor with corresponding residues of the rP2X4 receptor should remove residues involved in binding and decrease inhibition.

Of the 283 amino acids in the extracellular loop of the rP2X4 receptor, ~ 50% differ from the hP2X1 receptor. If variant residues were responsible for the differences in antagonist sensitivity, then to identify all the specific amino acids involved, the contribution of all 144 variant residues of the extracellular loop to antagonism would need to be evaluated. Chimera generation allowed the effect of swapping large numbers of amino acids to be tested quickly to identify important regions contributing to antagonism.

Many previous studies into antagonism at P2X receptors have tried to predict residues that may be contributing to antagonism and then tested these predictions through point mutation. These residues were chosen due to their specific properties, often the charge, as positive charges of the receptor have been predicted to interact with the negative charges of the antagonist molecules. There has been some success of this approach, which has led to the identification of several residues contributing to the high affinity of antagonists at the P2X1 receptor. The chimeric approach has also been used to identify residues that contribute to antagonist action, for example between the rat and human P2X4 receptor (Garcia-Guzman *et al.*, 1997). The residues that have been linked to antagonism at the P2X1 receptor are discussed in more detail below.

#### **4.1.1 Mutagenesis Studies into Suramin and NF449 Action at the P2X1 Receptor**

There are two studies that have demonstrated the importance of positive charge in the cysteine rich head region, adjacent to the agonist binding site in the sensitivity of the P2X1 receptor to suramin and NF449. In 2007 it was shown that the mouse P2X1 receptor showed little inhibition by 10 µM suramin, whilst the human P2X1 receptor showed near maximal inhibition at this concentration (Sim *et al.*, 2007; Ikeda, 2007). Sim *et al* therefore studied the molecular basis underlying the difference in suramin sensitivity between the two

species (Sim *et al.*, 2008). As suramin is negatively charged it was considered to be likely to interact with positively charged residues of the receptor. Positively charged lysine residues in the hP2X1 receptor subtype that were absent from the mP2X1 receptor were identified and the equivalent residues in the mouse receptor were mutated to lysine. Antagonism was tested by recording ATP potency in the presence and absence of suramin. At the WT mP2X1 receptor there was little or no effect of 10 µM suramin on the ATP concentration response curve. The introduction of a lysine at position 138 (N138K) resulted in a 40-fold decrease in ATP potency in the presence of suramin, demonstrating that the presence of a lysine at this position in the cysteine rich head region caused an increase in suramin sensitivity. NF449 was also less effective at the mouse than the human P2X1 receptor. At the mP2X1 receptor there was very little effect of 3 nM NF449 on ATP potency, but the agonist response was almost completely inhibited at 300 nM. The N138K mutation also greatly increased NF449 antagonism at the mP2X1 receptor, with nearly complete antagonism being seen at a concentration of 3 nM.

The reciprocal mutation in the hP2X1 receptor (K138E) caused the receptor to become less sensitive to both suramin and NF449 (Sim *et al.*, 2008). At the WT hP2X1 receptor 10 µM suramin shifted the ATP concentration response curve ~ 30-fold to the right. In the K138E mutant this shift was reduced to 10-fold. The mutation did not cause the suramin sensitivity to decrease to mP2X1 receptor like levels and other residues must therefore be contributing to the antagonist sensitivity (Sim *et al.*, 2008). The hP2X1 K138E mutant also had decreased sensitivity to NF449 compared to the WT receptor, however the mechanism was unclear as the maximum response to ATP of the mutant was also reduced.

A chimeric approach by El-Ajouz *et al* identified the cysteine rich head region as being important in suramin and NF449 antagonism (El-Ajouz *et al.*, 2012). In this study the head region was focussed on as this region is absent in P2X receptors from the species *Dictyostelium discoideum*, which are antagonist insensitive. It was therefore argued that these residues of the human P2X1 receptor, that were missing in the *Dictyostelium* receptors, could be contributing

to antagonist action. Deletion of the entire cysteine head region of the hP2X1 receptor left the receptor non-functional. Therefore to study the contribution of the head region a chimeric approach was used. The hP2X2 receptor has greatly reduced NF449 and suramin sensitivity compared to the hP2X1 subtype, and therefore initial chimeras were generated where the hP2X1 receptor head region was replaced with the corresponding region of the hP2X2 receptor and *vice versa*. This was then refined by making a series of sub-chimeras and point mutations. Replacing the whole head region of the hP2X1 receptor with that of the hP2X2 receptor caused an ~ 300 fold decrease in NF449 sensitivity, implicating residues in this region in NF449 action. Sub-chimeras made within this region showed that swapping residues between the third and fourth conserved cysteine residues, which were located at the base of the cysteine rich head region, caused a decrease in NF449 potency of ~ 1700 fold. Within this chimera are four positively charged residues that were identified to be responsible for the difference in NF449 sensitivity between this chimera and the WT hP2X1 receptor. Mutating residues K136, K138, R139 and K140 to the equivalent residues of the hP2X2 receptor (KAKRK to EADML) caused a 600 fold decrease compared to the hP2X1 receptor and therefore identified them as being important for the NF449 sensitivity of the hP2X1 receptor (figure 4.1a). The same mutant also showed an ~ 35-fold decrease in suramin sensitivity compared to the WT receptor,  $IC_{50} = 70$  and  $2 \mu M$  respectively (figure 4.1b). Introducing the charges into the hP2X2 receptor showed some increase in suramin sensitivity, although not to levels of the hP2X1 receptor (figure 4.1c). No NF449 sensitivity could be introduced to the hP2X2 receptor by introducing these positive charges (El-Ajouz *et al.*, 2012). This suggests that while the four charges are necessary for NF449 action, other variant regions/residues of the hP2X1 receptor must also be contributing.

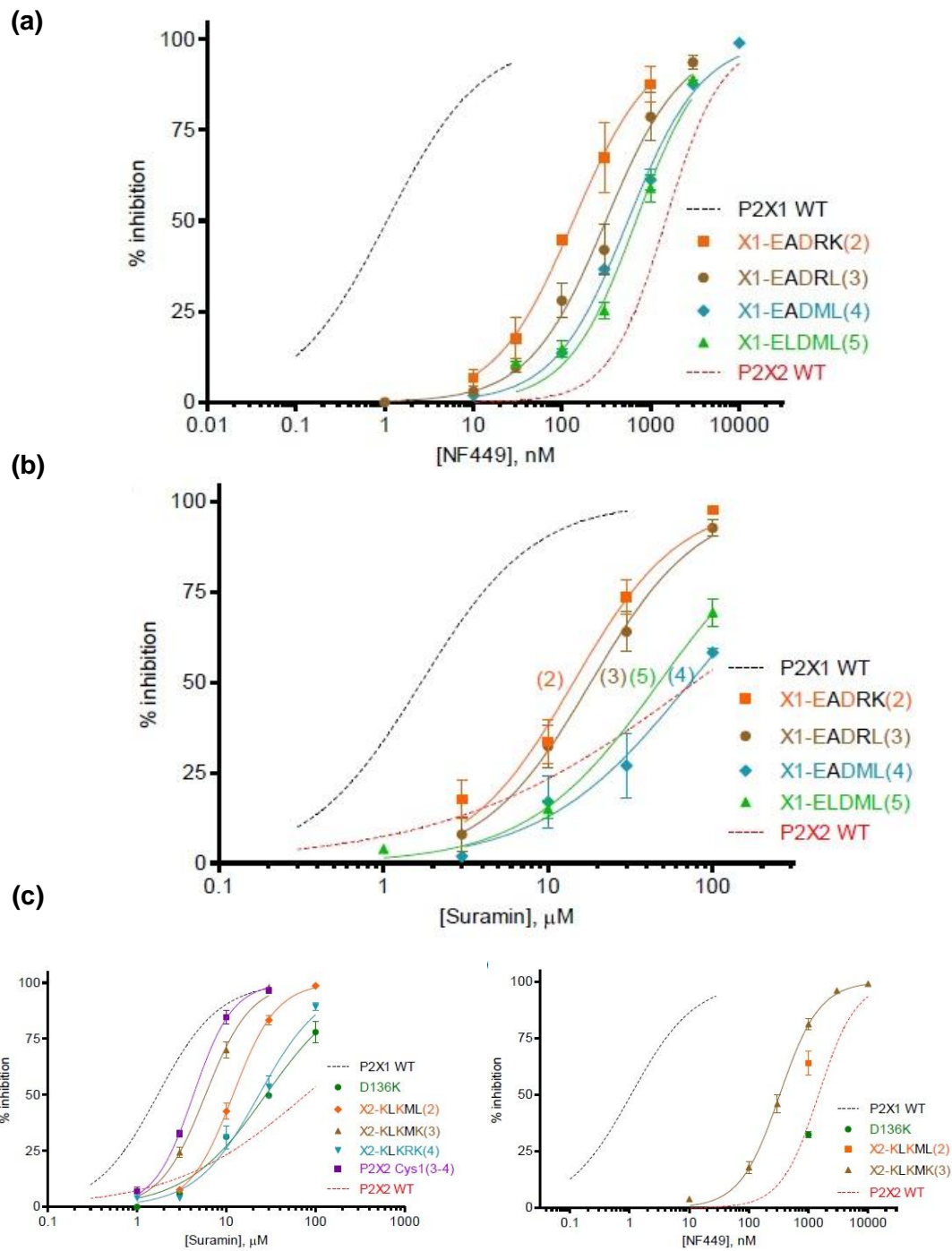


**Figure 4.1 Contribution of Residues in the Cysteine Rich Head Region to NF449 and Suramin Action (taken from (El-Ajouz, 2011)).** (a) NF449 inhibition at the point mutated hP2X1 receptors. Charged residues of the hP2X1 receptor (KAKRK) were replaced with the corresponding residues of the hP2X2 receptor (ELDML). The number of mutated residues is shown in brackets. (b) Suramin Inhibition at the hP2X1 receptor point mutations. (c) Effects of introduction of the four positive residues at the hP2X2 receptor on NF449 and suramin antagonism. Figures taken from (El-Ajouz, 2011).

#### **4.1.2 Mutagenesis Studies into PPADS Action at the P2X1 Receptor**

When the P2X4 receptor was first cloned it was seen that suramin, PPADS and P5P did not inhibit ATP induced currents at concentrations that would strongly inhibit the other subtypes (Buell *et al.*, 1996). It was noted that at high antagonist concentrations there was some inhibition of current (20-60%) by PPADS. This inhibition had a quicker onset and washed out more rapidly than at the other P2X subtypes. Because of this, the authors suggested that an aldehyde group present in the PPADS molecule may be forming a Schiff base with a lysine residue on the P2X1 and P2X2 receptors (Buell *et al.*, 1996). As this lysine was not conserved in the PPADS insensitive P2X4 receptor, and a glutamate was present instead, the mutation E249K was made and its PPADS sensitivity tested. Introduction of the lysine gave the P2X4 receptor P2X1-like PPADS sensitivity ( $IC_{50} = 2.6 \mu M$ ), supporting the Schiff base theory. The reciprocal mutation in the P2X2 receptor, K249E, removed PPADS potency at the receptor (Buell *et al.*, 1996). These findings support the theory that in order for PPADS to inhibit the receptor it must form a Schiff base with a lysine, in the case of P2X1, at position 249. However this lysine residue is not conserved at other P2X receptors which have PPADS sensitivity, e.g. the P2X3 receptor. PPADS can still bind to these receptors, despite the lack of a lysine residue in an equivalent position. This questions the necessity of a Schiff base at this position for PPADS antagonism.

Despite the success of these studies, other residues contributing to the antagonist binding site remain to be identified, and for this thesis it was felt that the wider contribution of variant residues within the extracellular loop should be evaluated, without any bias to particular amino acids. In order to do this, the chimeric method was chosen. Due to ~ 50% of residues within the extracellular loop of hP2X1 and rP2X4 receptors being variant, a method which could determine the contribution of large runs of amino acids to antagonism was preferred. The chimeric approach used in chapter 3 was therefore extended and developed for the hP2X1 and rP2X4 receptors, to screen large sections of the loop and identify them as, or exclude them from, being involved in antagonist action. Chimeras have previously been successfully used in the lab

to study antagonism at hP2X1 and rP2X4 receptors by El Ajouz *et al*, as discussed earlier. This chimeric approach provides a systematic way to identify regions of the extracellular loop which contribute to antagonist action, while reducing bias towards any particular residues.

### 4.1.3 Chapter Aims

The aim of this chapter was to determine the contribution of regions of the extracellular loops of hP2X1 and rP2X4 receptors to the difference in antagonist sensitivity between these two receptors. The P2X1 receptor antagonists suramin, NF449 and PPADS were used as these are potent at the hP2X1 receptor but the rP2X4 receptor is insensitive to these antagonists at micromolar concentrations.

## 4.2 Results

### 4.2.1 Designing Chimeras

Initial chimeras were designed by sequence analysis and looking at their location on the hP2X1 receptor homology model. The loop of the hP2X1 receptor was split into four sections that were designed to be of approximately equal size and bordered by sections of the sequence that were conserved between the two receptors. The conservation at the borders was important as it was thought that the transition from the hP2X1 to rP2X4 receptor sequence would be better tolerated at a point where there was minimal variance. To identify regions of conservation and variance between the two receptors, and therefore decide on the borders of the four sections, the sequences of the hP2X1 and rP2X4 receptors were compared in an amino acid line-up that was generated using the protein BLAST program (NCBI) and manually corrected (figure 4.2a). Throughout the line-up were spread islands where four or more amino acids were conserved or variant. Any runs of  $\geq 4$  conserved/variant amino acids were located on the hP2X1 receptor structure and (figure 4.2 c and d). Residues conserved between the two receptors tended to form more rigid structures of the P2X protein, such as  $\alpha$ -helices and  $\beta$ -sheets (figure 4.2c). The variant residues were mainly in the more mobile regions of the receptor e.g. the loops (figure 4.2d).

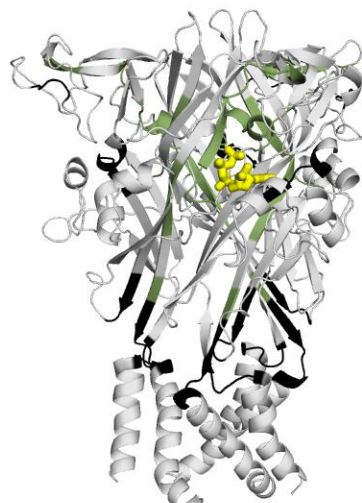
(a)

hP2X1	<b>YEKGYQTSSGLI</b> SSVSVKLKGAVTQLPGLGPQVWDVADYVFPAQGDNSFVVMTNFIVTP	110
rP2X4	W <u>ETDSVV</u> <u>TT</u> A <u>V</u> <u>NTSQ</u> <u>FRI</u> <u>I</u> <u>EE</u> <u>LFI</u> <u>M</u> <u>V</u>	109
hP2X1	<b>KQTQGYCAEHPE</b> -GGICKEDSGCTPGKAKRK <b>QAQGIRTGKCVAFN</b> DTVKTCEIFGWCPVEV	169
rP2X4	N <u>ST</u> <u>P</u> <u>I</u> <u>DKTS</u> <u>NS</u> <u>AD</u> <u>SVDTHSS</u> <u>VA</u> <u>R</u> <u>P</u> <u>ES</u> <u>VAA</u> <u>N</u>	169
hP2X1	<b>DDDI</b> PRPALLREAE <u>NTLFI</u> KNSISFPRFKVNRRNLVEEVNAAHMKTCLFHKT <u>LHPLCPV</u>	229
rP2X4	<u>VGV</u> <u>T</u> <u>F</u> <u>KA</u> <u>LV</u> <u>NIWY</u> <u>K</u> <u>NFSK</u> <u>ILPNITT</u> SYL <u>S</u> <u>IYNAQTD</u> <u>F</u> <u>I</u>	229
hP2X1	<b>FQLGYVVQESGQN</b> FSTLAEKGGVVGITIDWH <u>CDLDWHVRHC</u> PIYEFHGLYE---EKNLS	286
rP2X4	<u>R</u> <u>TI</u> <u>EDA</u> <u>HS</u> <u>QEM</u> <u>VE</u> <u>IM</u> <u>QIK</u> <u>D</u> <u>N</u> <u>RAASL</u> <u>L</u> <u>R</u> <u>S</u> <u>RR</u> <u>DTRDL</u> <u>H</u> <u>V</u>	289
hP2X1	<b>PGFNFRFARHFVE</b> -NGTNYRHLFKVFGIRFD <u>DILVDGKAG</u> KFDIIP	330
rP2X4	<u>KYYRDLA</u> <u>KEQ</u> <u>T</u> <u>T</u> <u>AY</u> <u>I</u> <u>F</u>	334

(b)

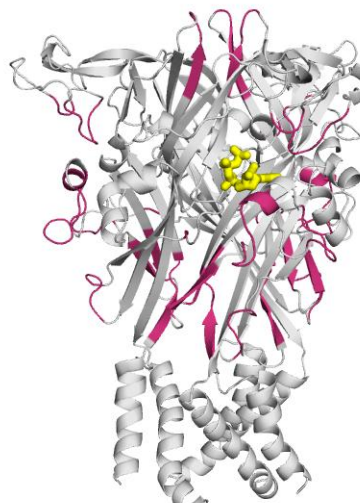
Region	Size (bp)	% conservation
A	81	54
B	51	53
C	76	35
D	69	55

(c)



Conserved

(d)



Variant

**Figure 4.2 Design of initial chimeras.** (a) The amino acids of the extracellular loop of the hP2X1 and rP2X4 receptors have been compared. Conserved residues are shown as a line in the rP2X4 receptor sequence. Using 5 conserved regions shown underlined in black, the loop region was split into four sections (A shown in purple, B in blue, C in green and D in orange). (b) Table comparing the size and % conservation of sections A-D. (c and d) Sections where  $\geq 4$  consecutive residues are either conserved (green) or variant (pink) are on the hP2X1 receptor homology models. The conserved regions used as swap over points for chimera generation are shown in black.

107

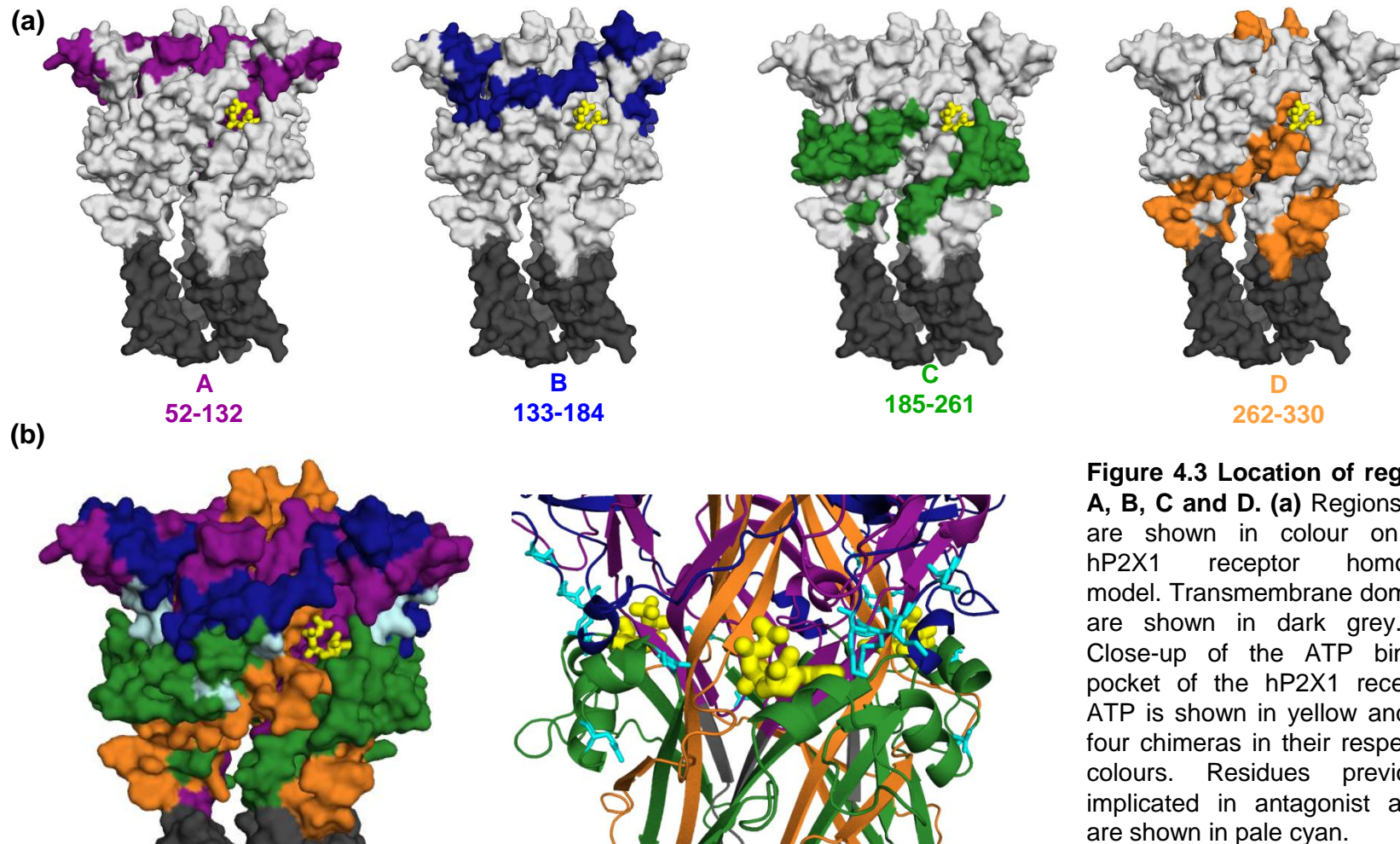


**Figure 4.3 Location of regions A, B, C and D. (a)** Regions A-D are shown in colour on the hP2X1 receptor homology model. Transmembrane domains are shown in dark grey. **(b)** Close-up of the ATP binding pocket of the hP2X1 receptor. ATP is shown in yellow and the four chimeras in their respective colours. Residues previously implicated in antagonist action are shown in pale cyan.

The four sections of the receptor that would be swapped to generate chimeras were chosen using the conserved residues. Four of these regions of conservation were 100% conserved and easy to choose as borders to regions A-D using the line-up. There was no obvious island of conservation in a suitable location to form the border between section C and D, so a section of 6 amino acids with > 65% conservation was chosen. The section surrounded a conserved cysteine residue (C261) important in receptor trafficking (Ennion & Evans, 2002a). Region A was the largest (81 bp), and B the smallest (51 bp). The residues contained within each section were 52-132 in A, 133-184 in B, 185-261 in C and 262-330 in D (hP2X1 receptor numbering). Of the residues in sections A, B and D, ~ 50% were conserved. Region C had the least conservation of the four, with only 35% sequence homology (figure 4.2b).

Sections A-D of the hP2X1 receptor were individually replaced with the corresponding residues of the rP2X4 receptor, to create four chimeras, shown in figure 4.3a. The nomenclature of the chimeras was the template receptor first, followed by the region that had been introduced. For example, chimera X1-AX4 consisted of the hP2X1 receptor, where section A had been replaced with that of the rP2X4 receptor. When the residues in each section were located on the homology model, it could be seen that regions A and B were located at the apex of the receptor, above the ATP binding pocket (figure 4.3a). Region C was adjacent to and immediately below the ATP binding pocket and the majority of region D is below the binding site, with some residues located at the apex of the receptor (figure 4.3a). Each of the chimeras contained a section of the residues in or around the ATP binding pocket (figure 4.3b). Although the residues in the binding pocket directly involved in ATP binding are conserved, and therefore cannot be contributing to the difference in antagonism between the receptors, previous studies suggest that the three antagonists may bind around the ATP binding pocket. Residues K136, K138, R139, K140 and K249 in the hP2X1 receptor and H241 in the rP2X4 receptor, that have previously been shown to be involved in antagonism, are all positioned in the proximity of the ATP binding pocket (figure 4.3b) (Buell *et al.*, 1996; Sim *et al.*, 2008; El-Ajouz *et al.*, 2012; Xiong *et al.*, 2004b). Therefore splitting the region around the ATP binding pocket between chimeras reduced any bias to a region that

has previously been implicated in antagonist action. The four chimeras gave full coverage of the extracellular loop of the hP2X1 and rP2X4 receptors (figure 4.3b) and allowed for the contribution to antagonism of all the residues within this region to be assessed.

#### 4.2.2 ATP Action at the hP2X1 Receptor Chimeras

Chimeras X1-BX4, X1-CX4 and X1-DX4 all produced inward currents in response to a 3 second maximal ATP application, with mean peak currents of  $4651 \pm 499$ ,  $8546 \pm 747$  and  $5265 \pm 546$  nA respectively. However X1-AX4 produced no change in current when ATP was applied, even up to a concentration of 1 mM (figure 4.4a). Surface biotinylation was used to label membrane proteins, and Western blotting showed that while the X1-AX4 protein was present at similar levels to the hP2X1 receptor in the whole oocyte, its expression in the membrane was much reduced (figure 4.4b). This suggests that the protein was made and assembled within the oocyte, but not trafficked efficiently to the cell surface. Some protein was present at the surface but there was no current recorded, suggesting that any expressed receptor was not functional. The original region that had been swapped consisted of residues 52-133. Using the P2X1 homology model it was seen that the variant residues in region 52-65 were not present on the surface of the trimeric receptor and were instead buried inside the protein (figure 4.4c). It is probable that only residues at the surface of the P2X protein will be available for antagonist binding, and these 14 residues buried in the protein were therefore unlikely to be directly contributing. Residues 52-65 were also positioned immediately next to the first transmembrane domain; this is an important structural element of the P2X receptor, anchoring it in the cell membrane. Swapping these residues may lead to misfolding of the protein and have been responsible for the reduced trafficking of the receptor. Chimera X1-AX4 was subsequently redesigned to omit residues 52-65 from the region swapped. This chimera was expressed at the oocyte surface and was functional in response to ATP application, with a mean peak current of  $1438 \pm 340$  nA. The current at the revised X1-AX4 chimera was smaller than that seen at the hP2X1 receptor (7598 nA),  $p < 0.0001$ . Residues 52-65 of the hP2X1 receptor may be contributing not only

to receptor trafficking but also to gating. From here on, X1-AX4 refers to the redesigned hP2X1 (66-133 rP2X4) receptor.

All four functional hP2X1 receptor based chimeras showed concentration dependent responses to ATP. Concentration response curves (0.1 - 300  $\mu$ M) were produced to identify any changes in ATP potency at the chimeras compared to the WT hP2X1 receptor (figure 4.5b). ATP potency at chimera X1-CX4 was unaffected compared to the WT hP2X1 receptor ( $pEC_{50}$  of  $6.17 \pm 0.06$  and  $6.31 \pm 0.04$  respectively). The other three chimeras all showed a decrease in ATP action. The potency at chimera X1-DX4 was reduced ~ 15-fold compared to the hP2X1 receptor ( $p < 0.0001$ ), and showed rP2X4 receptor-like sensitivity ( $pEC_{50} = 5.09 \pm 0.05$  and  $5.36 \pm 0.05$  respectively). The X1-AX4 ( $pEC_{50} = 4.39 \pm 0.08$ ,  $p < 0.0001$ ) and X1-BX4 ( $pEC_{50} = 4.26 \pm 0.03$ ,  $p < 0.0001$ ) chimeras were decreased 110-fold and 100-fold respectively compared to the hP2X1 receptor and ATP was also less potent at these chimeras than at the rP2X4 receptor ( $p < 0.0001$ ).

The time-course of the response to maximal ATP varied between the chimeras (figure 4.5a). The % desensitisation at the end of the 3 s ATP application for X1-AX4 and X1-CX4 was the same as at the hP2X1 receptor (% desensitisation =  $70.8 \pm 11.36$ ,  $74.7 \pm 2.9$  and  $80.3 \pm 4.3$  respectively). Chimera X1-BX4 had the slowest time-course of the hP2X1 receptor chimeras, with desensitisation ~ 2-fold slower ( $p < 0.001$ ) than that seen at the hP2X1 receptor, and unchanged compared to the rP2X4 receptor (X1-BX4 =  $40.5 \pm 2.9$  and rP2X4 =  $28.7 \pm 4.5\%$ ). X1-DX4 had a time-course intermediate between the two WT receptors, with a % desensitisation of  $59.9 \pm 2.5\%$ ,  $p < 0.01$ . Table 4.1 shows a summary of the effects of ATP at the hP2X1 receptor chimeras.

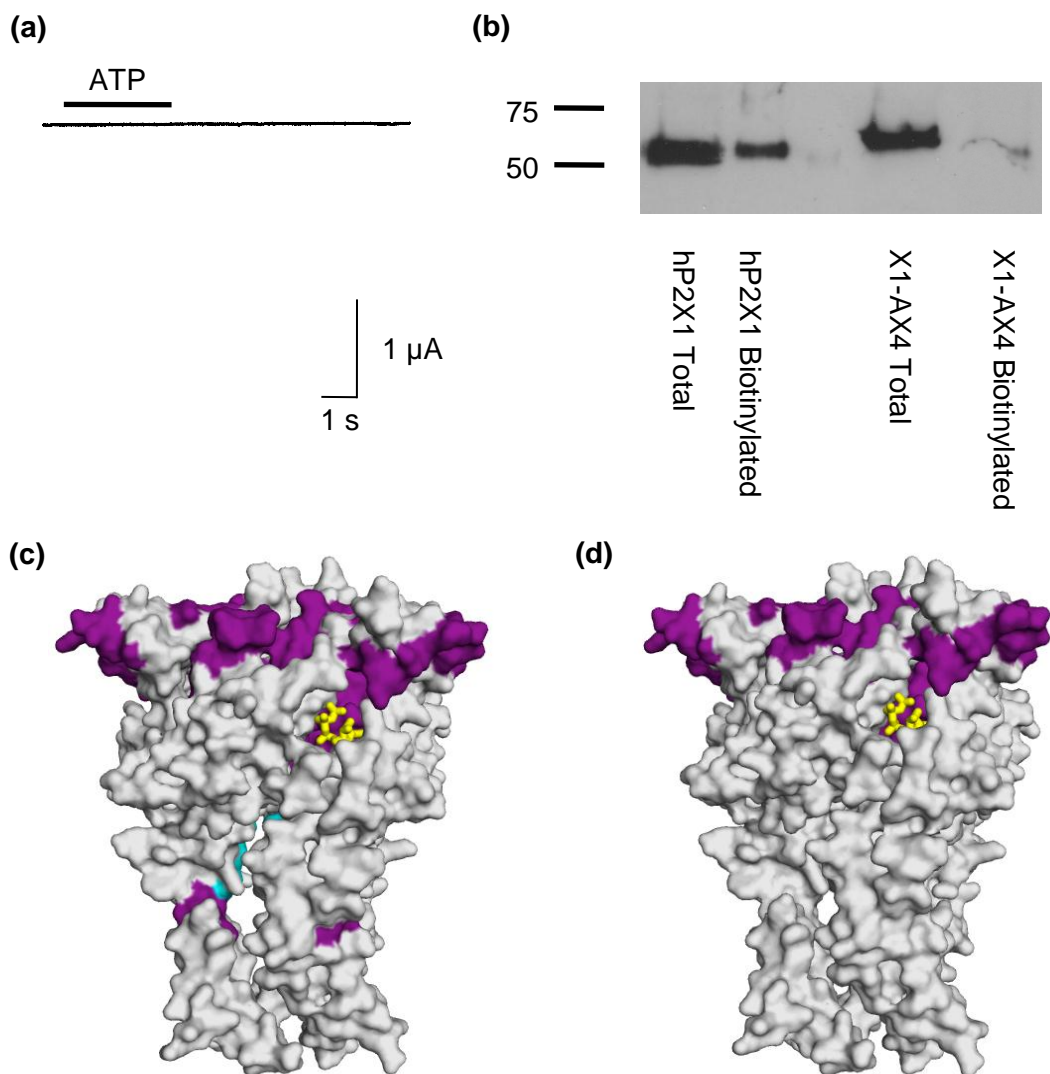
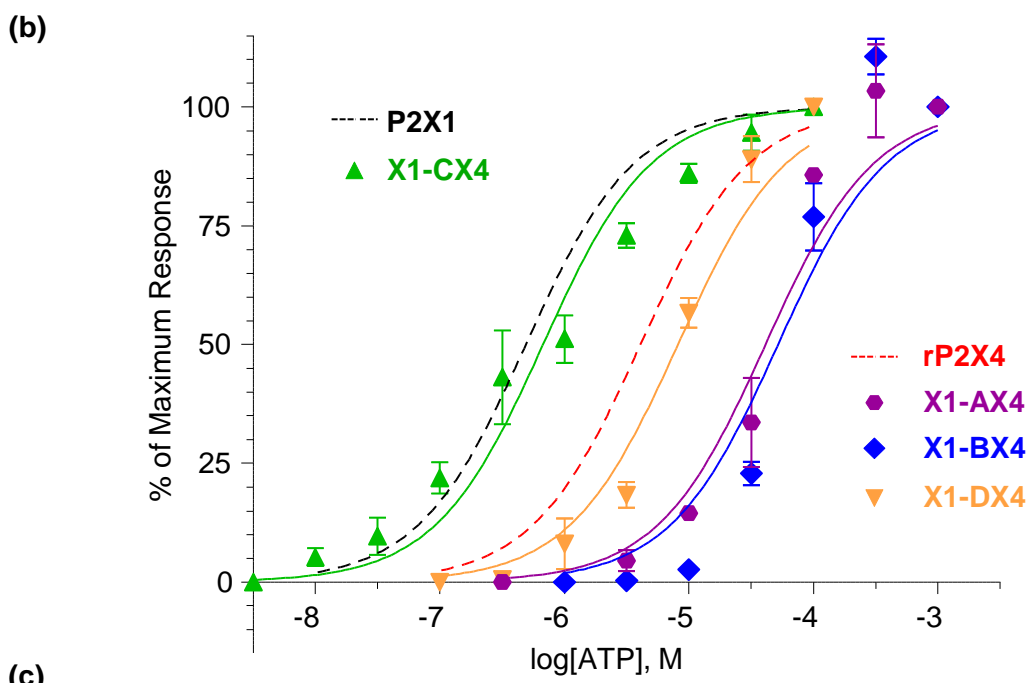
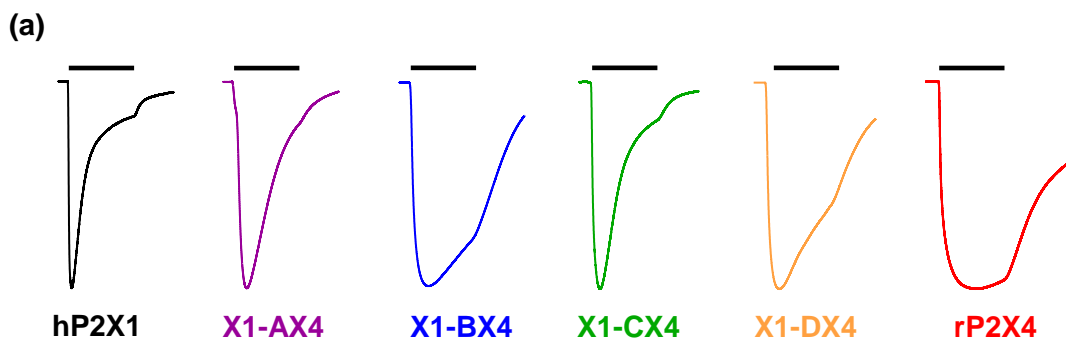


**Figure 4.4 Chimera X1-AX4 is Not Expressed at the Cell Surface.** (a) Representative trace of 10 mM ATP application to an oocyte expressing the X1-AX4 chimera. The bar represents a 3 s application. (b) Surface biotinylation and Western blotting showed that the receptor was present within the oocyte but was expressed at much lower levels than the hP2X1 receptor at the cell membrane. (c) hP2X1 receptor structure showing the location of chimera A (purple) and variant residues between amino acids 52-65 (cyan). The variant residues are not present at the surface of the receptor, but rather are buried within the structure. (d) The chimera was re-made omitting the first 14 amino acids (52-65) and the new chimera A is shown.



(c)

Receptor	pEC <sub>50</sub>	p value for difference from hP2X1	p value for difference from rP2X4
hP2X1	$6.3 \pm 0.04$	N/A	****
rP2X4	$5.39 \pm 0.06$	****	N/A
X1-AX4	$4.4 \pm 0.08$	****	****
X1-BX4	$4.3 \pm 0.09$	****	****
X1-CX4	$6.17 \pm 0.07$	ns	****
X1-DX4	$5.1 \pm 0.05$	****	ns

**Figure 4.5 ATP action at WT and chimeric receptors.** (a) Representative traces for WT and chimeric receptors at maximal ATP concentrations. The 3s application is shown by the bar. (b) Concentration response curves. (c) Table showing pEC<sub>50</sub> values. Stars indicate significant shifts. \*\*\*\* p<0.0001.

#### **4.2.3 NF449 Inhibition at the hP2X1 Receptor Chimeras**

To determine the contribution of variant residues within the chimeras to NF449 action, the sensitivity of each of the chimeras to NF449 was assessed and compared to the WT hP2X1 receptor. As ATP potency varied between the chimeras, the individual EC<sub>90</sub> concentration of ATP was deduced from the concentration response curves and used at each receptor in antagonist experiments to standardise the response of the receptors to ATP. All four chimeras showed a decrease in the sensitivity to NF449 (figure 4.6a,b). For X1-AX4 and X1-DX4 this decrease was less than 5-fold, with chimeras having pIC<sub>50</sub> values of  $8.20 \pm 0.05$ , p<0.01 and  $8.25 \pm 0.04$ , p<0.05 respectively. As these shifts were much smaller than the difference between the WT receptors, the residues in regions A and D were not focussed on in further studies into NF449 action.

In contrast, chimeras X1-BX4 (pIC<sub>50</sub> =  $7.35 \pm 0.08$ , p<0.0001) and X1-CX4 (pIC<sub>50</sub> =  $6.56 \pm 0.14$ , p<0.0001) displayed much larger decreases in inhibition by NF449 of ~ 60 fold and ~ 135 fold respectively (figure 4.6b). The Hill slopes of the inhibition curves of these chimeras were unchanged compared to that of the hP2X1 receptor (table 4.1). These large decreases in antagonist sensitivity suggest that residues within regions B and C are predominantly contributing to the differing effects of NF449 between the WT receptors. When regions B and C were located on the hP2X1 receptor homology model, it could be seen that region B contains residues positioned above the ATP binding pocket and includes the cysteine rich head region. Region C falls below both region B and the ATP binding pocket. These regions were subdivided into smaller chimeras and point mutations in chapter 5. The results show that studying chimeras is an appropriate method to identify residues contributing to NF449 antagonism at the hP2X1 receptor.

#### **4.2.4 Suramin Inhibition at the hP2X1 Receptor Chimeras**

As the chimera method had proven to be successful for identifying regions of the hP2X1 receptor involved in NF449 antagonism, suramin action

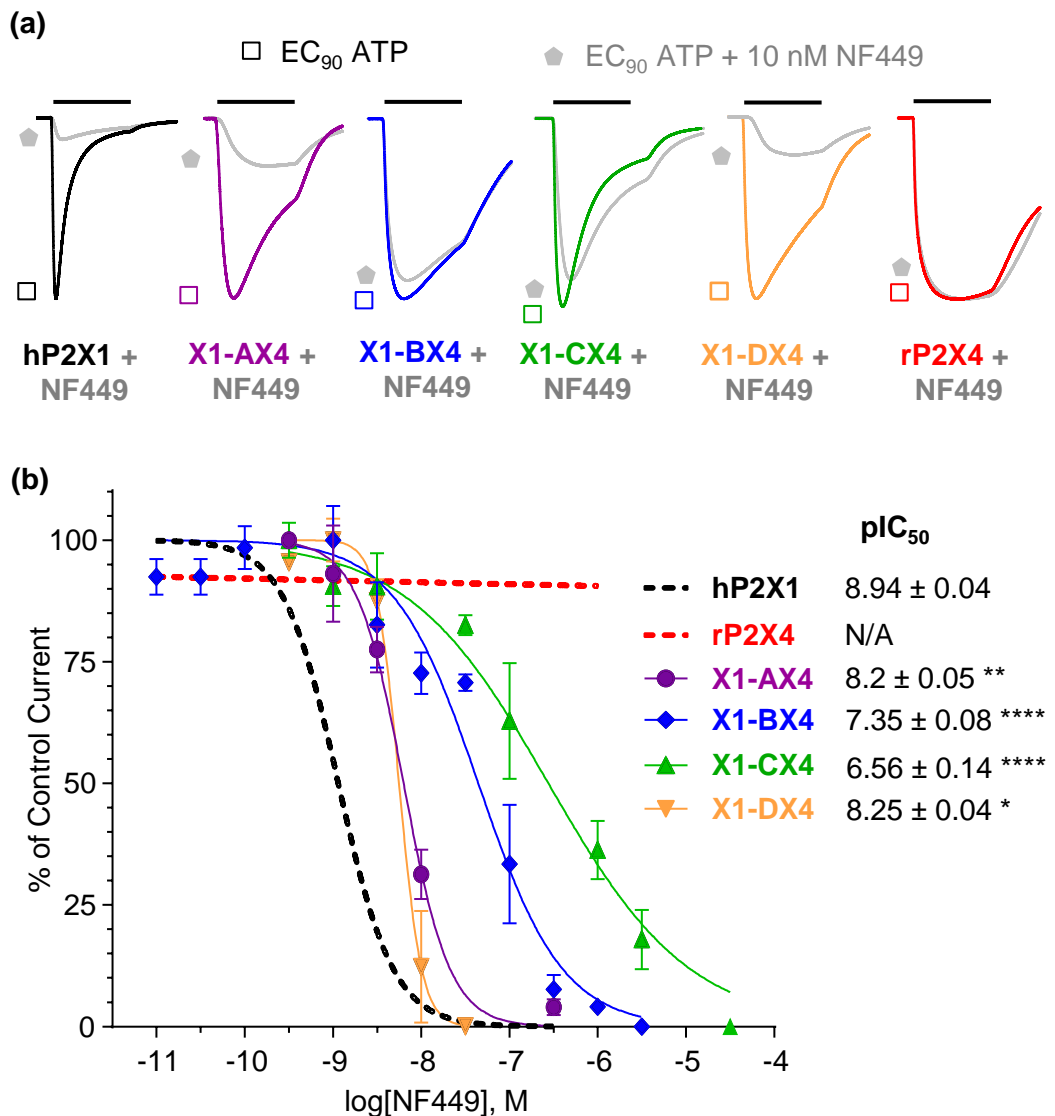


**Figure 4.6 NF449 Inhibition at Chimeric Receptors** **(a)** Representative traces showing the effect of NF449 application at *Xenopus* oocytes expressing WT and chimeric receptors. The bar indicates a 3s agonist/antagonist application **(b)** NF449 inhibition curves, pIC<sub>50</sub> values are given. Stars indicate significant shifts from hP2X1; \* p<0.05, \*\* p<0.01, \*\*\*\* p<0.0001.

was also studied. There was no change in suramin inhibition compared to the hP2X1 receptor at X1-BX4 or X1-CX4 with pIC<sub>50</sub> values of 5.56 ± 0.05 and 5.59 ± 0.06 respectively (figure 4.7b).

Interestingly chimeras X1-AX4 and X1-DX4 both showed a significant increase in suramin sensitivity compared to the hP2X1 receptor, even though the residues that were introduced were from a “less sensitive” receptor. The X1-AX4 and X1-DX4 chimeras had pIC<sub>50</sub> values of 6.59 ± 0.07, p<0.01 and 6.74 ± 0.04, p<0.001 respectively, compared to 5.98 ± 0.04 at the hP2X1 receptor (figure 4.7b). Although significant, the increase in suramin sensitivity seen due to swapping regions of the loop in chimeras was less than 10-fold. If the difference in antagonist sensitivity between the hP2X1 and rP2X4 receptors was due to variant residues, it would be expected that a decrease in suramin sensitivity would be seen when residues of P2X4 were introduced to the hP2X1 receptor.

#### **4.2.5 PPADS Inhibition at the hP2X1 Receptor Chimeras**

The inhibition by PPADS at the chimeras was also studied, to see if chimera generation could give insight into how PPADS acts at the hP2X1 receptor. Chimeras X1-AX4 and X1-CX4 had no change in PPADS sensitivity compared to the hP2X1 receptor, with pIC<sub>50</sub> values of 6.19 ± 0.04, 5.43 ± 0.07 and 5.8 ± 0.03 respectively (figure 4.8b). Chimeras X1-BX4 and X1-DX4 both showed significant shifts in the inhibition by PPADS. X1-DX4 showed an ~ 14 fold increase in the potency of the antagonist at the receptor with a pIC<sub>50</sub> value of 6.95 ± 0.03, p<0.001 (figure 4.8b). X1-BX4 showed a modest 3-fold decrease in PPADS sensitivity compared to the WT hP2X1 receptor (pIC<sub>50</sub> = 5.28 ± 0.08, p<0.01). The shift seen when region B had been swapped was very small when compared to the difference between the wildtype receptors. Therefore, as with suramin, it is likely that PPADS inhibition at the hP2X1 receptor is due to a combination of factors rather than solely individual variations in the amino acids between the two receptors. The chimera method was therefore not pursued as a method to investigate PPADS action at the hP2X1 receptor.

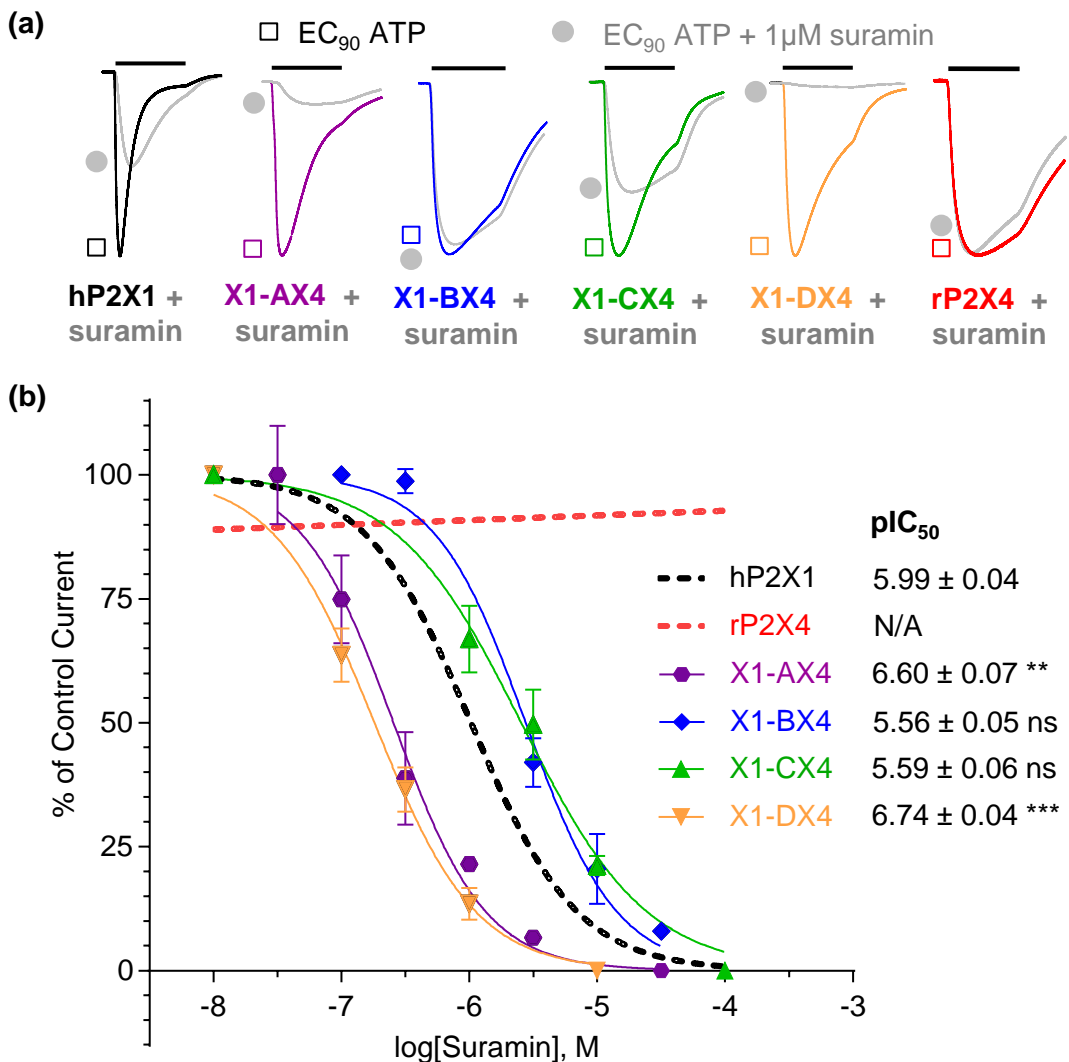


**Figure 4.7 Suramin Inhibition at Chimeric Receptors.** (a) Representative traces of EC<sub>90</sub> ATP (ATP<sub>90</sub>) and ATP<sub>90</sub> + suramin application to *Xenopus* oocytes expressing WT and chimeric receptors. A 3s agonist/antagonist application is indicated by the bar. Suramin was bath perfused around the oocyte for 5 minutes before co-application with ATP<sub>90</sub>. Traces are normalised to peak currents to allow for comparison. (b) Comparison of suramin action at WT receptors and chimeras. pIC<sub>50</sub> values are given and stars indicate significant shifts from the WT hP2X1 receptor. Stars indicate significant shifts from hP2X1; \*\* p<0.01, \*\*\* p<0.001.

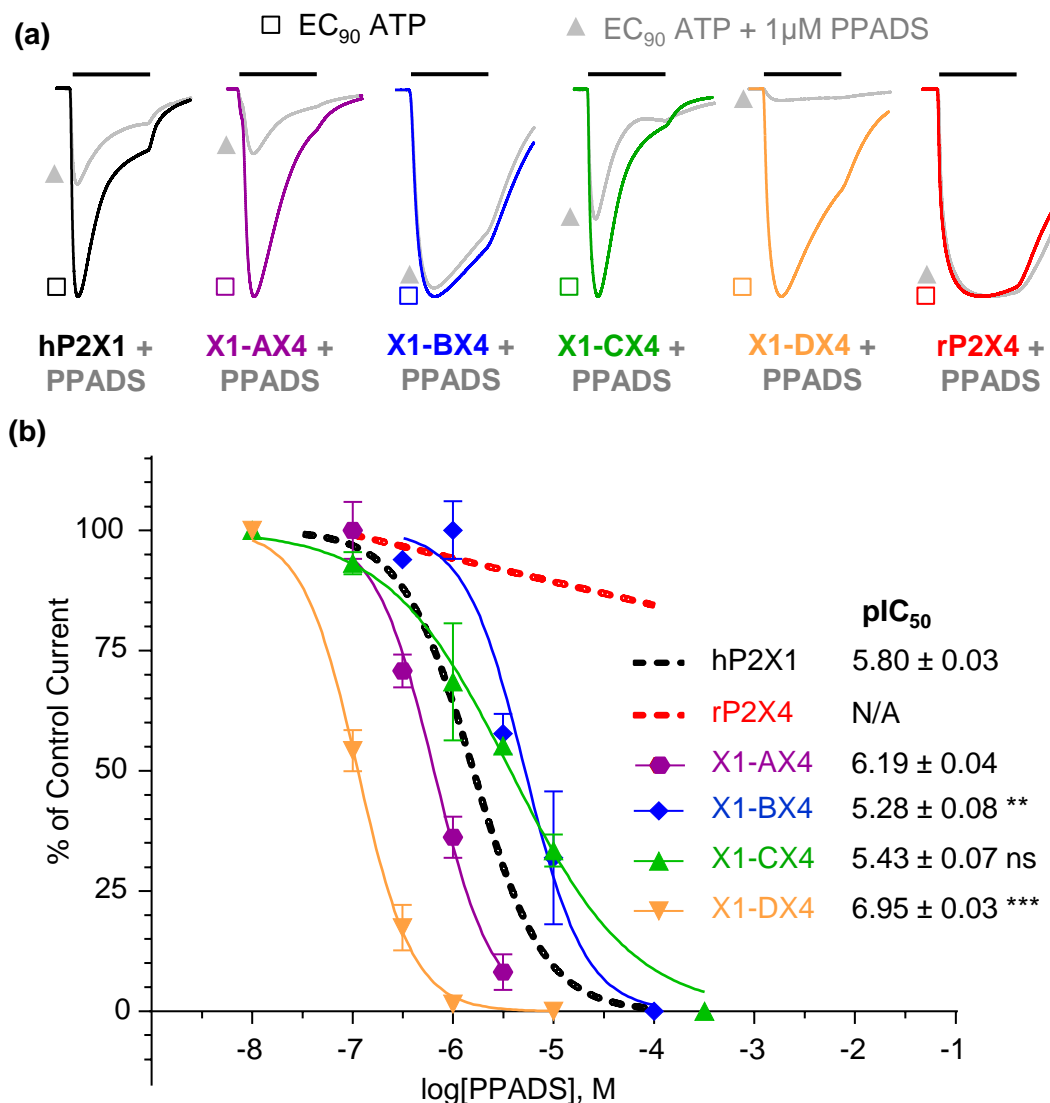


**Figure 4.8 PPADS Inhibition at Chimeric Receptors** (a) Representative traces showing effect of PPADS application at *Xenopus* oocytes expressing WT and chimeric receptors. A 3 s agonist/antagonist application is indicated by the bar. Traces are normalised to peak currents to allow comparison. PPADS was bath perfused around the oocyte for 5 minutes before co-application with ATP<sub>90</sub> (b) Inhibition curves and comparison with WT receptors. pIC<sub>50</sub> values are given and stars indicate significant shifts from WT P2X1. X1-AX4 and X1-CX4 showed no significant shift in PPADS potency. There was a small significant increase in inhibition at X1-DX4, and a small significant decrease for X1-BX4. Stars indicate significant shifts from hP2X1; \*\* p<0.01, \*\*\* p<0.001.

Receptor	ATP pEC <sub>50</sub>	ATP Rise Time (ms)	ATP % decay at 3s	Suramin pIC <sub>50</sub>	Suramin Hill Slope	PPADS pIC <sub>50</sub>	PPADS Hill Slope	NF449 pIC <sub>50</sub>	NF449 Hill Slope
hP2X1	6.31 ± 0.04	95.7 ± 5.1	80.3 ± 4.3	5.99 ± 0.04	1.05 ± 0.12	5.8 ± 0.03	1.23 ± 0.10	8.94 ± 0.04	1.40 ± 0.20
rP2X4	5.39 ± 0.06 ****	309.3 ± 32.0 ****	28.7 ± 4.5 ****	N/A	N/A	N/A	N/A	N/A	N/A
X1-AX4 (66-132)	4.39 ± 0.08 ****	145.6 ± 2.4 ns	70.8 ± 11.4 ns	6.60 ± 0.07 **	1.21 ± 0.20 ns	6.19 ± 0.04 ns	1.49 ± 0.04 ns	8.2 ± 0.05 **	1.65 ± 0.30 ns
X1-BX4 (133-184)	4.29 ± 0.09 ****	462.5 ± 41.2 ****	40.5 ± 2.9 ****	5.56 ± 0.05 ns	1.22 ± 0.18 ns	5.28 ± 0.08 ns	1.46 ± 0.32 ns	7.35 ± 0.08 ****	0.91 ± 0.12 ns
X1-CX4 (185-261)	6.17 ± 0.07 ns	180.2 ± 20.7 *	74.7 ± 2.9 ns	5.59 ± 0.06 ns	0.89 ± 0.14 ns	5.43 ± 0.07 ns	0.71 ± 0.10 ns	6.56 ± 0.14 ****	0.54 ± 0.07 ns
X1-DX4 (262-330)	5.09 ± 0.05 ****	191.1 ± 13.3 *	59.9 ± 2.1 **	6.74 ± 0.04 ***	1.10 ± 0.11 ns	6.95 ± 0.03 ***	1.58 ± 0.18 ns	8.25 ± 0.04 *	3.39 ± 0.50 ***

**Table 4.1 Summary of the Properties of ATP, Suramin, NF449 and PPADS at WT receptors and chimeras.** Boxes filled in red show a significant decrease compared to the hP2X1 receptor and those in blue show a significant increase. Stars indicate a significant difference from the WT hP2X1 receptor \* p<0.05, \*\* p<0.01, \*\*\* p<0.001. \*\*\*\* p<0.000. N/A = not applicable as was not determined.

#### **4.2.6 Generation of Inverse Chimeras X4-BX1 and X4-CX1**

As chimeras X1-BX4 and X1-CX4 had decreased NF449 inhibition compared to the hP2X1 receptor, the inverse chimeras, where regions B and C of the rP2X4 receptor had been replaced with the corresponding residues of the hP2X1 receptor, were made. These chimeras were named X4-BX1 and X4-CX1. When ATP was applied to the X4-CX1 chimera no change in the holding current was seen, even up to a concentration of 1mM (figure 4.9a). To test if the X4-CX1 RNA that had been injected into the oocyte was of a good quality an RNA gel was run (figure 4.9b). A bright band of ~ 7000 bp was seen for both the hP2X1 and X4-CX1 RNA, showing that the RNAs were similar. This was then repeated with a new batch of RNA and the same result seen (not shown). This suggests that the RNA is correct and that no current was seen as the receptor is non-functional, not expressed at the oocyte surface, or both.

#### **4.2.7 ATP Action at Chimera X4-BX1**

The X4-BX1 chimera was functional with a mean peak current of  $3617 \pm 570$  nA, (the same as the rP2X4 receptor). The time-course of the X4-BX1 chimera was unchanged compared to the rP2X4 and X1-BX4 receptors, with  $27.9 \pm 3.2\%$  desensitisation being seen at the end of the 3 second ATP application (figure 4.10a). ATP sensitivity of the X4-BX1 chimera was rP2X4 receptor-like, with a  $pEC_{50}$  of  $5.62 \pm 0.10$  (figure 4.10b). This shows that introduction of these residues of the hP2X1 receptor to the rP2X4 receptor has not introduced hP2X1 receptor-like time-course or ATP sensitivity.

#### **4.2.8 NF449 Action at Chimera X4-BX1**

As described previously, chimera X1-BX4 showed ~ 60-fold less inhibition by NF449 than the WT hP2X1 receptor which therefore implicated region B (residues 133-184) in the nanomolar potency of NF449 at the hP2X1 receptor. It was therefore investigated if the introduction of these residues to the rP2X4 receptor could cause an increased sensitivity to NF449. It was seen

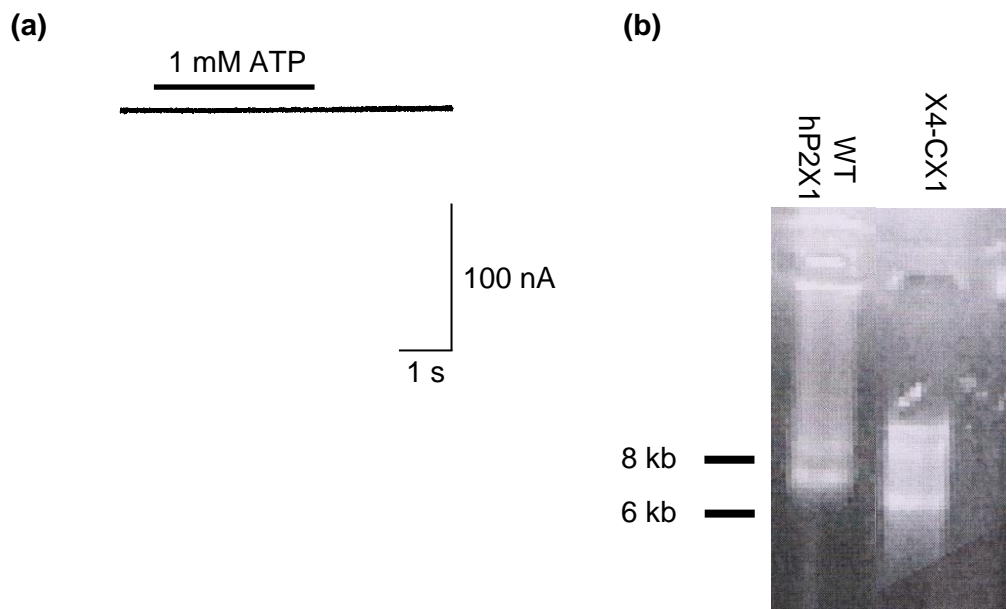


**Figure 4.9 ATP The X4-CX1 chimera was non-functional** (a) Representative trace of 1mM ATP application to a Xenopus oocyte injected with the X4-CX1 chimera. The bar represents a 3 s ATP application. (b) RNA gel of the WT hP2X1 and X4-CX1 receptor RNA. Both receptors show a strong band at ~ 7kb.

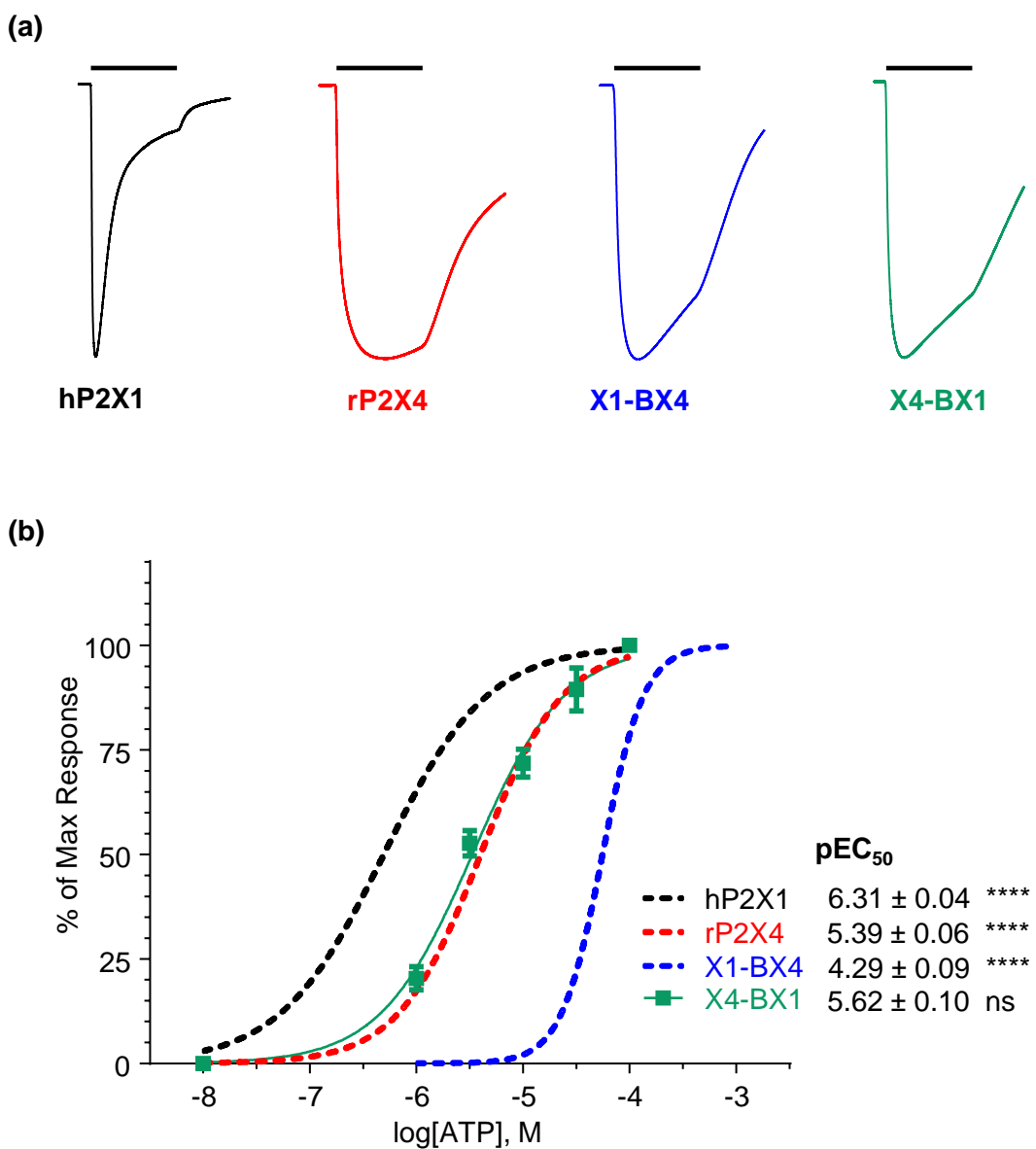


**Figure 4.10 ATP Action at Chimera X4-BX1.** (a) Representative traces of maximal ATP application at the hP2X1, rP2X4, X1-BX4 and X4-BX1 receptors. The bar represents a 3 second application. Traces have been normalised to peak currents to allow comparison. (b) Concentration response curves for the WT receptors and X1-BX4 and X4-BX1 chimeras.  $pEC_{50}$  values are shown. Stars represent a significant difference from the rP2X4 receptor. \*\*\*\*  $p < 0.0001$ .

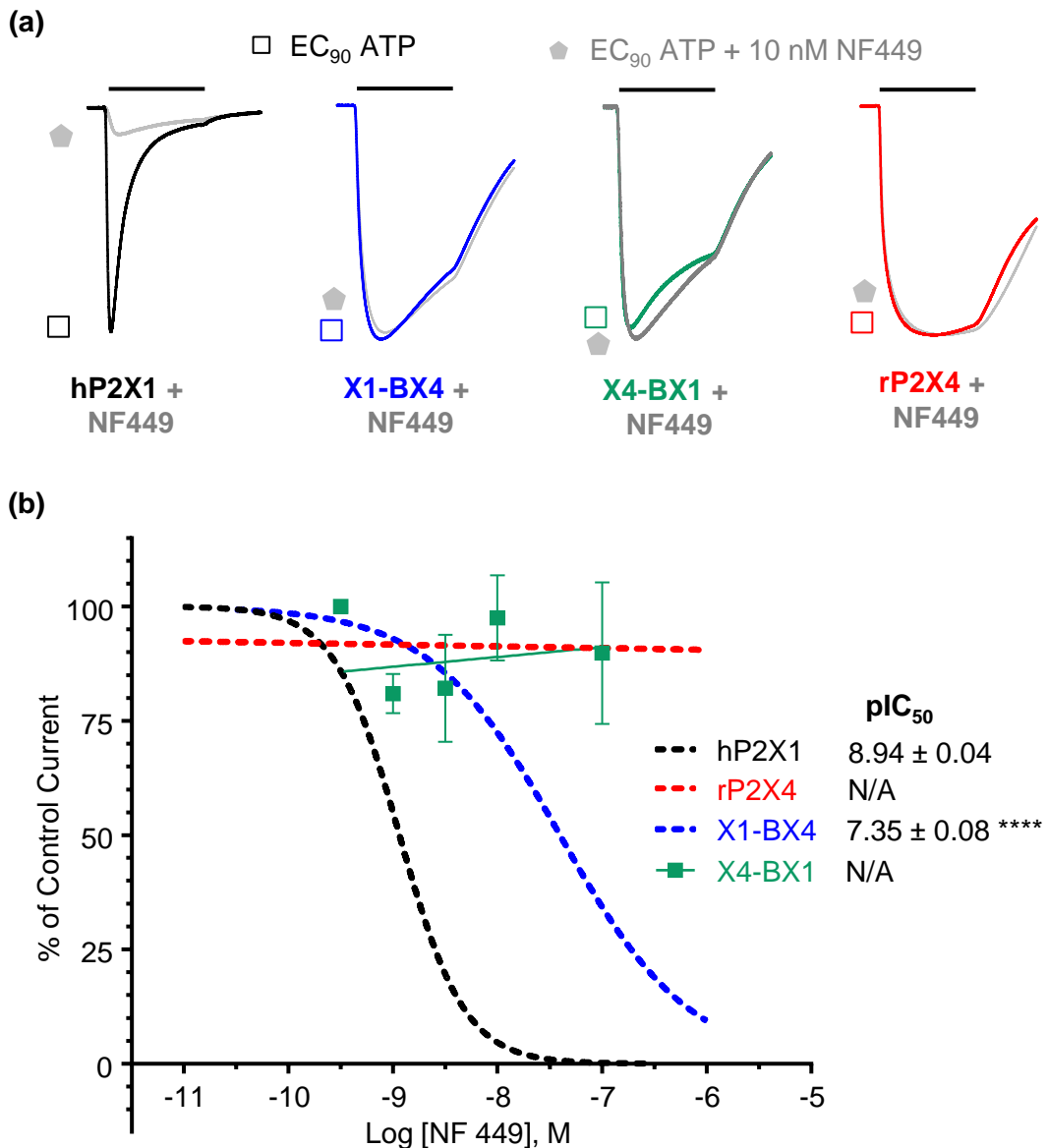


**Figure 4.11 NF449 Action at Chimera X4-BX1.** (a) Representative traces of EC<sub>90</sub> ATP (ATP<sub>90</sub>) and ATP<sub>90</sub> with NF449 application at the hP2X1, rP2X4, X1-BX4 and X4-BX1 receptors. The bar represents a 3 second application. Traces have been normalised to peak currents to allow comparison. NF449 was bath perfused around the oocyte for 5 minutes before co-application with ATP<sub>90</sub>. (b) Concentration response curves for the WT receptors and X1-BX4 and X4-BX1 chimeras. pIC<sub>50</sub> values are shown. Stars represent a significant difference from the hP2X1 receptor. \*\*\*\* p < 0.0001.

that co-application of 10 nM NF449 had no effect on the ATP induced current (figure 4.11a). This was the same as the application of the same concentration at the rP2X4 and X1-BX4 chimeras. An inhibition curve showed that the X4-BX1 chimera was not inhibited by NF449 up to a concentration of 300 nM, as was seen at the WT rP2X4 receptor (figure 4.11b). These results demonstrate that although replacing residues of region B of the hP2X1 receptor with those of the rP2X4 receptor caused a large decrease in NF449 sensitivity, the effect was not reciprocal as introduction of these residues of the hP2X1 receptor to the rP2X4 receptor did not alter NF449 action.

#### **4.2.9 Suramin Inhibition at Chimera X4-BX1**

Chimera X1-BX4 showed no decrease in suramin sensitivity compared to the hP2X1 receptor, suggesting that the residues within region B were not involved in the difference in suramin sensitivity between the two receptors. However, as the chimera had been generated, suramin inhibition at the X4-BX1 chimera was tested to see if introducing residues of region B from the hP2X1 receptor could introduce antagonist sensitivity to the rP2X4 receptor. 3  $\mu$ M suramin caused an ~ 40% decrease in the ATP induced current (figure 4.12a) and a full inhibition curve showed that the chimera was sensitive to suramin at hP2X1 receptor-like levels, with a  $pIC_{50}$  value of  $5.34 \pm 0.03$ . This was unexpected as swapping this region had had no effect on suramin inhibition at the hP2X1 receptor.

#### **4.2.10 PPADS Inhibition at Chimera X4-BX1**

The effect of PPADS on the X4-BX1 chimera was also examined. 1  $\mu$ M PPADS was seen to cause ~ 50% inhibition at X4-BX1, unchanged compared to the hP2X1 receptor (figure 4.13a). A full inhibition curve showed that the  $pIC_{50}$  value of X4-BX1 ( $5.62 \pm 0.10$ ) was hP2X1 receptor-like ( $5.80 \pm 0.03$ ), figure 4.13b. This showed that swapping residues 132-184 of the rP2X4 receptor with those of the hP2X1 receptor introduced both PPADS and suramin sensitivity to the receptor, but not NF449. These results are summarised in table 4.2 and further discussed in chapter 6.

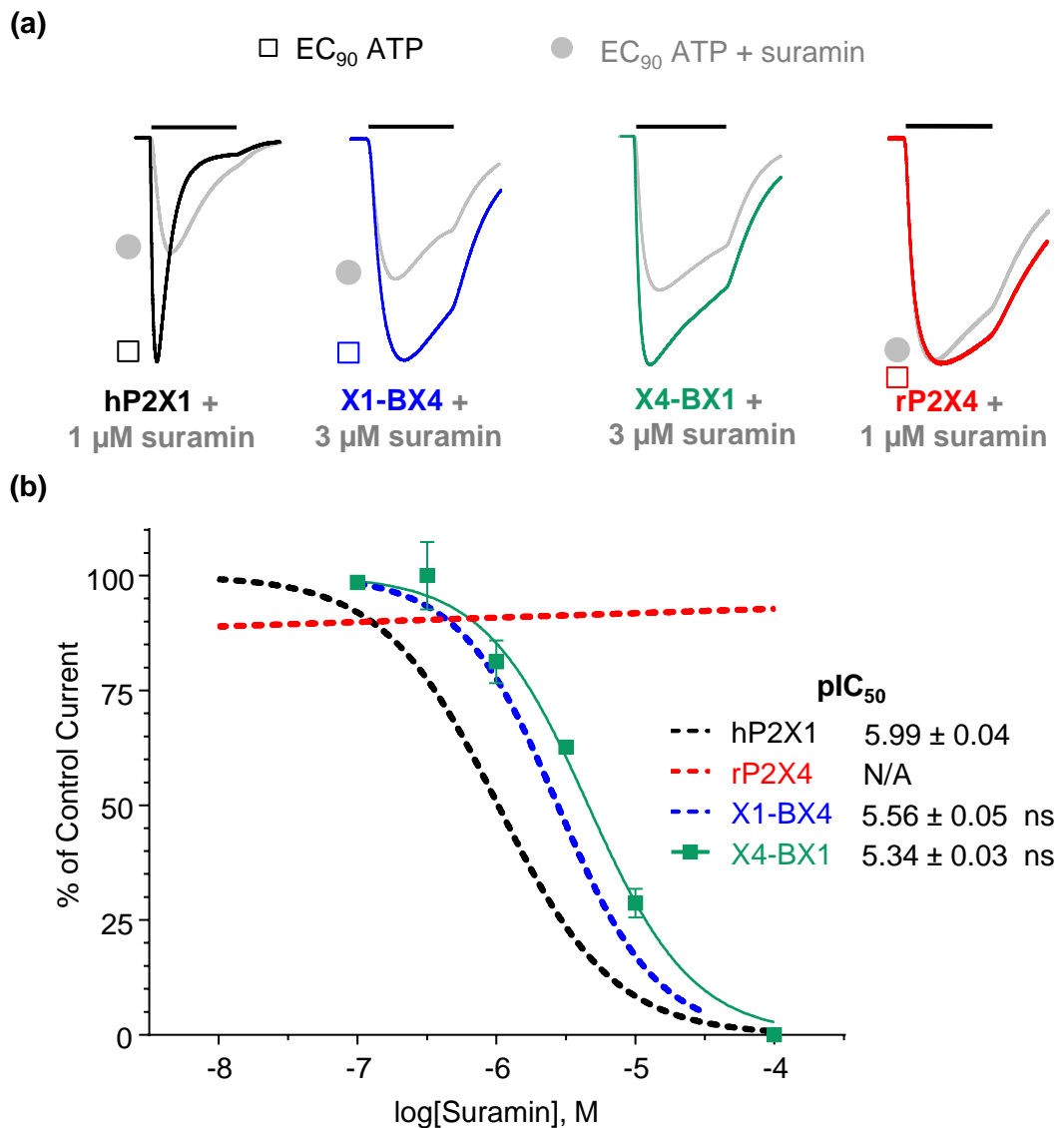
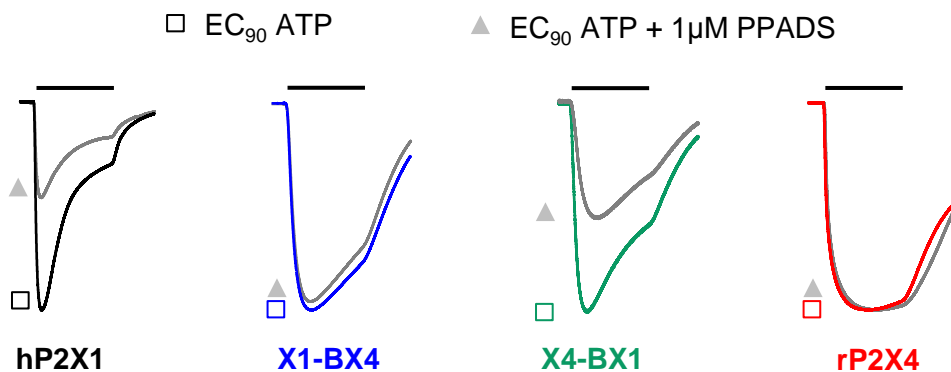


**Figure 4.12 Suramin Inhibition at Chimera X4-BX1.** (a) Representative traces of EC<sub>90</sub> ATP (open squares) and EC<sub>90</sub> ATP + suramin (closed circles) at the hP2X1, rP2X4, X1-BX4 and X4-BX1 receptors. The bar represents a 3 second application. (b) Suramin Inhibition curves for the WT receptors and X1-BX4 and X4-BX1 chimeras. pIC<sub>50</sub> values are shown. ns = not significantly different from the WT hP2X1 receptor.

(a)



(b)

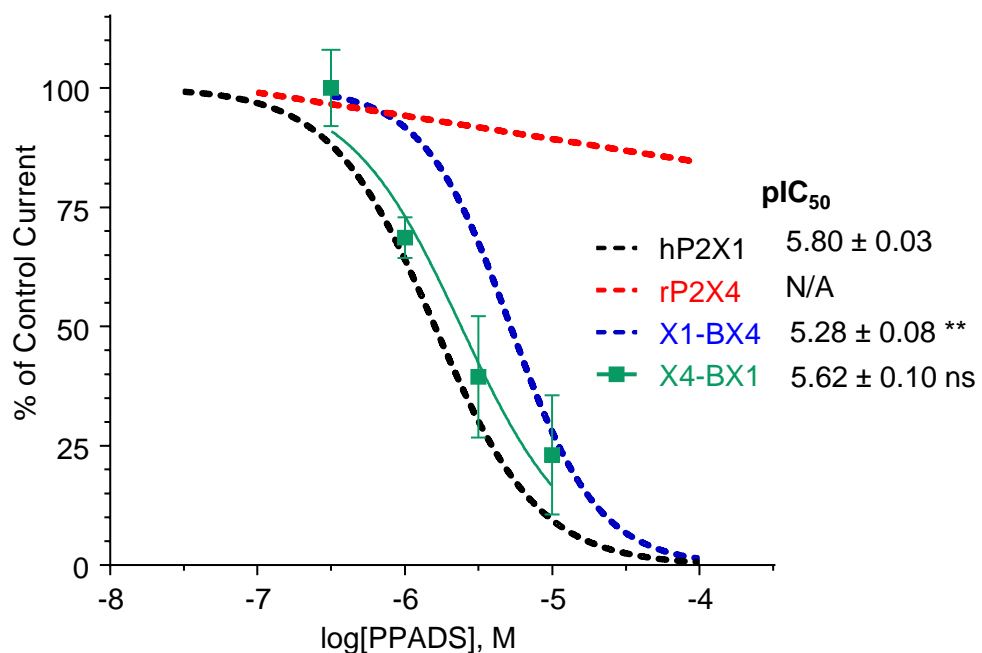


**Figure 4.13 PPADS Inhibition at Chimera X4-BX1.** (a) Representative traces of EC<sub>90</sub> ATP (open squares) and EC<sub>90</sub> ATP + 1 μM PPADS (closed triangles) at the hP2X1, rP2X4, X1-BX4 and X4-BX1 receptors. The bar represents a 3 second application. PPADS was bath perfused around the oocyte for 5 minutes before its co-application with ATP. (b) PPADS inhibition curves for the WT receptors and X1-BX4 and X4-BX1 chimeras. pIC<sub>50</sub> values are shown. Stars represent a significant difference from the hP2X1 receptor. \*\* p < 0.01.

Receptor	ATP pEC <sub>50</sub>	ATP Rise Time (ms)	ATP % decay at 3s	Suramin pIC <sub>50</sub>	Suramin Hill Slope	PPADS pIC <sub>50</sub>	PPADS Hill Slope
hP2X1	6.31 ± 0.04	95.7 ± 5.1	80.3 ± 4.3	5.99 ± 0.04	1.05 ± 0.12	5.8 ± 0.03	1.23 ± 0.10
rP2X4	5.39 ± 0.06 ****	309.3 ± 32.0 ****	28.7 ± 4.5 ****	N/A	N/A	N/A	N/A
X1-BX4 (133-184)	4.29 ± 0.09 ****	462.5 ± 41.2 ****	40.5 ± 2.9 ****	5.56 ± 0.05	1.22 ± 0.18	5.28 ± 0.08	1.46 ± 0.32
X4-BX1 (133-184)	5.62 ± 0.10 ****	204.0 ± 17.9 ****	27.9 ± 3.1 ****	5.34 ± 0.03	1.16 ± 0.10	5.62 ± 0.10	1.14 ± 0.27

**Table 4.2 Summary of ATP and antagonist properties at WT receptors and region B chimeras.** Boxes filled in red show a significant decrease compared to the hP2X1 receptor and those in blue show a significant increase. Grey boxes show no difference compared to the hP2X1 receptor. N/A = not applicable as value wasn't determined. Stars show significant difference from the WT hP2X1 receptor, \*\*\*\* = p<0.0001

## 4.3 Discussion

### 4.3.1 The Chimera Method Gives Insight into ATP Potency

There is an ~10-fold difference in ATP sensitivity between the hP2X1 and rP2X4 receptors and swapping residues of the hP2X1 receptor with those of the rP2X4 receptor affected the ATP potency of the receptor. ATP potency at chimera X1-CX4 was unchanged compared to the hP2X1 receptor and this suggests that variant residues in the region 185-261 do not contribute to the difference in ATP potency between the hP2X1 and rP2X4 receptors. Swapping residues 262-330 of the rP2X4 receptor into the hP2X1 receptor in the chimera X1-DX4 gave the receptor rP2X4 receptor-like ATP potency. This suggests that this region may contain residues which contribute to the ~ 10-fold difference in ATP potency between the two receptors. This supports the theory that variant residues between two P2X receptor subunits may be responsible for differences in their properties, in this case ATP potency. Residues located in the ATP binding pocket, known to be involved in ATP binding are conserved between all mammalian P2X receptors (Kaczmarek-Hajek *et al.*, 2012). Therefore these residues would not have been swapped as part of the chimera and cannot be responsible for the decrease in potency seen. Residues further outside the ATP binding pocket within these three chimeras must therefore be having an effect on ATP potency. This suggests that there is a complex interplay between residues in various parts of the P2X receptor, not just those in the ATP binding pocket, which contributes to ATP potency at the receptor.

Surprisingly the X1-AX4 and X1-BX4 chimeras were less sensitive to ATP than either the hP2X1 or rP2X4 receptors. At these receptors replacing residues in this region of the hP2X1 receptor with corresponding residues of the rP2X4 receptor has produced a mutant with an ATP sensitivity that is not similar or intermediate to either contributing receptor. It is therefore likely that swapping these residues has caused a conformational change at the receptor which alters ATP binding or gating at the receptor. The regions which were shown to have an effect on ATP potency are shown in figure 4.14a.

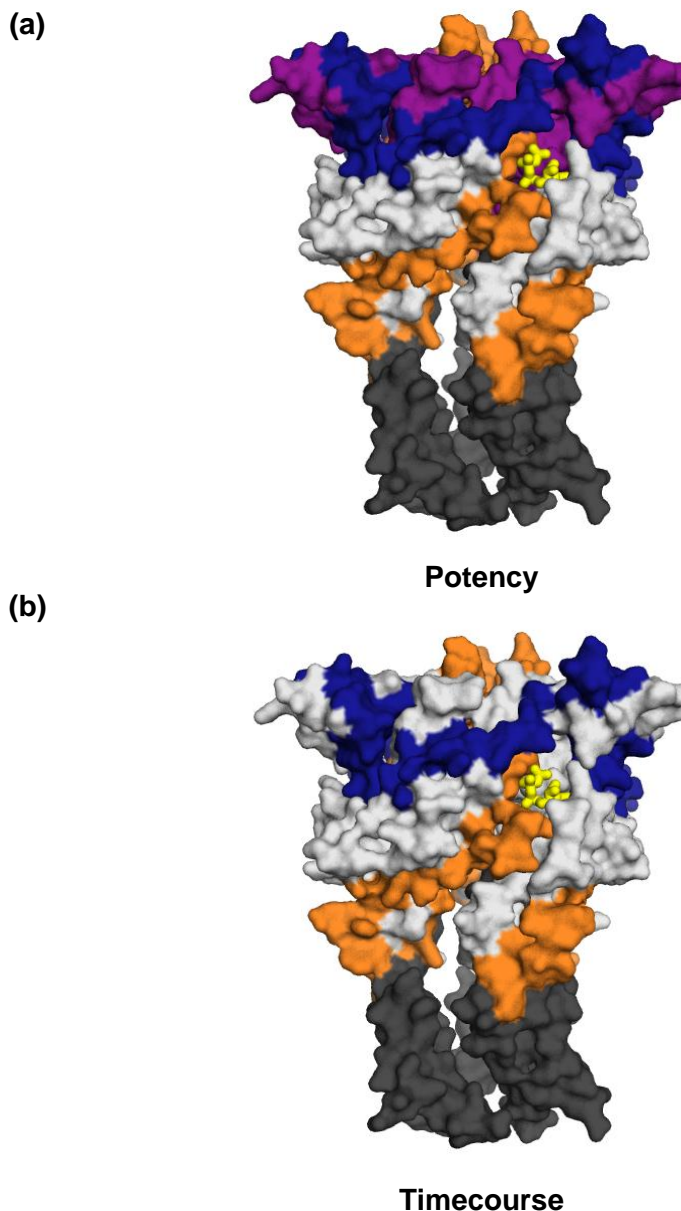


**Figure 4.14 Regions of the P2X Receptor Contributing to ATP potency and the Time-course of the ATP Response.** (a) Sections of the P2X receptor that had an effect on the potency of ATP at the hP2X1 receptor. Regions A (purple), B (blue) and D (orange) had an effect on ATP potency. Residues shown in light grey did not have an effect on ATP potency. Transmembrane domains are shown in dark grey and ATP is shown in yellow. (b) Sections of the P2X receptor that had an effect on the time-course of the response to ATP at the hP2X1 receptor. Regions B (blue) and D (orange) had an effect on the time-course of the ATP evoked response. Residues shown in dark grey had an effect on this property. Transmembrane domains are shown in dark grey and ATP is shown in yellow.

Interestingly, the effect of swapping residues was not reciprocal, as the X4-BX1 chimera had ATP potency similar to the rP2X4 receptor. This again suggests that multiple residues and regions of the receptor must be contributing to the difference in agonist potency and suggests that the effect on potency is not due to an alteration of residues directly involved in the ATP binding site.

#### 4.3.2 Insight into the Time-course of the ATP Evoked Response

The hP2X1 receptor has a characteristic fast time-course with near complete desensitisation (i.e. channel closure in the presence of ATP) during a 3 second ATP application, while the rP2X4 receptor shows intermediate desensitisation. The X1-AX4 and X1-CX4 chimeras had an unaffected time-course compared to the hP2X1 receptor. This suggests that differences in residues 52-132 and 185-261 are not contributing to the difference in time-course between the two receptors. Swapping residues of regions B and D of the hP2X1 receptor with those of the rP2X4 receptor affected the time-course of the receptors compared to the WT hP2X1 receptor. The X1-DX4 chimera had a time-course between the two WT receptors. This suggests that variant residues in the region 262-330 are having a contribution to the difference in time-course between the two receptors, but as the desensitisation was not as slow as at the WT rP2X4 receptor other residues must also be contributing. Chimera X1-BX4 had a time-course similar to the rP2X4 receptor, this suggests that residues in the region 133-184 of the rP2X4 receptor which has been introduced in this chimera are contributing to the slower time-course of the rP2X4 receptor. This effect was not reciprocal however, as introduction of the equivalent residues of the hP2X1 receptor into the rP2X4 receptor in chimera X4-BX1 did not introduce a P2X1 receptor-like rapid desensitisation. The regions of the receptor that have been implicated in the control of time-course in this chapter are shown in figure 4.14b.

Previous experiments using chimeras have demonstrated a strong contribution of the intracellular termini to receptor time-course (Werner *et al.*, 1996) (Allsopp & Evans, 2011). Splice variants of the P2X2 receptor have also implicated the intracellular regions in this property (Brandle *et al.*, 1997) (Smith *et al.*, 1999). Control of time-course at the P2X receptor is therefore complex,

with intracellular, extracellular and transmembrane components. There cannot be a physical interaction between the intracellular N terminus and the extracellular loop of the receptor and therefore these regions must be contributing in a different way. The transmembrane domains, in particular TM2, form the pore of the channel. Mutations of residues located in the intracellular and extracellular domains of the receptor which affect the time-course of the ATP response could be causing conformational changes to these regions of the receptor which in turn affect the transmembrane domains which are located between them. It has also been suggested that movement in the cysteine rich head region can be linked to desensitisation. Movement occurs in this region upon ATP binding which leads to channel opening (Hattori & Gouaux, 2012). Voltage clamp fluorometry experiments have shown that there is a slow increase in fluorescence upon ATP application when residues 121 and 125 were labelled by tetramethyl-rhodamine-maleimid (Lorinczi *et al.*, 2012). This fluorescence increase co-ordinated with desensitisation and movement that occurs at these residues has therefore been linked with this property.

#### **4.3.3 Insight into NF449 Binding**

Chimeras X1-BX4 and X1-CX4 showed large decreases in NF449 sensitivity compared to the hP2X1 receptor. This suggests that the difference in NF449 sensitivity between the hP2X1 and rP2X4 receptors is due to the rP2X4 receptor lacking the residues that form the NF449 binding site and implicates residues 133-261 in NF449 antagonism at the hP2X1 receptor, as their replacement with those of the antagonist insensitive rP2X4 receptor decreased NF449 sensitivity. The residues contained in region B are mostly located in the cysteine rich head region of the receptor (figure 4.15). This region has been implicated in NF449 antagonism previously, when residues K136, K138, R139 and K140 were shown to contribute to NF449 inhibition at the hP2X1 receptor (El-Ajouz *et al.*, 2012). These four residues are contained within region B and are likely to be contributing to the decrease in NF449 antagonism seen. In the El-Ajouz *et al* study, mutation of the four positive charges of the hP2X1 receptor to the equivalent charges in the hP2X2 receptor decreased antagonist sensitivity ~ 150-fold. In this thesis the same residues have been mutated to

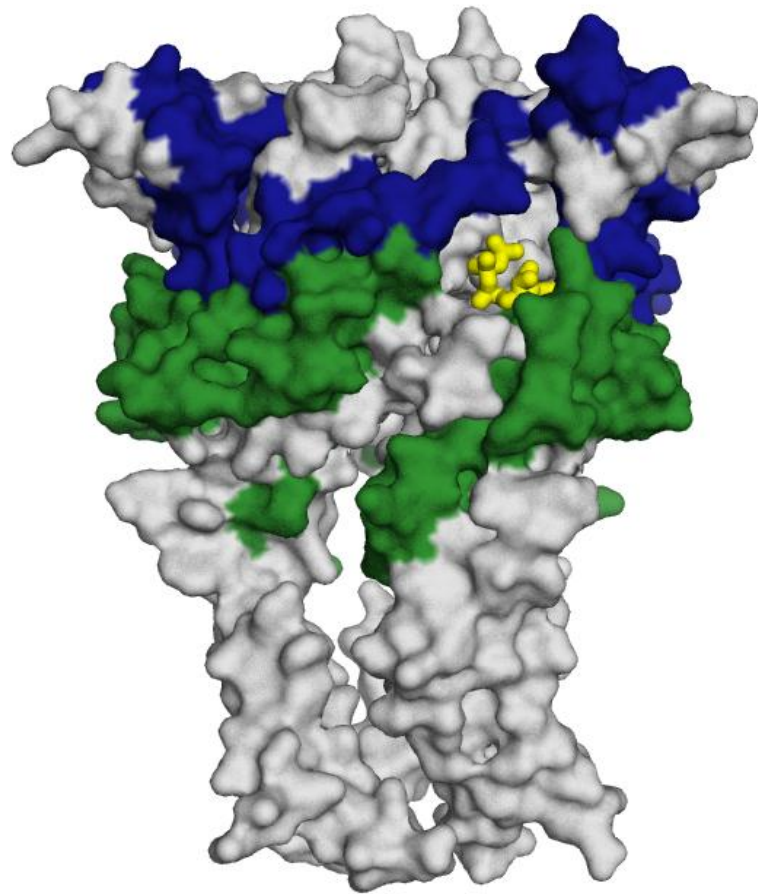


**Figure 4.15 Regions of the P2X Receptor Contributing to NF449 action.** Sections of the hP2X1 receptor that when swapped with the equivalent residues of the rP2X4 receptor caused a > 50-fold decrease in NF449 inhibition at the receptor are shown in colour on the ATP bound receptor. Section B, residues 133-184, is shown in blue. Section C, residues 185-261 are shown in green. ATP is shown in yellow.

the equivalent rP2X4 receptor amino acids, as part of chimera X1-BX4 in which residues 133-184 of the hP2X1 receptor were mutated to those of the rP2X4 receptor. This chimera had a shift of ~ 135-fold compared to the WT hP2X1 receptor, similar to the shift reported by El-Ajouz *et al.* It is therefore likely that the loss of these four charges is responsible for the shift seen in chimera X1-BX4, but as other variant residues have been swapped in this chimera it is possible that these might also be contributing to the loss in NF449 inhibition at the chimera. This will be tested in chapter 5. The residues located in region C (185-261) that were mutated as part of chimera X1-CX4 have not been previously indicated in NF449 action. These residues form a band around the centre of the receptor, including the region immediately below the positively charged residues in region B. This suggests that the NF449 molecule might be binding in this region so that it interacts with residues in both regions B and C. The specific residues within region C that are contributing to NF449 action will be investigated in chapter 5.

Although chimeras X1-AX4 and X1-DX4 showed a decrease in NF449 action, this shift was less than 5-fold. As the shift in the other two chimeras was much larger, it was assumed that regions A and D were not strongly contributing to NF449 action. As the hP2X1 receptor could not be made completely insensitive to NF449, as is seen at the rP2X4 receptor, it can be assumed that the differences between residues within regions B and C are not solely responsible for the difference in antagonist potency between the two receptors and a combination of chimeras or residues may be needed in order to completely eliminate NF449 inhibition at the hP2X1 receptor.

Chimera X4-BX1 was not inhibited by NF449. This shows that the effect of residues in region B was not reciprocal, and although the loss of these residues removed NF449 sensitivity from the hP2X1 receptor, the presence of them could not introduce sensitivity at the rP2X4 receptor. This demonstrates that antagonist sensitivity is a more complex process and other residues must also be necessary for NF449 action as part of a multi residues binding site. NF449 action at the hP2X1 receptor is further investigated in chapter 5.

#### **4.3.4 The Chimera Method Does Not Remove Suramin or PPADS Binding at the hP2X1 Receptor**

It was predicted that some variant residues in the hP2X1 receptor were responsible for high affinity suramin and PPADS binding and these were absent from the rP2X4 receptor, however none of the hP2X1 receptor based chimeras showed a decrease in either suramin or PPADS action. This suggests that the difference in antagonism between the two receptors is not a simple matter of a few variant residues but is more complex, with the conformation of the receptor having an important contribution.

Receptor conformation is important in antagonist action. It is known that the receptor is not a static structure, even at rest. For an antagonist to bind, as well as having the specific residues that form the binding site, the receptor must be in a conformation that allows antagonist action. This is known as the induced fit model, where the antagonist can cause movement that allows it to bind and exhibit its inhibitory effects. If variation in the sequence of a receptor causes a structural change that prevents it from entering this conformation then inhibition will not occur. This has been seen with the binding of ATP at the receptor, in the resting state the residues that co-ordinate ATP are too far apart to form a binding site, but ATP induces a conformational change which allows its binding and holds it in a conformation that allows ion flow (Hattori & Gouaux, 2012). The same is likely to be true for antagonists. If the difference in antagonism between the hP2X1 and rP2X4 receptors is due to differences in their conformation rather than in the residues that are directly involved in ATP binding then this would explain why the chimeric method did not give insight into their action.

This is in contrast to NF449, where the difference in antagonist sensitivity appears to be due to a difference in the residues which form the antagonist binding site. This makes sense as NF449 is selective for the hP2X1 receptor and has nanomolar potency at this receptor, suggesting that the residues it binds to are likely to be unique to this receptor subtype. Suramin and PPADS are less selective between P2X receptors and have a lower affinity than NF449. It can therefore be reasoned that the residues necessary for

suramin and PPADS binding are present in all P2X receptor subtypes and the antagonist sensitivity of each receptor is due to its conformation. The fact that the rP2X4 receptor is insensitive to all commonly used P2X receptor antagonists and that antagonists which do act at the receptor do not cause inhibition at other subtypes also supports the fact that the conformation the rP2X4 receptor adopts plays a large role in its antagonist sensitivity.

#### **4.3.5 Chimera X4-BX1 Introduced Suramin and PPADS Sensitivity to the rP2X4 Receptor**

An interesting find was that although replacing residues 133-184 of the hP2X1 receptor with those of the rP2X4 receptor had no effect on suramin inhibition, and very little effect on PPADS sensitivity of the hP2X1 receptor, the reciprocal mutation introducing hP2X1 receptor residues into the rP2X4 receptor led to the receptor being both PPADS and suramin sensitive. This demonstrates that antagonist sensitivity can be introduced to the antagonist insensitive rP2X4 receptor. A mutation which has previously been shown to introduce antagonist sensitivity to the P2X4 receptor is E249K (Buell *et al.*, 1996). This mutated P2X4 receptor was sensitive to PPADS with an IC<sub>50</sub> concentration of 2.6 μM. This residue has not been mutated as part of chimera X4-BX1 and therefore is not responsible for the PPADS sensitivity at this receptor. A second mutation which has introduced both suramin and PPADS sensitivity at the P2X4 receptor is H241A (Xiong *et al.*, 2004b). This residue has not been mutated as part of the X4-BX1 chimera and so is again unlikely to be contributing to the antagonist sensitivity of this mutant. The residues which have been shown to introduce antagonist sensitivity to the receptor are unlikely to be contributing to the binding site of the receptor as they are spread throughout the structure and are not clustered together in a binding pocket. They may therefore be inducing conformational changes to the receptor which allow antagonism to occur.

The introduction of antagonist sensitivity to the P2X4 receptor is particularly interesting as this is the only subtype of P2X receptor which has been crystallised is the antagonist insensitive zfP2X4 receptor. Therefore introducing antagonism to this subtype could lead to the generation of an

antagonist bound crystal structure for a P2X receptor. Crystallisation of a receptor in an antagonist bound state is a definitive way of locating the antagonist binding site and deducing the conformation that the receptor adopts when inhibition occurs. This has been seen for the antagonist TK40 at the NMDA receptor (Kvist *et al.*, 2013). The residues which have introduced suramin and PPADS inhibition to the rP2X4 receptor have been investigated in chapter 6.

In summary this chapter has given insight into regions of the receptor involved in ATP potency, time-course of the ATP evoked response and the NF449 binding site at the hP2X1 receptor. It has also shown regions of the hP2X1 receptor that when introduced to the rP2X4 receptor cause the receptor to become suramin and PPADS sensitive, likely by introducing a conformational change to the receptor. The particular residues within the regions identified that are contributing to these properties are investigated in more detail in later chapters.

## **Chapter 5: Sub-Chimeras and Point Mutations to Investigate NF449 Action**

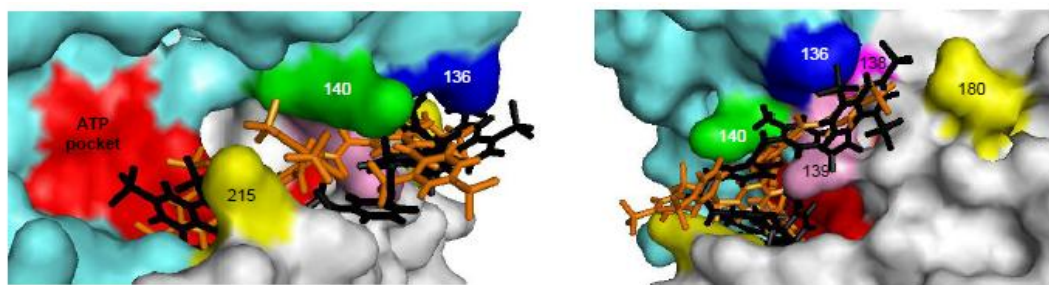
### **5.1 Introduction**

Initial chimeras identified residues in regions B and C of the hP2X1 receptor as contributing to the nanomolar potency of NF449 (chapter 4). These residues are located at the base of, and just below, the cysteine rich head region. Sub-division of these chimeras and the generation of point mutants was the next step to identify specific variant residues and regions contributing to NF449 action. Residues identified in these experiments were used to generate four potential NF449 bound *in silico* models of the hP2X1 receptor.

#### **5.1.1 Previous Studies into NF449 Binding and *in silico* Models**

In order to create an agonist/antagonist bound *in silico* model of a receptor, several residues which are known to be involved in the action of that molecule are required to be used as co-ordinates on the structure around which binding can be centred. The more residues that have been identified as contributing, the more accurate the binding studies will be. There are four charges present at the base of the cysteine rich head region of the hP2X1 receptor that have been shown to play an essential role in the high affinity of NF449 at the receptor (El-Ajouz *et al.*, 2012). These have previously been used as the basis for two *in silico* NF449 and suramin bound models of the hP2X1 receptor, with docking being centred around these 4 residues (El-Ajouz, 2011). The study predicted that suramin and NF449 would both bind in the same location, in close proximity to the four positive charges of the cysteine rich head region. In the first pose the centre of both antagonists bound between residues R139 and K140 and the arms of the molecules extended both into the ATP binding pocket, and around the rear of the cysteine rich head region, towards residue K136 (figure 5.1a) (El-Ajouz *et al.*, 2012). In the second pose the molecules bound further behind the cysteine rich head region and NF449 protruded downwards and displayed a possible interaction with residue H224 (figure 5.1b).

(a)



(b)

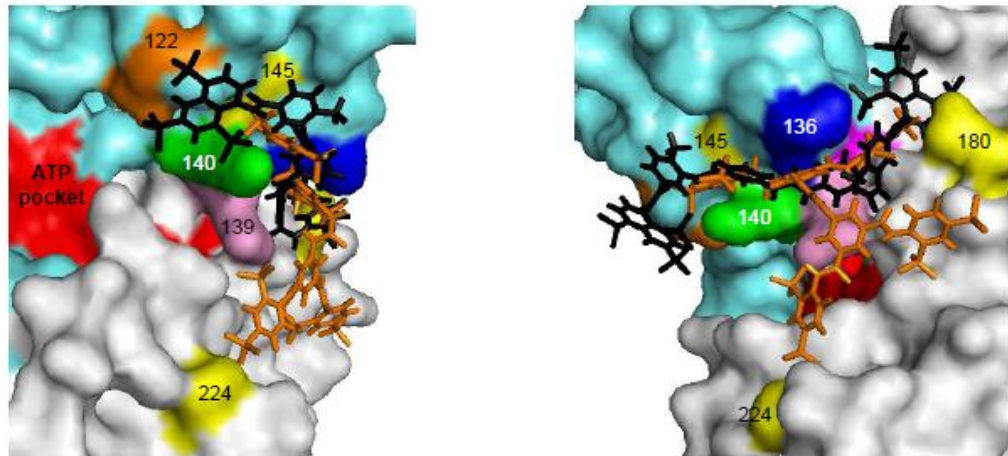


**Figure 5.1 Suramin and NF449 Bound Models from El Ajouz 2011. (a)** The model shows suramin (black) and NF449 (orange) molecules bound underneath the cysteine rich head region with the arms of the antagonists stretching into the ATP binding pocket. **(b)** A second potential model shows the antagonists docked further behind the cysteine rich head region, with NF449 extending further down the receptor than the suramin molecule. A possible interaction of NF449 with H224 is shown.

Multiple residues are known to be involved in ATP binding and NF449 is a much larger molecule than this agonist. Therefore it is likely that numerous residues are involved in the binding of NF449 to the hP2X1 receptor. Only four residues were identified and used as the basis of the *in silico* docking in the previous study, giving a fair possibility for error in these models. The experiments performed in this chapter to identify any residues in regions B or C that are contributing to NF449 action could be used to refine these models of NF449 binding by increasing the number of co-ordinates. Validation of previous models can also be carried out using these results as if mutating a residue located in close proximity to the previous bound NF449 molecule has an effect on NF449 inhibition, then this potentially supports that model. Identification of additional residues contributing to NF449 inhibition can therefore be used to increase the accuracy of antagonist bound models of the hP2X1 receptor.

### **5.1.2 Chapter Aims**

Results from chapter 4 suggested that residues located in regions B and C of the hP2X1 receptor are contributing to NF449 action. Therefore in this chapter sub-chimeras and point mutations within these regions were generated with the aim of highlighting specific residues or regions involved in inhibition by NF449. These findings could be used to provide a larger set of co-ordinates and additional parameters for the generation and validation of NF449 bound *in silico* models of the hP2X1 receptor.

## **5.2 Results**

### **5.2.1 ATP Sensitivity of Chimeras X1-BX4(2+) and X1-BX4(4+)**

The four positive charges previously shown to contribute to NF449 action (El-Ajouz *et al.*, 2012) are contained in section B of the hP2X1 receptor. Chimera X1-BX4 showed a large ~ 60-fold decrease in NF449 sensitivity compared to the hP2X1 receptor (chapter 4). As part of this chimera, the four positive charges had been replaced with uncharged or negatively charged residues. I wanted to identify if it was solely the loss of positive charge that was responsible for the decrease in NF449 sensitivity of X1-BX4, or if other residues within region B that had been swapped were also involved. Two mutant

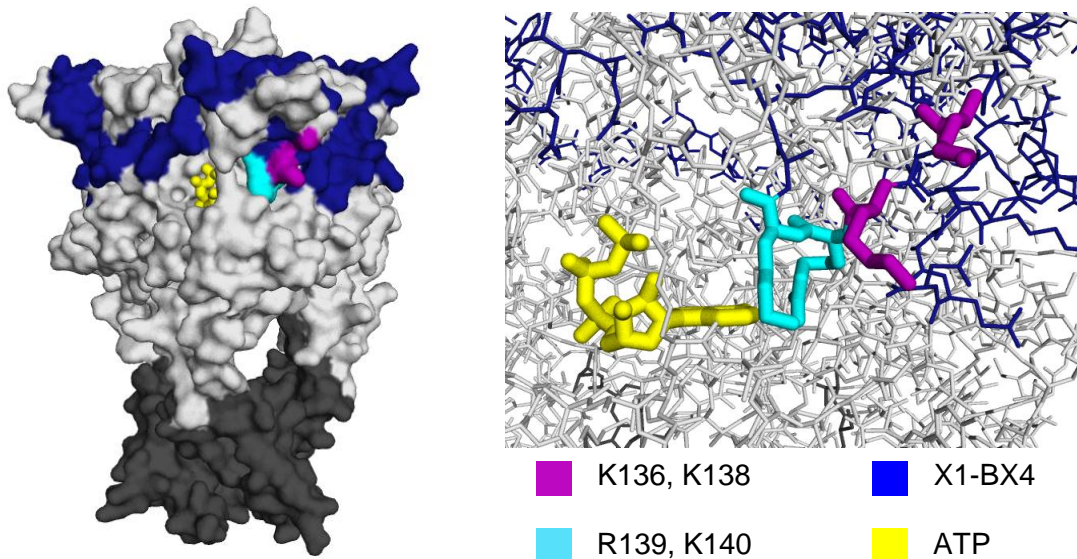
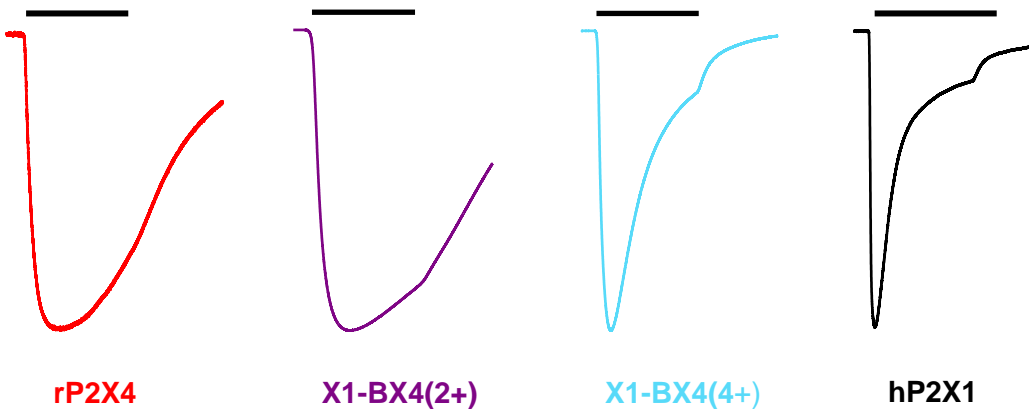


**Figure 5.2 Reintroducing Positive Charge to the Cysteine-Rich Head Region.** Homology model of the ATP-bound hP2X1 receptor. Four positive charges that are present in the hP2X1 receptor but not the rP2X4 receptor were mutated into chimera X1-BX4 (dark blue). The charges were mutated in two at a time. Chimera X1-BX4 (2+) contains K136 and K138 (purple). Chimera X1-BX4 (4+) also contains the additional R139 and K140 charges (cyan). The charges are located within the cysteine rich head region, near the ATP binding pocket. ATP is shown in yellow.

(a)



(b)

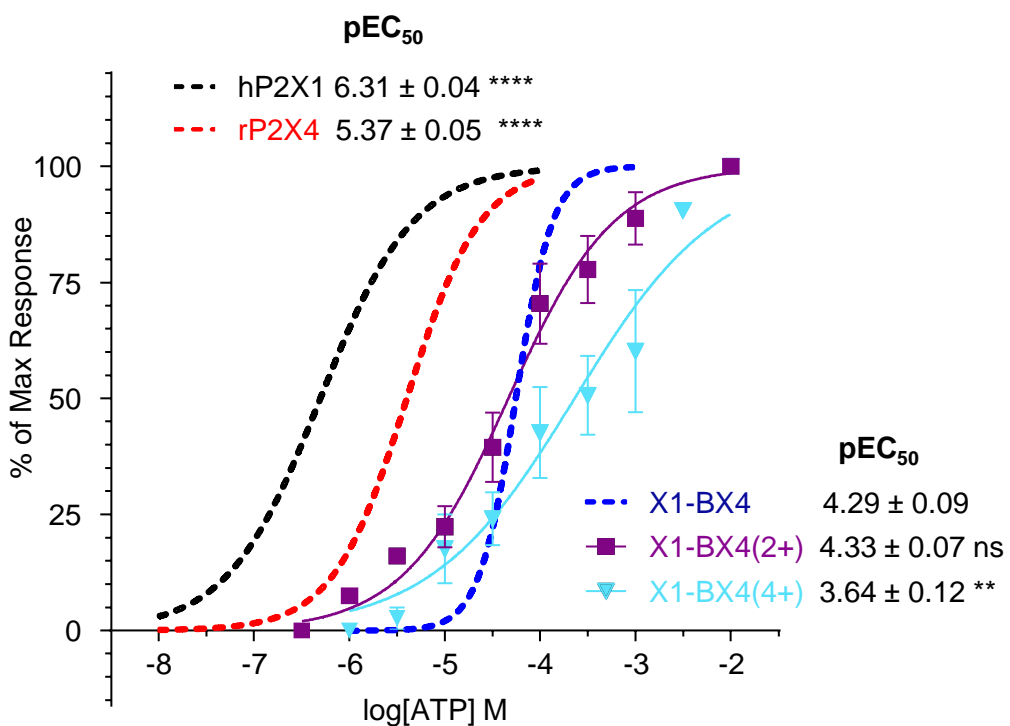


**Figure 5.3 ATP Action at the X1-BX4(2+) and X1-BX4(4+) Chimeras. (a)** Representative traces of maximal ATP application to *Xenopus* oocytes expressing the rP2X4, X4-BX1, X1-BX4(2+), X1-BX4(4+) and hP2X1 receptors. Bars represent a 3 s application. Traces have been normalised to peak currents to allow comparison. **(b)** Concentration response curves for the X1-BX4 mutants.  $\text{pEC}_{50}$  values are shown, stars represent a significant difference from the X1-BX4 chimera. \*\*  $p < 0.01$ , \*\*\*\*  $p < 0.0001$ .

receptors were made which re-introduced the WT residues of the hP2X1 receptor at these positions. X1-BX4(2+) consisted of chimera X1-BX4 with the mutations S136K and D138K (figure 5.2). X1-BX4(4+), used the X1-BX4(2+) template and contained additional T139R and H140K mutations. The residues were split this way as the studies by Sim *et al* and El-Ajouz *et al* had suggested that residues 136 and 138 were having the greatest contribution to suramin and NF449 sensitivity at the hP2X1 receptor (Sim *et al.*, 2008) (El-Ajouz *et al.*, 2012). The mutated residues were located near the ATP binding pocket, with R139 and K140 being closest to the pocket, and K136 and K138 slightly further out (figure 5.2).

ATP evoked currents at X1-BX4(2+) and X1-BX4(4+) with mean peak responses to ATP<sub>max</sub> (3 mM) of  $4540 \pm 434$  and  $3185 \pm 575$  nA respectively. A decrease in ATP potency compared to the hP2X1 and rP2X4 receptors was recorded at both chimeras, with pEC<sub>50</sub> values of  $4.33 \pm 0.07$  and  $3.64 \pm 0.12$  respectively  $p < 0.0001$  (figure 5.3b). ATP potency at X1-BX4(2+) was the same as the X1-BX4 chimera but the X1-BX4(4+) mutant was ~ 4-fold less sensitive than the X1-BX4 receptor,  $p < 0.01$ . Neither concentration response curve showed a difference from the hP2X1 receptor in Hill slope (table 5.1).

### **5.2.2 Time-course of the ATP Evoked Response of Chimeras X1-BX4(2+) and X1-BX4(4+)**

Chimera X1-BX4 had a rise time that was similar to the rP2X4 receptor, and > 4-fold slower than the hP2X1 receptor, suggesting that variant residues within region B were contributing to the difference in time-course between the two WT receptors (chapter 4). As with the X1-BX4 chimera, X1-BX4(2+) had a rP2X4 receptor-like rise time of  $356 \pm 25$  ms (figure 5.3a) . At the X1-BX4(4+) mutant, which had two further positive charges compared to X1-BX4(2+), the rise time was hP2X1 receptor-like ( $162 \pm 12.4$  ms), > 2 times faster than at the rP2X4, X1-BX4 and X1-BX4(2+) receptors ( $p < 0.01$ ) (figure 5.3a). As well as a difference in rise time between the X1-BX4, X1-BX4(2+) and X1-BX4(4+) chimeras, there was also a clear difference in the % desensitisation recorded at the end of the ATP application (figure 5.3a). It was seen in chapter 4 that

chimera X1-BX4 displayed rP2X4 receptor-like desensitisation, 2-fold less than the WT hP2X1 receptor. The X1-BX4(2+) mutant also showed rP2X4 and X1-BX4 –like desensitisation ( $28.2 \pm 3.5\%$ ) (figure 5.3a). This meant it desensitised nearly 3-fold less than the hP2X1 receptor during the presence of ATP,  $p < 0.0001$ . Again, introducing the two further charges in the X1-BX4(4+) mutant changed the time-course of the response compared to when only two charges were re-introduced. X1-BX4(4+) desensitised by  $84.3 \pm 1.7\%$ , similar to the hP2X1 receptor and ~ 3-fold faster than at the X1-BX4(2+) receptor,  $p < 0.0001$ ). These results show that the positively charged residues present in the cysteine rich head region of the WT hP2X1 receptor contribute to its characteristic fast time-course. This is interesting as although the X1-BX4(4+) mutant had the largest decrease in ATP potency from the hP2X1 receptor. It had a similar time-course. This will be discussed at the end of the chapter.

### 5.2.3 NF449 Action at X1-BX4 (2+) and X1-BX4(4+) Chimeras

If re-introduction of the essential positive charges to chimera X1-BX4 produced hP2X1-receptor like NF449 sensitivity, it could be assumed that it was only these residues within region B that were contributing to the difference in NF449 sensitivity between the hP2X1 and rP2X4 receptors. It was seen in chapter 4 that the presence of 10 nM NF449 caused no inhibition at the X1-BX4 chimera. A similar result was seen at the X1-BX4(2+) chimera, suggesting that the presence of positive charges at positions 136 and 138 has had no effect on the NF449 sensitivity of the receptor (figure 5.4a). In contrast, addition of two further positively charged residues at positions 139 and 140 in the X1-BX4(4+) chimera caused the receptor to be ~ 70% inhibited by 1 nM NF449 (figure 5.4a). NF449 inhibition curves showed that the X1-BX4 and X1-BX4(2+) chimeras were similarly blocked by NF449, with  $\text{pIC}_{50}$  values of  $7.35 \pm 0.08$  and  $7.53 \pm 0.06$  respectively (figure 5.4b). Both these receptors were ~ 40-fold less sensitive to NF449 than the hP2X1 receptor ( $p < 0.0001$ ). The X1-BX4(4+) chimera had an NF449 sensitivity similar to that of the hP2X1 receptor ( $\text{pIC}_{50} = 9.28 \pm 0.05$ ). This suggests that it was the loss of the positive charges from

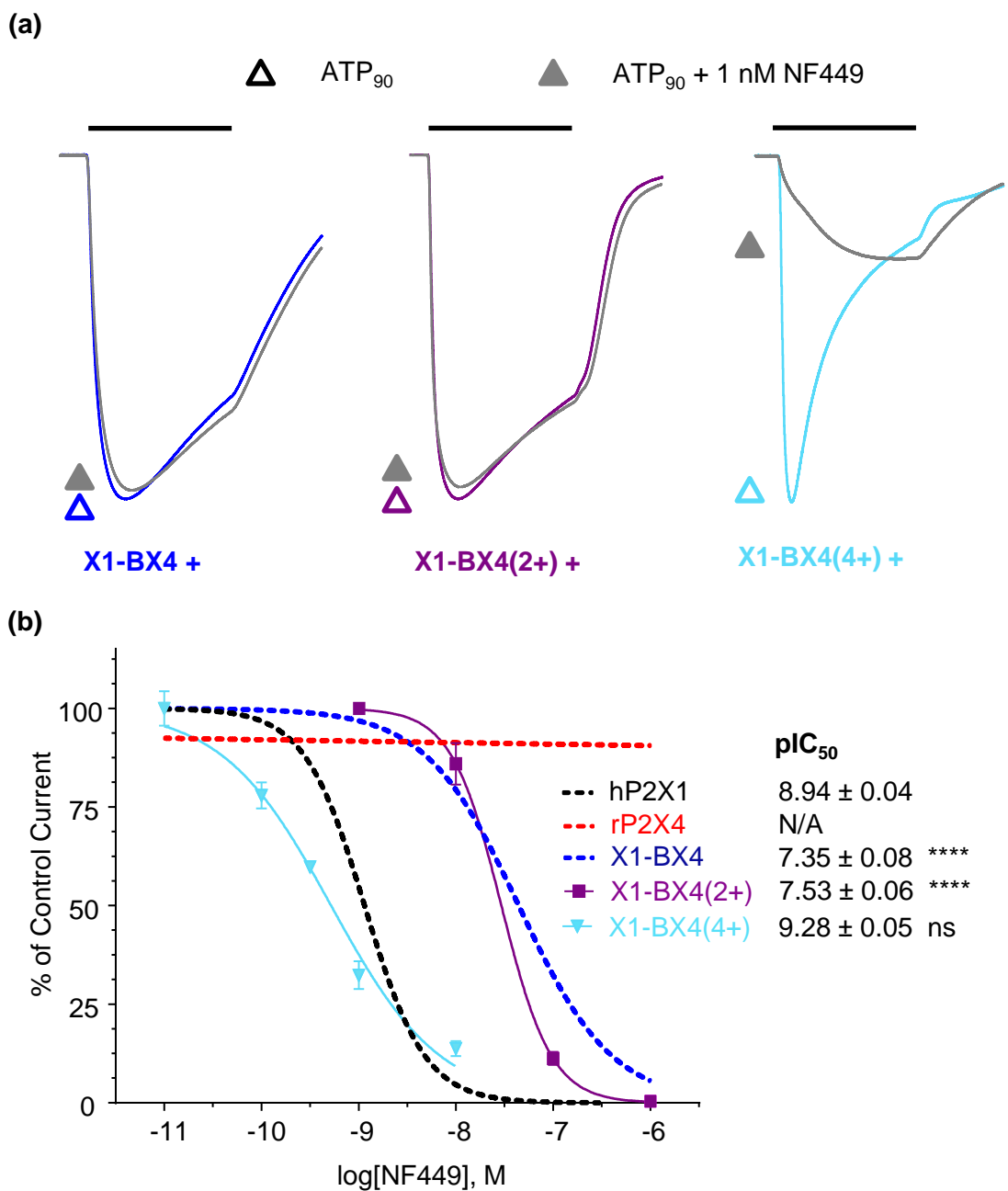


**Figure 5.4 NF449 Action at the X1-BX4 Point Mutations.** (a) Representative traces of ATP<sub>90</sub> (open triangles) and ATP<sub>90</sub> + NF449 (closed triangles) application. Bars indicate a 3 s application. Traces have been normalised to peak currents to allow for comparison. A 5-10 minute period was given between applications to allow for recovery from desensitisation. (b) NF449 inhibition curves. pIC<sub>50</sub> values are shown. Stars represent significant differences from the WT hP2X 1 receptor. \*\*\*\* p<0.0001.

	<b>Peak Current (nA)</b>	<b>Rise Time (ms)</b>	<b>% Desensitisation</b>	<b>ATP pEC<sub>50</sub></b>	<b>ATP Hill Slope</b>	<b>NF449 pIC<sub>50</sub></b>	<b>NF449 Hill Slope</b>
<b>hP2X1</b>	7598 ± 793	95.7 ± 5.1	80.3 ± 4.3	6.31 ± 0.04	0.89 ± 0.07	8.94 ± 0.04	1.40 ± 0.20
<b>rP2X4</b>	5320 ± 586	309.3 ± 32.0	28.7 ± 4.5	5.37 ± 0.05	1.07 ± 0.12	N/A	N/A
<b>X1-BX4</b>	4651 ± 499	462.5 ± 41.2	40.5 ± 2.9	4.29 ± 0.09	2.29 ± 0.28	7.35 ± 0.08	0.91 ± 0.12
<b>X1-BX4(2+)</b>	4540 ± 434	356 ± 25	28.2 ± 3.5	4.33 ± 0.07	0.78 ± 0.10	7.53 ± 0.06	1.68 ± 0.19
<b>X1-BX4(4+)</b>	3185 ± 575	162 ± 12	84.3 ± 1.7	3.64 ± 0.12	0.58 ± 0.09	9.28 ± 0.05	0.77 ± 0.08

**Table 5.1 ATP and NF449 action at the X1-BX4 mutations.** Boxes shaded in grey show no difference from the hP2X1 receptor. Blue represents a significant increase compared to the hP2X1 receptor and red represents a significant decrease. N/A = not applicable as the value was not determined.

the hP2X1 receptor that caused the decrease in NF449 sensitivity seen at chimera X1-BX4 and that the other variant residues in this region did not have important roles. Therefore no additional residues from region B were used in the generation of new *in silico* NF449 bound hP2X1 receptor models.

#### 5.2.4 X1-CX4 Sub-Chimeras

As chimera X1-CX4 showed an ~ 135-fold decrease in NF449 sensitivity compared to the hP2X1 receptor the contribution of this region (residues 185-261) to NF449 action was examined. To do this, region C was split into smaller sections from which sub-chimeras were generated.  $C_\alpha$  and  $C_\beta$ , were larger sections of 25 and 29 residues respectively and located either side of the four charged residues in region B (figure 5.5a). The residues swapped were 184-209 in chimera X1- $C_\alpha$ X4 and 232-261 in X1- $C_\beta$ X4. It was hypothesised that those residues within chimera C that were closest to the four positively charged residues in the cysteine rich head region were most likely to be involved in NF449 action. This region was therefore split into four smaller sections called  $C_\gamma$ ,  $C_\delta$ ,  $C_\varepsilon$  and  $C_\zeta$  (figure 5.5a). The smaller sub-chimeras allowed a more in-depth analysis of the contribution of residues closest to the positive charges to NF449 action. The residues contained within these chimeras were 210-215 in chimera X1- $C_\gamma$ X4, 216-220 in X1- $C_\delta$ X4, 221-226 in X1- $C_\varepsilon$ X4 and 227-231 in X1- $C_\zeta$ X4 (figure 5.5a).

#### 5.2.5 ATP at the Large X1-CX4 Sub-Chimeras

Application of ATP<sub>max</sub> produced responses in the X1- $C_\alpha$ X4 and X1- $C_\beta$ X4 chimeras with mean peak currents of  $6893 \pm 864$  and  $6117 \pm 669$  nA respectively. ATP potency at both X1- $C_\alpha$ X4 ( $pEC_{50} = 5.34 \pm 0.05$ ) and X1- $C_\beta$ X4 ( $pEC_{50} = 5.30 \pm 0.06$ ) was decreased ~ 10-fold compared to the hP2X1 and X1-CX4 receptors,  $p < 0.0001$ , and was rP2X4 receptor-like, as were the Hill slopes (figure 5.5c, table 5.2).

The time-course of the chimeras was also hP2X1 receptor-like with rise times of  $88.0 \pm 7.4$  ms and  $89.0 \pm 8.6$  ms for the X1- $C_\alpha$ X4 and X1- $C_\beta$ X4 chimeras respectively (figure 5.5b). The % desensitisation of both sub-chimeras

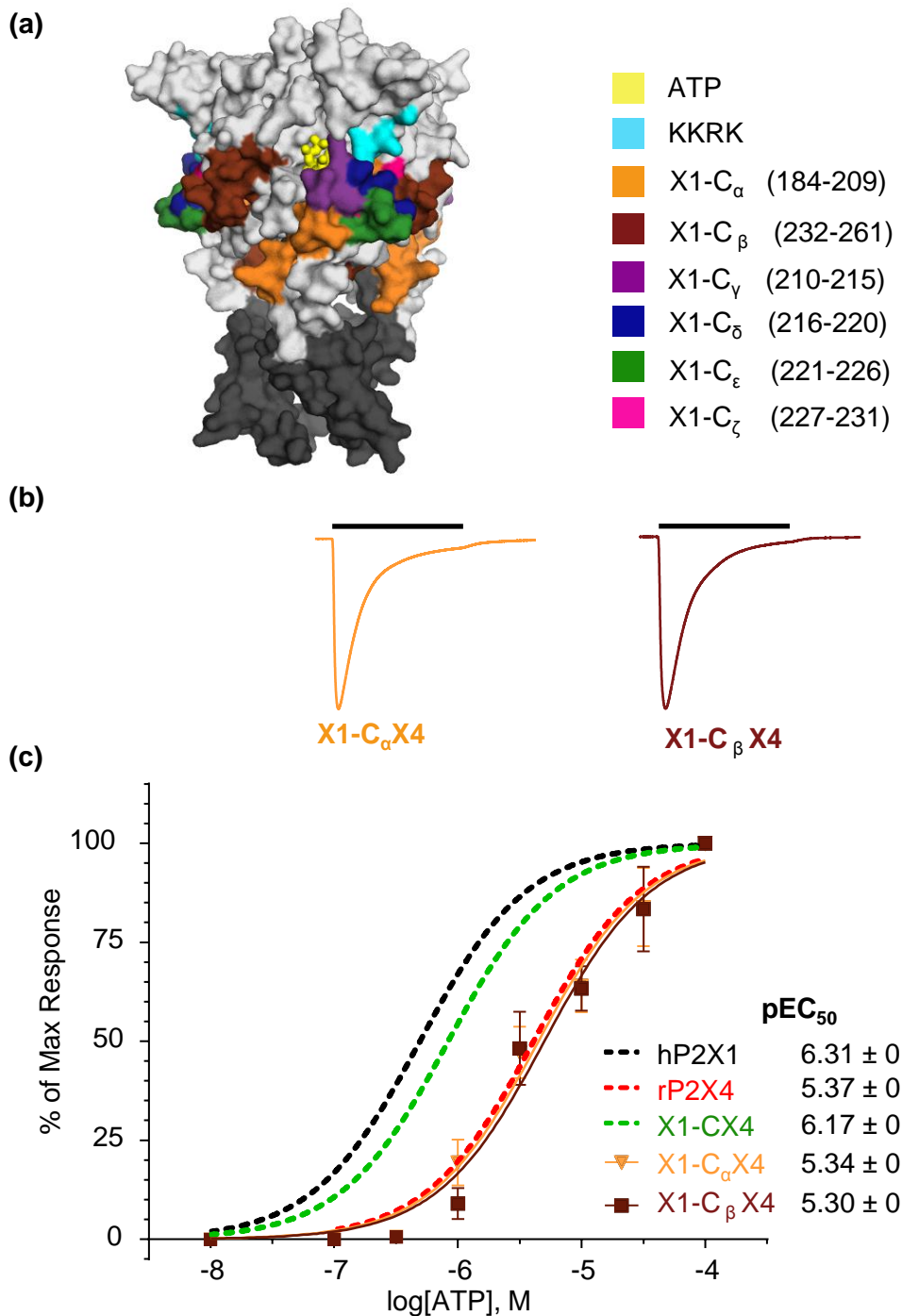
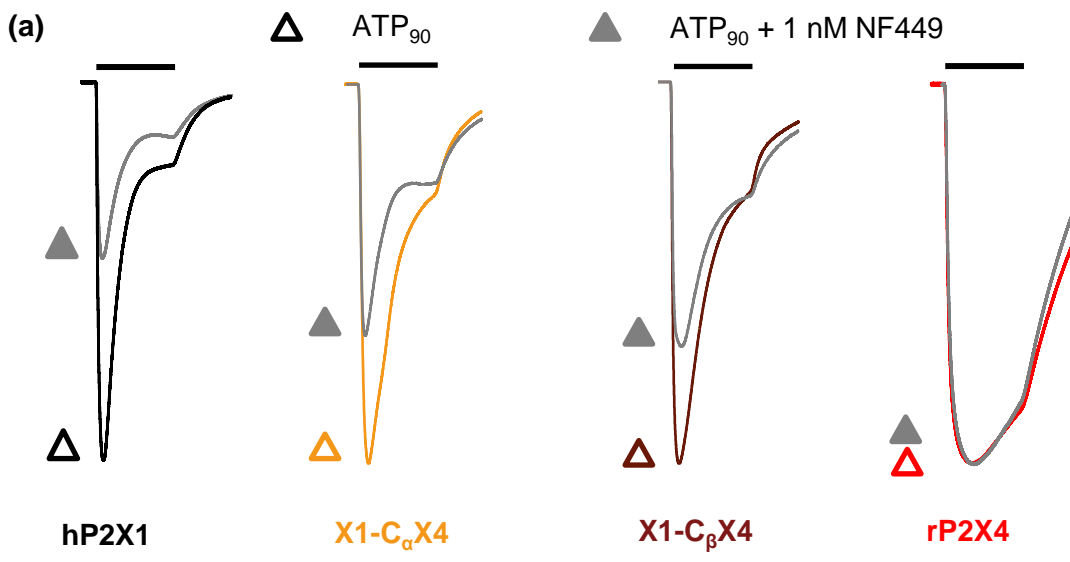


**Figure 5.5 Sub-chimeras Within X1-CX4 and Effects of ATP at Large Sub-chimeras.** (a) Region C, which is located below the four positive charges KKRK, was split into 6 sub-sections. Two large sub-chimeras (X1-C<sub>α</sub>X4 and X1-C<sub>β</sub>X4) and 4 smaller sub-chimeras (X1-C<sub>γ</sub>X4 X1-C<sub>δ</sub>, C<sub>ε</sub> and C<sub>ζ</sub>). (b) Representative traces to show maximal ATP application at the two large sub-chimeras. Bars indicate a 3 s application of ATP. Traces were normalised to peak currents to allow comparison (c) Concentration response curves for large sub chimeras. Stars show a significant difference in pEC<sub>50</sub> from the WT hP2X1 receptor. \*\*\*\* p<0.001



(b)

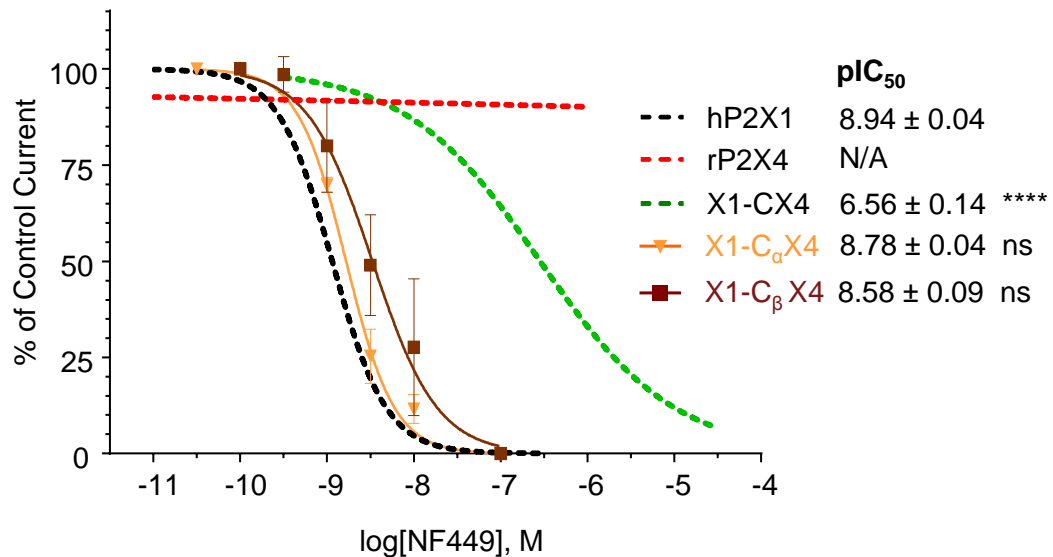


**Figure 5.6 NF449 Inhibition at the Large X1-CX4 Sub-Chimeras.** (a) Representative traces of EC<sub>90</sub> ATP (ATP<sub>90</sub> open triangles) and ATP<sub>90</sub> + 1 nM NF449 (closed triangles) application at *Xenopus* oocytes expressing the WT and X1-C<sub>α</sub>X4 and X1-C<sub>β</sub> X4 receptors. Bars indicate a 3 s application. Peaks have been normalised to allow for comparison. 5 minutes was given between repeat applications to allow for recovery from desensitisation. (b) Inhibition curves for NF449 at the large X1-CX4 sub-chimeras. pIC<sub>50</sub> values are shown. Stars indicate a significant difference from the hP2X1 receptor. \*\*\*\* p < 0.0001.

was  $89.4 \pm 1.5\%$  and  $84.8 \pm 8.2\%$  respectively. This shows that as with the X1-CX4 chimera, residues within regions  $C_\alpha$  and  $C_\beta$  were not involved in the varying time-course of the receptors in response to ATP. Residues which are contributing to time-course and potency of the hP2X1 receptor will be discussed in more detail at the end of this chapter.

### 5.2.6 NF449 Action at the Large X1-CX4 Sub-Chimeras

Both the X1- $C_\alpha$ X4 and X1- $C_\beta$ X4 chimeras displayed ~ 50% inhibition when 1 nM NF449 was co-applied with EC<sub>90</sub> ATP (figure 5.6a). Full NF449 inhibition curves showed that NF449 inhibition at X1- $C_\alpha$ X4 ( $pIC_{50} = 8.78 \pm 0.04$ ) and X1- $C_\beta$ X4 ( $pIC_{50} = 8.58 \pm 0.09$ ) was the same as the hP2X1 receptor (figure 5.6b). The Hill slopes also showed no difference from the hP2X1 receptor (table 5.2). This suggests that residues 184-209 and 232-261 of the hP2X1 receptor are not involved in the differences in NF449 inhibition between the hP2X1 and rP2X4 receptors.

### 5.2.7 Location of X1-CX4 Small Sub-Chimeras and ATP Sensitivity

The smaller X1-CX4 sub-chimeras each consisted of 5-6 residues and were located below both the ATP binding pocket and the four positively charged residues at positions 136-140 (figure 5.7a). The regions were X1- $C_\gamma$ X4 containing residues 210-215, X1- $C_\delta$ X4 containing residues 216-220, X1- $C_\epsilon$ X4 consisting of residues 221-226 and X1- $C_\zeta$ X4 which contained residues 227-231. Application of maximal ATP to the small sub-chimeras produced hP2X1 receptor-like peak currents (table 5.2). The X1- $C_\gamma$ X4 and X1- $C_\epsilon$ X4 chimeras had pEC<sub>50</sub> values of  $5.71 \pm 0.06$  and  $5.68 \pm 0.06$  respectively and showed similar ATP potency to both the hP2X1 and X1-CX4 receptors (figure 5.7b). The X1- $C_\delta$ X4 and X1- $C_\zeta$ X4 receptors had ~ 12 and 6-fold decreased ATP potency compared to the hP2X1 receptor, with pEC<sub>50</sub> values of  $5.21 \pm 0.04$ ,  $p < 0.0001$  and  $5.54 \pm 0.06$ ,  $p < 0.001$ . The Hill slopes of all the small sub-chimeras were hP2X1 receptor-like (table 5.2).

As with chimera X1-CX4, there was no difference in the time-course of the maximal responses of these chimeras compared to the hP2X1 receptor

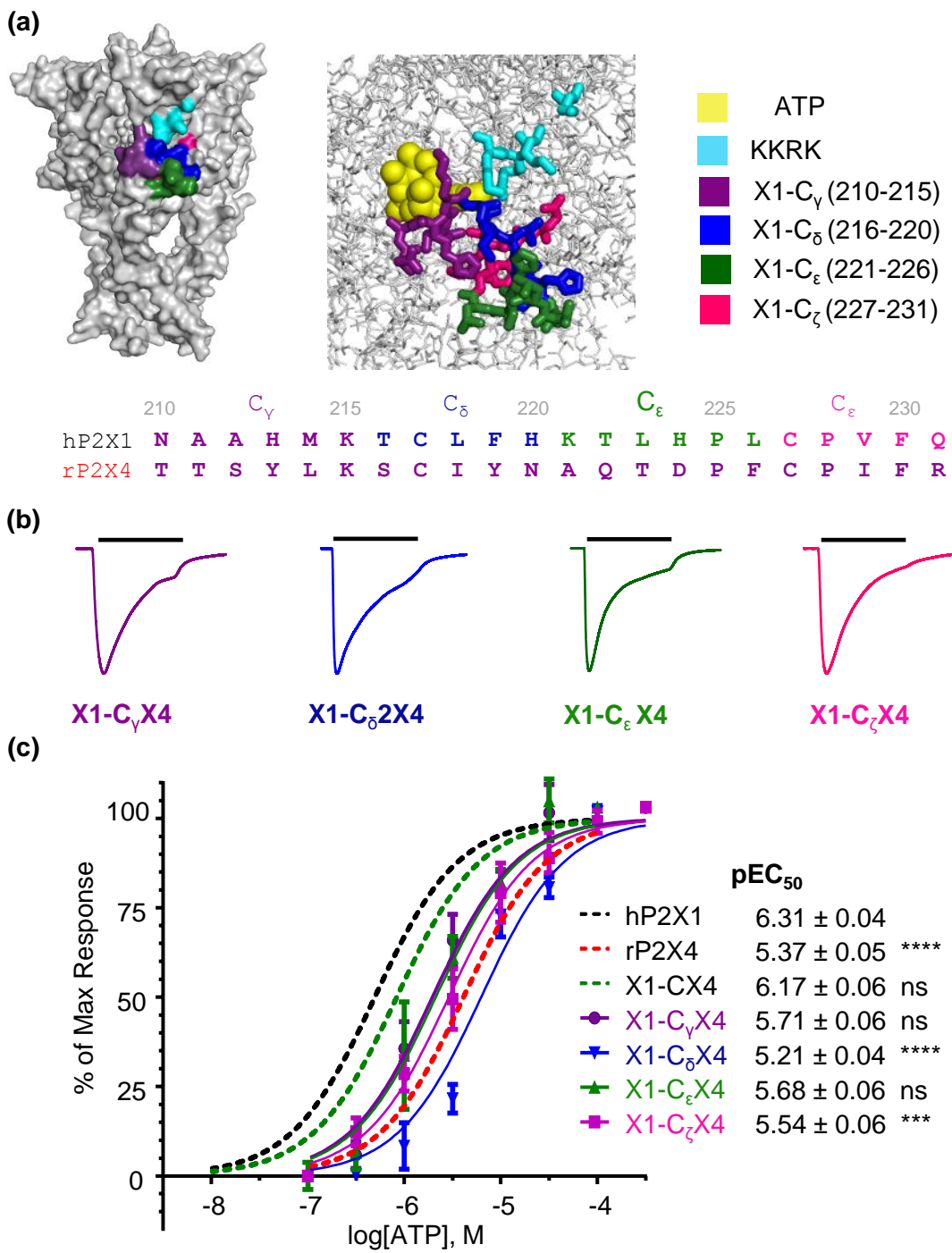


**Figure 5.7 The Effect of ATP at the Smaller X1-CX4 Sub-Chimeras.** (a) Line up of the sequences of the hP2X1 and rP2X4 receptors is shown and residues are coloured according to the region they fall within. Residues are also located on the hP2X1 receptor homology model. (b) Representative traces of maximal ATP at each of the small sub-chimeras. Bars represent a 3 s application. Traces are normalised to peak currents for comparison. (c) Concentration-response curves at the small sub-chimeras. pEC<sub>50</sub> values are shown. Stars represent a significant difference from the hP2X1 receptor. \*\*\* p < 0.001. \*\*\*\* < 0.0001.

(figure 5.7b). The rise times of the X1-C<sub>γ</sub>X4, X1-C<sub>δ</sub>X4, X1-C<sub>ε</sub>X4 and X1-C<sub>ζ</sub>X4 receptors were  $135.3 \pm 15.2$ ,  $110.7 \pm 9.1$ ,  $109.8 \pm 11.7$  and  $111.8 \pm 11.6$  ms respectively (figure 5.7b). At the WT hP2X1 receptor there was  $80.3 \pm 4.3\%$  desensitisation. The % desensitisation at the X1-C<sub>γ</sub>X4, X1-C<sub>δ</sub>X4, X1-C<sub>ε</sub>X4 and X1-C<sub>ζ</sub>X4 receptors was the hP2X1 receptor-like,  $65.9 \pm 2.3$ ,  $75.3 \pm 2.3$ ,  $76.5 \pm 3.7$  and  $81.0 \pm 8.2\%$  respectively (figure 5.7b). Taken together the region C sub-chimeras demonstrate that mutation within this region can affect ATP potency without affecting the time-course of the response to ATP at the hP2X1 receptor.

### 5.2.8 NF449 Sensitivity at the Small Sub-Chimeras

As neither the X1-C<sub>α</sub>X4 nor the X1-C<sub>γ</sub>X4 chimera showed any difference from the hP2X1 receptor in NF449 sensitivity, it was thought that the smaller sub-chimeras may contain the residues responsible for the decrease in NF449 sensitivity seen in chimera X1-CX4. The inhibition by NF449 at these chimeras was examined. Co-application of 1 nM NF449 with EC<sub>90</sub> ATP caused ~ 50% Inhibition at both the hP2X1 receptor and the X1-C<sub>γ</sub>X4 sub-chimera (figure 5.8a). The inhibition by 1 nM NF449 was slightly reduced at X1-C<sub>ε</sub>X4, where ~ 20% inhibition was seen. The X1-C<sub>δ</sub>X4 and X1-C<sub>ζ</sub>X4 sub-chimeras were only ~ 5% inhibited by 3 nM NF449. Full inhibition curves showed that only the X1-C<sub>γ</sub>X4 chimera ( $\text{pIC}_{50} = 8.78 \pm 0.06$ ) had hP2X1 receptor-like sensitivity to NF449 inhibition (figure 5.8b). The X1-C<sub>ε</sub>X4 chimera was ~ 4-fold less sensitive to NF449 than the hP2X1 receptor,  $\text{pIC}_{50}$  values =  $8.36 \pm 0.09$  and  $8.94 \pm 0.04$  respectively,  $p < 0.01$ . The X1-C<sub>δ</sub>X4 and X1-C<sub>ζ</sub>X4 sub-chimeras both had ~ 20-fold decreased NF449 sensitivity compared to the hP2X1 receptor, with  $\text{pIC}_{50}$  values of  $7.68 \pm 0.12$  and  $7.63 \pm 0.11$ ,  $p < 0.0001$ . Despite the X1-C<sub>δ</sub>X4, X1-C<sub>ε</sub>X4 and X1-C<sub>ζ</sub>X4 sub-chimeras being less inhibited by NF449 than the hP2X1 receptor, the chimeras were still > 10-fold more sensitive to NF449 than the X1-CX4 chimera. These results show, as predicted, that residues closest to the four positively charged residues in the cysteine rich head region within region C are contributing to NF449 sensitivity. This suggests that several residues are involved in NF449 action at the hP2X1 receptor, with contributions from both regions B and C.

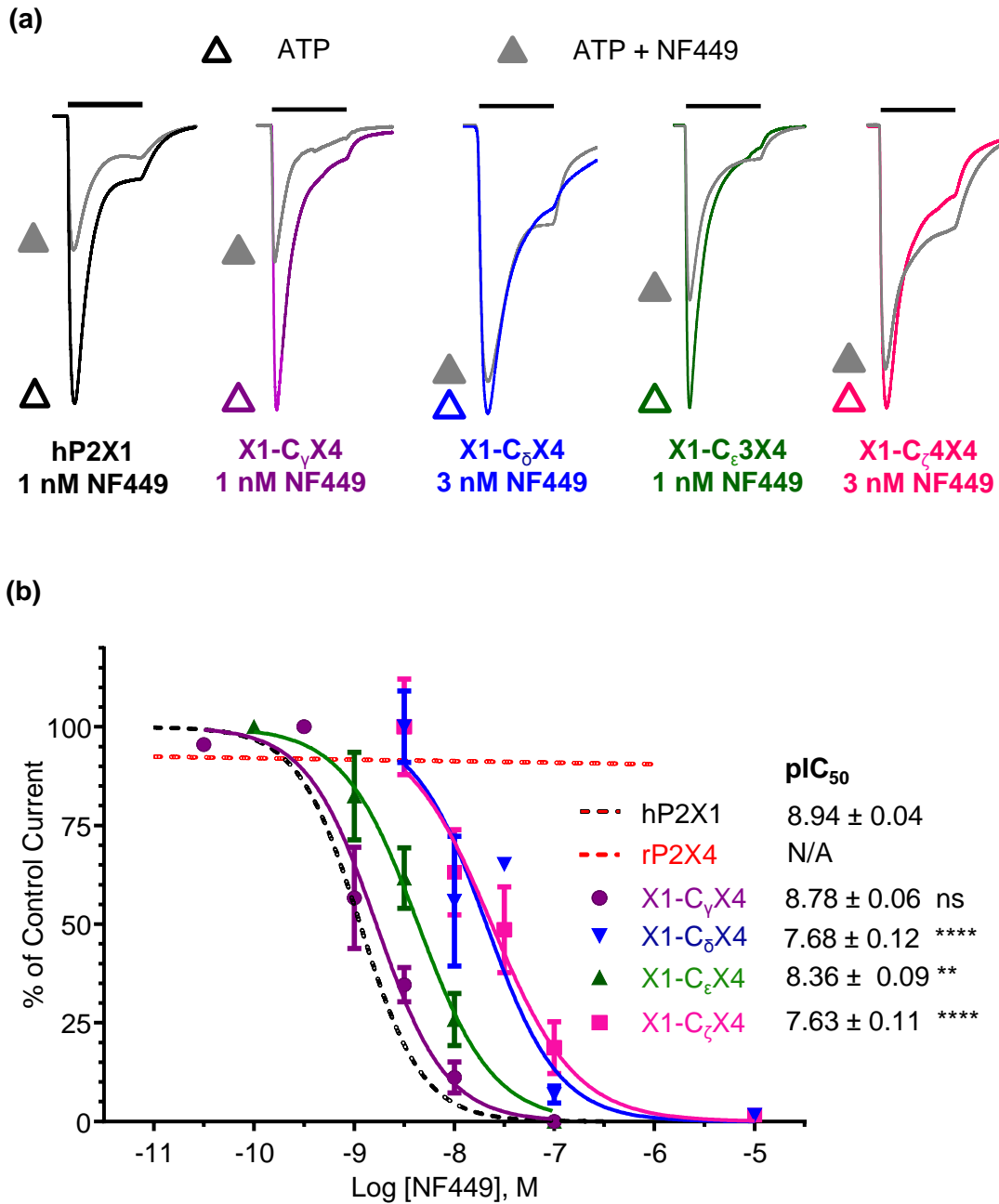


**Figure 5.8 NF449 Action at the X1-C $_{\beta}$ X4 Sub-Chimeras.** (a) Representative traces of EC $_{90}$  ATP (ATP $_{90}$ , open triangles) and ATP $_{90}$  + NF449 (closed triangles) application at Xenopus oocytes expressing the WT hP2X1 receptor and small sub-chimeras. Bars represent a 3 s application. Traces are normalised to peak currents to allow comparison. 5 mins was given between applications to allow for recovery from desensitization. (b) NF449 inhibition curves for the WT receptors and small sub-chimeras.  $\text{pIC}_{50}$  values are shown. Stars represent a significant difference from the hP2X1 receptor. \*\*  $p < 0.01$ , \*\*\*\*  $p < 0.0001$ .

	Peak Current (nA)	Rise Time (ms)	% Decay	ATP pEC <sub>50</sub>	ATP Hill Slope	NF449 pIC <sub>50</sub>	NF449 Hill Slope
<b>hP2X1</b>	7598 ± 793	95.7 ± 5.1	80.3 ± 4.3	6.31 ± 0.04	0.89 ± 0.07	8.94 ± 0.04	1.40 ± 0.20
<b>rP2X4</b>	5320 ± 586	309.3 ± 32.0	28.7 ± 4.5	5.37 ± 0.05	1.07 ± 0.12	N/A	N/A
<b>X1-CX4</b>	8546 ± 747	180.2 ± 20.7	74.7 ± 2.9 ns	6.17 ± 0.06	0.67 ± 0.06	6.56 ± 0.14	0.54 ± 0.07
<b>X1-C<sub>α</sub>X4</b>	6893 ± 864	88.0 ± 7.4	89.4 ± 1.5	5.34 ± 0.05	0.97 ± 0.11	8.78 ± 0.04	1.56 ± 0.22
<b>X1-C<sub>β</sub>X4</b>	6117 ± 669	89.0 ± 8.6	84.8 ± 8.2	5.30 ± 0.06	1.06 ± 0.14	8.58 ± 0.09	1.13 ± 0.09
<b>X1-C<sub>γ</sub>X4</b>	7623 ± 767	135.3 ± 15.2	65.9 ± 2.3	5.71 ± 0.06	1.13 ± 0.06	8.78 ± 0.06	1.25 ± 0.22
<b>X1-C<sub>δ</sub>X4</b>	8560 ± 800	110.7 ± 9.1	75.3 ± 2.3	5.21 ± 0.04	1.49 ± 0.18	7.68 ± 0.12	1.20 ± 0.32
<b>X1-C<sub>ε</sub>X4</b>	7047 ± 588	109.8 ± 11.7	76.5 ± 3.7	5.68 ± 0.06	1.20 ± 0.19	8.36 ± 0.09	1.16 ± 0.30
<b>X1-C<sub>ζ</sub>X4</b>	7450 ± 639	111.8 ± 11.6	81.0 ± 8.2	5.54 ± 0.06	0.94 ± 0.11	7.63 ± 0.11	1.04 ± 0.26

**Table 5.2 ATP and NF449 action at the X1-CX4 Sub-chimeras.** Boxes shaded in grey show no difference from the hP2X1 receptor. Blue represents a significant increase compared to the hP2X1 receptor and red represents a significant decrease. N/A = not applicable as the value was not determined.

### 5.2.9 ATP Action at X1-CX4 Point Mutations

Due to the shifts seen in the sensitivity to NF449 inhibition of the X1- $C_{\delta}X4$ , X1- $C_{\epsilon}X4$  and X1- $C_{\zeta}X4$  chimeras, individual point mutations were introduced to the hP2X1 receptor within these regions to replace residues with the corresponding variant residue of the rP2X4 receptor. This would allow the contribution of individual residues to NF449 sensitivity to be assessed. The mutated residues were chosen based on their proximity to the four positive charges in region B. Two histidine charges were also mutated due to previous implication of histidine residues in antagonist action (Xiong *et al.*, 2004b). The mutations made were T216S, L218I, H220N, H224D, V229I and Q231R (figure 5.9a). All of the mutants were functional, with hP2X1 receptor-like peak amplitudes at ATP<sub>max</sub> (table 5.3). Only the H220N mutant showed any difference from the WT hP2X1 receptor in time-course (figure 5.9b, table 5.3). The rise time was ~ 2.5 fold slower than that of the hP2X1 receptor ( $251.7 \pm 29.6$  and  $95.0 \pm 5.0$  respectively. There was also less desensitization at the H220N mutant than at the hP2X1 receptor ( $46.8 \pm 5.1\%$  compared to  $80.3 \pm 5.3\%$ ). The rise time and % desensitization of the H220N mutant was rP2X4 receptor-like, implicating H220 in the fast time-course of the hP2X1 receptor.

The H220N mutant showed an ~ 8-fold decrease in ATP potency compared to the hP2X1 receptor, with a pIC<sub>50</sub> value of  $5.41 \pm 0.03$  (figure 5.9c). This was the only point mutation studied which had an effect on ATP action compared to the WT receptor (table 5.3). The Hill slopes for the concentration response curves for all the point mutations were unaffected compared to the hP2X1 receptor, with the exception of H220N, which showed a significant increase (table 5.3). The point mutated residues therefore have no impact on the action of ATP at the hP2X1 receptor, with the exception of histidine 220, which showed a difference in both potency and time-course.

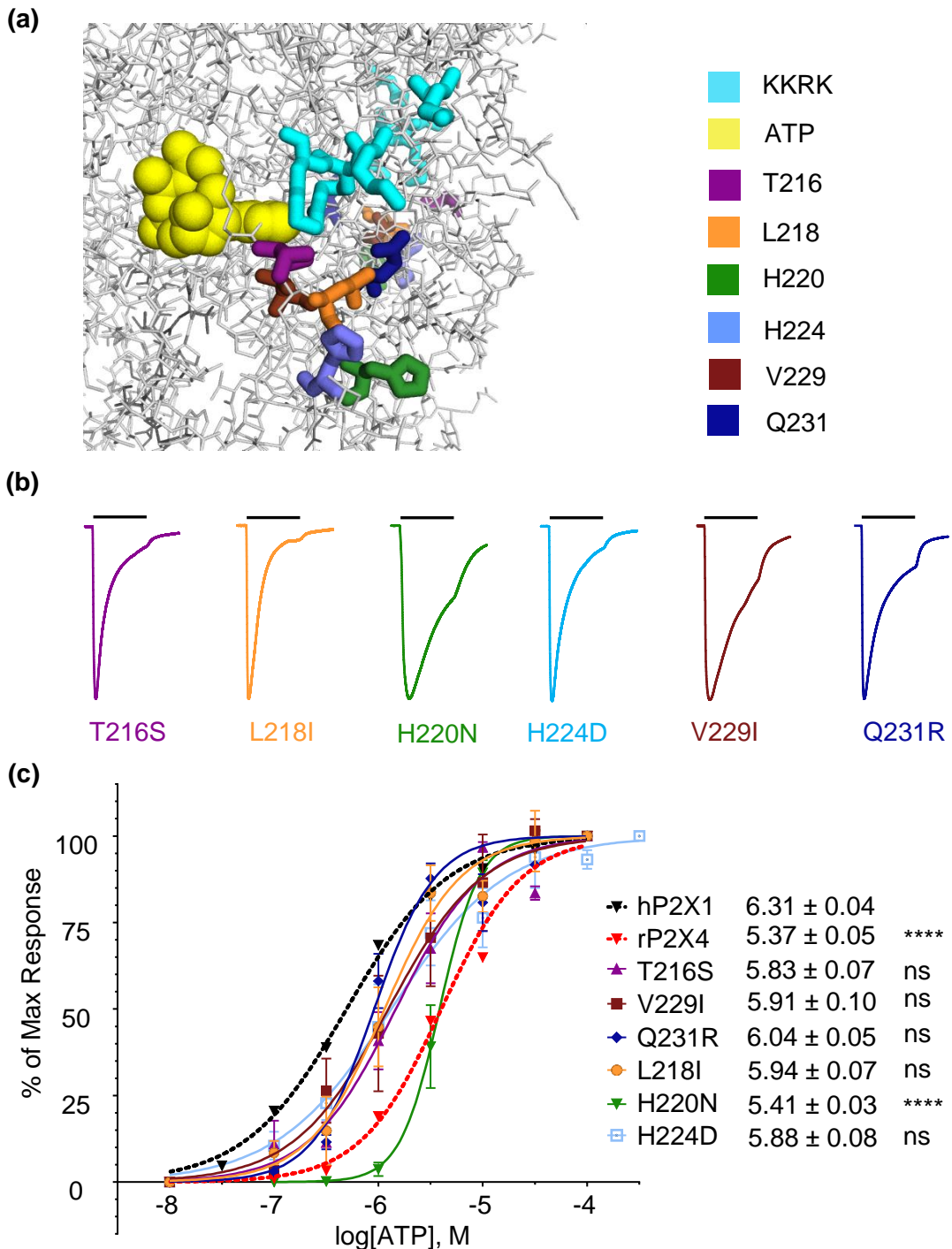
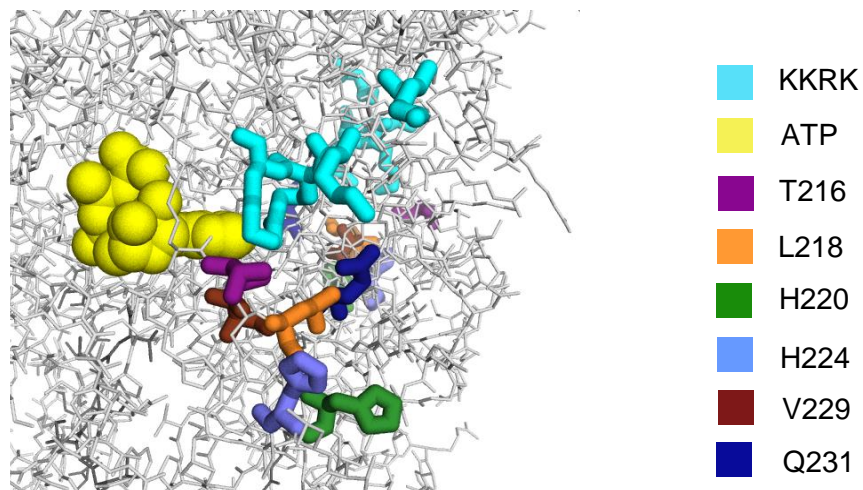


**Figure 5.9 ATP Action at X1-CX4 Point Mutations.** (a) Location of each of the mutated residues is shown on a homology model of the hP2X1 receptor. (b) Representative traces of application of a maximal concentration of ATP to the X1-CX4 point mutants. Bars represent a 3 s application. Traces have been normalised to peak current to allow comparison. (c) Concentration response curves for each of the point mutated receptors.  $pEC_{50}$  values are shown. Stars represent a significant difference from the hP2X1 receptor. \*\*\*\*  $p < 0.0001$ , ns not significant.

### **5.2.10 NF449 Action at X1-CX4 Point Mutations**

Inhibition by NF449 at the point mutated receptors was examined. Due to the large number of mutations, the fold-difference in NF449 sensitivity compared to the hP2X1 receptor control was reported, rather than the individual  $\text{pIC}_{50}$  values (figure 5.10). There was no change in inhibition by NF449 compared to the hP2X1 receptor for the L218I, H220N and V229I mutants. The H224D mutation, which introduced a negatively charged residue beneath the four positively charged residues in the cysteine head region, caused an ~ 6-fold decrease in NF449 sensitivity compared to the hP2X1 receptor. The Q231R mutation, which introduced a positively charged residue beneath these four charges also showed a decrease in NF449 sensitivity of ~ 7-fold. These results further implicate charged residues in NF449 action. The mutation at position 216, which mutated a threonine residue to a serine also had an effect on NF449 sensitivity, decreasing it ~ 7 fold. These residues can be used to generate *in silico* models of where NF449 is potentially binding to the hP2X1 receptor and this is described in the discussion below.

(a)



(b)

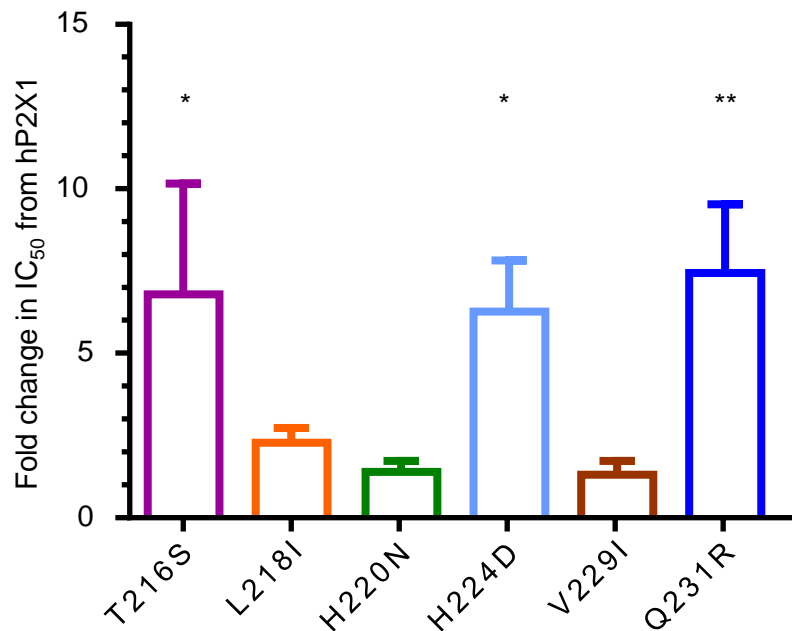


**Figure 5.10 NF449 Inhibition at X1-C<sub>β</sub>X4 point mutations.** (a) Location of each of the mutated residues shown on a homology model of the hP2X1 receptor. (b) The decrease in NF449 sensitivity of each of the X1-C<sub>β</sub>X4 point mutants compared to the hP2X1 receptor is shown. Stars represent a significant difference from the hP2X1 receptor. \* p < 0.05, \*\* p < 0.01.

	<b>Peak Current (nA)</b>	<b>Rise Time (ms)</b>	<b>% Desensitisation</b>	<b>ATP pEC<sub>50</sub></b>	<b>ATP Hill Slope</b>
<b>hP2X1</b>	7598 ± 793	95.7 ± 5.1	80.3 ± 4.3	6.31 ± 0.04	0.89 ± 0.07
<b>rP2X4</b>	5320 ± 586	309.3 ± 32.0	28.7 ± 4.5	5.37 ± 0.05	1.07 ± 0.12
<b>X1-CX4</b>	8546 ± 747	180.2 ± 20.7	74.7 ± 2.9	6.17 ± 0.06	0.67 ± 0.06
<b>T216S</b>	7549 ± 976	77.6 ± 6.5	84.6 ± 2.8	5.83 ± 0.07	1.04 ± 0.17
<b>L218I</b>	10042 ± 1326	125.8 ± 9.2	63.9 ± 3.5	5.94 ± 0.07	1.20 ± 0.07
<b>H220N</b>	9934 ± 521	251.7 ± 29.6	46.8 ± 5.1	5.41 ± 0.03	2.29 ± 0.34
<b>H224D</b>	6017 ± 688	78.0 ± 3.4	82.7 ± 4.4	5.88 ± 0.08	0.79 ± 0.11
<b>V229I</b>	7600 ± 8067	124.6 ± 25.3	63.9 ± 7.3	5.91 ± 0.10	0.96 ± 0.20
<b>Q231R</b>	7483 ± 732	122.5 ± 25.4	82.7 ± 1.9	6.04 ± 0.05	1.48 ± 0.24

**Table 5.3 ATP action at the X1-CX4 point mutations.** Boxes shaded in grey show no difference from the hP2X1 receptor. Blue represents a significant increase compared to the hP2X1 receptor and red represents a significant decrease.

### **5.3 Discussion**

Chimeras X1-BX4 and X1-CX4 had shown a contribution to both the ATP evoked response and the high affinity of NF449 action at the hP2X1 receptor in chapter 4. In this chapter sub-chimeras and point mutations were made within these regions and have shown a contribution of 7 residues to NF449 action. These residues have been used to generate an NF449 bound model of the hP2X1 receptor. Although the focus of this thesis is on antagonism, due to the difference in ATP potency and the time-course of the response between the WT hP2X1 and rP2X4 receptors, the experiments have also provided a breadth of information on the potency of ATP at the receptor and the time-course of the ATP evoked response and this is also discussed here.

#### **5.3.1 Residues in Regions B and C that Contribute to the Time-course of the ATP Evoked Response of the hP2X1 Receptor**

Introducing four positive charges at positions 136-140 of chimera X1-BX4 had a large effect on the time-course of chimera X1-BX4. As discussed in chapter 4, chimera X1-BX4 had an intermediate % desensitisation that was also seen at the rP2X4 receptor. The X1-BX4(4+) receptor which had these four positive charges mutated into it, had the rapid desensitisation of the hP2X1 receptor. This suggests that the four positive charges are important in the characteristic fast desensitisation of the hP2X1 receptor, and it was the loss of these charges which led to chimera X1-BX4 having rP2X4 receptor-like desensitisation. The study by El Ajouz *et al*, which removed these charges from the hP2X1 receptor and replaced them with equivalent residues form the slowly desensitising hP2X2 receptor showed no effect on the time-course of the ATP evoked response (El-Ajouz *et al.*, 2012). In this study a larger section of the receptor was replaced (section B) in order to cause the decrease in receptor desensitisation that was seen in chimera X1-BX4 and it was the re-introduction of the four charges that caused the return to WT hP2X1 receptor time-course of chimera X1-BX4(4+). This suggests that there are important reactions between residues in this region and other residues in the receptor that are contributing to the receptor time-course. These interactions appeared to be unaffected in El-

Ajouz's mutant, but were disrupted in chimera X1-BX4. Although these residues have a positive charge and ATP is a negatively charged molecule, it is unlikely that there is a direct interaction between the two as the binding site of ATP is well characterised and does not include these residues. The contribution of these residues is therefore likely to be to gating, or to maintaining a particular conformation at the receptor.

None of the sub-chimeras made within region C had any effect on the time-course of the ATP evoked response of the hP2X1 receptor. However the point mutation H220N, which falls within this region, showed a slower rise time and desensitisation than the WT. The Hill slope of this receptor was also increased compared to the WT receptors. Histidine residues have not been linked to the effects of ATP at the hP2X1 receptor, however they have previously been shown to have an impact on ATP action at the rP2X4 receptor (Xiong *et al.*, 2004a). In the previous study the rP2X4 H241A mutant has been shown to have a more rapid-rise time than the WT rP2X4 receptor and the mutation was suggested to have an effect on gating. This shows that mutation of histidine residues can affect ATP time-course; however the mutation which showed the largest effect in the study on the rP2X4 receptor by Xiong *et al* had the opposite effect to the hP2X1 H220N mutant in this thesis. This suggests that histidine residues have different contributions at different P2X receptor subtypes.

The location of the 5 residues within sections B and C which have had an effect on the time-course are shown on the hP2X1 receptor homology model in figure 5.11a. The four positive charges are located at the base of the cysteine rich head region, and H220 is located below these residues. The time-course of the ATP evoked response is associated with pore opening and closing, the P2X1 receptor opens rapidly and then quickly closes, the rP2X4 receptor is in the open conformation for a longer period of time. Movement of the cysteine rich head region has been shown to contribute to channel gating (Hattori & Gouaux, 2012) (Roberts *et al.*, 2012). It is not clear if the movement of the head region itself causes the receptor to move into a desensitised state or if the movement in the head region causes further movement in the

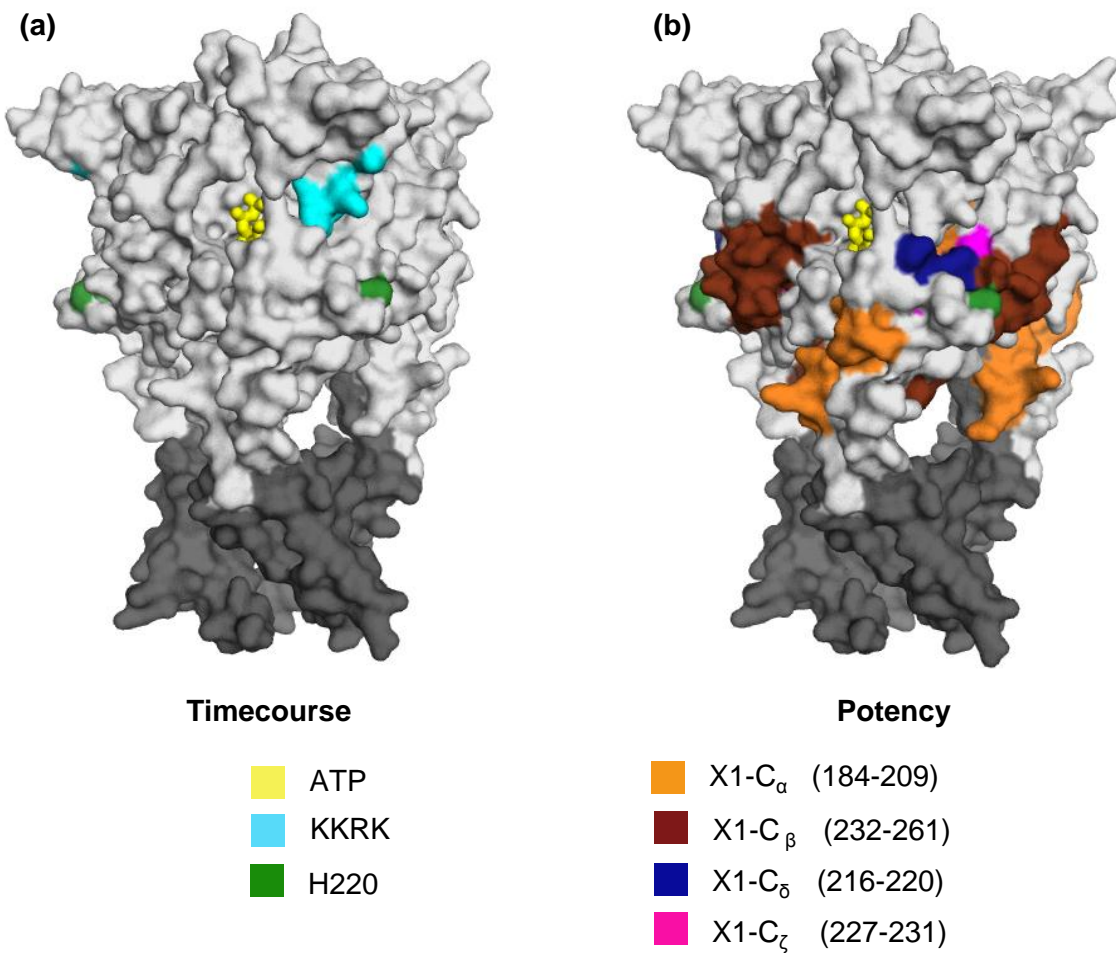


**Figure 5.11 Regions of the hP2X1 Receptor Which Affect the Properties of the ATP Evoked Response.** **(a)** The coloured residues on the structure are those which have been shown to affect the time-course of the ATP evoked response at the hP2X1 receptor. K136 – K140 are shown in cyan. H220 is shown in green. **(b)** Residues which affect the potency of ATP at the hP2X1 receptor are shown in colour. The X1-C<sub>α</sub>X4 and X1-C<sub>β</sub>X4 chimeras are shown in orange and brown respectively. X1-C<sub>δ</sub>X4 and X1-C<sub>ζ</sub>X4 are shown in dark blue and pink. and H220 is shown in green.

transmembrane domains and intracellular regions which leads to the closing of the channel and the flexibility of this region could mean that in certain conformations of the receptor these residues can interact with one another to bias the receptor toward a particular conformation and contribute to the fast time-course of the hP2X1 receptor. It is also possible that when ATP binds it interacts with both these residues and locks the receptor in a specific conformation which determines the fast time-course of the hP2X1 receptor. The absence of these residues in the rP2X4 receptor could therefore mean the receptor was not stabilised in this conformation upon ATP binding and instead a different conformation is adopted leading to the intermediate time-course of the rP2X4 receptor.

### **5.3.2 Residues in Regions B and C that contribute to ATP Sensitivity at the hP2X1 Receptor**

ATP potency at the X1-BX4(4+) chimera was > 450-fold decreased compared to the hP2X1 receptor, and ~ 4-fold decreased compared to the X1-BX4 chimera. While reintroducing the four positive charges at the X1-BX4 receptor returned the time-course to that of the hP2X1 receptor, it did not re-introduce ATP potency, but instead decreased it further compared to the hP2X1 receptor. This shows that mutation of the four charges can have an effect on ATP potency, but that their presence in the hP2X1 receptor is not responsible for the increased ATP potency compared to the rP2X4 receptor. The positive charges therefore contribute to the rapid time-course but not the high ATP potency of the hP2X1 receptor, suggesting that distinct residues control these two properties.

Chimeras X1-C<sub>α</sub>X4 and X1-C<sub>β</sub>X4 both showed rP2X4 receptor-like ATP potency which was decreased ~ 10-fold compared to the hP2X1 receptor. This suggests that the variant residues in regions 184-209 and 232-261 are potentially contributing to the difference in ATP potency between the hP2X1 and rP2X4 receptors or swapping them induced a conformational change which disrupted normal protein function. This was interesting as the X1-CX4 chimera, in which these residues had also been mutated, showed hP2X1 receptor-like ATP potency. This could occur as changing a large block of residues which

interact with each other does not disrupt the ATP potency, however changing a few of these residues could remove interacting pairs of residue and alter ATP potency. These chimeras had no effect on the time-course of the response to ATP, again suggesting that these two properties of the receptor are not controlled by the same residues.

The small X1-C<sub>δ</sub>X4 and X1-C<sub>ζ</sub>X4 sub-chimeras had decreased ATP potency compared to the hP2X1 receptor, implicating residues 216-220 and 227-231 in ATP potency. However these chimeras were still more sensitive to ATP than the rP2X4 receptor, suggesting that other residues are also involved. As these chimeras had a hP2X1 receptor-like time-course it again shows a difference in the residues that control ATP potency and the time-course of the ATP evoked response at the P2X receptor. The hP2X1 H220N mutant within this region also had an effect on ATP potency at the receptor. This mutant showed an ~ 8-fold decrease in sensitivity compared to the WT receptor. Histidine residues have not been previously linked with the ATP potency of the P2X1 receptor, but have shown a contribution to ATP sensitivity at the rP2X4 receptor (Xiong *et al.*, 2004b). Mutation of histidine 241 of the rP2X4 receptor to alanine has been shown to increase ATP potency at the receptor. Mutation of histidines 140 and 286 to alanine slightly decreased rP2X4 receptor ATP potency (~ 1.5 and 2-fold respectively). This shows that histidine residues may have different contributions to ATP potency in different subunits. All residues identified within this chapter as contributing ATP potency are shown in figure 5.11b. It can be seen that numerous residues in chimera C have been associated with the control of ATP potency. This suggests that the mechanism of this property is very complex, with residues that are distinct from ATP binding showing a role, possibly by altering the conformation of the receptor to one which encourages ATP binding. Components from all the chimeras in this thesis that have been identified as contributing to both ATP potency and time-course are discussed in chapter 7.

### **5.3.3 The Positive Residues at Positions 136-140 are Essential for NF449 Antagonism**

Residues 133-184 of the hP2X1 receptor were implicated in NF449 action in chapter 4. Within this region were residues K136, K138, R139 and K140 which had previously been shown to contribute to NF449 action at the hP2X1 receptor (El-Ajouz *et al.*, 2012). Introduction of two of these residues, K136 and K138 in the X1-BX4(2+) chimera had no effect on NF449 inhibition compared to the X1-BX4 chimera, demonstrating that these residues alone cannot convey NF449 action.

Mutating in a further two residues, R139 and K140 however caused the receptor to have hP2X1 receptor-like NF449 sensitivity. In the study by El-Ajouz *et al* replacement of these charges in the hP2X1 receptor with the equivalent residues of the hP2X2 receptor could decrease inhibition by NF449, but introduction of these charges to the hP2X2 receptor could not increase NF449 sensitivity (El-Ajouz *et al.*, 2012). In this thesis it was again shown that replacing these charges of the hP2X1 receptor could decrease NF449 inhibition, this time with the equivalent residues of the rP2X4 receptor as part of chimera X1-BX4. However, unlike the previous study, NF449 sensitivity could also be re-introduced to the X1-BX4 chimera through mutation of these residues. This is an important advance as it is easy to disrupt the structure and/or function of a receptor through mutation and cause the loss of a specific property, however introducing or reproducing a property shows the role of these residues more conclusively. In future experiments residues R139 and K140 could be introduced alone to test if these two residues could cause the X1-BX4 receptor to become NF449 sensitive in the absence of K136 and K138. The fact that the X1-BX4(4+) receptor had hP2X1 receptor-like NF449 inhibition suggests that the loss of these four residues alone was responsible for the decrease in NF449 inhibition seen at chimera X1-BX4 compared to the hP2X1 receptor. Other variant residues in the region 133-184 are unlikely to be contributing to the high potency and selectivity of NF449 at the hP2X1 receptor as the loss of these residues had no effect on NF449 action.

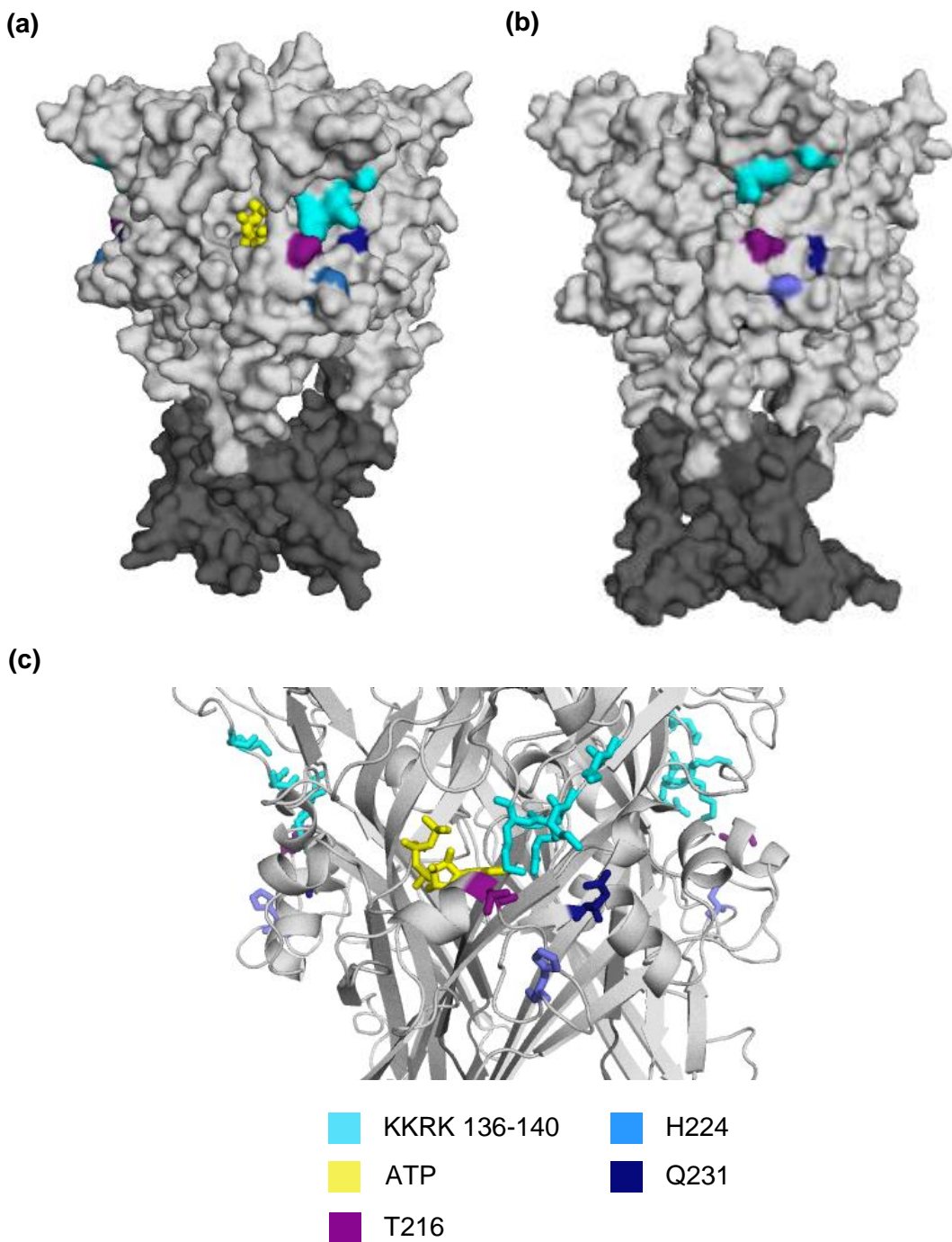


**Figure 5.12 Residues Identified as Contributing to NF449 action. Residues which have been shown to affect inhibition by NF449 are shown on the hP2X1 receptor homology model in colour** (a) Shows the surface of the agonist bound hP2X1 receptor and (b) shows the surface of the agonist unbound resting receptor. (c) Cartoon representation of the ATP bound hP2X1 receptor with contributing residues shown as sticks. The four positive residues K136, K138, R139 and K 140 are shown in cyan. T216, H224 and Q231 are shown in purple, light blue and dark respectively.

There are three ways that residues involved in NF449 and ATP binding can be related (figure 5.13). Firstly residues involved in the binding of ATP can be completely separate from those involved in NF449 (5.13a). Secondly the binding sites of each molecule can have some residues in common, but some residues are non-overlapping (figure 5.13b). Thirdly all residues involved in ATP action can also form the NF449 binding pocket (figure 5.13c). Chimera X1-BX4(4+) showed a large decrease in ATP potency but had no effect on NF449 inhibition compared to the WT hP2X1 receptor. This suggests that ATP and NF449 are not entirely sharing a binding site as this mutation has affected ATP action but not NF449 inhibition at the receptor. This would be expected as the NF449 molecule is much larger than ATP and therefore likely to be having more interactions with the receptor. If residues had a significant contribution to the binding of both molecules it would be expected that both properties would be affected. It is however possible that some residues that are involved in the binding of NF449 overlap with residues that are involved in ATP action (figure 5.13).

#### 5.3.4 Contribution of region C to NF449 sensitivity

Residues 185-261 of the hP2X1 receptor were identified as having an important role in NF449 action in chapter 4. Investigations into which specific residues within this section were important have highlighted several of the residues below the four positive charges. Chimeras X1-C<sub>α</sub>X4 and X1-C<sub>β</sub>X4 which contained residues of region C located further from these four charges showed no effect on NF449 sensitivity compared to the hP2X1 receptor and are therefore unlikely to be having a large contribution to NF449 action. The chimeras which did have an effect on NF449 inhibition were the X1-C<sub>δ</sub>X4 and X1-C<sub>ζ</sub>X4 receptors. These showed 6-fold and 12-fold decreases in NF449 sensitivity respectively and were therefore still much more sensitive to NF449 than the X1-CX4 chimera.

To identify which specific variant residues within regions C<sub>δ</sub> and C<sub>ζ</sub> were responsible for the decrease in NF449 inhibition seen at these chimeras, point mutations within these sections were generated. These demonstrated that

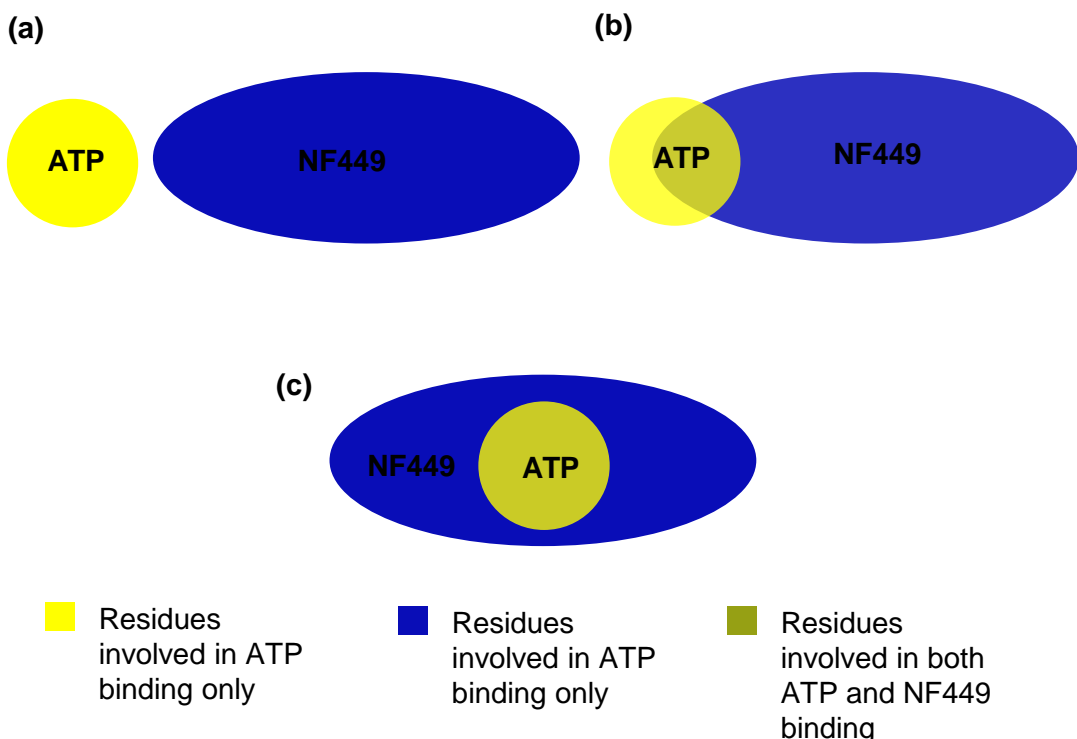


**Figure 5.13 Residues involved in ATP and NF449 binding.** There are a variety of ways residues that form the binding sites of ATP and NF449 can be related. **(a)** None of the residues of the ATP binding site can be shared with the NF449 binding site. **(b)** Some of the residues of the two sites can overlap. **(c)** All of the residues of the ATP binding site can also be involved in NF449 action. As the NF449 molecule is much larger than ATP it is highly likely that further residues would also be involved in the binding of the antagonist.

residues T216, H224 and Q231 contributed to the NF449 inhibition at the hP2X1 receptor, although as with chimeras X1-C<sub>δ</sub>X4, X1-C<sub>ε</sub>X4 and X1-C<sub>ζ</sub>X4, these mutants only caused small decreases in NF449 action compared to the ~130-fold decrease at chimera X1-CX4. This shows that swapping small sections of region C is not sufficient to cause a large decrease in NF449 sensitivity. This supports a multi-residue binding site for NF449 where mutation of individual residues involved in binding causes an incremented decrease in NF449 action, but numerous residues involved in NF449 binding need to be swapped in order to have a large effect on inhibition. It is therefore likely that the NF449 molecule interacts with residues both within regions C<sub>δ</sub> and C<sub>ζ</sub>, and with other residues in the receptor such as the four charges in region B. In future experiments chimeras which swap these sections simultaneously could be generated.

Interestingly the only point mutant which showed an effect on time-course (H220N) had no effect on NF449 action. This again demonstrates that distinct residues are involved in NF449 sensitivity and the gating of the hP2X1 receptor. The residues that were identified are located in close proximity to the four positive charges identified as being important in NF449 action in chimera B (figure 5.12). This gives support to the findings of this study as sub-chimera generation and point mutation has ultimately identified residues very close together on the receptor surface despite them originally being contained in separate chimeras.

None of the three residues identified as having a role in NF449 action from region C have been identified in NF449 sensitivity previously. Mutations H224D and Q231R altered the charge of the receptor and as the NF449 molecule is negatively charged interactions between these charges could be altering NF449 inhibition. The effect of the T216S mutant was unexpected as there is no difference in charge between these residues and they are both polar. Threonine does however have an extra methyl group compared to serine and so the mutation decreases the size of the residues at this position. H224 was previously suggested to be interacting with the NF449 molecule in model 2 in the previous NF449 binding study (figure 1) (El-Ajouz, 2011). The locations

of all the residues shown to contribute to NF449 action in this thesis is shown in figure 5.12. It can be seen that despite the residues coming from different initial chimeras (X1-BX4 and X-CX4) they are all located in close proximity to each other at the base of, and just below, the cysteine rich head region. Due to their proximity, it is highly likely that the large NF449 molecule could bind to all 7 residues. A comparison between the ATP bound and resting receptor homology models shows that movement of the receptor causes these residues to move towards each other on ATP binding (figure 5.12a,b). It is therefore possible that binding of NF449 in the resting state prevents the movement of the cysteine rich head region which in turn reduces ATP binding or prevents gating.

### **5.3.5 *In silico* Models of NF449 Binding at the hP2X1 Receptor**

The seven residues that have been identified in this chapter as contributing to the inhibition of the hP2X1 receptor by NF449 were used as co-ordinates around which to dock the NF449 molecule to the receptor. Four of these residues had been used in a previous NF449 bound model produced by Ralf Schmidt and Sam El-Ajouz (El-Ajouz, 2011), but in this thesis the three unique residues were also used to refine the model of NF449 binding. The location of these seven residues demonstrated that the NF449 molecule will potentially bind underneath the cysteine rich head region, adjacent to the ATP binding pocket (figure 5.12). Using these residues as co-ordinates for NF449 binding gave a variety of possible poses that the molecule could adopt at the receptor. Those with the highest modelling scores were individually studied and four solutions which fit the seven residues best are shown here (figure 5.13a). All four models bind at a similar location, with slight variations in the residues that they are likely to interact with. NF449 molecules were bound to an agonist unbound homology model of the hP2X1 receptor. This is because the ATP molecule does not have to be bound to the receptor in order for NF449 to bind, and binding of the antagonist may prevent the receptor adopting the open conformation. Due to the flexible nature of both NF449 and the P2X receptor it is possible that residues and bonds shown in these models may be orientated differently in the receptor. More refinement remains to be done to ensure that

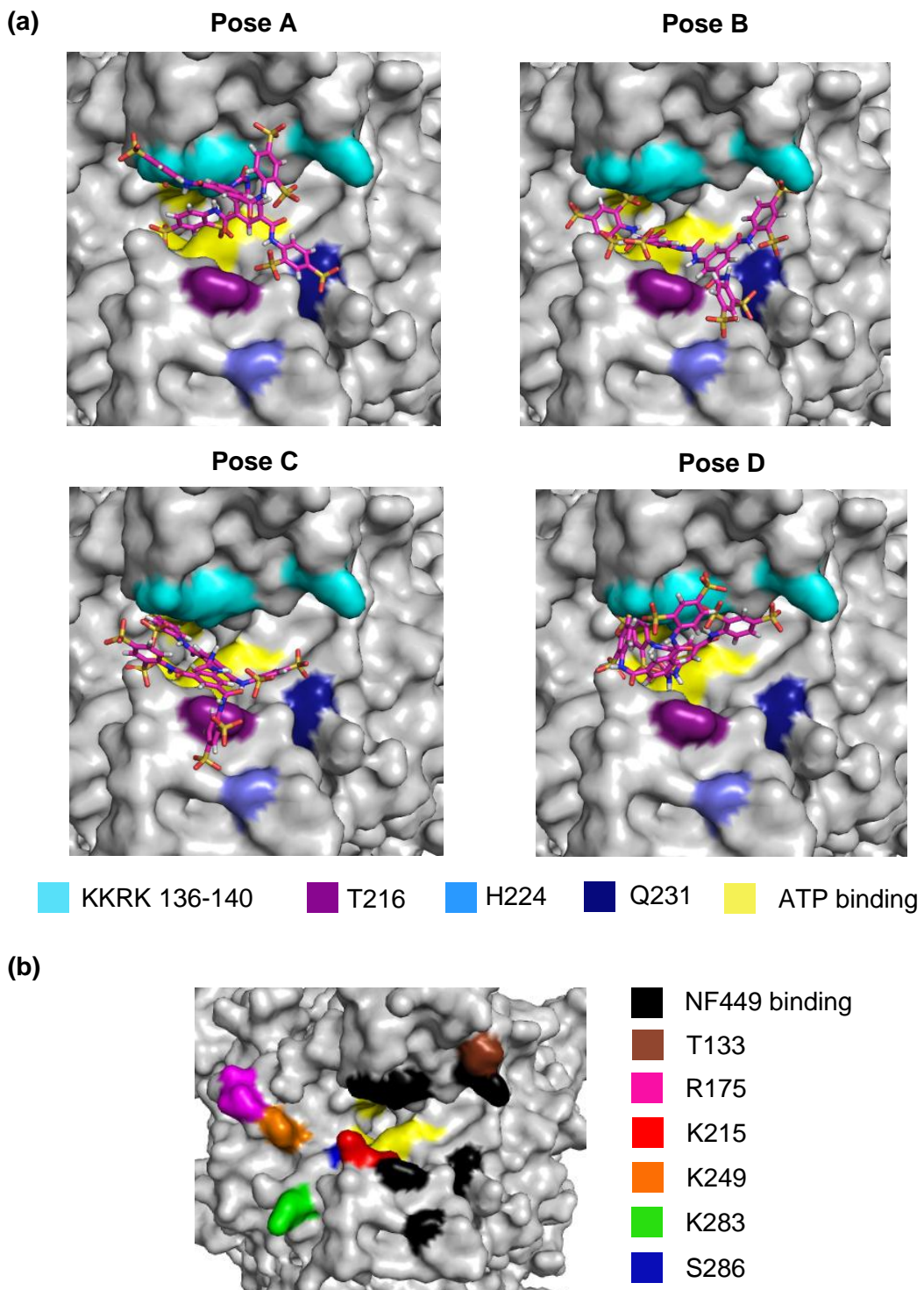


**Figure 5.14 Bound Poses of NF449 Binding at the hP2X1 Receptor.** (a) Four *in silico* models of NF449 binding at a homology model of the agonist unbound hP2X1 receptor. NF449 is shown coloured by element. Carbon is pink, hydrogen, grey, nitrogen blue, oxygen red and sulphur yellow. (b) Residues which have been highlighted for mutation in further studies to validate and refine these models. Residues previously suggested to be involved in NF449 action are shown in black.

both the receptor and the NF449 molecule are orientated in the most likely conformation based on the data.

All four poses show some overlap with residues known to contribute to ATP binding at the P2X receptor, although none of the poses show the majority of the ATP binding pocket to be occupied by the NF449 molecule (figure 5.13a). This suggests that NF449 may partially occupy the ATP binding pocket, but it is evident that residues outside this pocket are also having interactions with the molecule. If NF449 and ATP partially share a binding pocket then the presence of NF449 would be likely to disrupt ATP binding at the receptor by interacting with residues involved in ATP docking. This could explain why NF449 has a competitive nature at the receptor without completely sharing the ATP binding pocket.

Pose A shows strong interaction with the four charges and residues T216 and Q231, but there is not close proximity between the NF449 molecule and residue H224. Poses B and C show likely interaction with all residues identified as contributing to NF449 action in this thesis. Pose D is the most condensed of the docked poses and shows a strong interaction with the four positive charges but bond formation with the residues from region C appears less likely. Of the four poses, pose D is the most similar to model 1 generated in the work of Sam El-Ajouz, and poses B and C are most similar to model 2 (figure 5.1). All four poses could prevent the movement of the cysteine rich head region upon ATP binding (figure 5.14 a,b)

In order to further distinguish between and refine these potential poses, more point mutations could be made at the receptor in future studies to increase the number of co-ordinates for *in silico* docking, thus increasing accuracy. Cysteine mutants could be generated at which MTS reagents bind. There are a variety of MTS reagents with different sizes and charges and for this study negatively charged MTS reagents could be used to introduce negative charge at these introduced cysteine residues. As two negative charges repel each other, if introduction of a negative charge decreased NF449 inhibition at the hP2X1 receptor then it would be likely that the mutated residue

was located in close proximity to NF449. Differently sized MTS reagents could also be used to study the likely distances of these residues from the NF449 molecule, if a large diameter MTS reagent is needed then the residue is unlikely to be close to the molecule however if inhibition can be interrupted by a small MTS reagent then it is likely that the residue is situated immediately next to NF449. A similar study has been done using cysteine scanning mutagenesis to deduce residues involved in ATP potency (Allsopp *et al.*, 2011). The suggested cysteine mutations to investigate the NF449 bound models are T133C, R175C, K215C, K249C K283C and S286C (figure 5.14b). These residues have all been chosen based on their proximity to the NF449 poses and their ability to distinguish between the possible solutions.

For example if the K283C mutation shows a decrease in the presence of a negatively charged MTS reagent then this suggests that poses B and C are more likely to be correct. The residues suggested for mutation are located in other sections of the hP2X1 receptor which, when mutated as part of other chimeras, were shown to have no effect on NF449 action. These residues are therefore unlikely to be interacting with NF449 directly, but introduction of negative charge may interfere with the ability of NF449 to bind at the receptor if these residues are located in close proximity to the antagonist.

In summary, the residues involved in NF449 action that have been identified through chimera generation and point mutation are located adjacent to the ATP binding pocket, both in and below the cysteine rich head region. Some of these residues had previously been identified, but the residues located in region C are novel findings in this thesis. The seven residues have been used to generate *in silico* models of potential NF449 binding at the hP2X1 receptor. It is hypothesised that binding of the antagonist in the resting state of the receptor prevents movement of the cysteine rich head region which in turn inhibits channel activation. Additional mutations have been suggested which could further refine these models and determine which of them is most likely to be accurate.

## **Chapter 6: The Potential for Suramin and PPADS Bound P2X4 Crystal Structures**

### **6.1 Introduction**

In order to design novel potent and selective hP2X1 receptor antagonists, an understanding of how existing antagonists bind at the receptor is desirable. The most conclusive way of showing how an antagonist is binding at a receptor is to produce an antagonist bound crystal structure. Crystallisation is a complex process, with many months of trials and mutagenesis being necessary to optimise the crystallisation process. To date, the only subtype of P2X receptor that has been successfully crystallised is a truncated form of the zebrafish P2X4 (zfP2X4) receptor. P2X4 receptors are insensitive to the commonly used antagonists and this therefore means that an antagonist bound crystal structure has not been produced. If it were possible to introduce antagonist sensitivity to the zfP2X4 receptor through mutation then this receptor could be crystallised to give information on how the antagonists were binding.

#### **6.1.1 Introducing Antagonist Sensitivity to the P2X4 Receptor**

The rP2X4 receptor is known to be relatively insensitive to most commonly used antagonists, including suramin and PPADS. However mutations have been made which can increase antagonist sensitivity at the receptor. In 2004, Xiong *et al* introduced an alanine at position 241 (H241A) in the rP2X4 receptor (Xiong *et al.*, 2004b). This increased the inhibition by 100 µM suramin from 10% in the WT receptor to 76% for the H241A mutant, and the mutated receptor had an IC<sub>50</sub> concentration of 33.5 µM (Xiong *et al.*, 2004b). This demonstrates that a single point mutation can be sufficient to cause the rP2X4 receptor to become much more sensitive to an antagonist. The same mutation also introduced PPADS sensitivity to the receptor. 100 µM PPADS inhibited the WT receptor by 9%, but the H241A mutant was 67% inhibited at the same concentration and had an IC<sub>50</sub> concentration of 47.2 µM. This single point mutation could therefore introduce both suramin and PPADS sensitivity to the receptor, suggesting that they may be binding in a similar way. Although the rP2X4 receptor was now much more inhibited by suramin and PPADS than the WT receptor, a high concentration of antagonist (100 µM) was

still required to cause > 50% inhibition at the receptor. A mutation that introduced sensitivity at a lower antagonist concentration would be a better candidate for crystallisation. Also, the equivalent residue to H241 in the zfP2X4 receptor is glutamic acid, not histidine. It is therefore unlikely that mutation of this residue will affect the antagonist sensitivity of the zfP2X4 receptor and therefore could not contribute to the generation of an antagonist bound crystal structure.

PPADS sensitivity at the rP2X4 receptor has been introduced through the mutation E249K (Buell *et al.*, 1996). This mutation was made as the PPADS sensitive hP2X1 receptor has a lysine at the equivalent position and it was hypothesised that PPADS may be acting by forming a Schiff base with this residue. The IC<sub>50</sub> concentration of PPADS at the E249K mutant was hP2X1 receptor-like (2.6 µM). The same mutation was unable to introduce suramin inhibition to the receptor. The reciprocal mutation in the hP2X1 receptor was also unable to remove PPADS inhibition, although it did increase the reversibility of the inhibition. The P2X3 receptor which does not have a lysine at the equivalent position is still sensitive to PPADS inhibition (Buell *et al.*, 1996). This suggests that the residue is involved in, but not solely responsible for, PPADS inhibition. PPADS inhibition has also been introduced to the receptor in a chimera which introduced residues 81-183 of the hP2X4 receptor into the rP2X4 receptor (Garcia-Guzman *et al.*, 1997). The same study identified that the mutation Q78K could make the receptor suramin sensitive, but had no effect on PPADS action.

These previous studies demonstrate that mutation of various regions and residues of the rP2X4 receptor can introduce antagonist sensitivity to the rP2X4 receptor. These residues are not located near each other on the receptor structure and it is therefore unlikely that these residues are forming the antagonist binding sites but rather are involved in a more complex control of antagonism at the receptor. One possibility is that these mutations introduce conformational changes which allow the antagonists to bind to already existing residues in the receptor.

### **6.1.2 The Cysteine Rich Head Region and Antagonist Sensitivity**

Chimera X4-BX1 introduced residues 133-184 of the hP2X1 receptor into the rP2X4 receptor. This chimera was sensitive to both suramin and PPADS (chapter 4), suggesting that some residues within those that were swapped into the chimera were involved in antagonism in addition to H241. Within these residues were four positive charges unique to the P2X1 receptor (K136, K138, R139 and K140) known to be involved in NF449 action (chapter 5). As the X4-BX1 receptor was sensitive to suramin and PPADS it was tested to see if just introducing charged residues to positions 136, 138, 139 and 140 of the rP2X4 receptor would introduce PPADS and suramin sensitivity.

The study by El Ajouz *et al* had suggested that the first two charges at positions 136 and 138 were the most important in NF449 sensitivity and it was thought that similar effects might be seen for any contribution to suramin antagonism. Removing lysines from positions 136 and 138 caused a large ~ 140-fold decrease in the pIC<sub>50</sub> of NF449 from 9.07 to 6.85. Introducing an additional two charges at positions 139 and 140 only caused a further ~ 4-fold shift, suggesting that the first two charges were most important (El-Ajouz *et al.*, 2012). The study by Sim *et al* had also identified K138 as being important in suramin action (Sim *et al.*, 2008; El-Ajouz *et al.*, 2012). In this chapter it was tested to see if the introduction of the four charges alone had an effect on suramin and PPADS antagonism by mutating them into the rP2X4 receptor. If these charges caused the receptor to be inhibited then these minimally mutated receptors could have strong potential for crystallisation.

### **6.1.3 Chapter Aims**

Analysis of inhibition at chimera X4-BX1 suggested that a cluster of positively charged residues at the base of the cysteine rich head region, known to be involved in NF449 antagonism, may also contribute to suramin and PPADS action at the rP2X4 receptor. In this chapter it was determined if introducing four positive charges to the rP2X4 receptor could introduce suramin and PPADS sensitivity. If so they would also be introduced to the zfP2X4 receptor and the antagonism of these mutants tested. If it were possible,

introduction of low micromolar antagonist sensitivity to the zfP2X4 receptor would give a strong possibility of producing a P2X receptor crystal in the antagonist bound state.

## 6.2 Results

### 6.2.1 ATP Action at the rP2X4(2+) and rP2X4(4+) Mutants

Suramin and PPADS inhibited the X4-BX1 chimera at hP2X1 receptor-like levels. Within this chimera were four charges previously demonstrated to be important in NF449 and suramin action. To determine if these residues were contributing to the antagonist sensitivity of chimera X4-BX1, two rP2X4 receptor based mutants were generated which introduced the cluster of positively charged residues to the base of the cysteine rich head region of the rP2X4 receptor. The first, named rP2X4(2+), had two point mutations, S136K and D138K, which introduced two positive charges to the rP2X4 receptor. The second, named rP2X4(4+) also had these mutations and a further two mutations T139R and H140K. This gave the rP2X4(4+) receptor four additional positive charges compared to the WT rP2X4 receptor, located near the ATP binding pocket (figure 6.1a).

Both mutants were functional in response to a 3 second 300  $\mu$ M ATP application (figure 6.1b). rP2X4(2+) had a mean peak current of  $2226 \pm 271$  nA and rP2X4(4+) of  $2746 \pm 374$  nA. These currents were significantly smaller than those seen at the WT hP2X1 receptor which had a mean peak current of  $7598 \pm 793$  nA,  $p < 0.0001$ , but showed no difference in amplitude from currents at the WT rP2X4 receptor (mean peak current =  $5320 \pm 586$  nA). ATP potency at the rP2X4(2+) ( $\text{pIC}_{50} = 4.95 \pm 0.10$ ) and rP2X4(4+) ( $\text{pIC}_{50} = 5.02 \pm 0.05$ ) mutants was also the same as the WT rP2X4 receptor and was ~ 20-fold decreased compared to the hP2X1 receptor. The Hill slopes for the concentration response curves were similar to those of the WT receptors (table 6.1).

The rise times of rP2X4(2+) and rP2X4(4+) were  $447 \pm 24$  and  $247 \pm 64$  ms respectively. As with the WT rP2X4 receptor, both mutant receptors showed

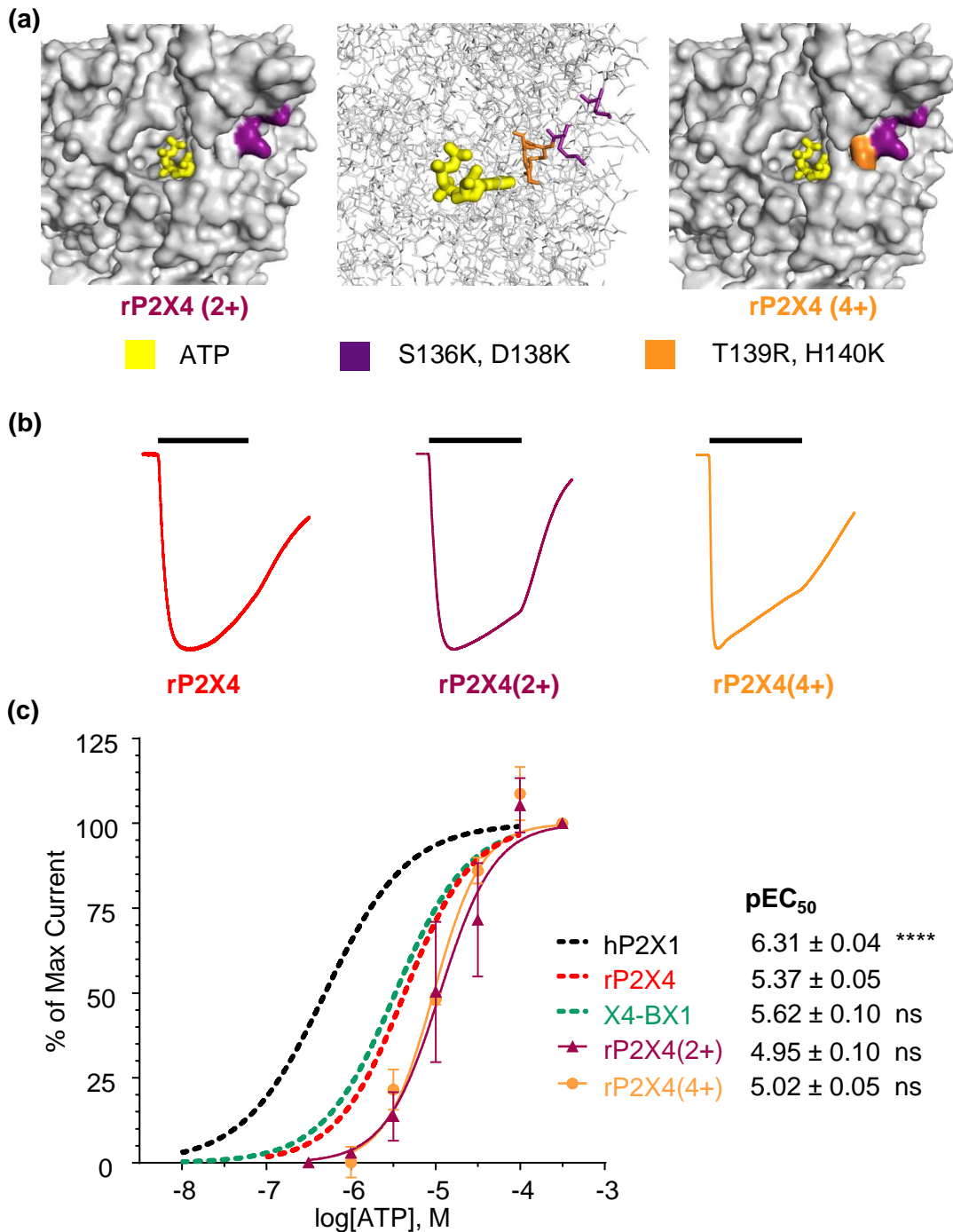


**Figure 6.1 ATP Action at rP2X4(2+) and rP2X4(4+).** (a) Four charges were introduced to the rP2X4 receptor. rP2X4(2+) contained K136 and K138, shown in purple and rP2X4(4+) also included R139 and K140 shown in orange. (b) Representative traces for maximal ATP application to *Xenopus* oocytes containing the mutated receptors. Bars represent a 3 s application. Traces have been normalised to peak currents to allow for comparison. (c) Concentration response curves for ATP at the mutated rP2X4 receptors.  $pEC_{50}$  values are shown. Stars represent a significant difference from the rP2X4 receptor. \*\*\*\* =  $p < 0.0001$ .

<50% desensitisation during the presence of ATP, with rP2X4(2+) desensitising by  $19.5 \pm 1.6\%$  and rP2X4(4+) desensitising by  $31.8 \pm 7.0\%$ . These results show that introduction of these positively charged residues to the rP2X4 receptor had no impact on the action of ATP in either potency or time-course.

### 6.2.2 Suramin Inhibition at the rP2X4(2+) and rP2X4(4+) Mutants

Suramin sensitivity at the rP2X4(2+) and rP2X4(4+) was tested to see if introduction of these residues could have caused the receptor to become suramin sensitive and was therefore responsible for the suramin sensitivity of the X4-BX1 chimera. Both the rP2X4(2+) and rP2X4(4+) receptors showed inhibition by 10  $\mu\text{M}$  suramin when co-applied with EC<sub>90</sub> ATP. The rP2X4(2+) receptor was inhibited by ~30% and the rP2X4(2+) receptor was more sensitive with ~75% inhibition (figure 6.2a). These results were a contrast to the WT rP2X4 receptor which was insensitive to suramin at all concentrations tested.

Suramin inhibition of ATP curves were produced for the rP2X4(2+) and rP2X4(4+) receptors (figure 6.2b). The rP2X4(2+) receptor had a pIC<sub>50</sub> for suramin of  $4.19 \pm 0.16$ , showing that the presence of two positive charges had induced suramin sensitivity from no inhibition at the rP2X4 receptor to a level intermediate between the hP2X1 and rP2X4 receptors. Introducing the two additional charges at positions 139 and 140 in the rP2X4(4+) mutant increased the suramin sensitivity of the receptor ~10-fold compared to rP2X4(2+), to a pIC<sub>50</sub> of  $5.16 \pm 0.09$ ,  $p < 0.0001$ . The Hill slopes of the rP2X4(2+) and rP2X4(4+) suramin inhibition curves were similar to the hP2X1 receptor (table 6.1). Although there was a significant increase in suramin sensitivity compared to the rP2X4 receptor, with the pIC<sub>50</sub> being only 3-fold less than that of the hP2X1 receptor, neither of the rP2X4 mutants became as sensitive to suramin as the hP2X1 receptor,  $p < 0.0001$ . This suggests that there are residues within the rP2X4 receptor that can co-ordinate suramin binding and allow it to inhibit the ATP induced currents.

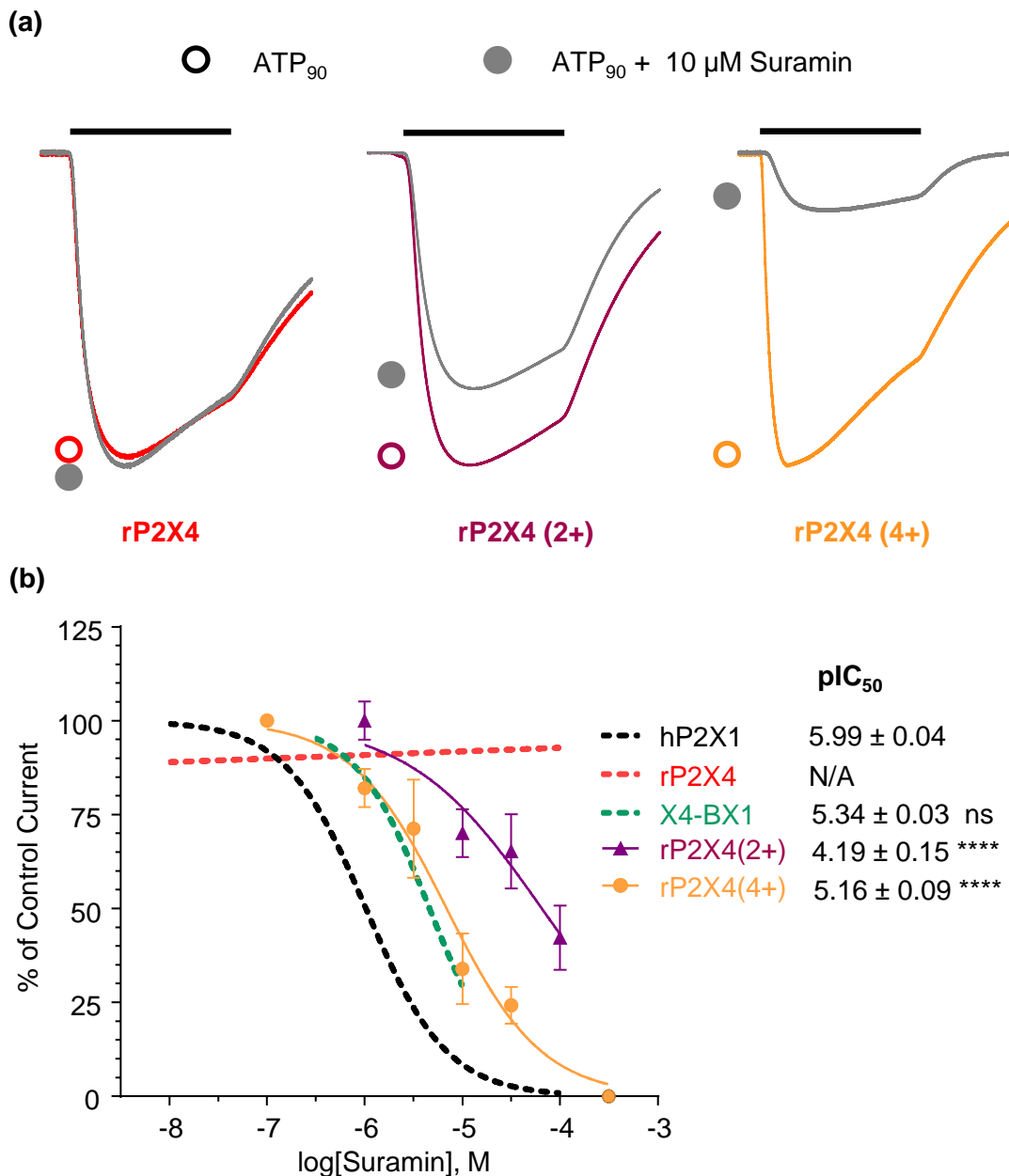


**Figure 6.2 Mutating Four Positive Charges into the rP2X4 Receptor Makes it Suramin Sensitive.** (a) Representative traces of EC<sub>90</sub> ATP (open circles) and EC<sub>90</sub> ATP + suramin (closed circles) at the rP2X4, rP2X4(2+) and rP2X4(4+) receptors. The bar represents a 3 s agonist/antagonist application. Traces have been normalised to peak currents to allow for comparison. (b) Inhibition curves for suramin at the rP2X4 mutant receptors. The pIC<sub>50</sub> values of suramin are shown. Stars represent a significant difference from the hP2X1 receptor. \*\*\*\* p< 0.0001.

### **6.2.3 PPADS Inhibition at the rP2X4(2+) and rP2X4(4+) Mutants**

As the X4-BX1 chimera had also shown PPADS sensitivity, it was thought that the presence of the four positively charged residues in the rP2X4 receptor may also make it sensitive to PPADS. When the antagonist was co-applied with EC<sub>90</sub> ATP at the rP2X4(2+) receptor, 10 µM PPADS caused ~ 70% inhibition (figure 6.3a). The pIC<sub>50</sub> for PPADS at the rP2X4(2+) receptor was 5.21 ± 0.05 which was the same as the hP2X1 receptor (pIC<sub>50</sub> = 5.80 ± 0.03) (figure 6.3b). The Hill slope of the rP2X4(2+) inhibition curve (1.6 ± 0.3) was unaffected compared to that of the hP2X1 receptor.

As with suramin, the rP2X4(4+) mutant, which had an additional two positive charges compared to rP2X4(2+), was even more sensitive to the antagonist. 1 µM PPADS caused ~70% inhibition (figure 6.3a). The rP2X4(4+) receptor was ~10-fold more inhibited by PPADS than the rP2X4(2+) mutant, with a pIC<sub>50</sub> of 6.32 ± 0.05, p<0.01 (figure 6.3b). PPADS inhibition at the rP2X4(4+) receptor was at the same levels as at the WT hP2X1 receptor. The Hill slope of the rP2X4(4+) inhibition curve (1.0 ± 0.1), was unaffected compared to the WT hP2X1 receptor. These results show that introduction of the four positive residues to the rP2X4 receptor can greatly increase suramin and PPADS inhibition at the receptor.

### **6.2.4 NF449 Sensitivity at the rP2X4(4+) Receptor**

The X1-BX4 receptor, from which charged residues at positions 136-140 had been removed as part of the mutation, showed decreased NF449 sensitivity, and addition of these charges to the X1-BX4 chimera reintroduced nanomolar NF449 sensitivity. These findings showed an important role of the charges in NF449 action. However the X4-BX1 chimera, which introduced the four positive charges to the rP2X4 receptor as part of a larger mutation, was not sensitive to NF449. This suggested that the four charges were not sufficient to introduce NF449 sensitivity to the receptor. However for completeness NF449 action at the rP2X4(4+) receptor was tested. When 1 µM ATP was co-applied with EC<sub>90</sub> ATP to the rP2X4(4+) receptor no inhibition of the peak current was seen (figure 6.4). The presence of positive charge in the cysteine rich head

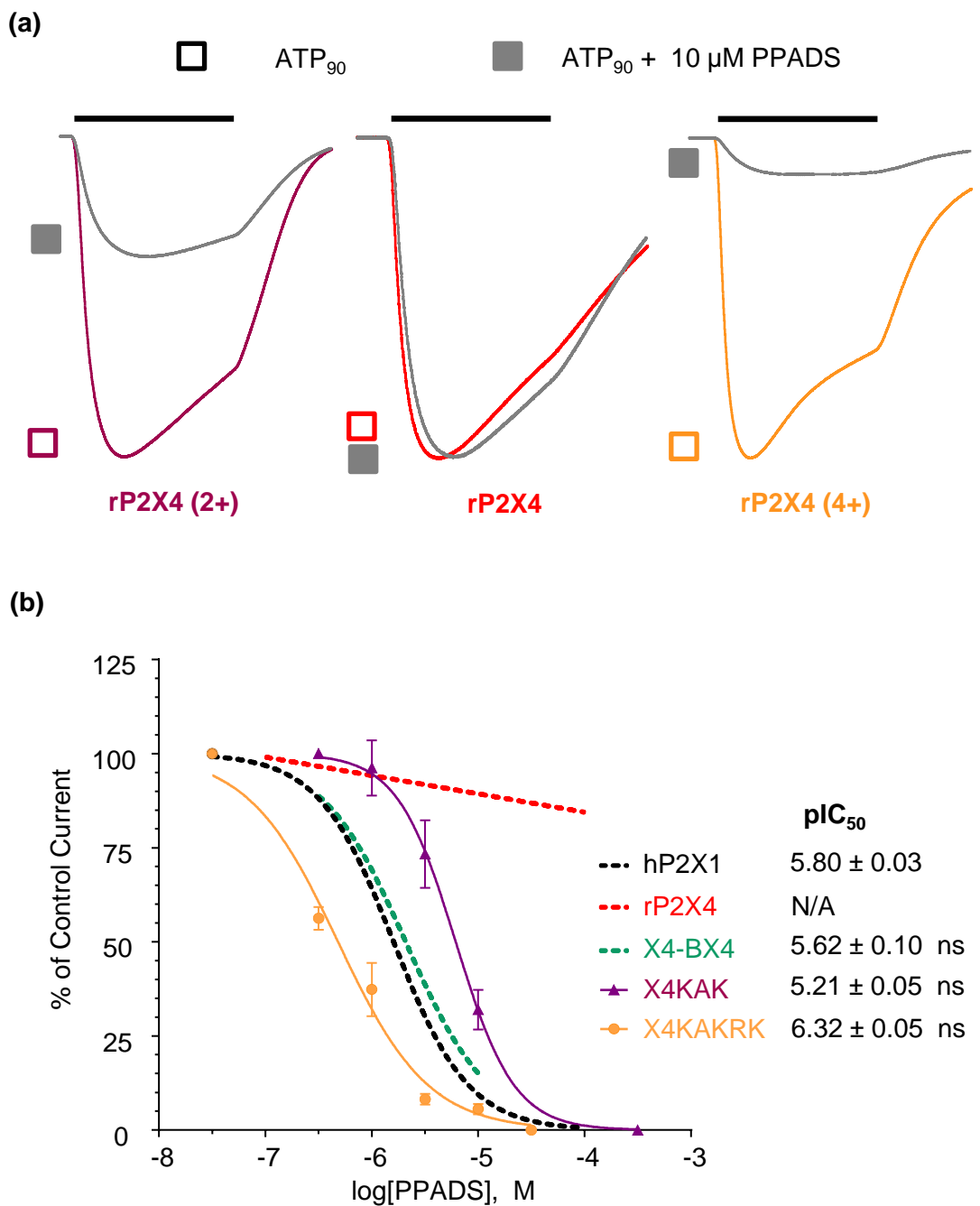


**Figure 6.3 Introducing Positive Charges to the Head Region of the rP2X4 Receptor Made it PPADS Sensitive** (a) Representative traces to show application of EC<sub>90</sub> ATP (open squares) and EC<sub>90</sub> ATP + PPADS (closed squares) to *Xenopus* oocytes expressing the rP2X4, rP2X4(2+) and rP2X4(4+) receptors. The bar represents a 3 s agonist/antagonist application. Traces have been normalised to peak currents to allow comparison. (b) PPADS inhibition curves. pIC<sub>50</sub> values are shown. ns = not significantly different from the WT hP2X1 receptor.

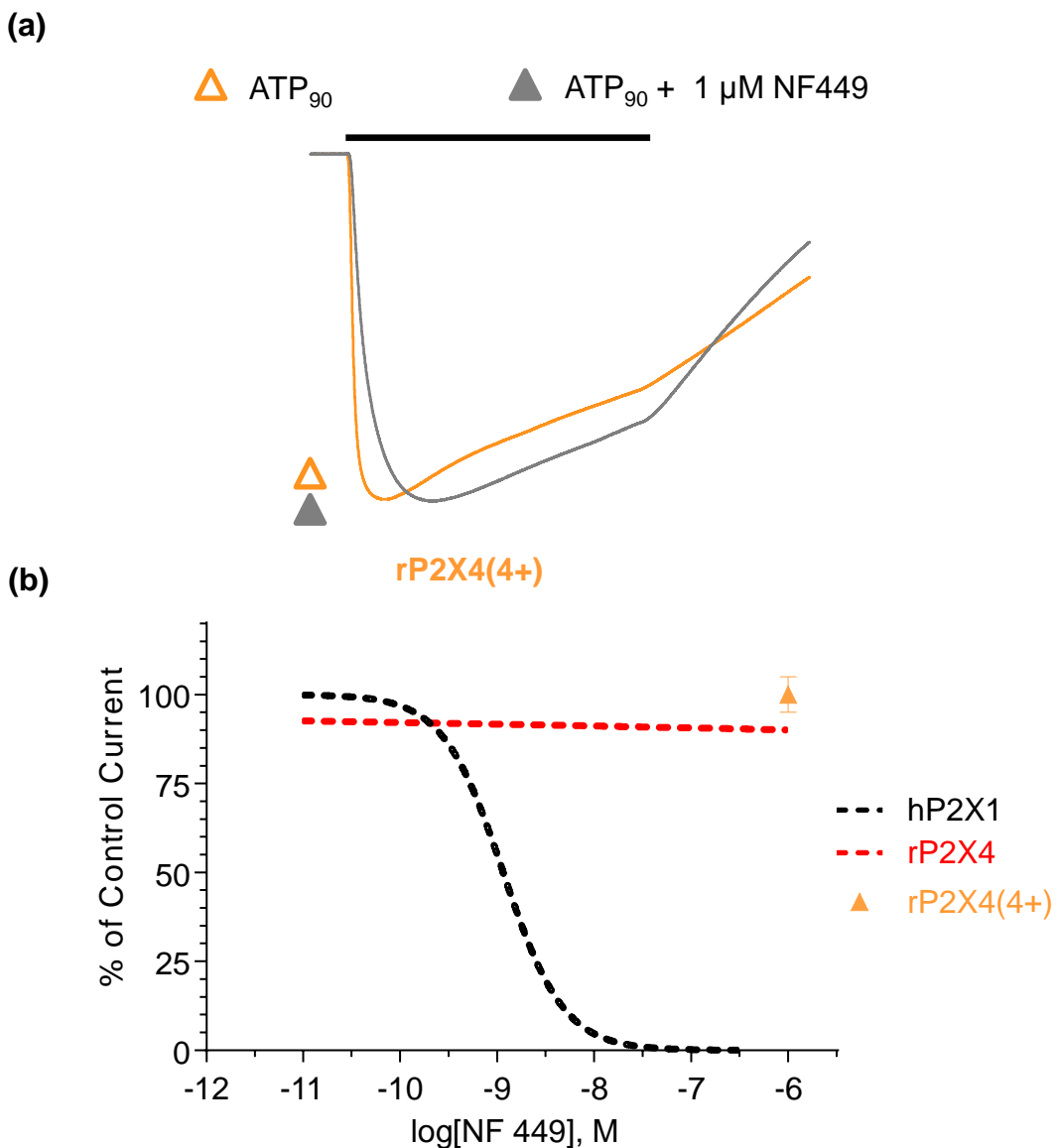


**Figure 6.4 The Presence of the Positive Charges does not Introduce NF449 Sensitivity at the rP2X4 Receptor.** (a) Four positive charges were introduced at positions 136,138,139 and 140 of the rP2X4 receptor. Representative traces of EC<sub>90</sub> ATP (orange) and EC<sub>90</sub> ATP + 1 μM NF449 (grey) application to Xenopus oocytes expressing the rP2X4 (4+) receptor. The bar represents a 3 s ATP application. For the EC<sub>90</sub> ATP + 1 μM NF449 application NF449 was bath perfused around the oocyte for 5 minutes before its co-application with ATP. (b) Inhibition curves for the WT receptors and the application of 1 μM NF449 at the rP2X4(4+) receptor.

region is therefore sufficient to allow suramin and PPADS, but not NF449, inhibition at the rP2X4 receptor.

### 6.2.5 ATP Action at the WT zfP2X4 Receptor

As the positive charges were shown to be important in suramin and PPADS action, it was tested to see if the equivalent mutations would introduce inhibition by these antagonists to the zfP2X4 receptor. This was tested in the zfP2X4 receptor subtype, which is the only subtype to have previously been crystallised. Sequence analysis (EMBL-EBI website) showed that the zfP2X4 nucleotide sequence shared 62% sequence homology with the rP2X4 receptor. The zfP2X4 receptor contained one charge at the base of the cysteine rich head region, equivalent to residue arginine 139 in the hP2X1 receptor, with the sequence at the equivalent positions being FNDAR (figure 6.7a). The WT zfP2X4 receptor will be referred to as zfP2X4 (FNDAR) in this thesis. When the zfP2X4 receptor was expressed in Xenopus oocytes, currents in response to ATP were very small, even at a very high concentration of 3mM ATP the mean peak current was only  $56.9 \pm 10.3$  nA, ~ 150-fold less than at the WT hP2X1 receptor,  $p < 0.0001$  (figure 6.5a). Therefore expression of the zfP2X4 receptor was optimised. The original zfP2X4 receptor was expressed in the pcDNA3 vector, but sequencing showed that unlike the other receptors that had been studied so far, did not have a polyadenylated (polyA) tail. A poly A tail is a series of adenosine bases 3' to the receptor sequence. The presence of a polyA tail stabilises RNA and helps with protein expression (Minvielle-Sebastia & Keller, 1999). Therefore the zfP2X4 receptor was sub-cloned into a pcDNA3.1 vector which contained a polyA tail 5' to the zfP2X4 receptor STOP codon.

Introducing a polyA tail after the stop codon of the zfP2X4 receptor increased the peak current in response to ATP ~ 5-fold,  $p < 0.001$  with the polyadenylated receptor having a peak current of  $325 \pm 73$  nA (figure 6.3b). This was the form of zfP2X4 receptor used in further experiments. Despite still having a greatly reduced current compared to the rP2X4 receptor, the time-courses of the rP2X4 and zfP2X4(FNDAR) receptors in response to maximal

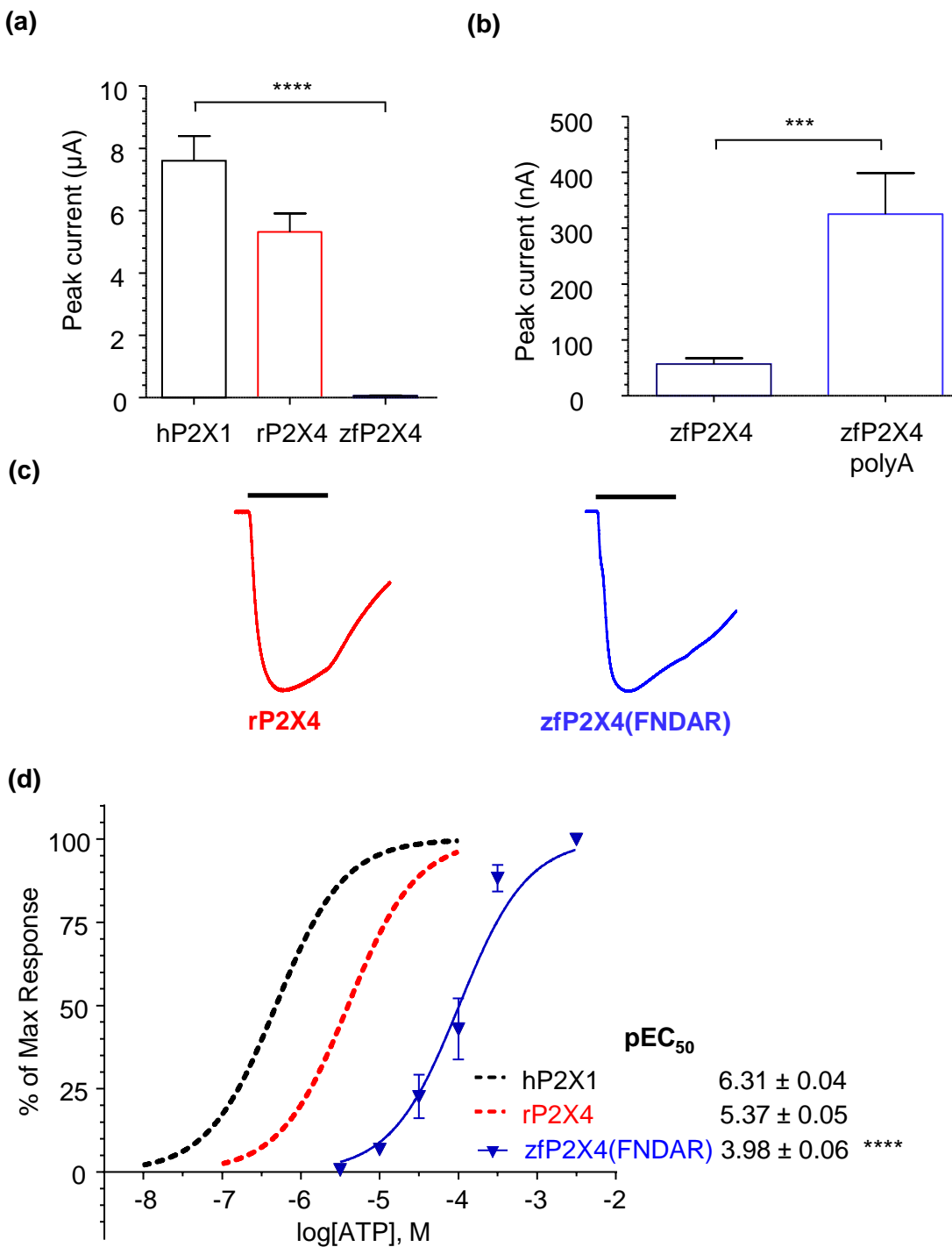


**Figure 6.5 ATP Action at the zfP2X4 Receptor.** (a) Effects of polyadenylation of the zfP2X4 receptor. Currents recorded from oocytes expressing the zfP2X4 protein without a polyA tail had a mean peak current of ~50 nA. (b) Polyadenylation was used to increase the currents at the zfP2X4 receptor to ~300 nA. Stars represent a significant difference. (c) Representative traces of maximal ATP application at the rP2X4 and zfP2X4 receptors. The bar shows a 3 s application. Traces have been normalised to peak current for comparison. (d) Concentration response curves for the WT receptors.  $\text{pEC}_{50}$  values are shown. Stars represent a significant shift from the hP2X1 receptor. \*\*\*  $p<0.001$  \*\*\*\*  $p<0.0001$ .

ATP were similar with % desensitisation being  $28.7 \pm 4.5$  and  $28.4 \pm 4.1\%$  respectively. The rise time at the zfP2X4(FNDAR) receptor was  $359 \pm 69$  ms, again similar to the rP2X4 receptor (figure 6.4c). The potency of ATP at the zfP2X4(FNDAR) receptor was ~ 100-fold reduced compared to both the hP2X1 and rP2X4 receptors,  $\text{pIC}_{50}$  values of  $3.98 \pm 0.06$ ,  $6.31 \pm 0.04$  and  $5.37 \pm 0.05$  respectively,  $p < 0.0001$  (figure 6.4d). The Hill slope of the zfP2X4(FNDAR) receptor ATP dose response curve was  $1.3 \pm 0.06$ , similar to those of the hP2X1 and rP2X4 receptors. A summary of the properties of the zfP2X4(FNDAR) receptor is given in table 6.1.

### 6.2.6 Suramin and PPADS at the zfP2X4 (FNDAR) receptor

The zfP2X4(FNDAR) receptor was insensitive to both suramin and PPADS when co-applied with EC<sub>90</sub> ATP, up to a concentration of  $100 \mu\text{M}$  suramin and  $300 \mu\text{M}$  PPADS (figure 6.6). This was the same as was seen at the rat P2X4 receptor and was expected as the P2X4 receptor of most species is insensitive to these commonly used antagonists (Kaczmarek-Hajek *et al.*, 2012). This antagonist insensitivity means that the zfP2X4 receptor has not been crystallised in an antagonist bound state, and as this is the only subtype of P2X receptor that has been crystallised so far, no antagonist bound P2X receptor crystal structure exists to date.

### 6.2.7 ATP Action at zfP2X4 (KNKAR) and zfP2X4 (KNKRR) Receptors

When the sequences of the hP2X1, rP2X4 and zfP2X4 receptors were compared it could be seen that the zfP2X4 receptor sequence already had a positively charged arginine residue at the equivalent position to K140 of the hP2X1 receptor (R143, zfP2X4 receptor numbering) but the other three charged residues were absent (figure 6.7a). Two mutant receptors were therefore made on the zfP2X4 receptor template. The first had mutations F139K and D141K introduced alongside the existing arginine at position 143, and this receptor is known as zfP2X4(KNKAR). This gave it an additional 2 positive charges compared to the WT zfP2X4 receptor, with three positive charges in this region overall. As there was a positive charge already present at position 143 in the WT receptor, and the number of mutations needed to

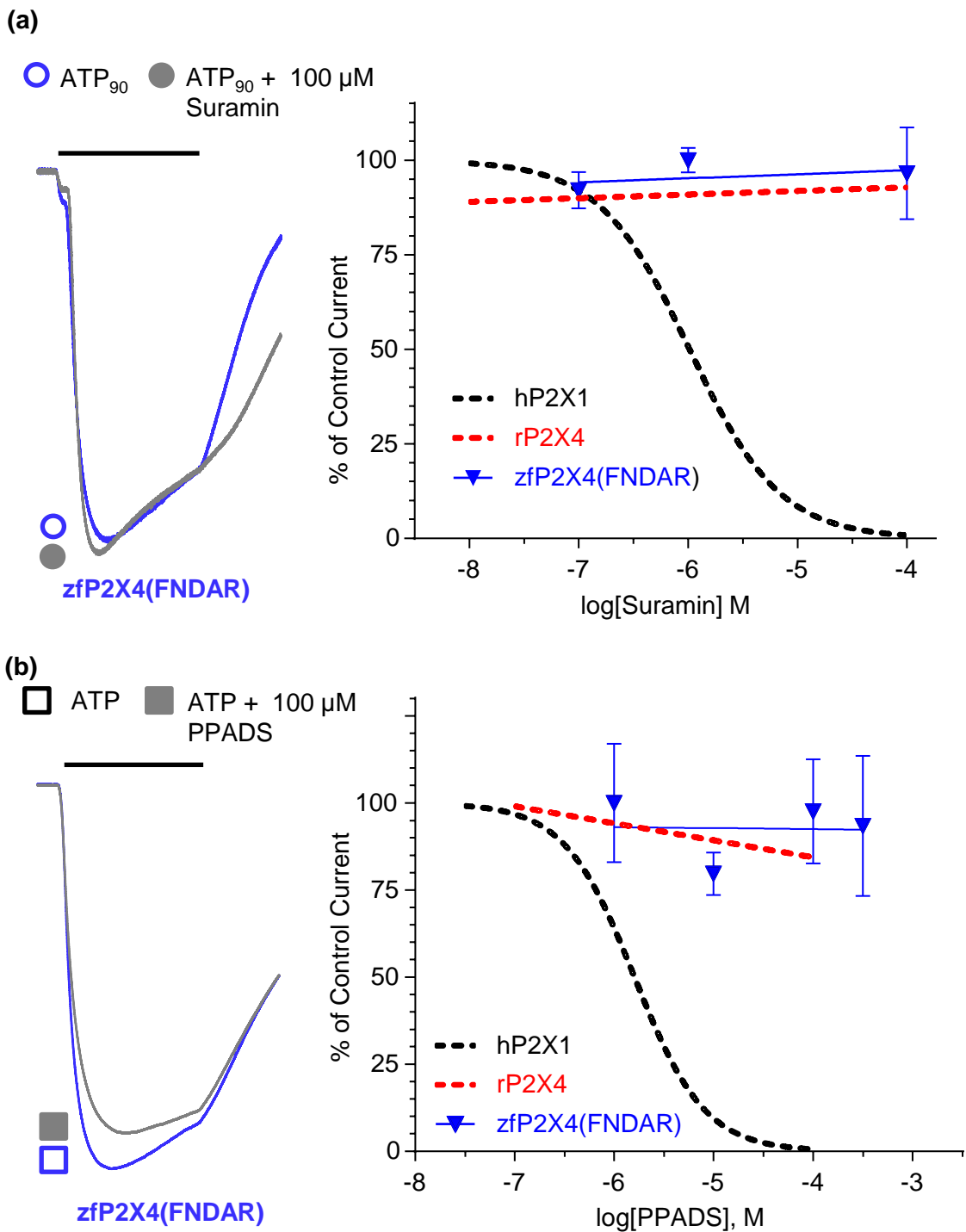


**Figure 6.6 The zfP2X4 Receptor is Insensitive to Suramin and PPADS** (a) Representative traces of EC<sub>90</sub> ATP (open circles) and EC<sub>90</sub> ATP + suramin (closed circles) application at the zfP2X4 receptor. The bar shows a 3 s application. Suramin inhibition curves are also shown. (b) Representative traces of EC<sub>90</sub> ATP (open squares) and EC<sub>90</sub> ATP + PPADS (closed squares) at the WT zfP2X4 receptor. The bar represents a 3 s application. PPADS inhibition curves are also shown.

(a)

hP2X1	K136	A137	K138	R139	K140
rP2X4	S136	V137	D138	T139	H140
zfP2X4(FNDAR)	F139	N140	D141	A142	R143
zfP2X4(KNKAR)	K139	N140	K141	A142	R143
zfP2X4(KNKRR)	K139	N140	K141	R142	R143

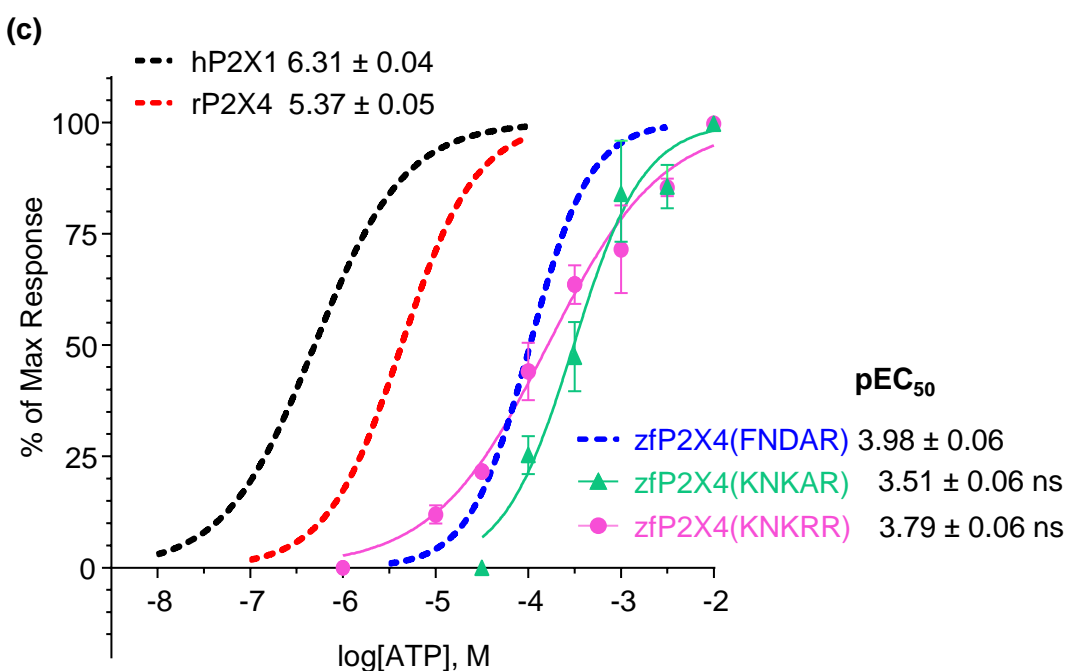
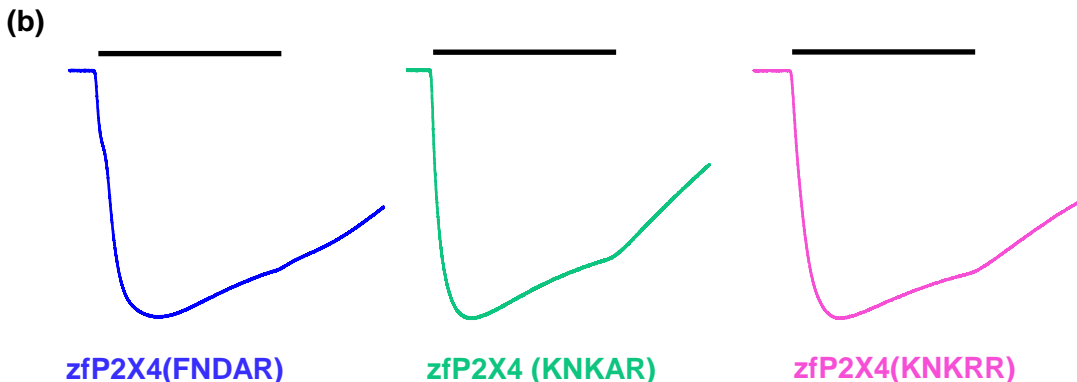


**Figure 6.7 ATP Action at the zfP2X4 Point Mutants** (a) Sequence alignment of the rP2X4, zfP2X4, zfP2X4(KNKAR) and zfP2X4(KNKRR) receptors. (b) Representative traces of maximal ATP at the WT and point mutated zfP2X4 receptors. The bars show a 3 s application. Traces have been normalised to peak currents to allow for comparison (c) Concentration response curves for the point mutated zfP2X4 receptors. pEC<sub>50</sub> values are given, ns = no significant shift from the WT zfP2X4 receptor.

introduce antagonist sensitivity was to be kept to a minimum, R143 was not mutated in this study. Only the A142R mutation was made in addition to form the zfP2X4(KNKRR) receptor. This mutant therefore had an additional 3 positive charges compared to the WT zfP2X4 receptor, with four positive charges present in this section of sequence overall (figure 6.6a).

Introducing the positive charges to the zfP2X4 receptor had no effect on the peak currents in response to ATP, with the zfP2X4(KNKAR) and zfP2X4(KNKRR) receptors recording mean peak currents of  $471 \pm 108$  and  $132 \pm 31$  nA respectively. The ATP potency of the zfP2X4(KNKAR) and zfP2X4(KNKRR) mutants was also unaffected compared to the WT zfP2X4 receptor,  $\text{pIC}_{50} = 3.59 \pm 0.06$ ,  $3.79 \pm 0.06$  and  $3.98 \pm 0.06$  respectively (figure 6.6c). The time-course of the zfP2X4 receptor point mutants was the same as at the WT zfP2X4 and rP2X4 receptors for both rise time and % desensitisation (figure 6.6b). The rise times for the zfP2X4(KNKAR) and zfP2X4(KNKRR) receptors were  $287.6 \pm 54.4$  ms and  $361.7 \pm 63.5$  ms respectively and the % desensitisation was  $27.0 \pm 3.6\%$  and  $12.7 \pm 3.3\%$ . This shows that as with the rP2X4 receptor mutants, introduction of positive charges to the zP2X4 receptor had no effect on how ATP was acting at the receptor.

### 6.2.8 Suramin Inhibition at the zfP2X4 Receptor Mutants

Mutating the positive charges into the head region of the zfP2X4 receptor had no effect on the action of ATP at the mutants compared to the WT zfP2X4(FNDAR) receptor, similar to what was seen when the equivalent mutations were made in the rat subtype. As the introduction of the four charged residues had made the rP2X4 receptor antagonist sensitive, it was tested to see if this was also true for the zfP2X4(KNKAR) and zfP2X4(KNKRR) mutants. Co-application of  $10 \mu\text{M}$  suramin with  $\text{EC}_{90}$  ATP caused  $\sim 40\%$  inhibition at the zfP2X4(KNKAR) mutant and  $\sim 50\%$  inhibition at the zfP2X4(KNKRR) mutant (figure 6.7a). The suramin sensitivity of zfP2X4(KNKAR) and zfP2X4(KNKRR) receptors was similar, with  $\text{pIC}_{50}$  values of  $4.52 \pm 0.05$  and  $4.90 \pm 0.05$  respectively (figure 4.7b). These results were in contrast to the WT zfP2X4 receptor which was insensitive to suramin up to a concentration of  $100 \mu\text{M}$ . The

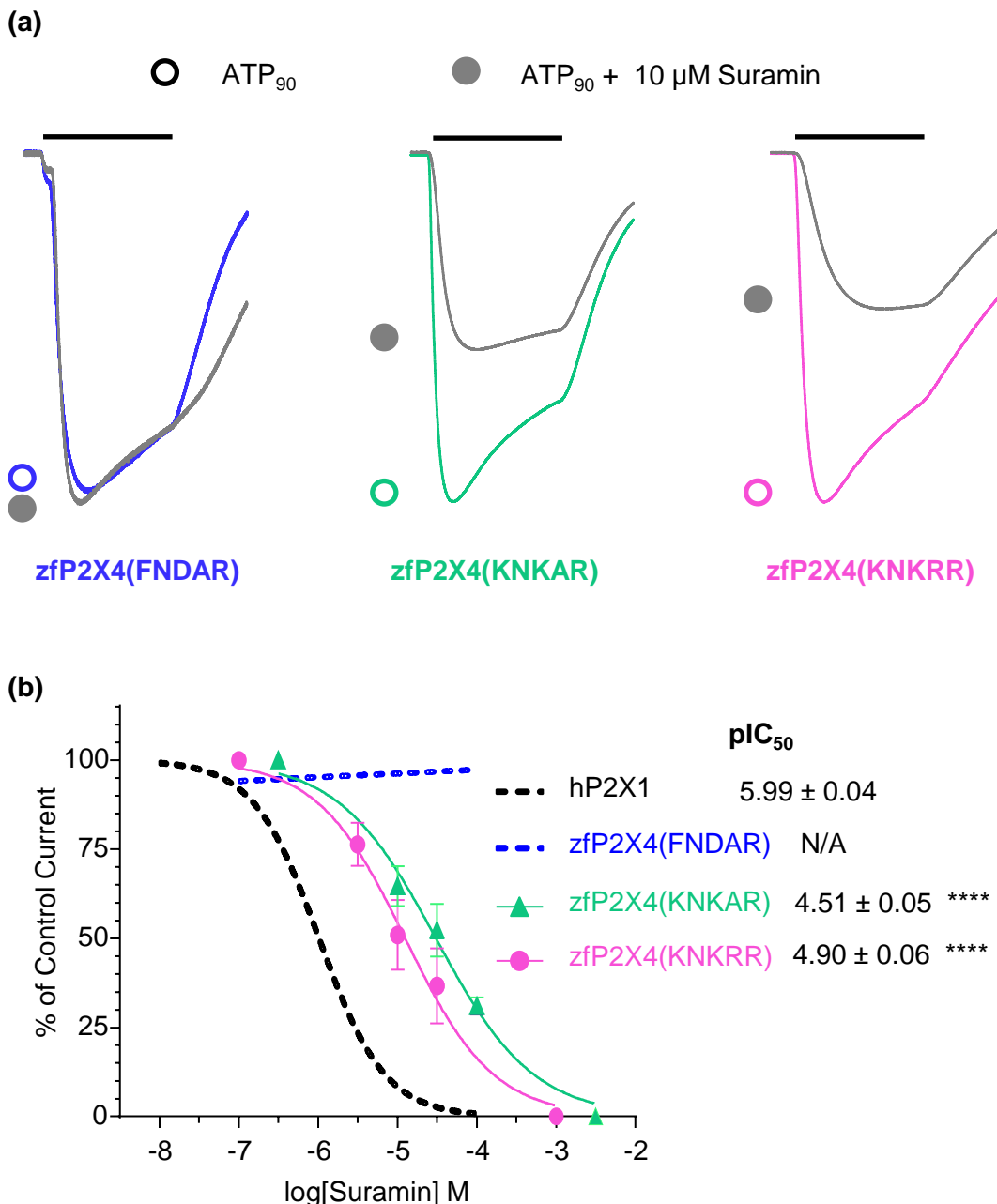


**Figure 6.8 Suramin Inhibition at zfP2X4 Point Mutations.** (a) Representative traces to show application of EC<sub>90</sub> ATP (open circles) and EC<sub>90</sub> ATP + suramin (closed circles) at WT and point mutated zfP2X4 receptors. The bars represent a 3 s application. Traces have been normalised to peak currents to allow for comparison (b) Suramin inhibition curves. pIC<sub>50</sub> values are shown. Stars represent a significant difference from the hP2X1 receptor. \*\*\*\* p < 0.0001

zfP2X4(KNKAR) and zfP2X4(KNKRR) mutants were ~ 30 and ~ 12-fold respectively less sensitive to suramin than the hP2X1 receptor,  $p < 0.0001$ , but showed no difference in the Hill slope of the inhibition curve compared to the hP2X1 receptor (table 6.1). These results show that the zfP2X4 (FNDAR) receptor can be made sensitive to suramin through introduction of two or three additional positive charges. Other residues within the zfP2X4 receptors are likely to also be co-ordinating suramin binding at the receptor, but the positive charges appear necessary for high affinity and potency at the receptor. These mutations could be useful when generating an antagonist bound crystal structure.

### 6.2.9 PPADS Inhibition at the zfP2X4 Receptor Mutants

As introduction of these two or three positive charges at positions 139 and 141 and 142, (along with the existing arginine at position 143 of the zfP2X4(FNDAR) receptor), made the receptor sensitive to suramin, it was tested to see if the zfP2X4(KNKAR) and zfP2X4(KNKRR) mutants were also sensitive to PPADS. PPADS caused no response at either receptor when applied in the absence of ATP and was pre-perfused around the oocyte for 5 minutes before being co-applied with EC<sub>90</sub> ATP. An application of 10  $\mu\text{M}$  PPADS caused ~ 50% inhibition at both the zfP2X4(KNKAR) and zfP2X4(KNKRR) mutants (figure 6.8a). There was again no difference in the potency of PPADS between the zfP2X4(KNKAR) and zfP2X4(KNKRR) mutants, with pIC<sub>50</sub> values of  $4.73 \pm 0.04$  and  $4.86 \pm 0.11$  respectively (figure 6.8b). The mutants were ~10-fold less sensitive to PPADS than the hP2X1 receptor ( $p < 0.001$ ), but showed a marked increase in inhibition compared to the WT zfP2X4(FNDAR) receptor which was insensitive to PPADS at the highest concentration tested (300  $\mu\text{M}$ ). The Hill slopes of the zfP2X4 receptor mutants were similar to the hP2X1 receptor (table 6.1). These results show that, as with suramin, the introduction of three additional positive charges to the zfP2X4(FNDAR) receptor could introduce PPADS sensitivity. As only 3 point mutations were necessary to introduce this sensitivity, these mutations could be used to generate antagonist bound crystal structures.

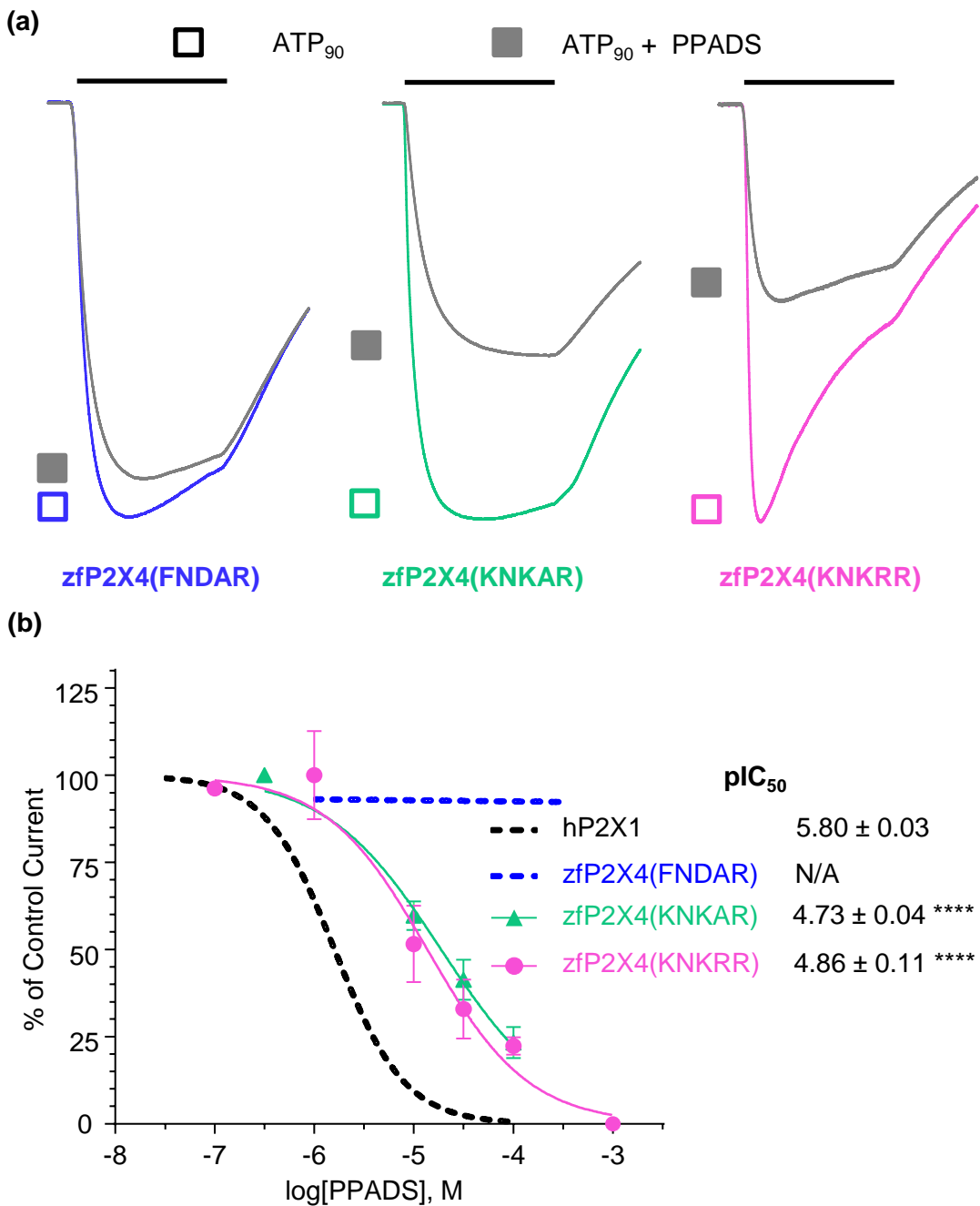


**Figure 6.9 PPADS Inhibition at the zfP2X4 Point Mutated Receptors.** (a) Representative traces to show application of EC<sub>90</sub> ATP (open squares) and EC<sub>90</sub> ATP + PPADS (closed squares) at WT and point mutated zfP2X4 receptors. Bars represent a 3 s application. Introducing positive charges at positions 139, 141 and 142 made the zfP2X4 receptor PPADS sensitive. Traces have been normalised to peak currents to allow comparison. (b) PPADS inhibition curves. pIC<sub>50</sub> values are shown. Stars indicate a significant difference from the hP2X1 receptor. \*\*\*\* = p <0.0001

	Mean Peak Current (nA)	Rise Time (ms)	% Decay	ATP pEC <sub>50</sub>	ATP Hill Slope	Suramin pIC <sub>50</sub>	Suramin Hill slope	PPADS pIC <sub>50</sub>	PPADS Hill slope
<b>hP2X1</b>	7598 ± 793	95 ± 5	80.29 ± 4.31	6.31 ± 0.04	0.89 ± 0.07	5.99 ± 0.04	1.05 ± 0.12	5.80 ± 0.03	1.23 ± 0.10
<b>rP2X4</b>	5320 ± 586	309.3 ± 32.04	28.65 ± 4.48	5.37 ± 0.05	1.07 ± 0.12	N/A	N/A	N/A	N/A
<b>rP2X4 (2+)</b>	2226 ± 271	447 ± 24	19.51 ± 1.6	4.95 ± 0.10	1.34 ± 0.34	4.19 ± 0.15	0.64 ± 0.16	5.21 ± 0.05	1.58 ± 0.28
<b>rP2X4 (4+)</b>	2746 ± 374	247 ± 64	31.83 ± 7.0	5.02 ± 0.05	1.53 ± 0.24	5.16 ± 0.09	0.89 ± 0.09	6.32 ± 0.05	1.03 ± 0.13
<b>zfP2X4(FN DAR)</b>	325 ± 73	359 ± 69	28.44 ± 4.07	3.98 ± 0.06	1.33 ± 0.23	N/A	N/A	N/A	N/A
<b>zfP2X4 (KNKAR)</b>	471 ± 108	287.6 ± 54.4	27.0 ± 3.6	3.51 ± 0.06	1.14 ± 0.17	4.51 ± 0.05	0.67 ± 0.08	4.73 ± 0.04	0.75 ± 0.07
<b>zfP2X4 (KNKRR)</b>	132 ± 31	361.7 ± 63.5	12.7 ± 3.3	3.79 ± 0.06	0.71 ± 0.06	4.9 ± 0.06	0.79 ± 0.10	4.86 ± 0.11	0.85 ± 0.19

**Table 6.1 ATP and NF449 action at the hP2X1 and P2X4 receptors and P2X4 mutants.** Boxes shaded in grey show no difference from the hP2X1 receptor. Blue represents a significant increase compared to the hP2X1 receptor and red represents a significant decrease.

### **6.2.10 Purification of the zfP2X4(KNKRR) Receptor**

Crystallisation of a receptor is a complicated process and it took seven years to crystallise the first P2X receptor (Young, 2010). One of the reasons the process takes so long is that many mutant forms of the receptor had to be trialled in order to find one that formed high resolution crystals. Therefore when attempting to crystallise the P2X4 receptor, it would be optimal to use the existing zfP2X4 receptor construct that has already been crystallised. This mutant is the zfP2X4C mutant which is both C and N-terminally truncated consisting of residues 28-365 of the WT zfP2X4(FNDAR) which has also had 2 glycosylation sites removed by point mutation (N78K and N187R) (Hattori & Gouaux, 2012). The zfP2X4C receptor is insensitive to suramin and PPADS, however introducing the three additional positive charges to the receptor may allow an antagonist bound crystal structure to be produced. Purification of the zfP2X4C(KNKRR) mutant on a small scale was attempted as an indication of whether crystallisation of the receptor in an antagonist bound state would be possible. These experiments were performed on a GFP-tagged zfP2X4C(FNDAR) receptor background which had a molecular weight of 66.2 kDa (figure 6.10a). The zfP2X4C(FNDAR) receptor was sub-cloned into a new vector named pLEICS-12 (figure 6.10b), and the 3 additional positive charges introduced in PCRs performed by the Protein Expression Laboratory, PROTEX (University of Leicester, Leicester, UK) to make the mutant zfP2X4C(KNKRR). The pLEICS-12 vector is based on the pcDNA3.1 vector and was chosen as it has routinely been used at the University of Leicester for protein expression in HEK cells and crystallisation experiments. The vector contained a CMV promoter and both FLAG and histidine tags in order to identify and immunoprecipitate the zfP2X4C(KNKRR) protein (figure 6.10). As the zfP2X4C construct used was also GFP tagged, a variety of options for protein identification and purification were available.

The zfP2X4C and zfP2X4C(KNKRR) constructs were transfected into Freestyle<sup>TM</sup> 293-F HEK cells (Invitrogen) and cultured in suspension. Two days after transfection cells were harvested and immunoprecipitation was performed using magnetic beads. The zfP2X4C(FNDAR) and zfP2X4C(KNKRR) receptors

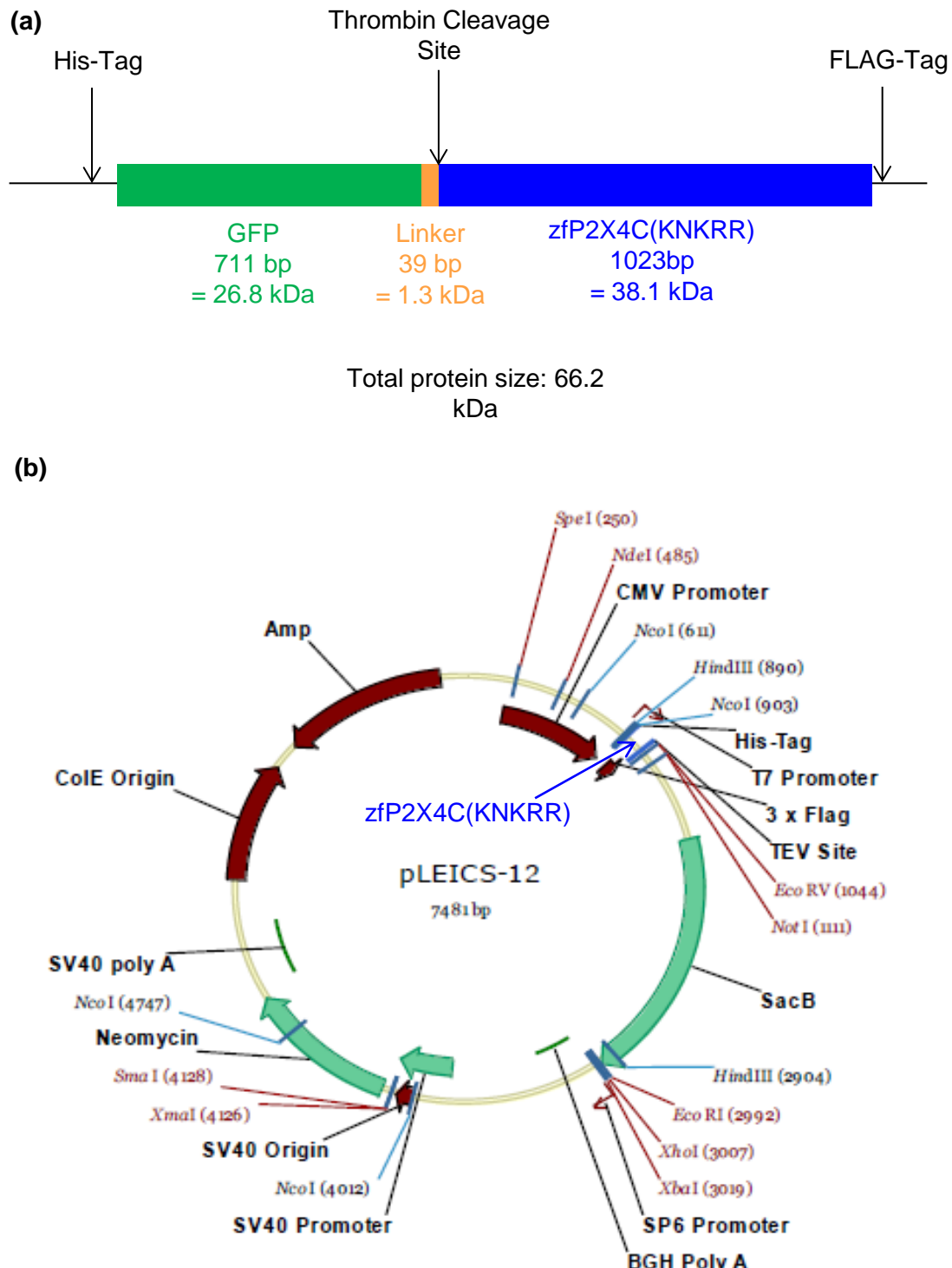


**Figure 6.10 Representations of the GFP tagged zfP2X4C(KNKRR) receptor and The pLEICS12 Vector.** (a) GFP-tagged zfP2X4C receptor drawn to scale. (b) pLeics12 vector map. The vector is 7481 bp in size and is based on the pcDNA3.1 vector. It contains ampicillin and neomycin resistance genes for selection. It uses a CMV promoter and has both His and FLAG tags in order to immunoprecipitate the zfP2X4C proteins.

were initially incubated with nickel beads which bound to the histidine tag. This method was chosen as the histidine tag had been used to pull down the zfP2X4C protein when the receptor had been crystallised previously, and also to save costs as the nickel beads were less expensive than the FLAG tagged ones (Kawate *et al.*, 2009). When the elutions from the nickel beads were run on a Bis-Tris gel and stained to identify any proteins present, there were numerous bands of different sizes, suggesting that while the zfP2X4 receptor proteins may have been present, the sample also contained lots of additional proteins and a pure sample could not be obtained (figure 6.11). Control cells were not used in this experiment, but as it was only performed to see if the histidine tag could be used for protein immunoprecipitation this does not affect the result. The reason that nickel beads were not successful in this study may be because the zfP2X4C(KNKRR) protein was expressed in HEK cells, whereas when the receptor was previously crystallised Sf9 cells were used. The nickel beads appear to be pulling down proteins present in the HEK cells. After discussions with structural biologists it was decided that the nickel beads were not the most effective method of purifying the protein and experiments should be repeated using anti-FLAG magnetic beads which would recognise the FLAG tag in the pLEICS-12 vector.

Two separate buffers were used in experiments using the anti-FLAG beads in order to optimise the protocol. The first (buffer A) was tris based and had routinely been used in the lab for protein purification experiments, the second (buffer B) was bis-tris based and was suggested by Dr Louise Fairal, University of Leicester (see methods). All experiments were run in parallel in both buffers. A control was performed using non-transfected cells (figure 6.12 a,b). For the control, only very faint bands could be seen in the elutions performed in either buffer on the coomassie stained protein gel (figure 6.12a), however when a Western blot was performed using an anti-flag antibody faint bands were seen in the elutions in both buffers (figure 6.12 b). The expected molecular weight for the unglycosylated GFP-tagged zfP2X4C(KNKRR) receptor was ~ 66 kDa, with GFP being ~27 kDa and the zfP2X4C(KNKRR) protein ~38 kDa (figure 6.10a). For the Western blot of the elution of control cells in buffer A there was a band at ~ 70 kDa. It was not clear what this

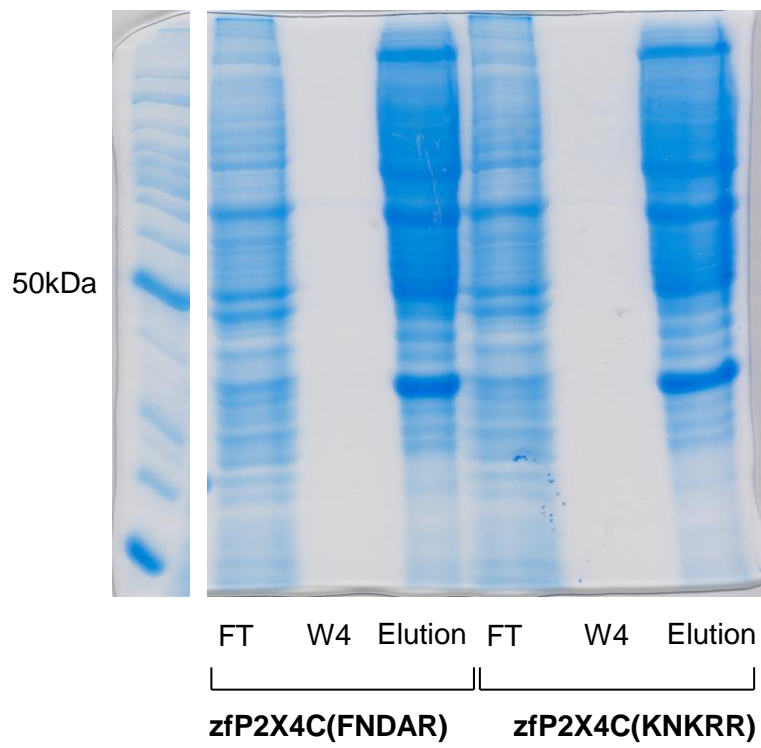


**Figure 6.11 Expressing the zfP2X4C(KNKRR) Protein in Freestyle™ 293-F HEK Cells.** Coomassie stained protein gel of HEK cells transfected with zfP2X4C or zfP2X4C(KNKRR) receptors. The zfP2X4C and zfP2X4C(KNKRR) receptors were pulled down using nickel beads which recognise the histidine tag. The samples have multiple bands meaning a pure zfP2X4C or zfP2X4C(KNKRR) protein has not been obtained. FT = flow through, W4 = wash 4.

band was, however it was likely to be too large to be confused with the zfP2X4C receptors in future experiments. There was no band present at a similar size in buffer B. Beads bound to the anti-FLAG antibody were therefore considered appropriate for purification of the zfP2X4C(KNKRR) protein.

When elutions from the zfP2X4C(KNKRR) sample were run on the protein gel, two very faint bands were seen at ~ 60 kDa in buffer B but no bands of the correct size were seen in cells treated with buffer A (figure 6.12c). Western blotting using an anti-FLAG antibody also showed two bands of a similar size of ~ 65kDa, suggesting that these bands could be the zfP2X4C(KNKRR) receptor (figure 6.12d). These bands were absent from the elution performed in buffer A. The bands were excised from the gel and sent for analysis by mass-spectrometry (PNACL, University of Leicester). Results showed that both bands contained the zfP2X4C(KNKRR) receptor protein. This meant that the protein could be identified and pulled down using the anti-FLAG beads. However there were still numerous other proteins present on the gel and so a pure sample of zfP2X4C(KNKRR) had not been obtained.

In order to increase the purity of the zfP2X4C(KNKRR) immunoprecipitated protein, membrane isolation was performed so that solely proteins present in the membrane of the cell would be incubated with the anti-FLAG beads. It was hoped that this would increase the purity of the protein. The membrane isolation was performed using a buffer which contained the detergent DDM that had been used to purify the chemokine receptor CCR1 (Allen *et al.*, 2009) (see methods). The immunoprecipitated membrane proteins were again run on a gel which was stained for protein (figure 6.12). This sample proved to be much purer, with only three bands being seen at ~ 65, ~ 75 and ~ 85 kDa. The predicted weight of the zfP2X4C(KNKRR) receptor was ~ 66 kDa. The bands were excised and sent for mass spectrometry. All three bands were identified as containing the zfP2X4C(KNKRR) receptor. Possible reasons for these multiple bands are discussed at the end of this chapter.

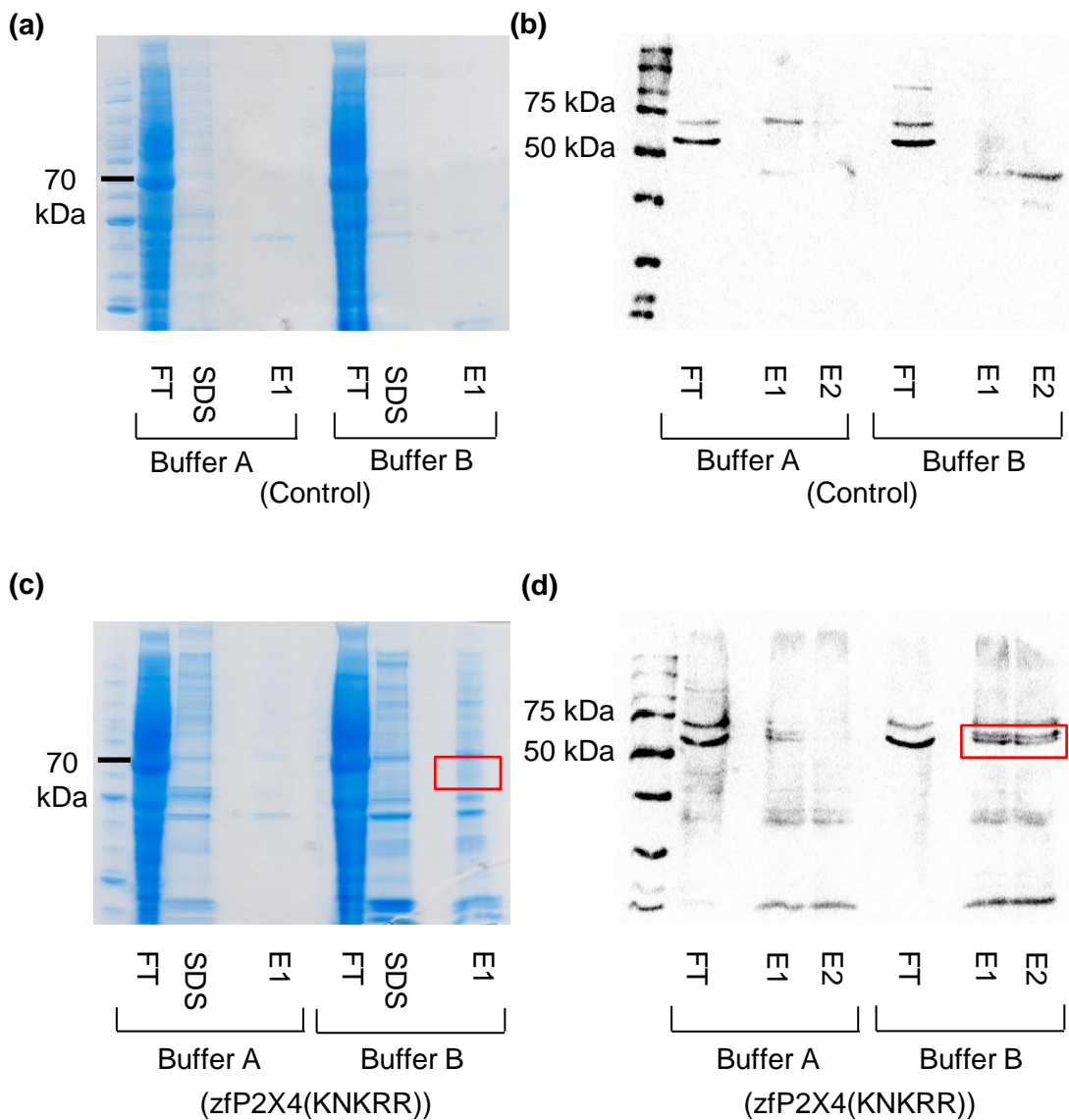


**Figure 6.12 Purifying the zfP2X4C(KNKRR) Receptor Protein in Different Buffers.** Harvested HEK cells were incubated with anti-FLAG beads and the flow through (FT) and elutions were run on protein gels which were stained with coomassie stain (**a and c**) or Western blots were performed using an anti-FLAG antibody (**b and d**). Non-transfected cells were used as a control and experiments were performed in parallel in two different buffers. Some bands were present in the Western blot for the control cells (**b**), however an additional band at the expected size (~ 66 kDa) was seen in the zfP2X4C(KNKRR) transfected cell samples (**d**). This suggests that it is this bands which contains the zfP2X4C(KNKRR) protein, highlighted in red. Buffer B produced better results than buffer A. The bands shown circled in red in gel (**c**) were excised and sent for analysis by mass spectrometry.

The bands for the zfP2X4C(KNKRR) protein were faint, so only a low concentration of protein was present. However this preparation had only used 90 ml of cells and only 20% of the protein from harvested cells was ultimately loaded on the gel. These results suggests that with optimisation a pure zfP2X4C(KNKRR) protein could be isolated in high concentrations for crystallisation if experiments were performed on a larger scale. An antagonist bound zfP2X4C(KNKRR) receptor crystal structure could give huge insights into how suramin and PPADS are acting at the hP2X1 receptor.

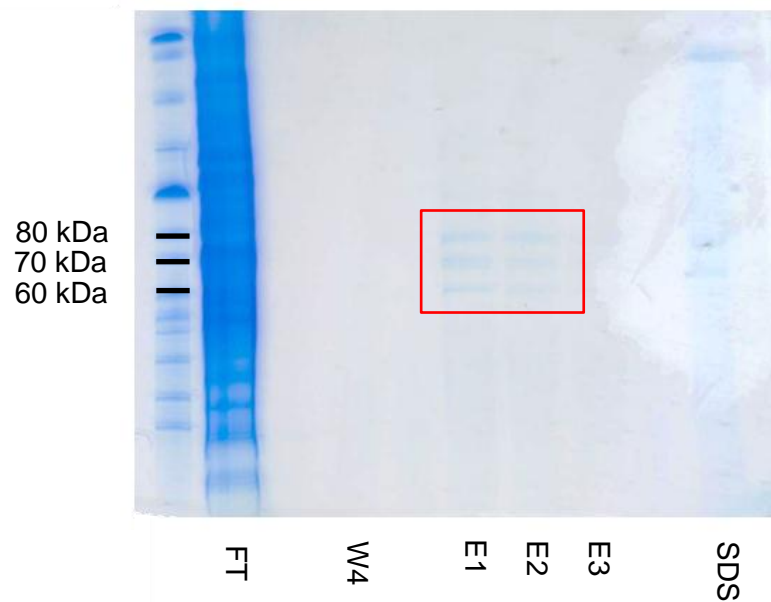


**Figure 6.13 Membrane Preparation of the zfP2X4C(KNKRR) Samples.** Membranes were isolated from the transfected HEK cells before being incubated with anti-FLAG magnetic beads. This meant that only proteins present in the cell membrane would be added to the protein gel. Three faint bands were seen at ~65, 75 and 85 kDa (shown in red). These bands were excised and sent for mass spectrometry. All three bands were seen to contain the zfP2X4C(KNKRR) protein, suggesting that differentially glycosylated forms of the protein may exist in the sample. FT = flow through, W4 = wash 4, E1, E2, E3 = elutions 1, 2 and 3. SDS = elution with SDS.

## **6.3 Discussion**

### **6.3.1 Introduction of the Positive Charges to the Head Region of the P2X4 Receptor had no Impact on ATP Action**

When either two or four positive charges were introduced to the rP2X4 receptor at positions 136-140, no effect on ATP potency or time-course was seen compared to the WT rP2X4 receptor. This suggests that residues S136, D138, T139 and H140 are not contributing to the difference in ATP potency or the time-course of the ATP evoked response between the hP2X1 and rP2X4 receptors. This is interesting as removal of these charges from the hP2X1 receptor as part of chimera X1-BX4 caused a decrease in the desensitisation seen, and their reintroduction to the receptor reintroduced the rapid hP2X1 receptor-like time-course. Swapping these charges with equivalent residues of the P2X2 receptor in a previous study also decreased ATP potency to P2X2 receptor levels but had no effect on the desensitisation, maintaining the rapid time-course of P2X1 at the receptor (El-Ajouz *et al.*, 2012). The time-course of the receptor may have been retained in the P2X2 study as only the four point mutations were made whereas in this thesis the charges were removed as part of a larger mutation. This shows that these charged residues are important for the rapid time-course of the hP2X1 receptor but that their presence alone cannot introduce this time-course to the slowly desensitising rP2X4 receptor. Introduction of these charges also had no effect on the time-course or potency of the hP2X2 receptor (El-Ajouz *et al.*, 2012). These residues are therefore part of a more complex control of receptor time-course, involving many residues both intracellular, extracellular and in the transmembrane domains (Werner *et al.*, 1996; Allsopp & Evans, 2011). There was also no effect on the time-course or ATP sensitivity of the zfP2X4(KNKAR) or zfP2X4(KNKRR) mutants compared to the WT zfP2X4(FNDAR) receptor. This suggests that no gross conformational changes have been introduced by the mutations as ATP binding and channel gating are still normal at the receptors. This is an important finding for the possibility of crystallisation, as a crystal structure is only informative if it is an accurate representation of the WT structure. Mutations which introduce conformational changes would not be a good target for crystallisation.

### **6.3.2 Introduction of the Positive Charges Introduced both Suramin and PPADS Sensitivity**

The WT rat and zebrafish P2X4 receptors showed no sensitivity to suramin or PPADS but both the rP2X4(2+) and rP2X4(4+) mutants were inhibited by these antagonists and this was mimicked in the zfP2X4(KNKAR) and zfP2X4(KNKRR) receptors. Therefore introducing positive charges at the base of the cysteine rich head region is sufficient to cause inhibition by suramin and PPADS at these receptors. The antagonists could either bind to these mutated residues, or the presence of these charged amino acids could allow the receptor to adopt a conformation at which antagonism can occur. The suramin and PPADS molecules are large and will bind to numerous residues in the receptor. As only three or four mutations have been made to these receptors in order to introduce this inhibition, even if suramin and PPADS are binding at these residues, other amino acids must also contribute to the binding site due to the size of the antagonist molecules. As removal of these charges had no effect on suramin and PPADS action (chapter 4) at the hP2X1 receptor it is likely that the antagonist molecules are not binding to these residues, but instead their presence causes a conformational change at the receptor which allows antagonism to occur. This is also supported by the fact that suramin and PPADS are structurally distinct with few common features, suramin is a competitive antagonist and PPADS non-competitive, and yet the mutation has had similar effects for both molecules. The residues are also missing from other suramin and PPADS sensitive receptors such as the hP2X2 receptor (El-Ajouz *et al.*, 2012).

Introduction of the four positive charges to the rP2X4 receptor caused the mutant to become sensitive to suramin and PPADS, but the removal of these charges as part of the X1-BX4 chimera did not decrease the action of these antagonists at the hP2X1 receptor. The opposite effect was seen for the contribution of the four positive charges to NF449 action. Introduction of the four positive charges to the rP2X4 receptor had no effect on NF449 action at the rP2X4 receptor, however the loss of these charges as part of the X1-BX4 chimera decreased NF449 inhibition. This shows that the charges are involved

in suramin, PPADS and NF449 action but are contributing to the effects of these antagonists in different ways. In the study by El Ajouz *et al* introduction of three of the four positive charges (E136K D138K and L140K) increased suramin sensitivity ~ 20-fold, but the additional M139R mutation caused the inhibition to return to WT hP2X2 receptor levels (El-Ajouz *et al.*, 2012). This supports the role of these positive charges in suramin action, but in this study the increase in antagonist sensitivity that has been seen is much greater, and the mutant in which four charges have been introduced also shows high suramin sensitivity. The greater effect of the mutant in this study could be due to suramin sensitivity being much lower at the rP2X4 receptor compared to the hP2X1 receptor. The H241A mutation did not have to be introduced to the rP2X4 receptor in order for it to become antagonist sensitive. This suggests that although this residue has been shown to be involved in the antagonist insensitivity of the rP2X4 receptor (Xiong *et al.*, 2004b), its presence does not prevent antagonism at the receptor, rather it just contributes to antagonist insensitivity. This again shows a complex, multifaceted control of antagonism at P2X receptors, with many different residues contributing to a receptor's antagonist sensitivity.

### **6.3.3 The Presence of the Four Charges in Other P2X Receptors**

The four positive charges are unlikely to be solely responsible for suramin and PPADS binding as they are not conserved in other receptors which are inhibited by these antagonists. For example PPADS is equally potent at the hP2X1 and hP2X2 receptors, and suramin also inhibits both receptors, but the hP2X2 receptor does not have charged residues at the equivalent positions. The rat P2X1 receptor is sensitive to suramin and contains three charges at positions equivalent to 136, 139 and 140, but interestingly lacks the charge at 138 which was shown to be particularly important in suramin inhibition by Sim *et al* (Sim *et al.*, 2008). It is possible that the introduction of the four charges at the rP2X4 receptor has helped it to adopt a conformation that is present in these other receptors.

### **6.3.4 Generation of an Antagonist Bound Crystal Structure**

The generation of an antagonist bound crystal structure for the P2X receptor is important as it would show where on the receptor the antagonist was binding. Little is currently known about how suramin and PPADS are binding at the receptor. The only subtype of P2X receptor that has been crystallised is the zfP2X4 receptor which is insensitive to antagonists and therefore an antagonist bound crystal structure has not been made. This chapter has shown that the introduction of the four charges to the zfP2X4C template may allow the P2X4 receptor to adopt a position where antagonists can bind to residues that already exist in the molecule, rather than the charges being involved in binding themselves. This would mean the crystal structure gave information on the native binding site of the suramin and PPADS molecules at P2X receptors. The zfP2X4C(KNKRR) receptor would be a strong target for crystallisation as only 3 point mutations have been introduced to the previously crystallised zfP2X4C receptor to make it antagonist sensitive. These mutations did not alter ATP sensitivity or the time-course of the ATP evoked response compared to the WT receptor, suggesting the receptor is still structurally similar and therefore is a good target for crystallisation.

The protein purification experiments at the end of this chapter have shown encouraging results for the generation of an antagonist bound crystal structure of the zfP2X4 receptor. It was seen that the zfP2X4C receptor could be purified when proteins were isolated from the membranes of Freestyle HEK cells. For a protein to be crystallised it needs to be a single molecular species, however in this study, three different sized bands were seen and it is currently unclear why this occurred. Differently glycosylated proteins have different sizes, and glycosylation of the P2X2 receptor has been reported to add ~ 15 kDa to the size of the protein (Newbolt *et al.*, 1998), it is therefore possible that the ~ 20 kDa difference in the size of the zfP2X4C(KNKRR) protein is due to glycosylation. In order to confirm this the protein could be deglycosylated using a protein deglycosylation kit (Sigma). Two glycosylation sites have been mutated out of the zfP2X4C(KNKRR) receptor and so other factors may be

contributing to the different molecular species seen such as modifications or interacting proteins (Kawate *et al.*, 2009).

Several modifications of the zfP2X4C(KNKRR) receptor were identified by mass spectrometry in the larger bands which could be responsible for an increase in size. These include oxidation of methionine residues and the addition of carbamidomethyl, which modifies the mass of cysteines and occurs when the protein is alkylated. It was also seen that additional proteins were contained in some of the bands with which the zfP2X4C(KNKRR) receptor could form a complex and account for this increased size. A further possible reason for these differently sized bands could be that the protein has not been completely denatured, and some more complex structure remains. The proteins were treated with 2-mercaptoethanol but were not heated and therefore the proteins could be heated to 95°C to make sure they are completely denatured before loading in future experiments. It remains to be seen what is responsible for these differences and this will be evaluated in further studies. An advantage of the zfP2X4C(KNKRR) receptor being both His and FLAG tagged is that both tags could be used to purify the receptor, for example an initial purification could be done using the FLAG tag and the experiment then repeated on this eluted sample using the nickel beads. This should increase the purity of the final protein as two methods of selection have been used. If the presence of three bands each containing the zfP2X4C(KNKRR) protein persists, then size exclusion chromatography could be used in order to isolate proteins that are less than 70 kDa in size., for example the EPPF-HiLoad Superdex-75pg 16/60 column. This should remove any variations of the receptor, giving a pure sample of the protein to be crystallised.

Protein expression will need to be increased in future experiments for crystallisation to be possible. There are several approaches can be taken to do this.

- (i) **A different method of elution.** In order to ensure the protein is eluted from the beads in the most efficient manner, members of the biochemistry department at the University of Leicester often

use a TEV protease recognition site in order to cleave the protein from the FLAG tag which has been used to bind the receptor to the beads. TEV protease is a cysteine protease engineered from the Tobacco Etch Virus Nla protease. A TEV site is included in the pLeics12 vector. A thrombin cleavage site is contained at the very beginning of the P2X4C(KNKRR) sequence which could also be used to cleave the protein from the beads.

- (ii) **Different Detergents.** In order to lyse cells and digest the membrane proteins, a detergent is added to the buffer when performing the membrane preparation. In this experiment I used 1% DDM. The concentration of DDM could be increased to ~ 5%. Different detergents could also be tried such as β-octylglucoside (OG) or Triton X-100.
- (iii) **Different Membrane Preparation Protocols.** Other protocols for membrane preparation could be researched and used which vary in the length and speed of centrifugation.
- (iv) **Removal of the GFP tag.** The GFP tag is a large (~ 26.8 kDa) protein and it is possible that its presence is interfering with the expression of the receptor. A zfP2X4C(KNKRR) protein without this tag could therefore be produced through mutation and purified. Another way to remove the tag is to cleave the zfP2X4C(KNKRR) mutant from the beads using the thrombin cleavage site (figure 6.10). This site is positioned between the zfP2X4C(KNKRR) receptor and the GFP tag and so cleavage here would just elute the receptor, leaving the GFP attached to the beads.

Although these experiments showed low expression, low volume (max 90 ml) cultures of cells were used and of these cultures only 20% was loaded onto the final gel. This shows that ~ 5 x more protein could be obtained from these low volume cultures and different buffers and methods could be tried to increase the amount of protein that is expressed. This suggests that enough protein could be purified in large scale experiments in order to allow crystallisation.

In summary this chapter has demonstrated that both the antagonist insensitive rP2X4 and zfP2X4 receptors can be made suramin and PPADS sensitive by the introduction of positively charged residues at the base of the cysteine rich head region. This shows the strong possibility for the generation of both suramin and PPADS bound crystal structures, which would give huge insight into the molecular basis of antagonist binding at P2X receptors. Initial experiments into protein purification have shown strong potential for the crystallisation of the zfP2X4C(KNKRR) receptor and work towards this is ongoing.

## **Chapter 7: General Discussion**

The main focus of this thesis was to determine the molecular basis of antagonist action at the hP2X1 receptor. To do this, residues were swapped between the hP2X1 receptor and the antagonist insensitive rP2X4 receptor to generate chimeras and point mutations. The results of these experiments have given a wealth of information on agonism, time-course and antagonism at both receptors. Drawing all the findings together has shown that a variety of different mutations could have an effect on ATP potency, time-course and antagonism. The mutant phenotype that was most common was a decrease in ATP potency and no mutation caused an increase in ATP sensitivity. It was seen that the residues controlling ATP potency and the time-course of the agonist evoked response were distinct. The NF449 binding site has been predicted to be localised at the base of and just below the cysteine rich head region, and several models of this binding have been generated. The basis of suramin and PPADS antagonism appears to be more complex, with the difference in inhibition seen between the two WT receptors likely to be due to differences in conformation.

### **7.1 Regions of the hP2X1 Receptor Contributing to ATP Potency**

The chimeras and point mutations described in this thesis have given an overview of the regions of the receptor which have an effect on two important features of ATP action, potency and the time-course of the ATP evoked response. ATP potency at the hP2X1 receptor was easily decreased through mutation (table 7.1). Replacing three of the four original sections of the hP2X1 receptor (A,B and D) with rP2X4 receptor residues decreased the potency of ATP between 15 and 110-fold (figure 7.1a). Swapping region C as a whole had no effect on ATP potency at the hP2X1 receptor, however when smaller sub-chimeras were made within this section, a 6-12-fold decrease in potency was seen, with ATP potency becoming rP2X4 receptor-like for regions X1-C<sub>α</sub>, X1-C<sub>β</sub>, X1-C<sub>δ</sub> and X1-C<sub>ζ</sub> and the residue His 220 (figure 7.1a). This demonstrated that mutation of residues spread throughout the extracellular loop could have an effect on ATP potency. The ATP binding site is conserved between receptors and well defined. It is unlikely that these residues are directly involved in ATP

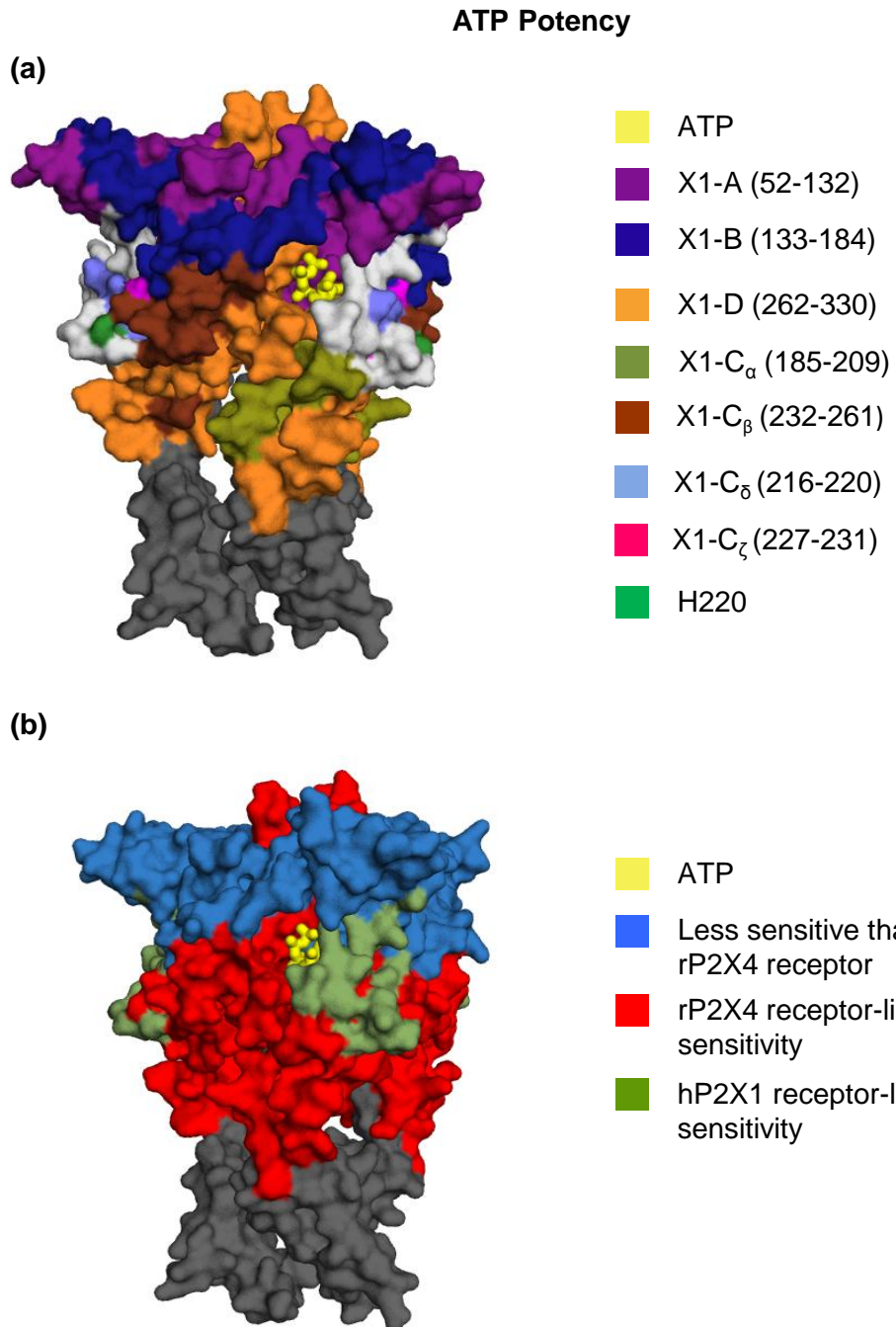


**Figure 7.1 Regions of the hP2X1 receptor identified as contributing to ATP potency** **(a)** Regions of the receptor which had an effect on ATP potency when mutated to the equivalent rP2X4 receptor residues are shown in colour on an homology model of the ATP bound hP2X1 receptor. **(b)** Regions where mutation of the hP2X1 receptor to equivalent residues of the rP2X4 receptor had an effect on ATP potency have been grouped according to how great the effect was. Residues shown in blue were less sensitive to ATP than the rP2X4 receptor. Residues shown in red had equivalent ATP sensitivity to the rP2X4 receptor and residues shown in black had hP2X1 receptor-like ATP potency.

binding. Therefore, as the original chimeras consisted of large swaps (> 50 residues), it was considered that they may have introduced conformational changes to the receptor that affected ATP binding. This could be through a subtle change in the structure of the ATP binding pocket which alters the affinity of the ATP molecule for the binding site, or through mutations which alter the gating of the receptor and decrease channel opening

This is supported by the finding that the effect on ATP potency of swapping region B was not reciprocal between the hP2X1 and rP2X4 receptors. Replacing residues of this region of the hP2X1 receptor with corresponding residues of the rP2X4 receptor decreased ATP potency, but the reciprocal mutation, replacing this region of the rP2X4 receptor with residues of the hP2X1 receptor had no effect on ATP potency. If the residues were involved in high affinity ATP binding, then their removal from the hP2X1 receptor would be likely to decrease the affinity of the molecule for the receptor, with some individual residues previously identified to be involved in ATP binding showing >1000-fold decrease in ATP potency when mutated (Ennion *et al.*, 2000). Further evidence that the effect is on conformation is that two of the mutations (regions A and B) have decreased potency compared to both the hP2X1 and rP2X4 receptors (figure 7.1b). If the effect were directly on gating or binding it would be likely that swapping residues between the two receptors would only introduce a phenotype that was either hP2X1 receptor or rP2X4 receptor like or was intermediate between the two. A gross structural change would be likely to greatly decrease agonist action.

These results show that ATP potency at the hP2X1 receptor can be easily decreased through mutation (table 7.1). It was for this reason that an EC<sub>90</sub> concentration of ATP was used in antagonism experiments at the mutated receptors as it standardised any change in antagonism that was due to altered ATP potency.

## **7.2 Regions of the Receptor Contributing to the Time-course of the ATP Evoked Response**

The chimeras have also given an overview of how the desensitization of the ATP evoked response is controlled at the receptor. Only four mutants had slowed desensitization, while ~ 50% of mutants showed a decrease in ATP potency, demonstrating that it was possible to decrease ATP potency without affecting desensitization (table 7.1). Two of the four original chimeras (X1-BX4 and X1-DX4) desensitized less than the hP2X1 receptor (figure 7.2). Chimera X1-BX4 became rP2X4 receptor-like in its desensitization, suggesting that residues in this region could contribute to the difference in time-course between the two receptors.

Only one point mutation affected the time-course and this was H220N, this was also the only point mutation which had an effect on receptor potency. All of the hP2X1 receptor based mutants which had an effect on time-course also decreased ATP potency, but five mutations affected potency but not time-course (table 7.1). It is hypothesized that mutations which affect potency but not time-course are causing a conformational change which decreases the affinity of ATP for the receptor, but once ATP binds there is no effect on gating (which is largely controlled by the transmembrane and intracellular domains). It is therefore likely that the change in conformation is subtle and mapping residues on the homology models has shown it is most likely to be located around the binding pocket.

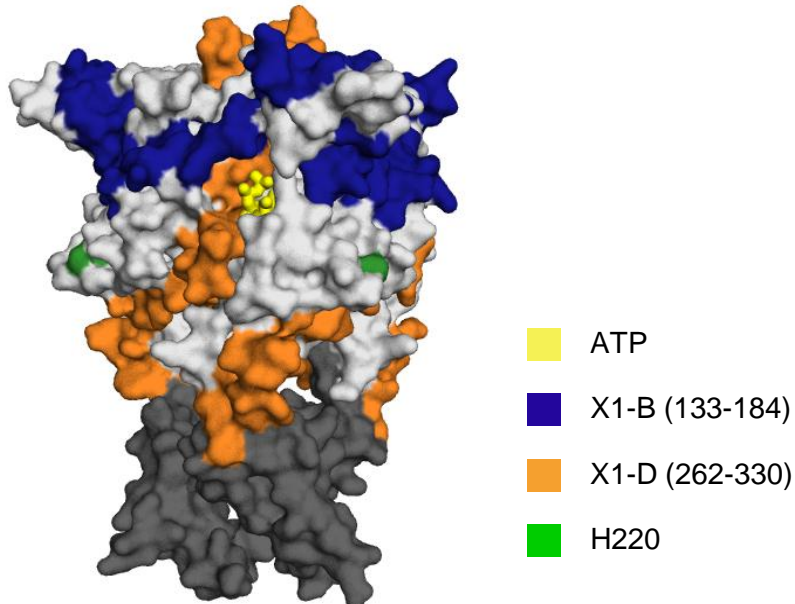
There is one example in this thesis of a mutation which affects the time-course, but not the potency of ATP, chimera X1-BX4(4+). The X1-BX4 chimera had rP2X4 receptor-like time-course and decreased ATP potency compared to the rP2X4 receptor. Introduction of the four charges to the mutant to make the X1-BX4(4+) chimera dramatically increased the amount of desensitization seen but had no effect on the ATP potency or peak amplitude compared to X1-BX4. This suggests that these residues may be involved in gating of the hP2X1 receptor. As the peak current was unaffected, the X1-BX4 and X1-BX4(4+) receptors are opening to the same extent, but the X1-BX4(4+) chimera is

Receptor	ATP Potency	Timecourse
rP2X4	↓	↓
X1-AX4	↓	-
X1-BX4	↓	↓
X1-CX4	-	-
X1-DX4	↓	↓
X1-C <sub>α</sub> X4	↓	-
X1-C <sub>β</sub> X4	↓	-
X1-C <sub>γ</sub> X4	-	-
X1-C <sub>δ</sub> X4	↓	-
X1-C <sub>ε</sub> X4	-	-
X1-C <sub>ζ</sub> X4	↓	-
T216S	-	-
L218I	-	-
H220N	↓	↓
H224D	-	-
V229I	-	-
Q231R	-	-

**Table 7.1 Table to show the difference in ATP potency and the time-course of the ATP evoked response between chimeric and point mutated receptors compared to the hP2X1 receptor.** Mutations which cause a decrease in ATP potency are shown by ↓ and highlighted in blue. Mutations which had no effect are highlighted in grey.

### Desensitisation of the ATP Evoked Response

(a)



(b)

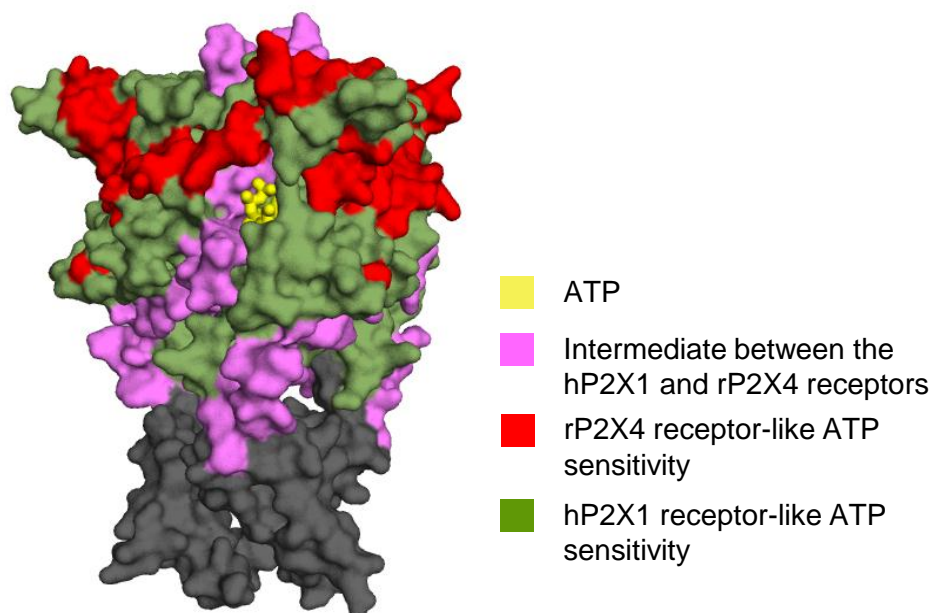


**Figure 7.2 Regions of the hP2X1 receptor identified as contributing to desensitisation** (a) Regions of the hP2X1 receptor which had an effect on desensitisation of the ATP evoked response when mutated to the equivalent rP2X4 receptor residue are shown in colour on a homology model of the ATP bound hP2X1 receptor. (b) Regions where mutation of the hP2X1 receptor to equivalent residues of the rP2X4 receptor had an effect on desensitisation have been grouped according to how great the effect was.

closing more rapidly. The four residues are located in the cysteine rich head region which is thought to move downwards upon ATP binding (Hattori & Gouaux, 2012; Roberts *et al.*, 2012). This movement could cause further conformational changes in the transmembrane domains of the receptor affecting channel gating and causing desensitization. The loss of these charges from the hP2X1 receptor as part of chimera X1-BX4 could have decreased or altered this movement, decreasing the desensitization. Reintroduction of the charges has then allowed this increased movement of the hP2X1 receptor head region to return. If the four positive charges are involved in movement of the head region, and this movement causes rapid desensitisation, then this could contribute to the difference in desensitisation seen between the WT hP2X1 and rP2X4 receptors as more movement has been reported in the head region of the hP2X1 receptor than was seen at the zfP2X4 receptor crystal structure (Lorinczi *et al.*, 2012) and the positive charges are absent in the rat and zebrafish P2X4 receptors. It was seen in this study that introducing the four charges to the rP2X4 receptor did not affect the time-course of the receptor and this was supported by the El Ajouz study which showed that introduction of the residues to the hP2X2 receptor also had no effect on time-course (El-Ajouz, 2011). This suggests that there are residues, likely to be negatively charged, in the hP2X1 receptor but not the hP2X2 or rP2X4 receptors which the four charges are interacting with to influence time-course. Figure 7.3a shows the presence of positive and negative charge around the KKRK residues.

In general the results of the chimeras on the effects of ATP show that it is easy to decrease opening at the receptor through mutation but harder to affect the desensitization.

### **7.3 The Effects of Suramin and PPADS Track Together at Mutated Receptors**

Suramin and PPADS sensitivity at the chimeras and point mutated receptors tracked together. If a receptor showed a decrease in suramin sensitivity compared to the hP2X1 or rP2X4 receptor, it also showed a decrease in PPADS sensitivity (Table 7.1 and 7.2). NF449 did not follow the same pattern, with similar effects to suramin and PPADS at one of the original

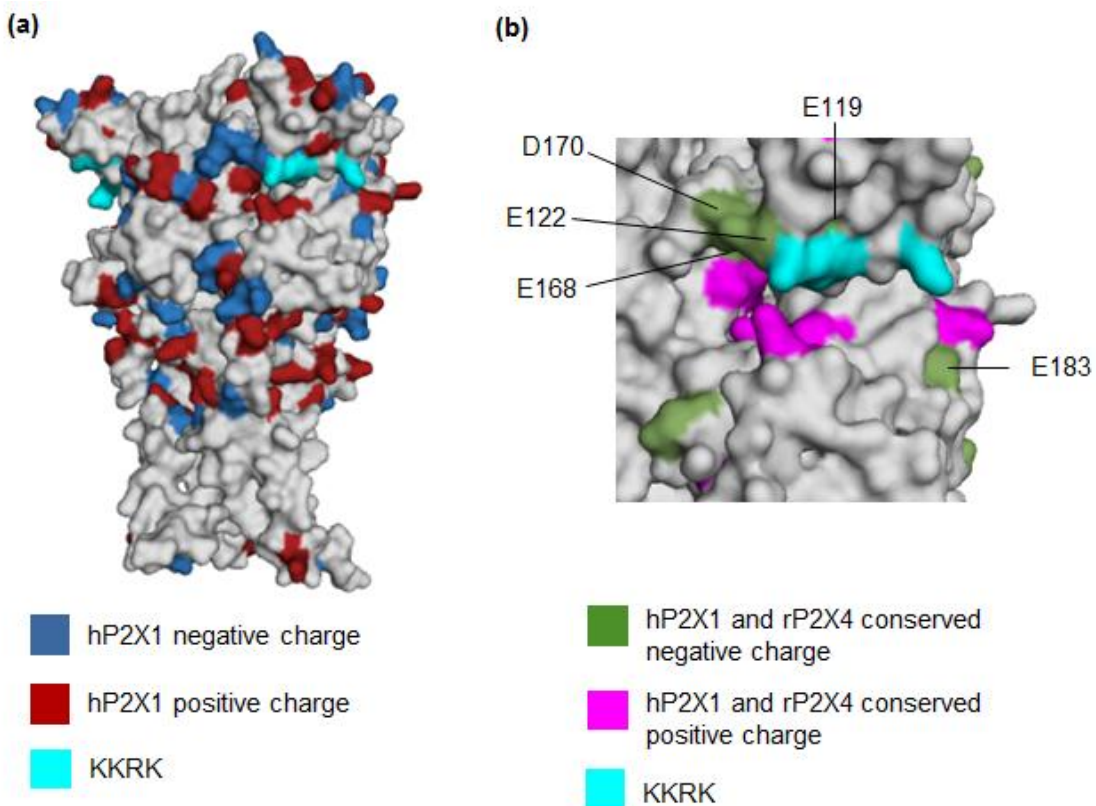


**Figure 7.3 Positive and negatively charged residues at the hP2X1 receptor.** **(a)** All charged residues of the hP2X1 receptor are highlighted in colour on the receptor homology model. **(b)** Close up of the region around the KKRK residues shows charged residues which are conserved between the hP2X1 and rP2X4 receptors.

chimeras but different effects at the other three. It might have been expected that if any two antagonists were going to track together that it would be suramin and NF449 as NF449 is a suramin derivative and in the previous chimeric study by El-Ajouz *et al* it was seen that these two antagonists did have similar effects at the chimeras (El-Ajouz *et al.*, 2012). 3D modelling of these molecules however shows that there is a significant difference between their structures and a difference in their action is therefore not unexpected.

A study on the effect of histidine residues of the rP2X4 receptor on antagonism has shown that a single mutation of H241 to an alanine could increase both suramin and PPADS sensitivity (Xiong *et al.*, 2004b). Other studies on antagonism have identified mutations which introduce either suramin or PPADS inhibition but have no effect on the other antagonist. For example the mutation E249K in the rP2X4 receptor could introduce PPADS but not suramin inhibition and the mutation Q78K at the same receptor had the opposite effect, introducing suramin but not PPADS inhibition (Buell *et al.*, 1996; Garcia-Guzman *et al.*, 1997). A chimera which introduced residues 81-183 of the hP2X4 receptor into the rP2X4 receptor was also shown to introduce PPADS but not suramin sensitivity (Garcia-Guzman *et al.*, 1997). This shows that separate residues are contributing to the action of each molecule.

It is unclear if suramin and PPADS share a binding site. Although NF449 is a suramin derivative the structures of the molecules are not particularly similar, with NF449 being larger and less linear. A previous study by El-Ajouz *et al* suggested that the two antagonists did share a binding site at the hP2X1 receptor (El-Ajouz *et al.*, 2012) however in this study chimeras which had an effect on NF449 action did not alter suramin inhibition. This may be because different P2X receptors were used in these two studies (P2X1 and P2X2 by El Ajouz and P2X1 and P2X4 in this thesis). It could also be explained by suramin and PPADS sharing part, but not all of a binding site, similar to what was described for ATP and NF449 in figure 5.13. This way some mutations could affect both suramin and NF449 whilst other mutations would affect only one of the antagonists.

Receptor	ATP potency	NF449 Inhibition	Suramin Inhibition	PPADS Inhibition
rP2X4	↓	↓	↓	↓
X1-AX4	↓	↓	↑	↑
X1-BX4	↓	↓	↓	↓
X1-CX4	-	↓	-	-
X1-DX4	↓	↓	↑	↑

**Table 7.2 Comparison of the Effects of ATP and Antagonists at Chimeras and the hP2X1 Receptor.** ↓ represents a decrease compared to the hP2X1 receptor and is highlighted in blue. ↑ represents an increase and is highlighted in red. Receptors which showed no difference are highlighted in grey.

Receptor	ATP potency	NF449 Inhibition	Suramin Inhibition	PPADS Inhibition
X4-BX1	-	-	↑	↑
rP2X4 (2+)	-	ND	↑	↑
rP2X4(4+)	-	-	↑	↑
zfP2X4 (FNDAR)	↓	ND	-	-
zfP2X4 (KNKAR)	↓	ND	↑	↑
zfP2X4 (KNKRR)	↓	ND	↑	↑

**Table 7.3 Comparison of the effects of ATP and antagonists at chimeras and the rP2X4 receptor.** ↓ represents a decrease compared to the rP2X4 receptor and is highlighted in blue. ↑ represents an increase and is highlighted in red. Receptors which showed no difference are highlighted in grey. ND = not determined.

The mutations by El-Ajouz *et al* had similar effects on suramin and NF449, with mutation of the KKRK residues to those of the hP2X2 receptor decreasing the inhibition by both antagonists. However mutation of the same residues to those of the rP2X4 receptor in this thesis only decreased NF449 inhibition. This could be because the chimeras and point mutations in these two studies were made between different receptors. In this thesis the residues KKRK of the hP2X1 receptor were mutated to SDTH and in the El Ajouz study were mutated to EDML. As the four charges are involved in the binding of NF449 to the hP2X1 receptor, the replacement of these residues with those of either hP2X2 or rP2X4 would cause a loss of antagonism by this molecule at the receptor. However I predict that the role of the residues in suramin sensitivity is through an effect on the conformation of the receptor, rather than the binding site of the suramin molecule. Therefore replacement of these residues with those of the hP2X2 receptor has caused a structural change at the hP2X1 receptor which prevents antagonist binding, however the replacement with those of the rP2X4 receptor has not induced this structural change.

#### **7.4. The Molecular Basis of Antagonism at the hP2X1 and rP2X4 Receptors**

As part of this thesis I have developed an NF449 bound model of the hP2X1 receptor, with seven residues predicted to be involved in the binding of this antagonist. The model is discussed in detail in chapter 5.3. I have also been able to introduce suramin and PPADS sensitivity to the rP2X4 receptor through introduction of four of the residues identified as contributing to NF449 action at the hP2X1 receptor (KKRK). NF449 sensitivity could not be introduced to the rP2X4 receptor through these mutations.

For an antagonist to bind, the receptor must have both the residues that the molecule binds to, and adopt a conformation that allows binding. The fact that the same mutation was able to introduce antagonism by two molecules with considerably different structures suggests that the mutated residues are involved in gating/conformation rather than binding and that the WT rP2X4 receptor contains residues necessary for suramin and PPADS binding, but

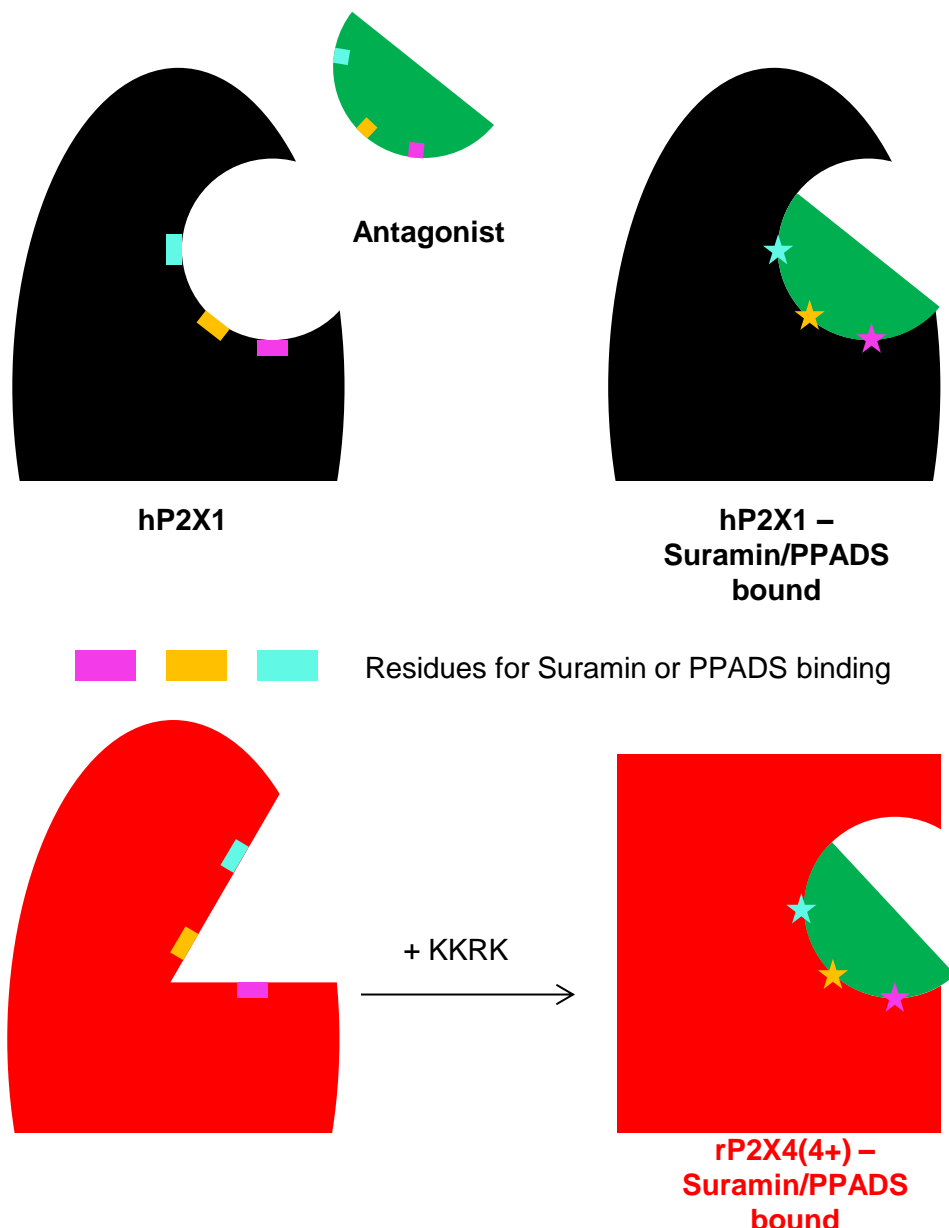


**Figure 7.4 Simple Cartoon Predicting the Molecular Basis of Suramin and PPADS Binding at the hP2X1 and rP2X4 Receptors.** It is predicted that the hP2X1 receptor has both the conformation and residues necessary for suramin and PPADS action. The antagonist does not fit tightly into the pocket but is able to bind, meaning that it is not particularly potent or selective between subunits. The rP2X4 receptor is predicted to have the residues necessary for these antagonists to bind but not have the conformation. Introduction of the residues KKRK allows the rP2X4 to adopt a conformation that allows these molecules to bind and antagonism therefore occurs. Stars represent interactions between the antagonist molecule and the receptor.

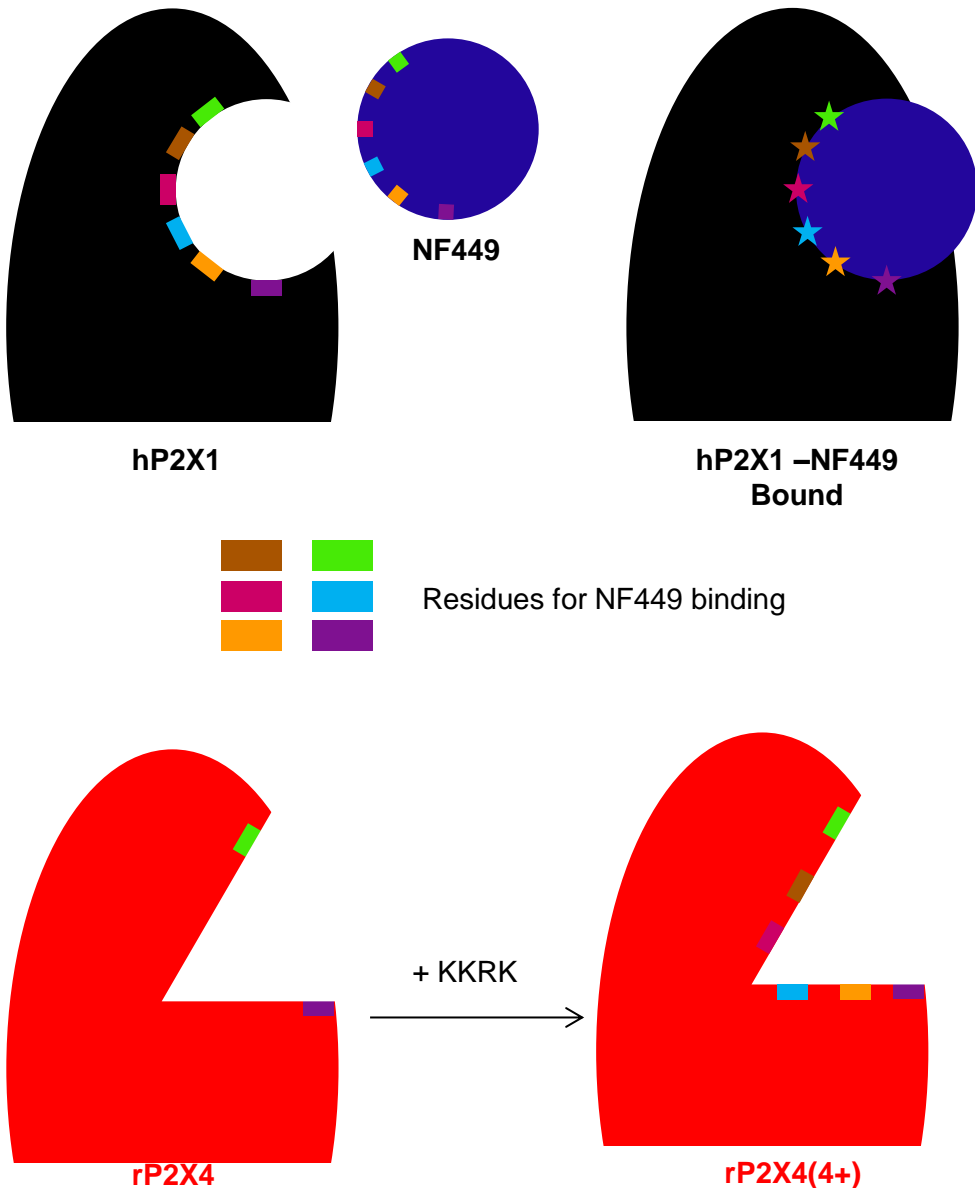


**Figure 7.5 Simple Cartoon Predicting the Molecular Basis of NF449 Binding at the hP2X1 and rP2X4 Receptors.** It is predicted that the hP2X1 receptor has both the conformation and residues necessary for NF449 action. The antagonist fits tightly into the binding site, giving high potency and selectivity. In contrast the rP2X4 receptor has neither the binding site nor the conformation. Therefore introducing residues necessary for binding (KKRK) cannot introduce NF449 action to the rP2X4 receptor as the necessary conformation for antagonist binding cannot be adopted. Stars represent interactions between the antagonist molecule and the receptor.

adopts a conformation that the antagonist cannot bind to (figure 7.4). The introduction of the four positive charges then allows the receptor to adopt a conformation at which suramin and PPADS can bind/stabilise the receptor in this antagonist sensitive conformation. This would explain why suramin and PPADS inhibition could not be removed at the hP2X1 receptor through chimera generation. If the WT rP2X4 receptor contains the majority of residues necessary for suramin and PPADS binding then as the hP2X1 receptor is inhibited by these molecules, it is likely that these residues were among those conserved between the two receptors and therefore swapping residues would have no effect on the binding of these molecules. Instead, the conformation of the hP2X1 receptor would need to be changed to mimic that of the rP2X4 receptor if suramin and PPADS antagonism were to be decreased. The structure of a receptor is something that the whole subunit contributes too, with a change in the extracellular loop likely to link to changes in the transmembrane domains and intracellular termini and vice versa. It would therefore be very difficult to cause the structure of the hP2X4 receptor to mimic that of the rP2X4 receptor through mutation of part of the receptor only (i.e. a chimera). Swapping the whole loop of the receptor with that of the hP2X2 receptor in chapter 3 did reduce suramin and PPADS antagonism at the molecule as this very large swap could have introduced a conformational change that mimicked the hP2X2 receptor. Despite this, introduction of four residues appears to have caused a conformational change at the rP2X4 receptor that allows antagonist binding. It is likely that these mutations have not caused the receptor structure to completely mimic that of the hP2X1 receptor, but rather have allowed the cysteine rich head region, around which several residues predicted to be involved in suramin and PPADS binding are located, to adopt a conformation at which the antagonists can bind (figure 7.4). These four residues cannot be responsible for the selectivity of suramin and PPADS as they are not present in other receptor subtypes which are inhibited by these antagonists. It is likely that residues are conserved between the hP2X1 and rP2X4 receptors that interact with the four residues to effect conformation. As the residues are positively charged, the interacting residues are likely to be negative. Negatively charged residues around the cysteine rich head region are shown in figure 7.3. Further

mutations could be performed to remove these charges from the hP2X1 receptor to see if antagonism is affected.

The residues that were responsible for the loss of NF449 sensitivity at the hP2X1 receptor when mutated to the equivalent residues of the rP2X4 receptor, were located in close proximity to each other, despite being contained in different original regions (B and C). This suggests that they form part of a binding site for NF449, and that the rP2X4 receptor is NF449 insensitive as it does not contain these residues necessary for NF449 binding. As introduction of these residues to the rP2X4 receptor could not introduce NF449 sensitivity, it is likely that as well as lacking these residues necessary for NF449 action, the receptor also adopts a conformation at which NF449 cannot bind (figure 7.5).

These findings could give insight into the differences in selectivity for the antagonists between P2X receptor subtypes. If most or all P2X receptor subtypes contain the residues necessary for suramin and PPADS binding, but conformation prevents the antagonism, then this could explain why these antagonists are less sensitive. In contrast the residues necessary for NF449 binding appear to be unique to the hP2X1 receptor, increasing selectivity at this receptor.

I have therefore shown that four residues located in the base of the cysteine rich head region of the hP2X1 receptor contribute to the suramin, PPADS and NF449 sensitivity of the receptor in different ways. For suramin and PPADS these residues are involved in allowing the antagonist molecule to stabilise the receptor in a conformation which prevents agonist action. However the residues are also part of the NF449 binding site at the receptor. In future studies the model of NF449 binding at the hP2X1 receptor will be refined through cysteine mutagenesis (see section 5.3.5). Protein purification of the zfP2X4C(KNKRR) receptor will also be optimised with the hope of entering the receptor into trials to generate suramin and PPADS bound crystal structures.

Future studies would further refine the NF449 binding models by using cysteine mutagenesis and negatively charged MTS reagents to assess the

distance of residues form the bound NF449 molecule. This should allow the four models to be distinguished between and the most likely pose identified. The purification of the zfP2X4C(KNKRR) receptor would continue to be optimised in order for crystal trials to begin to attempt to crystallise the receptor in an antagonist bound state.

The overall results of this thesis have shown a new, more detailed model of NF449 binding at the P2X1 receptor, and demonstrated that antagonism can be induced at the rP2X4 receptor. Insight has also been gained into why the rP2X4 receptor is antagonist insensitive with results suggesting that this is due to the conformation of the WT receptor. The findings will hopefully be used to develop an antagonist bound crystal structure of the rP2X4 receptor. To conclude, this study has furthered the understanding of both high potency antagonism at the hP2X1 receptor and the antagonist insensitivity of the rP2X4 receptor.

## References

- Abberley, L., Bebius, A., Beswick, P.J., Billinton, A., Collis, K.L., Dean, D.K., Fonfria, E., Gleave, R.J., Medhurst, S.J., Michel, A.D., Moses, A.P., Patel, S., Roman, S.A., Scoccitti, T., Smith, B., Steadman, J.G., Walter, D.S., 2010. Identification of 2-oxo-N-(phenylmethyl)-4-imidazolidinecarboxamide antagonists of the P2X(7) receptor. *Bioorganic & Medicinal Chemistry Letters*. **20**, 6370-6374.
- Abdi, M.H., Beswick, P.J., Billinton, A., Chambers, L.J., Charlton, A., Collins, S.D., Collis, K.L., Dean, D.K., Fonfria, E., Gleave, R.J., Lejeune, C.L., Livermore, D.G., Medhurst, S.J., Michel, A.D., Moses, A.P., Page, L., Patel, S., Roman, S.A., Senger, S., Slingsby, B., Steadman, J.G., Stevens, A.J., Walter, D.S., 2010. Discovery and structure-activity relationships of a series of pyroglutamic acid amide antagonists of the P2X7 receptor. *Bioorganic & Medicinal Chemistry Letters*. **20**, 5080-5084.
- Ali, Z., Laurijssens, B., Ostenfeld, T., McHugh, S., Stylianou, A., Scott-Stevens, P., Hosking, L., Dewit, O., Richardson, J.C., Chen, C., 2013. Pharmacokinetic and pharmacodynamic profiling of a P2X7 receptor allosteric modulator GSK1482160 in healthy human subjects. *British Journal of Clinical Pharmacology*. **75**, 197-207.
- Allen, S.J., Ribeiro, S., Horuk, R., Handel, T.M., 2009. Expression, purification and in vitro functional reconstitution of the chemokine receptor CCR1. *Protein Expression and Purification*. **66**, 73-81.
- Allsopp, R.C., El Ajouz, S., Schmid, R., Evans, R.J., 2011. Cysteine scanning mutagenesis (residues Glu52-Gly96) of the human P2X1 receptor for ATP: mapping agonist binding and channel gating. *The Journal of Biological Chemistry*. **286**, 29207-29217.
- Allsopp, R.C. & Evans, R.J., 2011. The intracellular amino terminus plays a dominant role in desensitization of ATP-gated P2X receptor ion channels. *The Journal of Biological Chemistry*. **286**, 44691-44701.
- Allsopp, R.C., Farmer, L.K., Fryatt, A.G., Evans, R.J., 2013. P2X receptor chimeras highlight roles of the amino terminus to partial agonist efficacy, the carboxyl terminus to recovery from desensitization, and independent regulation of channel transitions. *The Journal of Biological Chemistry*. **288**, 21412-21421.
- Anderson, C.M. & Nedergaard, M., 2006. Emerging challenges of assigning P2X7 receptor function and immunoreactivity in neurons. *Trends in Neurosciences*. **29**, 257-262.
- Antonio, L.S., Stewart, A.P., Xu, X.J., Varanda, W.A., Murrell-Lagnado, R.D., Edwardson, J.M., 2011. P2X4 receptors interact with both P2X2 and P2X7 receptors in the form of homotrimers. *British Journal of Pharmacology*. **163**, 1069-1077.
- Asatryan, L., Popova, M., Perkins, D., Trudell, J.R., Alkana, R.L., Davies, D.L., 2010. Ivermectin antagonizes ethanol inhibition in purinergic P2X4 receptors. *The Journal of Pharmacology and Experimental Therapeutics*. **334**, 720-728.

Aschrafi, A., Sadtler, S., Niculescu, C., Rettinger, J., Schmalzing, G., 2004. Trimeric architecture of homomeric P2X2 and heteromeric P2X1+2 receptor subtypes. *Journal of Molecular Biology*. **342**, 333-343.

Balazs, B., Danko, T., Kovacs, G., Koles, L., Hediger, M.A., Zsembery, A., 2013. Investigation of the inhibitory effects of the benzodiazepine derivative, 5-BDBD on P2X4 purinergic receptors by two complementary methods. *Cellular Physiology and Biochemistry : International Journal of Experimental Cellular Physiology, Biochemistry, and Pharmacology*. **32**, 11-24.

Ballini, E., Virginio, C., Medhurst, S.J., Summerfield, S.G., Aldegheri, L., Buson, A., Carignani, C., Chen, Y.H., Giacometti, A., Lago, I., Powell, A.J., Jarolimek, W., 2011. Characterization of three diaminopyrimidines as potent and selective antagonists of P2X3 and P2X2/3 receptors with in vivo efficacy in a pain model. *British Journal of Pharmacology*. **163**, 1315-1325.

Banfi, C., Ferrario, S., De Vincenti, O., Ceruti, S., Fumagalli, M., Mazzola, A., D'Ambrosi, N., Volonte, C., Fratto, P., Vitali, E., Burnstock, G., Beltrami, E., Parolari, A., Polvani, G., Biglioli, P., Tremoli, E., Abbracchio, M.P., 2005. P2 receptors in human heart: upregulation of P2X6 in patients undergoing heart transplantation, interaction with TNFalpha and potential role in myocardial cell death. *Journal of Molecular and Cellular Cardiology*. **39**, 929-939.

Barrera, N.P., Ormond, S.J., Henderson, R.M., Murrell-Lagnado, R.D., Edwardson, J.M., 2005. Atomic force microscopy imaging demonstrates that P2X2 receptors are trimers but that P2X6 receptor subunits do not oligomerize. *The Journal of Biological Chemistry*. **280**, 10759-10765.

Bean, B.P., Williams, C.A., Ceelen, P.W., 1990. ATP-activated channels in rat and bullfrog sensory neurons: current-voltage relation and single-channel behavior. *The Journal of Neuroscience : The Official Journal of the Society for Neuroscience*. **10**, 11-19.

Beani, L., Bianchi, C., Crema, A., 1971. Vagal non-adrenergic inhibition of guinea-pig stomach. *The Journal of Physiology*. **217**, 259-279.

Beggs, S. & Salter, M.W., 2010. Microglia-neuronal signalling in neuropathic pain hypersensitivity 2.0. *Current Opinion in Neurobiology*. **20**, 474-480.

Bennett, A. & Fleshler, B., 1969. A hyoscine-resistant excitatory nerve pathway in guinea-pig colon. *The Journal of Physiology*. **203**, 62P-63P.

Ben-Selma, W., Ben-Kahla, I., Boukadida, J., Harizi, H., 2011. Contribution of the P2X7 1513A/C loss-of-function polymorphism to extrapulmonary tuberculosis susceptibility in Tunisian populations. *FEMS Immunology and Medical Microbiology*. **63**, 65-72.

Bhattacharya, A., Wang, Q., Ao, H., Shoblock, J.R., Lord, B., Aluisio, L., Fraser, I., Nepomuceno, D., Neff, R.A., Welty, N., Lovenberg, T.W., Bonaventure, P., Wickenden, A.D., Letavic, M.A., 2013. Pharmacological characterization of a novel centrally permeable P2X7 receptor antagonist: JNJ-47965567. *British Journal of Pharmacology*. **170**, 624-640.

Bian, X., Ren, J., DeVries, M., Schnegelsberg, B., Cockayne, D.A., Ford, A.P., Galligan, J.J., 2003. Peristalsis is impaired in the small intestine of mice lacking the P2X3 subunit. *The Journal of Physiology*. **551**, 309-322.

Blanchard, D.K., Wei, S., Duan, C., Pericle, F., Diaz, J.I., Djeu, J.Y., 1995. Role of extracellular adenosine triphosphate in the cytotoxic T-lymphocyte-mediated lysis of antigen presenting cells. *Blood*. **85**, 3173-3182.

Bo, X., Zhang, Y., Nassar, M., Burnstock, G., Schoepfer, R., 1995. A P2X purinoceptor cDNA conferring a novel pharmacological profile. *FEBS Letters*. **375**, 129-133.

Boue-Grabot, E., Archambault, V., Seguela, P., 2000. A protein kinase C site highly conserved in P2X subunits controls the desensitization kinetics of P2X(2) ATP-gated channels. *The Journal of Biological Chemistry*. **275**, 10190-10195.

Boumechache, M., Masin, M., Edwardson, J.M., Gorecki, D.C., Murrell-Lagnado, R., 2009. Analysis of assembly and trafficking of native P2X4 and P2X7 receptor complexes in rodent immune cells. *The Journal of Biological Chemistry*. **284**, 13446-13454.

Bradley, H.J., Baldwin, J.M., Goli, G.R., Johnson, B., Zou, J., Sivaprasadarao, A., Baldwin, S.A., Jiang, L.H., 2011. Residues 155 and 348 contribute to the determination of P2X7 receptor function via distinct mechanisms revealed by single-nucleotide polymorphisms. *The Journal of Biological Chemistry*. **286**, 8176-8187.

Brake, A.J., Wagenbach, M.J., Julius, D., 1994. New structural motif for ligand-gated ion channels defined by an ionotropic ATP receptor. *Nature*. **371**, 519-523.

Brandle, U., Spielmanns, P., Osteroth, R., Sim, J., Surprenant, A., Buell, G., Ruppersberg, J.P., Plinkert, P.K., Zenner, H.P., Glowatzki, E., 1997. Desensitization of the P2X(2) receptor controlled by alternative splicing. *FEBS Letters*. **404**, 294-298.

Braun, K., Rettinger, J., Ganso, M., Kassack, M., Hildebrandt, C., Ullmann, H., Nickel, P., Schmalzing, G., Lambrecht, G., 2001. NF449: a subnanomolar potency antagonist at recombinant rat P2X1 receptors. *Naunyn-Schmiedeberg's Archives of Pharmacology*. **364**, 285-290.

Broom, D.C., Matson, D.J., Bradshaw, E., Buck, M.E., Meade, R., Coombs, S., Matchett, M., Ford, K.K., Yu, W., Yuan, J., Sun, S.H., Ochoa, R., Krause, J.E., Wustrow, D.J., Cortright, D.N., 2008. Characterization of N-(adamantan-1-ylmethyl)-5-[(3R-amino-pyrrolidin-1-yl)methyl]-2-chloro-benzamide, a P2X7 antagonist in animal models of pain and inflammation. *The Journal of Pharmacology and Experimental Therapeutics*. **327**, 620-633.

Brotherton-Pleiss, C.E., Dillon, M.P., Ford, A.P., Gever, J.R., Carter, D.S., Gleason, S.K., Lin, C.J., Moore, A.G., Thompson, A.W., Villa, M., Zhai, Y., 2010. Discovery and optimization of RO-85, a novel drug-like, potent, and selective P2X3 receptor antagonist. *Bioorganic & Medicinal Chemistry Letters*. **20**, 1031-1036.

Brown, S.G., Townsend-Nicholson, A., Jacobson, K.A., Burnstock, G., King, B.F., 2002. Heteromultimeric P2X(1/2) receptors show a novel sensitivity to extracellular pH. *The Journal of Pharmacology and Experimental Therapeutics*. **300**, 673-680.

Browne, L.E., Nunes, J.P., Sim, J.A., Chudasama, V., Bragg, L., Caddick, S., Alan North, R., 2014. Optical control of trimeric P2X receptors and acid-sensing ion channels. *Proceedings of the National Academy of Sciences of the United States of America*. **111**, 521-526.

Buckingham, S.D., Pym, L., Sattelle, D.B., 2006. Oocytes as an expression system for studying receptor/channel targets of drugs and pesticides. *Methods in Molecular Biology (Clifton, N.J.)*. **322**, 331-345.

Buell, G., Lewis, C., Collo, G., North, R.A., Surprenant, A., 1996. An antagonist-insensitive P2X receptor expressed in epithelia and brain. *The EMBO Journal*. **15**, 55-62.

Bulanova, E. & Bulfone-Paus, S., 2010. P2 receptor-mediated signaling in mast cell biology. *Purinergic Signalling*. **6**, 3-17.

Bultmann, R., Wittenburg, H., Pause, B., Kurz, G., Nickel, P., Starke, K., 1996. P2-purinoceptor antagonists: III. Blockade of P2-purinoceptor subtypes and ecto-nucleotidases by compounds related to suramin. *Naunyn-Schmiedeberg's Archives of Pharmacology*. **354**, 498-504.

Burgard, E.C., Niforatos, W., van Biesen, T., Lynch, K.J., Touma, E., Metzger, R.E., Kowaluk, E.A., Jarvis, M.F., 1999. P2X receptor-mediated ionic currents in dorsal root ganglion neurons. *Journal of Neurophysiology*. **82**, 1590-1598.

Burnstock, G., 2013. Introduction and perspective, historical note. *Frontiers in Cellular Neuroscience*. **7**, 227.

Burnstock, G., 2009. Purinergic cotransmission. *F1000 Biology Reports*. **1**, 46-46.

Burnstock, G., 2004. Introduction: P2 receptors. *Current Topics in Medicinal Chemistry*. **4**, 793-803.

Burnstock, G., 1976. Do some nerve cells release more than one transmitter? *Neuroscience*. **1**, 239-248.

Burnstock, G., 1972. Purinergic nerves. *Pharmacological Reviews*. **24**, 509-581.

BURNSTOCK, G., CAMPBELL, G., BENNETT, M., HOLMAN, M.E., 1964. Innervation of the Guinea-Pig Taenia Coli: are there Intrinsic Inhibitory Nerves which are Distinct from Sympathetic Nerves? *International Journal of Neuropharmacology*. **3**, 163-166.

BURNSTOCK, G., CAMPBELL, G., BENNETT, M., HOLMAN, M.E., 1963. Inhibition of the Smooth Muscle on the Taenia Coli. *Nature*. **200**, 581-582.

Burnstock, G., Campbell, G., Satchell, D., Smythe, A., 1970. Evidence that adenosine triphosphate or a related nucleotide is the transmitter substance

released by non-adrenergic inhibitory nerves in the gut. *British Journal of Pharmacology*. **40**, 668-688.

Burnstock, G., Cocks, T., Crowe, R., Kasakov, L., 1978. Purinergic innervation of the guinea-pig urinary bladder. *British Journal of Pharmacology*. **63**, 125-138.

Burnstock, G. & Kennedy, C., 1985. Is there a basis for distinguishing two types of P2-purinoceptor? *General Pharmacology*. **16**, 433-440.

Burnstock, G. & Knight, G.E., 2004. Cellular distribution and functions of P2 receptor subtypes in different systems. *International Review of Cytology*. **240**, 31-304.

Calvert, J.A. & Evans, R.J., 2004. Heterogeneity of P2X receptors in sympathetic neurons: contribution of neuronal P2X1 receptors revealed using knockout mice. *Molecular Pharmacology*. **65**, 139-148.

Calvert, R.C., Shabbir, M., Thompson, C.S., Mikhailidis, D.P., Morgan, R.J., Burnstock, G., 2004. Immunocytochemical and pharmacological characterisation of P2-purinoceptor-mediated cell growth and death in PC-3 hormone refractory prostate cancer cells. *Anticancer Research*. **24**, 2853-2859.

Cao, L., Young, M.T., Broomhead, H.E., Fountain, S.J., North, R.A., 2007. Thr339-to-serine substitution in rat P2X2 receptor second transmembrane domain causes constitutive opening and indicates a gating role for Lys308. *The Journal of Neuroscience : The Official Journal of the Society for Neuroscience*. **27**, 12916-12923.

Carmo, M.R., Menezes, A.P., Nunes, A.C., Pliassova, A., Rolo, A.P., Palmeira, C.M., Cunha, R.A., Canas, P.M., Andrade, G.M., 2014. The P2X7 receptor antagonist Brilliant Blue G attenuates contralateral rotations in a rat model of Parkinsonism through a combined control of synaptotoxicity, neurotoxicity and gliosis. *Neuropharmacology*.

Casas-Pruneda, G., Reyes, J.P., Perez-Flores, G., Perez-Cornejo, P., Arreola, J., 2009. Functional interactions between P2X4 and P2X7 receptors from mouse salivary epithelia. *The Journal of Physiology*. **587**, 2887-2901.

Cavaliere, F., Amadio, S., Dinkel, K., Reymann, K.G., Volonte, C., 2007. P2 receptor antagonist trinitrophenyl-adenosine-triphosphate protects hippocampus from oxygen and glucose deprivation cell death. *The Journal of Pharmacology and Experimental Therapeutics*. **323**, 70-77.

Chambers, L.J., Stevens, A.J., Moses, A.P., Michel, A.D., Walter, D.S., Davies, D.J., Livermore, D.G., Fonfria, E., Demont, E.H., Vimal, M., Theobald, P.J., Beswick, P.J., Gleave, R.J., Roman, S.A., Senger, S., 2010. Synthesis and structure-activity relationships of a series of (1H-pyrazol-4-yl)acetamide antagonists of the P2X7 receptor. *Bioorganic & Medicinal Chemistry Letters*. **20**, 3161-3164.

Chaumont, S., Jiang, L.H., Penna, A., North, R.A., Rassendren, F., 2004. Identification of a trafficking motif involved in the stabilization and polarization of P2X receptors. *The Journal of Biological Chemistry*. **279**, 29628-29638.

Cheewatrakoolpong, B., Gilchrest, H., Anthes, J.C., Greenfeder, S., 2005. Identification and characterization of splice variants of the human P2X7 ATP channel. *Biochemical and Biophysical Research Communications*. **332**, 17-27.

Chen, B.C., Lee, C.M., Lin, W.W., 1996. Inhibition of ecto-ATPase by PPADS, suramin and reactive blue in endothelial cells, C6 glioma cells and RAW 264.7 macrophages. *British Journal of Pharmacology*. **119**, 1628-1634.

Chen, C.C., Akopian, A.N., Sivilotti, L., Colquhoun, D., Burnstock, G., Wood, J.N., 1995. A P2X purinoceptor expressed by a subset of sensory neurons. *Nature*. **377**, 428-431.

Chen, L. & Brosnan, C.F., 2006. Exacerbation of experimental autoimmune encephalomyelitis in P2X7R-/- mice: evidence for loss of apoptotic activity in lymphocytes. *Journal of Immunology (Baltimore, Md.: 1950)*. **176**, 3115-3126.

Chen, X., Pierce, B., Naing, W., Grapperhaus, M.L., Phillion, D.P., 2010. Discovery of 2-chloro-N-((4,4-difluoro-1-hydroxycyclohexyl)methyl)-5-(5-fluoropyrimidin-2-yl)b enzamide as a potent and CNS penetrable P2X7 receptor antagonist. *Bioorganic & Medicinal Chemistry Letters*. **20**, 3107-3111.

Cheson, B.D., Levine, A.M., Mildvan, D., Kaplan, L.D., Wolfe, P., Rios, A., Groopman, J.E., Gill, P., Volberding, P.A., Poiesz, B.J., 1987. Suramin therapy in AIDS and related disorders. Report of the US Suramin Working Group. *JAMA : The Journal of the American Medical Association*. **258**, 1347-1351.

Chessell, I.P., Hatcher, J.P., Bountra, C., Michel, A.D., Hughes, J.P., Green, P., Egerton, J., Murfin, M., Richardson, J., Peck, W.L., Grahames, C.B., Casula, M.A., Yianguo, Y., Birch, R., Anand, P., Buell, G.N., 2005. Disruption of the P2X7 purinoceptor gene abolishes chronic inflammatory and neuropathic pain. *Pain*. **114**, 386-396.

Clyne, J.D., Wang, L.F., Hume, R.I., 2002. Mutational analysis of the conserved cysteines of the rat P2X2 purinoceptor. *The Journal of Neuroscience : The Official Journal of the Society for Neuroscience*. **22**, 3873-3880.

Cockayne, D.A., Dunn, P.M., Zhong, Y., Rong, W., Hamilton, S.G., Knight, G.E., Ruan, H.Z., Ma, B., Yip, P., Nunn, P., McMahon, S.B., Burnstock, G., Ford, A.P., 2005. P2X2 knockout mice and P2X2/P2X3 double knockout mice reveal a role for the P2X2 receptor subunit in mediating multiple sensory effects of ATP. *The Journal of Physiology*. **567**, 621-639.

Cockayne, D.A., Hamilton, S.G., Zhu, Q.M., Dunn, P.M., Zhong, Y., Novakovic, S., Malmberg, A.B., Cain, G., Berson, A., Kassotakis, L., Hedley, L., Lachnit, W.G., Burnstock, G., McMahon, S.B., Ford, A.P., 2000. Urinary bladder hyporeflexia and reduced pain-related behaviour in P2X3-deficient mice. *Nature*. **407**, 1011-1015.

Collo, G., Neidhart, S., Kawashima, E., Kosco-Vilbois, M., North, R.A., Buell, G., 1997. Tissue distribution of the P2X7 receptor. *Neuropharmacology*. **36**, 1277-1283.

Collo, G., North, R.A., Kawashima, E., Merlo-Pich, E., Neidhart, S., Surprenant, A., Buell, G., 1996. Cloning OF P2X5 and P2X6 receptors and the distribution and properties of an extended family of ATP-gated ion channels. *The Journal of Neuroscience : The Official Journal of the Society for Neuroscience*. **16**, 2495-2507.

Compan, V., Ullmann, L., Stel'mashenko, O., Chemin, J., Chaumont, S., Rassendren, F., 2012. P2X2 and P2X5 subunits define a new heteromeric receptor with P2X7-like properties. *The Journal of Neuroscience : The Official Journal of the Society for Neuroscience*. **32**, 4284-4296.

Connolly, G.P., 1995. Differentiation by pyridoxal 5-phosphate, PPADS and IsoPPADS between responses mediated by UTP and those evoked by alpha, beta-methylene-ATP on rat sympathetic ganglia. *British Journal of Pharmacology*. **114**, 727-731.

Cook, S.P., Vulchanova, L., Hargreaves, K.M., Elde, R., McCleskey, E.W., 1997. Distinct ATP receptors on pain-sensing and stretch-sensing neurons. *Nature*. **387**, 505-508.

Coutinho-Silva, R. & Persechini, P.M., 1997. P2Z purinoceptor-associated pores induced by extracellular ATP in macrophages and J774 cells. *The American Journal of Physiology*. **273**, C1793-800.

Craigie, E., Birch, R.E., Unwin, R.J., Wildman, S.S., 2013. The relationship between P2X4 and P2X7: a physiologically important interaction? *Frontiers in Physiology*. **4**, 216.

Damer, S., Niebel, B., Czeche, S., Nickel, P., Ardanuy, U., Schmalzing, G., Rettinger, J., Mutschler, E., Lambrecht, G., 1998. NF279: a novel potent and selective antagonist of P2X receptor-mediated responses. *European Journal of Pharmacology*. **350**, R5-6.

Dao-Ung, L.P., Fuller, S.J., Sluyter, R., SkarRatt, K.K., Thunberg, U., Tobin, G., Byth, K., Ban, M., Rosenquist, R., Stewart, G.J., Wiley, J.S., 2004. Association of the 1513C polymorphism in the P2X7 gene with familial forms of chronic lymphocytic leukaemia. *British Journal of Haematology*. **125**, 815-817.

De Clercq, E., 1979. Suramin: a potent inhibitor of the reverse transcriptase of RNA tumor viruses. *Cancer Letters*. **8**, 9-22.

Deuchars, S.A., Atkinson, L., Brooke, R.E., Musa, H., Milligan, C.J., Batten, T.F., Buckley, N.J., Parson, S.H., Deuchars, J., 2001. Neuronal P2X7 receptors are targeted to presynaptic terminals in the central and peripheral nervous systems. *The Journal of Neuroscience : The Official Journal of the Society for Neuroscience*. **21**, 7143-7152.

Devries, M.P., Vessalo, M., Galligan, J.J., 2010. Deletion of P2X2 and P2X3 receptor subunits does not alter motility of the mouse colon. *Frontiers in Neuroscience*. **4**, 22.

Di Virgilio, F., Pizzo, P., Zanovello, P., Bronte, V., Collavo, D., 1990. Extracellular ATP as a possible mediator of cell-mediated cytotoxicity. *Immunology Today*. **11**, 274-277.

Diaz-Hernandez, M., Diez-Zaera, M., Sanchez-Nogueiro, J., Gomez-Villafuertes, R., Canals, J.M., Alberch, J., Miras-Portugal, M.T., Lucas, J.J., 2009. Altered P2X7-receptor level and function in mouse models of Huntington's disease and therapeutic efficacy of antagonist administration. *FASEB Journal : Official Publication of the Federation of American Societies for Experimental Biology*. **23**, 1893-1906.

Donnelly-Roberts, D.L., Namovic, M.T., Surber, B., Vaidyanathan, S.X., Perez-Medrano, A., Wang, Y., Carroll, W.A., Jarvis, M.F., 2009.  $[^3\text{H}]$ 2-cyano-1-[(1S)-1-phenylethyl]-3-quinolin-5-ylguanidine) is a novel, potent, and selective antagonist radioligand for P2X7 receptors. *Neuropharmacology*. **56**, 223-229.

Drury, A.N. & Szent-Gyorgyi, A., 1929. The physiological activity of adenine compounds with especial reference to their action upon the mammalian heart. *The Journal of Physiology*. **68**, 213-237.

Dunn, P.M. & Blakeley, A.G., 1988. Suramin: a reversible P2-purinoceptor antagonist in the mouse vas deferens. *British Journal of Pharmacology*. **93**, 243-245.

Duplantier, A.J., Dombroski, M.A., Subramanyam, C., Beaulieu, A.M., Chang, S.P., Gabel, C.A., Jordan, C., Kalgutkar, A.S., Kraus, K.G., Labasi, J.M., Mussari, C., Perregaux, D.G., Shepard, R., Taylor, T.J., Trevena, K.A., Whitney-Pickett, C., Yoon, K., 2011. Optimization of the physicochemical and pharmacokinetic attributes in a 6-azauracil series of P2X7 receptor antagonists leading to the discovery of the clinical candidate CE-224,535. *Bioorganic & Medicinal Chemistry Letters*. **21**, 3708-3711.

Ehre, C., Ridley, C., Thornton, D.J., 2014. Cystic fibrosis: An inherited disease affecting mucin-producing organs. *The International Journal of Biochemistry & Cell Biology*.

El-Ajouz, S., 2011. *Molecular basis of antagonist action at the P2X1 receptor*. Ph. D. University of Leicester.

El-Ajouz, S., Ray, D., Allsopp, R.C., Evans, R.J., 2012. Molecular basis of selective antagonism of the P2X1 receptor for ATP by NF449 and suramin: contribution of basic amino acids in the cysteine-rich loop. *British Journal of Pharmacology*. **165**, 390-400.

Elliott, J.I. & Higgins, C.F., 2004. Major histocompatibility complex class I shedding and programmed cell death stimulated through the proinflammatory P2X7 receptor: a candidate susceptibility gene for NOD diabetes. *Diabetes*. **53**, 2012-2017.

Ennion, S., Hagan, S., Evans, R.J., 2000. The role of positively charged amino acids in ATP recognition by human P2X1 receptors. *The Journal of Biological Chemistry*. **275**, 35656.

Ennion, S.J. & Evans, R.J., 2002a. Conserved cysteine residues in the extracellular loop of the human P2X(1) receptor form disulfide bonds and are involved in receptor trafficking to the cell surface. *Molecular Pharmacology*. **61**, 303-311.

Ennion, S.J. & Evans, R.J., 2002b. P2X(1) receptor subunit contribution to gating revealed by a dominant negative PKC mutant. *Biochemical and Biophysical Research Communications*. **291**, 611-616.

Erlinge, D., 2011. P2Y receptors in health and disease. *Advances in Pharmacology (San Diego, Calif.)*. **61**, 417-439.

Evans, R.J., Lewis, C., Buell, G., Valera, S., North, R.A., Surprenant, A., 1995. Pharmacological characterization of heterologously expressed ATP-gated cation channels (P2x purinoceptors). *Molecular Pharmacology*. **48**, 178-183.

Evans, R.J., Lewis, C., Virginio, C., Lundstrom, K., Buell, G., Surprenant, A., North, R.A., 1996. Ionic permeability of, and divalent cation effects on, two ATP-gated cation channels (P2X receptors) expressed in mammalian cells. *The Journal of Physiology*. **497 ( Pt 2)**, 413-422.

Feldberg, W. & Hebb, C., 1948. The stimulating action of phosphate compounds on the perfused superior cervical ganglion of the cat. *The Journal of Physiology*. **107**, 210-221.

Feng, Y.H., Li, X., Wang, L., Zhou, L., Gorodeski, G.I., 2006. A truncated P2X7 receptor variant (P2X7-j) endogenously expressed in cervical cancer cells antagonizes the full-length P2X7 receptor through hetero-oligomerization. *The Journal of Biological Chemistry*. **281**, 17228-17237.

Ferrini, F., Trang, T., Mattioli, T.A., Laffray, S., Del'Guidice, T., Lorenzo, L.E., Castonguay, A., Doyon, N., Zhang, W., Godin, A.G., Mohr, D., Beggs, S., Vandal, K., Beaulieu, J.M., Cahill, C.M., Salter, M.W., De Koninck, Y., 2013. Morphine hyperalgesia gated through microglia-mediated disruption of neuronal Cl(-) homeostasis. *Nature Neuroscience*. **16**, 183-192.

Finger, T.E., Danilova, V., Barrows, J., Bartel, D.L., Vigers, A.J., Stone, L., Hellekant, G., Kinnamon, S.C., 2005. ATP signaling is crucial for communication from taste buds to gustatory nerves. *Science (New York, N.Y.)*. **310**, 1495-1499.

Ford, A.P. & Undem, B.J., 2013. The therapeutic promise of ATP antagonism at P2X3 receptors in respiratory and urological disorders. *Frontiers in Cellular Neuroscience*. **7**, 267.

Fortes, P.A., Ellory, J.C., Lew, V.L., 1973. Suramin: a potent ATPase inhibitor which acts on the inside surface of the sodium pump. *Biochimica Et Biophysica Acta*. **318**, 262-272.

Fujiwara, Y., Keceli, B., Nakajo, K., Kubo, Y., 2009. Voltage- and [ATP]-dependent gating of the P2X(2) ATP receptor channel. *The Journal of General Physiology*. **133**, 93-109.

Garcia-Guzman, M., Soto, F., Gomez-Hernandez, J.M., Lund, P.E., Stuhmer, W., 1997. Characterization of recombinant human P2X4 receptor reveals pharmacological differences to the rat homologue. *Molecular Pharmacology*. **51**, 109-118.

Garcia-Guzman, M., Soto, F., Laube, B., Stuhmer, W., 1996. Molecular cloning and functional expression of a novel rat heart P2X purinoceptor. *FEBS Letters*. **388**, 123-127.

Gayle, S. & Burnstock, G., 2005. Immunolocalisation of P2X and P2Y nucleotide receptors in the rat nasal mucosa. *Cell and Tissue Research*. **319**, 27-36.

Gever, J.R., Cockayne, D.A., Dillon, M.P., Burnstock, G., Ford, A.P., 2006. Pharmacology of P2X channels. *Pflugers Archiv : European Journal of Physiology*. **452**, 513-537.

Gever, J.R., Soto, R., Henningsen, R.A., Martin, R.S., Hackos, D.H., Panicker, S., Rubas, W., Oglesby, I.B., Dillon, M.P., Milla, M.E., Burnstock, G., Ford, A.P., 2010. AF-353, a novel, potent and orally bioavailable P2X3/P2X2/3 receptor antagonist. *British Journal of Pharmacology*. **160**, 1387-1398.

Glass, R., Loesch, A., Bodin, P., Burnstock, G., 2002. P2X4 and P2X6 receptors associate with VE-cadherin in human endothelial cells. *Cellular and Molecular Life Sciences : CMLS*. **59**, 870-881.

Gleave, R.J., Walter, D.S., Beswick, P.J., Fonfria, E., Michel, A.D., Roman, S.A., Tang, S.P., 2010. Synthesis and biological activity of a series of tetrasubstituted-imidazoles as P2X(7) antagonists. *Bioorganic & Medicinal Chemistry Letters*. **20**, 4951-4954.

Gong, Q.J., Li, Y.Y., Xin, W.J., Zang, Y., Ren, W.J., Wei, X.H., Li, Y.Y., Zhang, T., Liu, X.G., 2009. ATP induces long-term potentiation of C-fiber-evoked field potentials in spinal dorsal horn: the roles of P2X4 receptors and p38 MAPK in microglia. *Glia*. **57**, 583-591.

Greig, A.V., Linge, C., Healy, V., Lim, P., Clayton, E., Rustin, M.H., McGrouther, D.A., Burnstock, G., 2003. Expression of purinergic receptors in non-melanoma skin cancers and their functional roles in A431 cells. *The Journal of Investigative Dermatology*. **121**, 315-327.

Guerrero-Alba, R., Valdez-Morales, E., Juarez, E.H., Miranda-Morales, M., Ramirez-Martinez, J.F., Espinosa-Luna, R., Barajas-Lopez, C., 2010. Two suramin binding sites are present in guinea pig but only one in murine native P2X myenteric receptors. *European Journal of Pharmacology*. **626**, 179-185.

Guns, P.J., Hendrickx, J., Van Assche, T., Fransen, P., Bult, H., 2010. P2Y receptors and atherosclerosis in apolipoprotein E-deficient mice. *British Journal of Pharmacology*. **159**, 326-336.

Guo, C., Masin, M., Qureshi, O.S., Murrell-Lagnado, R.D., 2007. Evidence for functional P2X4/P2X7 heteromeric receptors. *Molecular Pharmacology*. **72**, 1447-1456.

Haines, W.R., Torres, G.E., Voigt, M.M., Egan, T.M., 1999. Properties of the novel ATP-gated ionotropic receptor composed of the P2X(1) and P2X(5) isoforms. *Molecular Pharmacology*. **56**, 720-727.

Hattori, M. & Gouaux, E., 2012. Molecular mechanism of ATP binding and ion channel activation in P2X receptors. *Nature*. **485**, 207-212.

Hechler, B. & Gachet, C., 2011. P2 receptors and platelet function. *Purinergic Signalling*. **7**, 293-303.

Hechler, B., Lenain, N., Marchese, P., Vial, C., Heim, V., Freund, M., Cazenave, J.P., Cattaneo, M., Ruggeri, Z.M., Evans, R., Gachet, C., 2003. A role of the fast ATP-gated P2X1 cation channel in thrombosis of small arteries in vivo. *The Journal of Experimental Medicine*. **198**, 661-667.

Hechler, B., Magnenat, S., Zighetti, M.L., Kassack, M.U., Ullmann, H., Cazenave, J.P., Evans, R., Cattaneo, M., Gachet, C., 2005. Inhibition of platelet functions and thrombosis through selective or nonselective inhibition of the platelet P2 receptors with increasing doses of NF449 [4,4',4'',4''-(carbonylbis(imino-5,1,3-benzenetriylbis-(carbonylimino))))tetrakis -benzene-1,3-disulfonic acid octasodium salt. *The Journal of Pharmacology and Experimental Therapeutics*. **314**, 232-243.

Heppner, T.J., Werner, M.E., Nausch, B., Vial, C., Evans, R.J., Nelson, M.T., 2009. Nerve-evoked purinergic signalling suppresses action potentials, Ca<sup>2+</sup> flashes and contractility evoked by muscarinic receptor activation in mouse urinary bladder smooth muscle. *The Journal of Physiology*. **587**, 5275-5288.

Hernandez-Olmos, V., Abdelrahman, A., El-Tayeb, A., Freudendahl, D., Weinhausen, S., Muller, C.E., 2012. N-substituted phenoxazine and acridone derivatives: structure-activity relationships of potent P2X4 receptor antagonists. *Journal of Medicinal Chemistry*. **55**, 9576-9588.

Hoebertz, A., Townsend-Nicholson, A., Glass, R., Burnstock, G., Arnett, T.R., 2000. Expression of P2 receptors in bone and cultured bone cells. *Bone*. **27**, 503-510.

HOLTON, F.A. & HOLTON, P., 1954. The capillary dilator substances in dry powders of spinal roots; a possible role of adenosine triphosphate in chemical transmission from nerve endings. *The Journal of Physiology*. **126**, 124-140.

HOLTON, P., 1959. The liberation of adenosine triphosphate on antidromic stimulation of sensory nerves. *The Journal of Physiology*. **145**, 494-504.

Honore, P., Donnelly-Roberts, D., Namovic, M., Zhong, C., Wade, C., Chandran, P., Zhu, C., Carroll, W., Perez-Medrano, A., Iwakura, Y., Jarvis, M.F., 2009. The antihyperalgesic activity of a selective P2X7 receptor antagonist, A-839977, is lost in IL-1alpha/beta knockout mice. *Behavioural Brain Research*. **204**, 77-81.

Honore, P., Donnelly-Roberts, D., Namovic, M.T., Hsieh, G., Zhu, C.Z., Mikusa, J.P., Hernandez, G., Zhong, C., Gauvin, D.M., Chandran, P., Harris, R., Medrano, A.P., Carroll, W., Marsh, K., Sullivan, J.P., Faltynek, C.R., Jarvis, M.F., 2006. A-740003 [N-(1-{[(cyanoimino)(5-quinolinylamino) methyl]amino}-2,2-dimethylpropyl)-2-(3,4-dimethoxyphenyl)acetamide], a novel and selective P2X7

receptor antagonist, dose-dependently reduces neuropathic pain in the rat. *The Journal of Pharmacology and Experimental Therapeutics*. **319**, 1376-1385.

Hou, M., Malmsjo, M., Moller, S., Pantev, E., Bergdahl, A., Zhao, X.H., Sun, X.Y., Hedner, T., Edvinsson, L., Erlinge, D., 1999. Increase in cardiac P2X1-and P2Y2-receptor mRNA levels in congestive heart failure. *Life Sciences*. **65**, 1195-1206.

Housley, G.D., Luo, L., Ryan, A.F., 1998. Localization of mRNA encoding the P2X2 receptor subunit of the adenosine 5'-triphosphate-gated ion channel in the adult and developing rat inner ear by *in situ* hybridization. *The Journal of Comparative Neurology*. **393**, 403-414.

Hracsko, Z., Baranyi, M., Csolle, C., Goloncser, F., Madarasz, E., Kittel, A., Sperlagh, B., 2011. Lack of neuroprotection in the absence of P2X7 receptors in toxin-induced animal models of Parkinson's disease. *Molecular Neurodegeneration*. **6**, 28-1326-6-28.

Hu, B., Mei, Q.B., Yao, X.J., Smith, E., Barry, W.H., Liang, B.T., 2001. A novel contractile phenotype with cardiac transgenic expression of the human P2X4 receptor. *FASEB Journal : Official Publication of the Federation of American Societies for Experimental Biology*. **15**, 2739-2741.

Huang, S., Chen, Y., Wu, W., Ouyang, N., Chen, J., Li, H., Liu, X., Su, F., Lin, L., Yao, Y., 2013. miR-150 promotes human breast cancer growth and malignant behavior by targeting the pro-apoptotic purinergic P2X7 receptor. *PLoS One*. **8**, e80707.

Huang, Y.A., Stone, L.M., Pereira, E., Yang, R., Kinnamon, J.C., Dvoryanchikov, G., Chaudhari, N., Finger, T.E., Kinnamon, S.C., Roper, S.D., 2011. Knocking out P2X receptors reduces transmitter secretion in taste buds. *The Journal of Neuroscience : The Official Journal of the Society for Neuroscience*. **31**, 13654-13661.

Hulsmann, M., Nickel, P., Kassack, M., Schmalzing, G., Lambrecht, G., Markwardt, F., 2003. NF449, a novel picomolar potency antagonist at human P2X1 receptors. *European Journal of Pharmacology*. **470**, 1-7.

Ikeda, M., 2007. Characterization of functional P2X(1) receptors in mouse megakaryocytes. *Thrombosis Research*. **119**, 343-353.

Ishii, K., Kaneda, M., Li, H., Rockland, K.S., Hashikawa, T., 2003. Neuron-specific distribution of P2X7 purinergic receptors in the monkey retina. *The Journal of Comparative Neurology*. **459**, 267-277.

Jahangir, A., Alam, M., Carter, D.S., Dillon, M.P., Bois, D.J., Ford, A.P., Gever, J.R., Lin, C., Wagner, P.J., Zhai, Y., Zira, J., 2009. Identification and SAR of novel diaminopyrimidines. Part 2: The discovery of RO-51, a potent and selective, dual P2X(3)/P2X(2/3) antagonist for the treatment of pain. *Bioorganic & Medicinal Chemistry Letters*. **19**, 1632-1635.

Jaime-Figueroa, S., Greenhouse, R., Padilla, F., Dillon, M.P., Gever, J.R., Ford, A.P., 2005. Discovery and synthesis of a novel and selective drug-like P2X(1) antagonist. *Bioorganic & Medicinal Chemistry Letters*. **15**, 3292-3295.

Jarvis, M.F., 2010. The neural-glial purinergic receptor ensemble in chronic pain states. *Trends in Neurosciences*. **33**, 48-57.

Jarvis, M.F., Bianchi, B., Uchic, J.T., Cartmell, J., Lee, C.H., Williams, M., Faltynek, C., 2004. 3HJA-317491, a novel high-affinity non-nucleotide antagonist that specifically labels human P2X2/3 and P2X3 receptors. *The Journal of Pharmacology and Experimental Therapeutics*. **310**, 407-416.

Jarvis, M.F., Burgard, E.C., McGaraughty, S., Honore, P., Lynch, K., Brennan, T.J., Subieta, A., Van Biesen, T., Cartmell, J., Bianchi, B., Niforatos, W., Kage, K., Yu, H., Mikusa, J., Wismer, C.T., Zhu, C.Z., Chu, K., Lee, C.H., Stewart, A.O., Polakowski, J., Cox, B.F., Kowaluk, E., Williams, M., Sullivan, J., Faltynek, C., 2002. A-317491, a novel potent and selective non-nucleotide antagonist of P2X3 and P2X2/3 receptors, reduces chronic inflammatory and neuropathic pain in the rat. *Proceedings of the National Academy of Sciences of the United States of America*. **99**, 17179-17184.

Jarvis, M.F. & Khakh, B.S., 2009. ATP-gated P2X cation-channels. *Neuropharmacology*. **56**, 208-215.

Jelassi, B., Chantome, A., Alcaraz-Perez, F., Baroja-Mazo, A., Cayuela, M.L., Pelegrin, P., Surprenant, A., Roger, S., 2011. P2X(7) receptor activation enhances SK3 channels- and cystein cathepsin-dependent cancer cells invasiveness. *Oncogene*. **30**, 2108-2122.

Jiang, L.H., Rassendren, F., Surprenant, A., North, R.A., 2000. Identification of amino acid residues contributing to the ATP-binding site of a purinergic P2X receptor. *The Journal of Biological Chemistry*. **275**, 34190-34196.

Jiang, R., Lemoine, D., Martz, A., Taly, A., Gonin, S., Prado de Carvalho, L., Specht, A., Grutter, T., 2011. Agonist trapped in ATP-binding sites of the P2X2 receptor. *Proceedings of the National Academy of Sciences of the United States of America*. **108**, 9066-9071.

Jiang, R., Taly, A., Grutter, T., 2013. Moving through the gate in ATP-activated P2X receptors. *Trends in Biochemical Sciences*. **38**, 20-29.

Jiang, R., Taly, A., Lemoine, D., Martz, A., Cunrath, O., Grutter, T., 2012. Tightening of the ATP-binding sites induces the opening of P2X receptor channels. *The EMBO Journal*. **31**, 2134-2143.

Kaan, T.K., Yip, P.K., Patel, S., Davies, M., Marchand, F., Cockayne, D.A., Nunn, P.A., Dickenson, A.H., Ford, A.P., Zhong, Y., Malcangio, M., McMahon, S.B., 2010. Systemic blockade of P2X3 and P2X2/3 receptors attenuates bone cancer pain behaviour in rats. *Brain : A Journal of Neurology*. **133**, 2549-2564.

Kaczmarek-Hajek, K., Lorinczi, E., Hausmann, R., Nicke, A., 2012. Molecular and functional properties of P2X receptors--recent progress and persisting challenges. *Purinergic Signalling*. **8**, 375-417.

Kamiya, A. & Togawa, T., 1980. Adaptive regulation of wall shear stress to flow change in the canine carotid artery. *The American Journal of Physiology*. **239**, H14-21.

Kaplan, L.D., Wolfe, P.R., Volberding, P.A., Feorino, P., Levy, J.A., Abrams, D.I., Kiprov, D., Wong, R., Kaufman, L., Gottlieb, M.S., 1987. Lack of response to suramin in patients with AIDS and AIDS-related complex. *The American Journal of Medicine*. **82**, 615-620.

Kaur, M., Reed, E., Sartor, O., Dahut, W., Figg, W.D., 2002. Suramin's development: what did we learn? *Investigational New Drugs*. **20**, 209-219.

Kawate, T., Michel, J.C., Birdsong, W.T., Gouaux, E., 2009. Crystal structure of the ATP-gated P2X(4) ion channel in the closed state. *Nature*. **460**, 592-598.

Kawate, T., Robertson, J.L., Li, M., Silberberg, S.D., Swartz, K.J., 2011. Ion access pathway to the transmembrane pore in P2X receptor channels. *The Journal of General Physiology*. **137**, 579-590.

Ke, H.Z., Qi, H., Weidema, A.F., Zhang, Q., Panupinthu, N., Crawford, D.T., Grasser, W.A., Paralkar, V.M., Li, M., Audoly, L.P., Gabel, C.A., Jee, W.S., Dixon, S.J., Sims, S.M., Thompson, D.D., 2003. Deletion of the P2X7 nucleotide receptor reveals its regulatory roles in bone formation and resorption. *Molecular Endocrinology (Baltimore, Md.)*. **17**, 1356-1367.

Kennedy, C., 2013. The importance of drug discovery for treatment of cardiovascular diseases. *Future Medicinal Chemistry*. **5**, 355-357.

Keystone, E.C., Wang, M.M., Layton, M., Hollis, S., McInnes, I.B., D1520C00001 Study Team, 2012. Clinical evaluation of the efficacy of the P2X7 purinergic receptor antagonist AZD9056 on the signs and symptoms of rheumatoid arthritis in patients with active disease despite treatment with methotrexate or sulphasalazine. *Annals of the Rheumatic Diseases*. **71**, 1630-1635.

Khakh, B.S., Burnstock, G., Kennedy, C., King, B.F., North, R.A., Seguela, P., Voigt, M., Humphrey, P.P., 2001. International union of pharmacology. XXIV. Current status of the nomenclature and properties of P2X receptors and their subunits. *Pharmacological Reviews*. **53**, 107-118.

Khakh, B.S., Michel, A., Humphrey, P.P., 1994. Estimates of antagonist affinities at P2X purinoceptors in rat vas deferens. *European Journal of Pharmacology*. **263**, 301-309.

Khakh, B.S., Proctor, W.R., Dunwiddie, T.V., Labarca, C., Lester, H.A., 1999. Allosteric control of gating and kinetics at P2X(4) receptor channels. *The Journal of Neuroscience : The Official Journal of the Society for Neuroscience*. **19**, 7289-7299.

Kidd, E.J., Grahames, C.B., Simon, J., Michel, A.D., Barnard, E.A., Humphrey, P.P., 1995. Localization of P2X purinoceptor transcripts in the rat nervous system. *Molecular Pharmacology*. **48**, 569-573.

King, B.F., Wildman, S.S., Townsend-Nicholson, A., Burnstock, G., 1998. Antagonism of an adenosine/ATP receptor in follicular Xenopus oocytes. *The Journal of Pharmacology and Experimental Therapeutics*. **285**, 1005-1011.

Kotnis, S., Bingham, B., Vasilyev, D.V., Miller, S.W., Bai, Y., Yeola, S., Chanda, P.K., Bowlby, M.R., Kaftan, E.J., Samad, T.A., Whiteside, G.T., 2010. Genetic and functional analysis of human P2X5 reveals a distinct pattern of exon 10 polymorphism with predominant expression of the nonfunctional receptor isoform. *Molecular Pharmacology*. **77**, 953-960.

Kracun, S., Chaptal, V., Abramson, J., Khakh, B.S., 2010. Gated access to the pore of a P2X receptor: structural implications for closed-open transitions. *The Journal of Biological Chemistry*. **285**, 10110-10121.

Kvist, T., Steffensen, T.B., Greenwood, J.R., Mehrzad Tabrizi, F., Hansen, K.B., Gajhede, M., Pickering, D.S., Traynelis, S.F., Kastrup, J.S., Brauner-Osborne, H., 2013. Crystal structure and pharmacological characterization of a novel N-methyl-D-aspartate (NMDA) receptor antagonist at the GluN1 glycine binding site. *The Journal of Biological Chemistry*. **288**, 33124-33135.

Kwon, H.J., 2012. Extracellular ATP signaling via P2X(4) receptor and cAMP/PKA signaling mediate ATP oscillations essential for prechondrogenic condensation. *The Journal of Endocrinology*. **214**, 337-348.

Labasi, J.M., Petrushova, N., Donovan, C., McCurdy, S., Lira, P., Payette, M.M., Brissette, W., Wicks, J.R., Audoly, L., Gabel, C.A., 2002. Absence of the P2X7 receptor alters leukocyte function and attenuates an inflammatory response. *Journal of Immunology (Baltimore, Md.: 1950)*. **168**, 6436-6445.

Lalo, U., Pankratov, Y., Wichert, S.P., Rossner, M.J., North, R.A., Kirchhoff, F., Verkhratsky, A., 2008. P2X1 and P2X5 subunits form the functional P2X receptor in mouse cortical astrocytes. *The Journal of Neuroscience : The Official Journal of the Society for Neuroscience*. **28**, 5473-5480.

Lambrecht, G., Braun, K., Damer, M., Ganso, M., Hildebrandt, C., Ullmann, H., Kassack, M.U., Nickel, P., 2002. Structure-activity relationships of suramin and pyridoxal-5'-phosphate derivatives as P2 receptor antagonists. *Current Pharmaceutical Design*. **8**, 2371-2399.

Lambrecht, G., Fribe, T., Grimm, U., Windscheif, U., Bungardt, E., Hildebrandt, C., Baumert, H.G., Spatz-Kumbel, G., Mutschler, E., 1992. PPADS, a novel functionally selective antagonist of P2 purinoceptor-mediated responses. *European Journal of Pharmacology*. **217**, 217-219.

Langer, S.Z. & Pinto, J.E., 1976. Possible involvement of a transmitter different from norepinephrine in the residual responses to nerve stimulation of the cat nictitating membrane after pretreatment with reserpine. *The Journal of Pharmacology and Experimental Therapeutics*. **196**, 697-713.

Le, K.T., Babinski, K., Seguela, P., 1998. Central P2X4 and P2X6 channel subunits coassemble into a novel heteromeric ATP receptor. *The Journal of Neuroscience : The Official Journal of the Society for Neuroscience*. **18**, 7152-7159.

Le, K.T., Boue-Grabot, E., Archambault, V., Seguela, P., 1999. Functional and biochemical evidence for heteromeric ATP-gated channels composed of P2X1 and P2X5 subunits. *The Journal of Biological Chemistry*. **274**, 15415-15419.

Le, K.T., Paquet, M., Nouel, D., Babinski, K., Seguela, P., 1997. Primary structure and expression of a naturally truncated human P2X ATP receptor subunit from brain and immune system. *FEBS Letters*. **418**, 195-199.

Lecut, C., Faccinetto, C., Delierneux, C., van Oerle, R., Spronk, H.M., Evans, R.J., El Benna, J., Bours, V., Oury, C., 2012. ATP-gated P2X1 ion channels protect against endotoxemia by dampening neutrophil activation. *Journal of Thrombosis and Haemostasis : JTH*. **10**, 453-465.

Lecut, C., Frederix, K., Johnson, D.M., Deroanne, C., Thiry, M., Faccinetto, C., Maree, R., Evans, R.J., Volders, P.G., Bours, V., Oury, C., 2009. P2X1 ion channels promote neutrophil chemotaxis through Rho kinase activation. *Journal of Immunology (Baltimore, Md.: 1950)*. **183**, 2801-2809.

Leff, P., Wood, B.E., O'Connor, S.E., 1990. Suramin is a slowly-equilibrating but competitive antagonist at P2x-receptors in the rabbit isolated ear artery. *British Journal of Pharmacology*. **101**, 645-649.

Lemoine, D., Habermacher, C., Martz, A., Mery, P.F., Bouquier, N., Diverchy, F., Taly, A., Rassendren, F., Specht, A., Grutter, T., 2013. Optical control of an ion channel gate. *Proceedings of the National Academy of Sciences of the United States of America*. **110**, 20813-20818.

Lewis, C., Neidhart, S., Holy, C., North, R.A., Buell, G., Surprenant, A., 1995. Coexpression of P2X2 and P2X3 receptor subunits can account for ATP-gated currents in sensory neurons. *Nature*. **377**, 432-435.

Li, C., 2000. Novel mechanism of inhibition by the P2 receptor antagonist PPADS of ATP-activated current in dorsal root ganglion neurons. *Journal of Neurophysiology*. **83**, 2533-2541.

Li, C., Aguayo, L., Peoples, R.W., Weight, F.F., 1993. Ethanol inhibits a neuronal ATP-gated ion channel. *Molecular Pharmacology*. **44**, 871-875.

Li, C., Peoples, R.W., Weight, F.F., 1998. Ethanol-induced inhibition of a neuronal P2X purinoceptor by an allosteric mechanism. *British Journal of Pharmacology*. **123**, 1-3.

Li, J., Liu, D., Ke, H.Z., Duncan, R.L., Turner, C.H., 2005. The P2X7 nucleotide receptor mediates skeletal mechanotransduction. *The Journal of Biological Chemistry*. **280**, 42952-42959.

Li, M., Chang, T.H., Silberberg, S.D., Swartz, K.J., 2008. Gating the pore of P2X receptor channels. *Nature Neuroscience*. **11**, 883-887.

Li, M., Kawate, T., Silberberg, S.D., Swartz, K.J., 2010. Pore-opening mechanism in trimeric P2X receptor channels. *Nature Communications*. **1**, 44.

Li, M., Silberberg, S.D., Swartz, K.J., 2013a. Subtype-specific control of P2X receptor channel signaling by ATP and Mg<sup>2+</sup>. *Proceedings of the National Academy of Sciences of the United States of America*. **110**, E3455-63.

Li, X., Kang, L., Li, G., Zeng, H., Zhang, L., Ling, X., Dong, H., Liang, S., Chen, H., 2013b. Intrathecal leptin inhibits expression of the P2X2/3 receptors and alleviates neuropathic pain induced by chronic constriction sciatic nerve injury. *Molecular Pain*. **9**, 65-8069-9-65.

Liu, M., Yang, H., Fang, D., Yang, J.J., Cai, J., Wan, Y., Chui, D.H., Han, J.S., Xing, G.G., 2013. Upregulation of P2X3 receptors by neuronal calcium sensor protein VILIP-1 in dorsal root ganglions contributes to the bone cancer pain in rats. *Pain*. **154**, 1551-1568.

LOMINSKI, I. & GRAY, S., 1961. Inhibition of lysozyme by 'Suramin'. *Nature*. **192**, 683.

Lorca, R.A., Rozas, C., Loyola, S., Moreira-Ramos, S., Zeise, M.L., Kirkwood, A., Huidobro-Toro, J.P., Morales, B., 2011. Zinc enhances long-term potentiation through P2X receptor modulation in the hippocampal CA1 region. *The European Journal of Neuroscience*. **33**, 1175-1185.

Lorinczi, E., Bhargava, Y., Marino, S.F., Taly, A., Kaczmarek-Hajek, K., Barrantes-Freer, A., Dutertre, S., Grutter, T., Rettinger, J., Nicke, A., 2012. Involvement of the cysteine-rich head domain in activation and desensitization of the P2X1 receptor. *Proceedings of the National Academy of Sciences of the United States of America*. **109**, 11396-11401.

Lucae, S., Salyakina, D., Barden, N., Harvey, M., Gagne, B., Labbe, M., Binder, E.B., Uhr, M., Paez-Pereda, M., Sillaber, I., Ising, M., Bruckl, T., Lieb, R., Holsboer, F., Muller-Myhsok, B., 2006. P2RX7, a gene coding for a purinergic ligand-gated ion channel, is associated with major depressive disorder. *Human Molecular Genetics*. **15**, 2438-2445.

Lustig, K.D., Shiau, A.K., Brake, A.J., Julius, D., 1993. Expression cloning of an ATP receptor from mouse neuroblastoma cells. *Proceedings of the National Academy of Sciences of the United States of America*. **90**, 5113-5117.

Lynch, K.J., Touma, E., Niforatos, W., Kage, K.L., Burgard, E.C., van Biesen, T., Kowaluk, E.A., Jarvis, M.F., 1999. Molecular and functional characterization of human P2X(2) receptors. *Molecular Pharmacology*. **56**, 1171-1181.

Ma, W., Korngreen, A., Weil, S., Cohen, E.B., Priel, A., Kuzin, L., Silberberg, S.D., 2006. Pore properties and pharmacological features of the P2X receptor channel in airway ciliated cells. *The Journal of Physiology*. **571**, 503-517.

MacKenzie, A.B., Mahaut-Smith, M.P., Sage, S.O., 1996. Activation of receptor-operated cation channels via P2X1 not P2T purinoceptors in human platelets. *The Journal of Biological Chemistry*. **271**, 2879-2881.

Mallard, N., Marshall, R., Sithers, A., Spriggs, B., 1992. Suramin: a selective inhibitor of purinergic neurotransmission in the rat isolated vas deferens. *European Journal of Pharmacology*. **220**, 1-10.

Marcellino, D., Suarez-Boomgaard, D., Sanchez-Reina, M.D., Aguirre, J.A., Yoshitake, T., Yoshitake, S., Hagman, B., Kehr, J., Agnati, L.F., Fuxe, K., Rivera, A., 2010. On the role of P2X(7) receptors in dopamine nerve cell degeneration in

a rat model of Parkinson's disease: studies with the P2X(7) receptor antagonist A-438079. *Journal of Neural Transmission (Vienna, Austria : 1996)*. **117**, 681-687.

Marquez-Klaka, B., Rettinger, J., Bhargava, Y., Eisele, T., Nicke, A., 2007. Identification of an intersubunit cross-link between substituted cysteine residues located in the putative ATP binding site of the P2X1 receptor. *The Journal of Neuroscience : The Official Journal of the Society for Neuroscience*. **27**, 1456-1466.

Marquez-Klaka, B., Rettinger, J., Nicke, A., 2009. Inter-subunit disulfide cross-linking in homomeric and heteromeric P2X receptors. *European Biophysics Journal : EBJ*. **38**, 329-338.

Masin, M., Young, C., Lim, K., Barnes, S.J., Xu, X.J., Marschall, V., Brutkowski, W., Mooney, E.R., Gorecki, D.C., Murrell-Lagnado, R., 2012. Expression, assembly and function of novel C-terminal truncated variants of the mouse P2X7 receptor: re-evaluation of P2X7 knockouts. *British Journal of Pharmacology*. **165**, 978-993.

Matute, C., Torre, I., Perez-Cerda, F., Perez-Samartin, A., Alberdi, E., Etxebarria, E., Arranz, A.M., Ravid, R., Rodriguez-Antiguedad, A., Sanchez-Gomez, M., Domercq, M., 2007. P2X(7) receptor blockade prevents ATP excitotoxicity in oligodendrocytes and ameliorates experimental autoimmune encephalomyelitis. *The Journal of Neuroscience : The Official Journal of the Society for Neuroscience*. **27**, 9525-9533.

McGaraughty, S., Chu, K.L., Namovic, M.T., Donnelly-Roberts, D.L., Harris, R.R., Zhang, X.F., Shieh, C.C., Wismer, C.T., Zhu, C.Z., Gauvin, D.M., Fabiyi, A.C., Honore, P., Gregg, R.J., Kort, M.E., Nelson, D.W., Carroll, W.A., Marsh, K., Faltynek, C.R., Jarvis, M.F., 2007. P2X7-related modulation of pathological nociception in rats. *Neuroscience*. **146**, 1817-1828.

McIlwrath, S.L., Davis, B.M., Bielefeldt, K., 2009. Deletion of P2X3 receptors blunts gastro-oesophageal sensation in mice. *Neurogastroenterology and Motility : The Official Journal of the European Gastrointestinal Motility Society*. **21**, 890-e66.

McLaren, G.J., Lambrecht, G., Mutschler, E., Baumert, H.G., Sneddon, P., Kennedy, C., 1994. Investigation of the actions of PPADS, a novel P2x-purinoceptor antagonist, in the guinea-pig isolated vas deferens. *British Journal of Pharmacology*. **111**, 913-917.

Mei, Q. & Liang, B.T., 2001. P2 purinergic receptor activation enhances cardiac contractility in isolated rat and mouse hearts. *American Journal of Physiology. Heart and Circulatory Physiology*. **281**, H334-41.

Minvielle-Sebastia, L. & Keller, W., 1999. mRNA polyadenylation and its coupling to other RNA processing reactions and to transcription. *Current Opinion in Cell Biology*. **11**, 352-357.

Mio, K., Kubo, Y., Ogura, T., Yamamoto, T., Sato, C., 2005. Visualization of the trimeric P2X2 receptor with a crown-capped extracellular domain. *Biochemical and Biophysical Research Communications*. **337**, 998-1005.

Mitsuya, H., Matsushita, S., Yarchoan, R., Broder, S., 1984. Protection of T cells against infectivity and cytopathic effect of HTLV-III in vitro. *Princess Takamatsu Symposia*. **15**, 277-288.

Mulryan, K., Gitterman, D.P., Lewis, C.J., Vial, C., Leckie, B.J., Cobb, A.L., Brown, J.E., Conley, E.C., Buell, G., Pritchard, C.A., Evans, R.J., 2000. Reduced vas deferens contraction and male infertility in mice lacking P2X1 receptors. *Nature*. **403**, 86-89.

Nagata, K., Imai, T., Yamashita, T., Tsuda, M., Tozaki-Saitoh, H., Inoue, K., 2009. Antidepressants inhibit P2X4 receptor function: a possible involvement in neuropathic pain relief. *Molecular Pain*. **5**, 20-8069-5-20.

Nakajima, M., DeChavigny, A., Johnson, C.E., Hamada, J., Stein, C.A., Nicolson, G.L., 1991. Suramin. A potent inhibitor of melanoma heparanase and invasion. *The Journal of Biological Chemistry*. **266**, 9661-9666.

Nakanishi, H. & Takeda, H., 1973. The possible role of adenosine triphosphate in chemical transmission between the hypogastric nerve terminal and seminal vesicle in the guinea-pig. *Japanese Journal of Pharmacology*. **23**, 479-490.

Nawa, G., Miyoshi, Y., Yoshikawa, H., Ochi, T., Nakamura, Y., 1999. Frequent loss of expression or aberrant alternative splicing of P2XM, a p53-inducible gene, in soft-tissue tumours. *British Journal of Cancer*. **80**, 1185-1189.

Newbolt, A., Stoop, R., Virginio, C., Suprenant, A., North, R.A., Buell, G., Rassendren, F., 1998. Membrane topology of an ATP-gated ion channel (P2X receptor). *The Journal of Biological Chemistry*. **273**, 15177-15182.

Nichols, C.G. & Lopatin, A.N., 1997. Inward rectifier potassium channels. *Annual Review of Physiology*. **59**, 171-191.

Nicke, A., 2008. Homotrimeric complexes are the dominant assembly state of native P2X7 subunits. *Biochemical and Biophysical Research Communications*. **377**, 803-808.

Nicke, A., Baumert, H.G., Rettinger, J., Eichele, A., Lambrecht, G., Mutschler, E., Schmalzing, G., 1998. P2X1 and P2X3 receptors form stable trimers: a novel structural motif of ligand-gated ion channels. *The EMBO Journal*. **17**, 3016-3028.

Nicke, A., Kerschensteiner, D., Soto, F., 2005. Biochemical and functional evidence for heteromeric assembly of P2X1 and P2X4 subunits. *Journal of Neurochemistry*. **92**, 925-933.

Nicke, A., Kuan, Y.H., Masin, M., Rettinger, J., Marquez-Klaka, B., Bender, O., Gorecki, D.C., Murrell-Lagnado, R.D., Soto, F., 2009. A functional P2X7 splice variant with an alternative transmembrane domain 1 escapes gene inactivation in P2X7 knock-out mice. *The Journal of Biological Chemistry*. **284**, 25813-25822.

Norenberg, W., Sobottka, H., Hempel, C., Plotz, T., Fischer, W., Schmalzing, G., Schaefer, M., 2012. Positive allosteric modulation by ivermectin of human but not murine P2X7 receptors. *British Journal of Pharmacology*. **167**, 48-66.

North, R.A., 2002. Molecular physiology of P2X receptors. *Physiological Reviews*. **82**, 1013-1067.

North, R.A. & Surprenant, A., 2000. Pharmacology of cloned P2X receptors. *Annual Review of Pharmacology and Toxicology*. **40**, 563-580.

Ostrovskaya, O., Asatryan, L., Wyatt, L., Popova, M., Li, K., Peoples, R.W., Alkana, R.L., Davies, D.L., 2011. Ethanol is a fast channel inhibitor of P2X4 receptors. *The Journal of Pharmacology and Experimental Therapeutics*. **337**, 171-179.

Oury, C., Kuijpers, M.J., Toth-Zsamboki, E., Bonnefoy, A., Danloy, S., Vreys, I., Feijge, M.A., De Vos, R., Vermeylen, J., Heemskerk, J.W., Hoylaerts, M.F., 2003. Overexpression of the platelet P2X1 ion channel in transgenic mice generates a novel prothrombotic phenotype. *Blood*. **101**, 3969-3976.

Palygin, O., Lalo, U., Verkhratsky, A., Pankratov, Y., 2010. Ionotropic NMDA and P2X1/5 receptors mediate synaptically induced Ca<sup>2+</sup> signalling in cortical astrocytes. *Cell Calcium*. **48**, 225-231.

Peng, W., Cotrina, M.L., Han, X., Yu, H., Bekar, L., Blum, L., Takano, T., Tian, G.F., Goldman, S.A., Nedergaard, M., 2009. Systemic administration of an antagonist of the ATP-sensitive receptor P2X7 improves recovery after spinal cord injury. *Proceedings of the National Academy of Sciences of the United States of America*. **106**, 12489-12493.

Popova, M., Asatryan, L., Ostrovskaya, O., Wyatt, L.R., Li, K., Alkana, R.L., Davies, D.L., 2010. A point mutation in the ectodomain-transmembrane 2 interface eliminates the inhibitory effects of ethanol in P2X4 receptors. *Journal of Neurochemistry*. **112**, 307-317.

Qureshi, O.S., Paramasivam, A., Yu, J.C., Murrell-Lagnado, R.D., 2007. Regulation of P2X4 receptors by lysosomal targeting, glycan protection and exocytosis. *Journal of Cell Science*. **120**, 3838-3849.

Ralevic, V. & Burnstock, G., 1998. Receptors for purines and pyrimidines. *Pharmacological Reviews*. **50**, 413-492.

Rassendren, F., Buell, G., Newbolt, A., North, R.A., Surprenant, A., 1997a. Identification of amino acid residues contributing to the pore of a P2X receptor. *The EMBO Journal*. **16**, 3446-3454.

Rassendren, F., Buell, G.N., Virginio, C., Collo, G., North, R.A., Surprenant, A., 1997b. The permeabilizing ATP receptor, P2X7. Cloning and expression of a human cDNA. *The Journal of Biological Chemistry*. **272**, 5482-5486.

Ren, J., Bian, X., DeVries, M., Schnegelsberg, B., Cockayne, D.A., Ford, A.P., Galligan, J.J., 2003. P2X2 subunits contribute to fast synaptic excitation in

myenteric neurons of the mouse small intestine. *The Journal of Physiology*. **552**, 809-821.

Resende, R.R., Britto, L.R., Ulrich, H., 2008. Pharmacological properties of purinergic receptors and their effects on proliferation and induction of neuronal differentiation of P19 embryonal carcinoma cells. *International Journal of Developmental Neuroscience : The Official Journal of the International Society for Developmental Neuroscience*. **26**, 763-777.

Rettinger, J., Braun, K., Hochmann, H., Kassack, M.U., Ullmann, H., Nickel, P., Schmalzing, G., Lambrecht, G., 2005. Profiling at recombinant homomeric and heteromeric rat P2X receptors identifies the suramin analogue NF449 as a highly potent P2X1 receptor antagonist. *Neuropharmacology*. **48**, 461-468.

Rettinger, J., Schmalzing, G., Damer, S., Muller, G., Nickel, P., Lambrecht, G., 2000. The suramin analogue NF279 is a novel and potent antagonist selective for the P2X(1) receptor. *Neuropharmacology*. **39**, 2044-2053.

Rieg, T., Gerasimova, M., Boyer, J.L., Insel, P.A., Vallon, V., 2011. P2Y(2) receptor activation decreases blood pressure and increases renal Na(+) excretion. *American Journal of Physiology.Regulatory, Integrative and Comparative Physiology*. **301**, R510-8.

Roberts, J.A., Allsopp, R.C., El Ajouz, S., Vial, C., Schmid, R., Young, M.T., Evans, R.J., 2012. Agonist binding evokes extensive conformational changes in the extracellular domain of the ATP-gated human P2X1 receptor ion channel. *Proceedings of the National Academy of Sciences of the United States of America*. **109**, 4663-4667.

Roberts, J.A. & Evans, R.J., 2006. Contribution of conserved polar glutamine, asparagine and threonine residues and glycosylation to agonist action at human P2X1 receptors for ATP. *Journal of Neurochemistry*. **96**, 843-852.

Roberts, J.A. & Evans, R.J., 2004. ATP binding at human P2X1 receptors. Contribution of aromatic and basic amino acids revealed using mutagenesis and partial agonists. *The Journal of Biological Chemistry*. **279**, 9043-9055.

Rong, W., Gourine, A.V., Cockayne, D.A., Xiang, Z., Ford, A.P., Spyer, K.M., Burnstock, G., 2003. Pivotal role of nucleotide P2X2 receptor subunit of the ATP-gated ion channel mediating ventilatory responses to hypoxia. *The Journal of Neuroscience : The Official Journal of the Society for Neuroscience*. **23**, 11315-11321.

Rothwell, S.W., Stansfeld, P.J., Bragg, L., Verkhratsky, A., North, R.A., 2014. Direct Gating of ATP-activated Ion Channels (P2X2 Receptors) by Lipophilic Attachment at the Outer End of the Second Transmembrane Domain. *The Journal of Biological Chemistry*. **289**, 618-626.

Royle, S.J., Bobanovic, L.K., Murrell-Lagnado, R.D., 2002. Identification of a non-canonical tyrosine-based endocytic motif in an ionotropic receptor. *The Journal of Biological Chemistry*. **277**, 35378-35385.

Rubio, M.E. & Soto, F., 2001. Distinct Localization of P2X receptors at excitatory postsynaptic specializations. *The Journal of Neuroscience : The Official Journal of the Society for Neuroscience*. **21**, 641-653.

Ryten, M., Dunn, P.M., Neary, J.T., Burnstock, G., 2002. ATP regulates the differentiation of mammalian skeletal muscle by activation of a P2X5 receptor on satellite cells. *The Journal of Cell Biology*. **158**, 345-355.

Ryten, M., Yang, S.Y., Dunn, P.M., Goldspink, G., Burnstock, G., 2004. Purinoceptor expression in regenerating skeletal muscle in the mdx mouse model of muscular dystrophy and in satellite cell cultures. *FASEB Journal : Official Publication of the Federation of American Societies for Experimental Biology*. **18**, 1404-1406.

Samways, D.S., Khakh, B.S., Dutertre, S., Egan, T.M., 2011. Preferential use of unobstructed lateral portals as the access route to the pore of human ATP-gated ion channels (P2X receptors). *Proceedings of the National Academy of Sciences of the United States of America*. **108**, 13800-13805.

Sanz, J.M., Chiozzi, P., Ferrari, D., Colaianna, M., Idzko, M., Falzoni, S., Fellin, R., Trabace, L., Di Virgilio, F., 2009. Activation of microglia by amyloid  $\beta$  requires P2X7 receptor expression. *Journal of Immunology (Baltimore, Md.: 1950)*. **182**, 4378-4385.

Saugstad, J.A., Roberts, J.A., Dong, J., Zeitouni, S., Evans, R.J., 2004. Analysis of the membrane topology of the acid-sensing ion channel 2a. *The Journal of Biological Chemistry*. **279**, 55514-55519.

Saul, A., Hausmann, R., Kless, A., Nicke, A., 2013. Heteromeric assembly of P2X subunits. *Frontiers in Cellular Neuroscience*. **7**, 250.

Savi, P., Labouret, C., Delesque, N., Guette, F., Lupker, J., Herbert, J.M., 2001. P2y(12), a new platelet ADP receptor, target of clopidogrel. *Biochemical and Biophysical Research Communications*. **283**, 379-383.

Scase, T.J., Heath, M.F., Allen, J.M., Sage, S.O., Evans, R.J., 1998. Identification of a P2X1 purinoceptor expressed on human platelets. *Biochemical and Biophysical Research Communications*. **242**, 525-528.

Schachter, J.B., Li, Q., Boyer, J.L., Nicholas, R.A., Harden, T.K., 1996. Second messenger cascade specificity and pharmacological selectivity of the human P2Y1-purinoceptor. *British Journal of Pharmacology*. **118**, 167-173.

SCHUMANN, H.J., 1958. Noradrenalin and ATP content of sympathetic nerves. *Naunyn-Schmiedebergs Archiv Fur Experimentelle Pathologie Und Pharmakologie*. **233**, 296-300.

Schwindt, T.T., Trujillo, C.A., Negraes, P.D., Lameu, C., Ulrich, H., 2011. Directed differentiation of neural progenitors into neurons is accompanied by altered expression of P2X purinergic receptors. *Journal of Molecular Neuroscience : MN*. **44**, 141-146.

Sharp, A.J., Polak, P.E., Simonini, V., Lin, S.X., Richardson, J.C., Bongarzone, E.R., Feinstein, D.L., 2008. P2x7 deficiency suppresses development of experimental autoimmune encephalomyelitis. *Journal of Neuroinflammation*. **5**, 33-2094-5-33.

Shen, J.B., Shutt, R., Agosto, M., Pappano, A., Liang, B.T., 2009. Reversal of cardiac myocyte dysfunction as a unique mechanism of rescue by P2X4 receptors in cardiomyopathy. *American Journal of Physiology.Heart and Circulatory Physiology*. **296**, H1089-95.

Silberberg, S.D. & Swartz, K.J., 2009. Structural biology: Trimeric ion-channel design. *Nature*. **460**, 580-581.

Sim, J.A., Broomhead, H.E., North, R.A., 2008. Ectodomain lysines and suramin block of P2X1 receptors. *The Journal of Biological Chemistry*. **283**, 29841-29846.

Sim, J.A., Chaumont, S., Jo, J., Ulmann, L., Young, M.T., Cho, K., Buell, G., North, R.A., Rassendren, F., 2006. Altered hippocampal synaptic potentiation in P2X4 knock-out mice. *The Journal of Neuroscience : The Official Journal of the Society for Neuroscience*. **26**, 9006-9009.

Sim, J.A., Park, C.K., Oh, S.B., Evans, R.J., North, R.A., 2007. P2X1 and P2X4 receptor currents in mouse macrophages. *British Journal of Pharmacology*. **152**, 1283-1290.

Sindrup, S.H., Otto, M., Finnerup, N.B., Jensen, T.S., 2005. Antidepressants in the treatment of neuropathic pain. *Basic & Clinical Pharmacology & Toxicology*. **96**, 399-409.

Smith, F.M., Humphrey, P.P., Murrell-Lagnado, R.D., 1999. Identification of amino acids within the P2X2 receptor C-terminus that regulate desensitization. *The Journal of Physiology*. **520 Pt 1**, 91-99.

Smolen, J.E. & Weissmann, G., 1978. Mg<sup>2+</sup>-ATPase as a membrane ectoenzyme of human granulocytes. Inhibitors, activators and response to phagocytosis. *Biochimica Et Biophysica Acta*. **512**, 525-538.

Sneddon, P., 1992. Suramin inhibits excitatory junction potentials in guinea-pig isolated vas deferens. *British Journal of Pharmacology*. **107**, 101-103.

Sneddon, P. & Burnstock, G., 1984. ATP as a co-transmitter in rat tail artery. *European Journal of Pharmacology*. **106**, 149-152.

Solle, M., Labasi, J., Perregaux, D.G., Stam, E., Petrushova, N., Koller, B.H., Griffiths, R.J., Gabel, C.A., 2001. Altered cytokine production in mice lacking P2X(7) receptors. *The Journal of Biological Chemistry*. **276**, 125-132.

Sonin, D., Zhou, S.Y., Cronin, C., Sonina, T., Wu, J., Jacobson, K.A., Pappano, A., Liang, B.T., 2008. Role of P2X purinergic receptors in the rescue of ischemic heart failure. *American Journal of Physiology.Heart and Circulatory Physiology*. **295**, H1191-H1197.

Soto, F., Garcia-Guzman, M., Gomez-Hernandez, J.M., Hollmann, M., Karschin, C., Stuhmer, W., 1996a. P2X4: an ATP-activated ionotropic receptor cloned from rat brain. *Proceedings of the National Academy of Sciences of the United States of America*. **93**, 3684-3688.

Soto, F., Garcia-Guzman, M., Karschin, C., Stuhmer, W., 1996b. Cloning and tissue distribution of a novel P2X receptor from rat brain. *Biochemical and Biophysical Research Communications*. **223**, 456-460.

Soto, F., Lambrecht, G., Nickel, P., Stuhmer, W., Busch, A.E., 1999. Antagonistic properties of the suramin analogue NF023 at heterologously expressed P2X receptors. *Neuropharmacology*. **38**, 141-149.

Souslova, V., Cesare, P., Ding, Y., Akopian, A.N., Stanfa, L., Suzuki, R., Carpenter, K., Dickenson, A., Boyce, S., Hill, R., Nebenuis-Oosthuizen, D., Smith, A.J., Kidd, E.J., Wood, J.N., 2000. Warm-coding deficits and aberrant inflammatory pain in mice lacking P2X3 receptors. *Nature*. **407**, 1015-1017.

Spehr, J., Spehr, M., Hatt, H., Wetzel, C.H., 2004. Subunit-specific P2X-receptor expression defines chemosensory properties of trigeminal neurons. *The European Journal of Neuroscience*. **19**, 2497-2510.

Spelta, V., Jiang, L.H., Surprenant, A., North, R.A., 2002. Kinetics of antagonist actions at rat P2X2/3 heteromeric receptors. *British Journal of Pharmacology*. **135**, 1524-1530.

Stokes, L., Jiang, L.H., Alcaraz, L., Bent, J., Bowers, K., Fagura, M., Furber, M., Mortimore, M., Lawson, M., Theaker, J., Laurent, C., Braddock, M., Surprenant, A., 2006. Characterization of a selective and potent antagonist of human P2X(7) receptors, AZ11645373. *British Journal of Pharmacology*. **149**, 880-887.

Stokes, L., Scurrah, K., Ellis, J.A., Cromer, B.A., Skarratt, K.K., Gu, B.J., Harrap, S.B., Wiley, J.S., 2011. A loss-of-function polymorphism in the human P2X4 receptor is associated with increased pulse pressure. *Hypertension*. **58**, 1086-1092.

Stoop, R., Surprenant, A., North, R.A., 1997. Different sensitivities to pH of ATP-induced currents at four cloned P2X receptors. *Journal of Neurophysiology*. **78**, 1837-1840.

Sun, B., Li, J., Okahara, K., Kambayashi, J., 1998. P2X1 purinoceptor in human platelets. Molecular cloning and functional characterization after heterologous expression. *The Journal of Biological Chemistry*. **273**, 11544-11547.

Surprenant, A., 1996. Functional properties of native and cloned P2X receptors. *Ciba Foundation Symposium*. **198**, 208-19; discussion 219-22.

Surprenant, A., Rassendren, F., Kawashima, E., North, R.A., Buell, G., 1996. The cytolytic P2Z receptor for extracellular ATP identified as a P2X receptor (P2X7). *Science (New York, N.Y.)*. **272**, 735-738.

Surprenant, A., Schneider, D.A., Wilson, H.L., Galligan, J.J., North, R.A., 2000. Functional properties of heteromeric P2X(1/5) receptors expressed in HEK cells

and excitatory junction potentials in guinea-pig submucosal arterioles. *Journal of the Autonomic Nervous System*. **81**, 249-263.

Telang, R.S., Paramananthasivam, V., Vlajkovic, S.M., Munoz, D.J., Housley, G.D., Thorne, P.R., 2010. Reduced P2x(2) receptor-mediated regulation of endocochlear potential in the ageing mouse cochlea. *Purinergic Signalling*. **6**, 263-272.

Tempest, H.V., Dixon, A.K., Turner, W.H., Elneil, S., Sellers, L.A., Ferguson, D.R., 2004. P2X and P2X receptor expression in human bladder urothelium and changes in interstitial cystitis. *BJU International*. **93**, 1344-1348.

Thimmaiah, K.N., Horton, J.K., Seshadri, R., Israel, M., Houghton, J.A., Harwood, F.C., Houghton, P.J., 1992. Synthesis and chemical characterization of N-substituted phenoxazines directed toward reversing vinca alkaloid resistance in multidrug-resistant cancer cells. *Journal of Medicinal Chemistry*. **35**, 3358-3364.

Tian, M., Abdelrahman, A., Weinhausen, S., Hinz, S., Weyer, S., Dosa, S., El-Tayeb, A., Muller, C.E., 2014. Carbamazepine derivatives with P2X4 receptor-blocking activity. *Bioorganic & Medicinal Chemistry*. **22**, 1077-1088.

Torres, G.E., Egan, T.M., Voigt, M.M., 1999. Hetero-oligomeric assembly of P2X receptor subunits. Specificities exist with regard to possible partners. *The Journal of Biological Chemistry*. **274**, 6653-6659.

Torres, G.E., Egan, T.M., Voigt, M.M., 1998a. N-Linked glycosylation is essential for the functional expression of the recombinant P2X2 receptor. *Biochemistry*. **37**, 14845-14851.

Torres, G.E., Egan, T.M., Voigt, M.M., 1998b. Topological analysis of the ATP-gated ionotropic [correction of ionotrophic] P2X2 receptor subunit. *FEBS Letters*. **425**, 19-23.

Torres, G.E., Haines, W.R., Egan, T.M., Voigt, M.M., 1998c. Co-expression of P2X1 and P2X5 receptor subunits reveals a novel ATP-gated ion channel. *Molecular Pharmacology*. **54**, 989-993.

Toulme, E., Garcia, A., Samways, D., Egan, T.M., Carson, M.J., Khakh, B.S., 2010. P2X4 receptors in activated C8-B4 cells of cerebellar microglial origin. *The Journal of General Physiology*. **135**, 333-353.

TOWN, B.W., WILLS, E.D., WILSON, E.J., WORMALL, A., 1950. Studies on suramin; the action of the drug on enzymes and some other proteins. General considerations. *The Biochemical Journal*. **47**, 149-158.

Trang, T. & Salter, M.W., 2012. P2X4 purinoceptor signaling in chronic pain. *Purinergic Signalling*. **8**, 621-628.

Trezise, D.J., Kennedy, I., Humphrey, P.P., 1994. The use of antagonists to characterize the receptors mediating depolarization of the rat isolated vagus nerve by alpha, beta-methylene adenosine 5'-triphosphate. *British Journal of Pharmacology*. **112**, 282-288.

Trujillo, C.A., Nery, A.A., Martins, A.H., Majumder, P., Gonzalez, F.A., Ulrich, H., 2006. Inhibition mechanism of the recombinant rat P2X(2) receptor in glial cells by suramin and TNP-ATP. *Biochemistry*. **45**, 224-233.

Tsuda, M., Kuboyama, K., Inoue, T., Nagata, K., Tozaki-Saitoh, H., Inoue, K., 2009. Behavioral phenotypes of mice lacking purinergic P2X4 receptors in acute and chronic pain assays. *Molecular Pain*. **5**, 28-8069-5-28.

Tsuda, M., Masuda, T., Tozaki-Saitoh, H., Inoue, K., 2013. P2X4 receptors and neuropathic pain. *Frontiers in Cellular Neuroscience*. **7**, 191.

Tsuda, M., Shigemoto-Mogami, Y., Koizumi, S., Mizokoshi, A., Kohsaka, S., Salter, M.W., Inoue, K., 2003. P2X4 receptors induced in spinal microglia gate tactile allodynia after nerve injury. *Nature*. **424**, 778-783.

Ulmann, L., Hatcher, J.P., Hughes, J.P., Chaumont, S., Green, P.J., Conquet, F., Buell, G.N., Reeve, A.J., Chessell, I.P., Rassendren, F., 2008. Up-regulation of P2X4 receptors in spinal microglia after peripheral nerve injury mediates BDNF release and neuropathic pain. *The Journal of Neuroscience : The Official Journal of the Society for Neuroscience*. **28**, 11263-11268.

Ulmann, L., Hirbec, H., Rassendren, F., 2010. P2X4 receptors mediate PGE2 release by tissue-resident macrophages and initiate inflammatory pain. *The EMBO Journal*. **29**, 2290-2300.

Urano, T., Nishimori, H., Han, H., Furuhata, T., Kimura, Y., Nakamura, Y., Tokino, T., 1997. Cloning of P2XM, a novel human P2X receptor gene regulated by p53. *Cancer Research*. **57**, 3281-3287.

Valera, S., Hussy, N., Evans, R.J., Adami, N., North, R.A., Surprenant, A., Buell, G., 1994. A new class of ligand-gated ion channel defined by P2x receptor for extracellular ATP. *Nature*. **371**, 516-519.

Valera, S., Talabot, F., Evans, R.J., Gos, A., Antonarakis, S.E., Morris, M.A., Buell, G.N., 1995. Characterization and chromosomal localization of a human P2X receptor from the urinary bladder. *Receptors & Channels*. **3**, 283-289.

Venkova, K., Milne, A., Krier, J., 1994. Contractions mediated by alpha 1-adrenoceptors and P2-purinoceptors in a cat colon circular muscle. *British Journal of Pharmacology*. **112**, 1237-1243.

Verdonk, M.L., Cole, J.C., Hartshorn, M.J., Murray, C.W., Taylor, R.D., 2003. Improved protein-ligand docking using GOLD. *Proteins*. **52**, 609-623.

Verkhratsky, A. & Steinhauser, C., 2000. Ion channels in glial cells. *Brain Research.Brain Research Reviews*. **32**, 380-412.

Vial, C. & Evans, R.J., 2002. P2X(1) receptor-deficient mice establish the native P2X receptor and a P2Y6-like receptor in arteries. *Molecular Pharmacology*. **62**, 1438-1445.

Vial, C. & Evans, R.J., 2000. P2X receptor expression in mouse urinary bladder and the requirement of P2X(1) receptors for functional P2X receptor responses in

the mouse urinary bladder smooth muscle. *British Journal of Pharmacology*. **131**, 1489-1495.

Vial, C., Hechler, B., Leon, C., Cazenave, J.P., Gachet, C., 1997. Presence of P2X1 purinoceptors in human platelets and megakaryoblastic cell lines. *Thrombosis and Haemostasis*. **78**, 1500-1504.

Vial, C., Rolf, M.G., Mahaut-Smith, M.P., Evans, R.J., 2002. A study of P2X1 receptor function in murine megakaryocytes and human platelets reveals synergy with P2Y receptors. *British Journal of Pharmacology*. **135**, 363-372.

Virginio, C., MacKenzie, A., Rassendren, F.A., North, R.A., Surprenant, A., 1999. Pore dilation of neuronal P2X receptor channels. *Nature Neuroscience*. **2**, 315-321.

Vlaskovska, M., Kasakov, L., Rong, W., Bodin, P., Bardini, M., Cockayne, D.A., Ford, A.P., Burnstock, G., 2001. P2X3 knock-out mice reveal a major sensory role for urothelial released ATP. *The Journal of Neuroscience : The Official Journal of the Society for Neuroscience*. **21**, 5670-5677.

von Kugelgen, I. & Wetter, A., 2000. Molecular pharmacology of P2Y-receptors. *Naunyn-Schmiedeberg's Archives of Pharmacology*. **362**, 310-323.

Voogd, T.E., Vansterkenburg, E.L., Wilting, J., Janssen, L.H., 1993. Recent research on the biological activity of suramin. *Pharmacological Reviews*. **45**, 177-203.

Vulchanova, L., Arvidsson, U., Riedl, M., Wang, J., Buell, G., Surprenant, A., North, R.A., Elde, R., 1996. Differential distribution of two ATP-gated channels (P2X receptors) determined by immunocytochemistry. *Proceedings of the National Academy of Sciences of the United States of America*. **93**, 8063-8067.

Walker, J.E., Saraste, M., Runswick, M.J., Gay, N.J., 1982. Distantly related sequences in the alpha- and beta-subunits of ATP synthase, myosin, kinases and other ATP-requiring enzymes and a common nucleotide binding fold. *The EMBO Journal*. **1**, 945-951.

Wang, J.C., Raybould, N.P., Luo, L., Ryan, A.F., Cannell, M.B., Thorne, P.R., Housley, G.D., 2003. Noise induces up-regulation of P2X2 receptor subunit of ATP-gated ion channels in the rat cochlea. *Neuroreport*. **14**, 817-823.

Wareham, K., Vial, C., Wykes, R.C., Bradding, P., Seward, E.P., 2009. Functional evidence for the expression of P2X1, P2X4 and P2X7 receptors in human lung mast cells. *British Journal of Pharmacology*. **157**, 1215-1224.

Webb, T.E., Simon, J., Krishek, B.J., Bateson, A.N., Smart, T.G., King, B.F., Burnstock, G., Barnard, E.A., 1993. Cloning and functional expression of a brain G-protein-coupled ATP receptor. *FEBS Letters*. **324**, 219-225.

Weight, F.F., Li, C., Peoples, R.W., 1999. Alcohol action on membrane ion channels gated by extracellular ATP (P2X receptors). *Neurochemistry International*. **35**, 143-152.

Werner, P., Seward, E.P., Buell, G.N., North, R.A., 1996. Domains of P2X receptors involved in desensitization. *Proceedings of the National Academy of Sciences of the United States of America*. **93**, 15485-15490.

Westfall, D.P., Sedaa, K.O., Shinozuka, K., Bjur, R.A., Buxton, I.L., 1990. ATP as a cotransmitter. *Annals of the New York Academy of Sciences*. **603**, 300-310.

Westfall, D.P., Stitzel, R.E., Rowe, J.N., 1978. The postjunctional effects and neural release of purine compounds in the guinea-pig vas deferens. *European Journal of Pharmacology*. **50**, 27-38.

White, C.W., Choong, Y.T., Short, J.L., Exintaris, B., Malone, D.T., Allen, A.M., Evans, R.J., Ventura, S., 2013. Male contraception via simultaneous knockout of alpha1A-adrenoceptors and P2X1-purinoceptors in mice. *Proceedings of the National Academy of Sciences of the United States of America*. **110**, 20825-20830.

Wildman, S.S., King, B.F., Burnstock, G., 1999. Modulatory activity of extracellular H<sup>+</sup> and Zn<sup>2+</sup> on ATP-responses at rP2X1 and rP2X3 receptors. *British Journal of Pharmacology*. **128**, 486-492.

Windscheif, U., Pfaff, O., Ziganshin, A.U., Hoyle, C.H., Baumert, H.G., Mutschler, E., Burnstock, G., Lambrecht, G., 1995. Inhibitory action of PPADS on relaxant responses to adenine nucleotides or electrical field stimulation in guinea-pig taenia coli and rat duodenum. *British Journal of Pharmacology*. **115**, 1509-1517.

Windscheif, U., Ralevic, V., Baumert, H.G., Mutschler, E., Lambrecht, G., Burnstock, G., 1994. Vasoconstrictor and vasodilator responses to various agonists in the rat perfused mesenteric arterial bed: selective inhibition by PPADS of contractions mediated via P2x-purinoceptors. *British Journal of Pharmacology*. **113**, 1015-1021.

Wolf, C., Rosefort, C., Fallah, G., Kassack, M.U., Hamacher, A., Bodnar, M., Wang, H., Illes, P., Kless, A., Bahrenberg, G., Schmalzing, G., Hausmann, R., 2011. Molecular determinants of potent P2X2 antagonism identified by functional analysis, mutagenesis, and homology docking. *Molecular Pharmacology*. **79**, 649-661.

Wong, A.Y., Burnstock, G., Gibb, A.J., 2000. Single channel properties of P2X ATP receptors in outside-out patches from rat hippocampal granule cells. *The Journal of Physiology*. **527 Pt 3**, 529-547.

Woolf, C.J., 2004. Dissecting out mechanisms responsible for peripheral neuropathic pain: implications for diagnosis and therapy. *Life Sciences*. **74**, 2605-2610.

Wu, T., Dai, M., Shi, X.R., Jiang, Z.G., Nuttall, A.L., 2011. Functional expression of P2X4 receptor in capillary endothelial cells of the cochlear spiral ligament and its role in regulating the capillary diameter. *American Journal of Physiology. Heart and Circulatory Physiology*. **301**, H69-78.

Xiong, K., Hu, X.Q., Stewart, R.R., Weight, F.F., Li, C., 2005. The mechanism by which ethanol inhibits rat P2X4 receptors is altered by mutation of histidine 241. *British Journal of Pharmacology*. **145**, 576-586.

Xiong, K., Li, C., Weight, F.F., 2000. Inhibition by ethanol of rat P2X(4) receptors expressed in Xenopus oocytes. *British Journal of Pharmacology*. **130**, 1394-1398.

Xiong, K., Peoples, R.W., Montgomery, J.P., Chiang, Y., Stewart, R.R., Weight, F.F., Li, C., 1999. Differential modulation by copper and zinc of P2X2 and P2X4 receptor function. *Journal of Neurophysiology*. **81**, 2088-2094.

Xiong, K., Stewart, R.R., Hu, X.Q., Werby, E., Peoples, R.W., Weight, F.F., Li, C., 2004a. Role of extracellular histidines in agonist sensitivity of the rat P2X4 receptor. *Neuroscience Letters*. **365**, 195-199.

Xiong, K., Stewart, R.R., Weight, F.F., Li, C., 2004b. Role of extracellular histidines in antagonist sensitivity of the rat P2X4 receptor. *Neuroscience Letters*. **367**, 197-200.

Yamamoto, K., Korenaga, R., Kamiya, A., Ando, J., 2000a. Fluid shear stress activates Ca(2+) influx into human endothelial cells via P2X4 purinoceptors. *Circulation Research*. **87**, 385-391.

Yamamoto, K., Korenaga, R., Kamiya, A., Qi, Z., Sokabe, M., Ando, J., 2000b. P2X(4) receptors mediate ATP-induced calcium influx in human vascular endothelial cells. *American Journal of Physiology. Heart and Circulatory Physiology*. **279**, H285-92.

Yamamoto, K., Sokabe, T., Matsumoto, T., Yoshimura, K., Shibata, M., Ohura, N., Fukuda, T., Sato, T., Sekine, K., Kato, S., Isshiki, M., Fujita, T., Kobayashi, M., Kawamura, K., Masuda, H., Kamiya, A., Ando, J., 2006. Impaired flow-dependent control of vascular tone and remodeling in P2X4-deficient mice. *Nature Medicine*. **12**, 133-137.

Yan, D., Zhu, Y., Walsh, T., Xie, D., Yuan, H., Sirmaci, A., Fujikawa, T., Wong, A.C., Loh, T.L., Du, L., Grati, M., Vlajkovic, S.M., Blanton, S., Ryan, A.F., Chen, Z.Y., Thorne, P.R., Kachar, B., Tekin, M., Zhao, H.B., Housley, G.D., King, M.C., Liu, X.Z., 2013. Mutation of the ATP-gated P2X(2) receptor leads to progressive hearing loss and increased susceptibility to noise. *Proceedings of the National Academy of Sciences of the United States of America*. **110**, 2228-2233.

Yang, R. & Liang, B.T., 2012. Cardiac P2X(4) receptors: targets in ischemia and heart failure? *Circulation Research*. **111**, 397-401.

Young, M.T., 2010. P2X receptors: dawn of the post-structure era. *Trends in Biochemical Sciences*. **35**, 83-90.

Young, M.T., Fisher, J.A., Fountain, S.J., Ford, R.C., North, R.A., Khakh, B.S., 2008. Molecular shape, architecture, and size of P2X4 receptors determined using fluorescence resonance energy transfer and electron microscopy. *The Journal of Biological Chemistry*. **283**, 26241-26251.

Zhong, Y., Dunn, P.M., Xiang, Z., Bo, X., Burnstock, G., 1998. Pharmacological and molecular characterization of P2X receptors in rat pelvic ganglion neurons. *British Journal of Pharmacology*. **125**, 771-781.

Ziganshin, A.U., Hoyle, C.H., Bo, X., Lambrecht, G., Mutschler, E., Baumert, H.G., Burnstock, G., 1993. PPADS selectively antagonizes P2X-purinoceptor-mediated responses in the rabbit urinary bladder. *British Journal of Pharmacology*. **110**, 1491-1495.

Ziganshin, A.U., Hoyle, C.H., Lambrecht, G., Mutschler, E., Baumert, H.G., Burnstock, G., 1994. Selective antagonism by PPADS at P2X-purinoceptors in rabbit isolated blood vessels. *British Journal of Pharmacology*. **111**, 923-929.

Zsembery, A., Boyce, A.T., Liang, L., Peti-Peterdi, J., Bell, P.D., Schwiebert, E.M., 2003. Sustained calcium entry through P2X nucleotide receptor channels in human airway epithelial cells. *The Journal of Biological Chemistry*. **278**, 13398-13408.

Zsembery, A., Fortenberry, J.A., Liang, L., Bebok, Z., Tucker, T.A., Boyce, A.T., Braunstein, G.M., Welty, E., Bell, P.D., Sorscher, E.J., Clancy, J.P., Schwiebert, E.M., 2004. Extracellular zinc and ATP restore chloride secretion across cystic fibrosis airway epithelia by triggering calcium entry. *The Journal of Biological Chemistry*. **279**, 10720-10729.